Landolt-Börnstein / New Series

Springer

Berlin
Heidelberg
New York
Barcelona
Budapest
Hong Kong
London
Milan
Paris
Singapore
Tokyo

Landolt-Börnstein

Numerical Data and Functional Relationships in Science and Technology

New Series
Editor in Chief: W. Martienssen

Units and Fundamental Constants in Physics and Chemistry

Elementary Particles, Nuclei and Atoms (Group I)
(Formerly: Nuclear and Particle Physics)

Molecules and Radicals (Group II)
(Formerly: Atomic and Molecular Physics)

Condensed Matter (Group III)
(Formerly: Solid State Physics)

Physical Chemistry (Group IV)
(Formerly: Macroscopic Properties of Matter)

Geophysics (Group V)

Astronomy and Astrophysics (Group VI)

Biophysics (Group VII)

Some of the group names have been changed to provide a better description of their contents

Landolt-Börnstein
Numerical Data and Functional Relationships in Science and Technology
New Series / Editor in Chief: W. Martienssen

Group I: Elementary Particles, Nuclei and Atoms
Volume 17

Photon and Electron Interactions with Atoms, Molecules and Ions

Subvolume A
Interactions of Photons and Electrons with Atoms

S.J. Buckman, J.W. Cooper, M.T. Elford
M. Inokuti, Y. Itikawa, H. Tawara

Edited by Y. Itikawa

Springer

ISSN 1615-1844 (Elementary Particles, Nuclei and Atoms)

ISBN 3-540-64296-X Springer-Verlag Berlin Heidelberg New York

Library of Congress Cataloging in Publication Data
Zahlenwerte und Funktionen aus Naturwissenschaften und Technik, Neue Serie
Editor in Chief: W. Martienssen
Vol. I/17A: Editor: Y. Itikawa
At head of title: Landolt-Börnstein. Added t.p.: Numerical data and functional relationships in science and technology.
Tables chiefly in English.
Intended to supersede the Physikalisch-chemische Tabellen by H. Landolt and R. Börnstein of which the 6th ed. began publication in 1950 under title: Zahlenwerte und Funktionen aus Physik, Chemie, Astronomie, Geophysik und Technik.
Vols. published after v. 1 of group I have imprint: Berlin, New York, Springer-Verlag
Includes bibliographies.
1. Physics--Tables. 2. Chemistry--Tables. 3. Engineering--Tables.
I. Börnstein, R. (Richard), 1852-1913. II. Landolt, H. (Hans), 1831-1910.
III. Physikalisch-chemische Tabellen. IV. Title: Numerical data and functional relationships in science and technology.
QC61.23 502'.12 62-53136

Printed in Germany

Cover layout: Erich Kirchner, Heidelberg
Typesetting: Redaktion Landolt-Börnstein, Darmstadt
Printing: Computer to plate, Mercedes-Druck, Berlin
Binding: Lüderitz & Bauer, Berlin

SPIN: 1054 7143 63/3020 - 5 4 3 2 1 0 – Printed on acid-free paper

Editor

Y. Itikawa
Institute of Space and Astronautical Science,
3-1-1 Yoshinodai, Sagamihara, Kanagawa 229-8510, Japan
e-mail: itikawa@pub.isas.ac.jp

Contributers

S.J. Buckman
Research School of Physical Sciences,
Australian National University,
Canberra, ACT 0200, Australia
e-mail: stephen.buckman@anu.edu.au
Electron collisions with atoms

John W. Cooper
Institute for Physical Science and Technology,
University of Maryland,
College Park, MD 20742, USA
e-mail: jc153@umail.umd.edu
Photon interactions with atoms

M.T. Elford
Research School of Physical Sciences,
Australian National University,
Canberra, ACT 0200, Australia
e-mail: mte107@rsphysse.anu.edu.au
Electron collisions with atoms

M. Inokuti
Physics Division, Argonne National Laboratory,
9700 South Cass Avenue,
Argonne, IL 60439-4843, USA
e-mail: inokuti@anl.gov
Electron collisions with atoms

Y. Itikawa
Institute of Space and Astronautical Science,
3-1-1 Yoshinodai, Sagamihara,
Kanagawa 229-8510, Japan
e-mail: itikawa@pub.isas.ac.jp
General introduction

H. Tawara
National Institute for Fusion Science,
Toki 509-5292, Japan
e-mail: tawara@nifs.ac.jp

Physics Department, Kansas State University,
Manhattan, Kansas 66506-2601, USA
e-mail: tawara@phys.ksu.edu
Electron collisions with atoms

Landolt-Börnstein

Editorial Office
Gagernstr. 8, D-64283 Darmstadt,
Germany
fax: +49 (6151) 171760
e-mail: lb@springer.de

Internet
http://www.springer.de/newmedia/laboe/lbhome.htm

Preface

Interactions of photons and electrons with atoms, molecules, and ions are fundamental elementary processes in a wide variety of neutral or ionized gases in nature or laboratory. The data on the cross sections or related quantities for those processes are eagerly needed in many fields of application such as astrophysics, atmospheric science, plasma science, radiation physics and chemistry, etc. They are also important in understanding physical or chemical properties of atoms, molecules, and their ions.

Volume I/17 provides cross section data and related quantitative information on the collisions of (*1*) photons with atoms, (*2*) electrons with atoms, and (*3*) electrons with atomic ions. In particular subvolume A of volume I/17 deals with the interactions of photons and electrons with neutral atoms. The scope and the outline of the contents are given in the General Introduction. With the continuing development of experimental technique, as well as with the increasing demands from the application fields, the relevant data are constantly produced. The present volume includes the data available as of early summer of 1999.

I thank all the authors for their enormous efforts to survey uncounted number of publications and to critically compile data from them to be assembled in this volume.

Sagamihara, March 2000 **The Editor**

General introduction

Motivations for and objectives of the present volume

Atomic and molecular collision processes have played a fundamental role in the development of quantum mechanics since its early stage. Through the collision processes, many new phenomena of importance in atomic and molecular physics have been revealed. Atomic and molecular collisions are elementary processes in various application fields such as astrophysics, environmental science, plasma physics, gaseous electronics and radiation science. Thus the knowledge of atomic and molecular collision processes is of essential significance both in the atomic and molecular physics and in those application fields.

The Landolt-Börnstein published a volume on atoms and ions in 1950. It includes cross section data for a number of collision processes involving electrons, atoms and molecules. Since then the field of atomic and molecular physics has been expanded greatly. With the development of experimental techniques (e.g., an achievement of high quality vacuum, precise electromagnetic control of colliding particles, laser technology for preparation and detection of relevant states of target particles, accelerator-based facilities like synchrotron radiation source and ion storage ring) many detailed and accurate data on collision processes have been produced. An increasing capability of computer has enabled sophisticated, as well as large-scale, calculations. Results of those calculations are of significance in understanding and evaluating experimental data. If the theoretical values are sufficiently accurate, they can supplement the experimental data when the latter are difficult to obtain. Atomic and molecular collision processes are now applied to much wider fields than in 1950. Opening of new fields such as space research and nuclear fusion science has widened the requirement of collision data. A recent application of low-temperature plasmas to industry has created another demand of collision data on a large scale. Considering these situations, it is clearly needed to construct a new comprehensive data base on the collision processes.

The present volume of the Landolt-Börnstein new series is the first attempt of the new comprehensive data compilation on atomic and molecular collisions. It is concerned with the interaction of photons and electrons with atoms, molecules and their ions. This category of collision processes is rather simple, because one of the collision partners is restricted to a photon or an electron. The other partner of the collision (i.e., atoms, molecules, or their ions) , however, may be of a wide variety so that any comprehensive data compilation is still difficult. In principle the present volume is intended to include the relevant collision data for all the atomic and molecular species. In reality, however, reliable data are available only for a limited number of species. This volume presents all of those reliable data. Sometimes collision data are needed for other atoms or molecules than those presented here. In

such cases it is helpful to resort to some simple calculation or empirical formulas. Information about those approximate methods of obtaining data is provided also in the present volume.

Finally it should be noted that the style of the presentation of numerical data is not uniform over the subchapters in the volume. This reflects the present stage of experimental or theoretical studies of the respective collision process. Each author has expended his effort to present the best available data as far as possible. Each subchapter starts with a rather extensive introduction to show the state of the subfield and availability of the respective data.

Outline of the volume

The present volume deals with the following collision processes

i) interaction of photons with atoms
ii) interaction of photons with molecules
iii) electron collisions with atoms
iv) electron collisions with atomic ions
v) electron collisions with molecules

When photons interact with a free atom, they are either scattered or absorbed. The scattering process occurs with (inelastic) or without (elastic) absorption of a part of the incident photon energy. Following the photoabsorption, the atom is excited to a discrete state (i.e., excited state) or a continuum. The latter process (i.e., photoionization) results in an atomic ion and one or more free electrons. The data on photoionization and photon scattering in a photon interaction with neutral atoms are presented in Chapter 1. In some experiments for photoionization, the quantity actually measured is a degree of attenuation of incident photons in an atomic gas. There is, however, no significant difference between the photoattenuation cross section and the photoionization one, unless the photon energy is very high (say, larger than 10 keV). No discrete excitation (i.e., bound-bound transition) is covered by this volume. Those data (i.e., atomic transition probability) can be found in other data bases.

Photon interaction with molecules is very similar to that with atoms, except for the process resulting in a dissociation of the molecule. In Chapter 6, cross section data are presented for the photoionization and photodissociation for a number representative molecules.

Photon interaction with atomic (positive) ions has a special situation. It is a general subject but has been studied much less extensively than for neutral atoms. Experiment is very difficult to do. Usually photon interaction with ions is so weak that we need high density of target ions and powerful light source. It is very difficult, however, to prepare ion targets of sufficient density. Though a small number of experimental results are available for singly charged ions, we have virtually no

experimental data for multi-charged ions. There are theoretical calculations of the photoionization cross section for light ions, particularly for the ions of astrophysical interest. The resulting values, however, have not been confirmed experimentally. For these reasons, no data on the photoionization of ions are included in this volume.

When an electron collides with atoms, elastic and inelastic processes occur. The latter includes excitation and ionization of atoms. Besides the cross sections for these processes, there are two physically important category of cross sections: total scattering cross section and momentum transfer cross section. The total scattering cross section is the sum of the cross sections for all the (elastic and inelastic) processes. It serves as an upper bound of any cross section for the respective atom. The momentum transfer cross section represents the degree of momentum transfer during the collision. It plays a fundamental role in the study of electron transport in a gas. Chapter 2 deals with the cross section data for all the processes in the electron-atom collision: elastic scattering, excitation, ionization, total scattering and momentum transfer.

An electron collision with atomic ions has been studied extensively in recent decades. In some cases the features of electron-ion collision are similar to those of electron-atom collision, but in other cases (particularly in the cases involving highly charged ions) they are very different. In the electron-ion collision, elastic scattering results in a divergent cross section in the forward direction (i.e., the Rutherford scattering). Only the inelastic processes (i.e., excitation and ionization) have a physical significance. One particular process relevant to the electron-ion collision is recombination of ions. In this process, one electron attaches to the target ion to reduce its charge by one. Electron-impact excitation and ionization of atomic ions and electron-ion recombination are dealt with in Chapter 3.

Electron-molecule collision is very similar to the electron-atom collision described above. Only exception in the former system is a dissociation process. This process looks simple, but it is difficult to reach a comprehensive understanding of the process. Dissociation results in many kinds of products: atoms, molecules (often radicals), and (positive and negative) ions. Another complicated feature of the molecule is its nuclear motion. Electron collision induces an excitation of rotational and vibrational motions of the molecule. A further difficulty in the data compilation for molecules is the number of the target molecules. There is no limit for the number. In conclusion, it is more difficult to make a comprehensive compilation of electron-molecule collision than in the case of electron-atom collisions. Chapters 5 and 6 cover all the collision processes between electrons and molecules, but for a limited number of target molecules.

1 Photon interactions with atoms

1.1 Introduction

When a photon collides with an atom in its free state a number of things can happen. The photon may be absorbed and the atom left in an excited state or one or more atomic electrons may be removed and the atom becomes a singly or multiply charged ion. Alternatively, the photon may be scattered elastically without loss of energy or inelastically with subsequent excitation or single or multiple ionization of the atom. These processes are of fundamental importance for a wide variety of applications since the interactions of photons with atomic systems forms the basis of our understanding of the interaction of radiation with matter in general. It is the aim of this chapter to present a large subset of the basic experimental data on these processes.

Since photons can have energies (or wavelengths) over a broad range and the number of experiments which have been performed by alternative techniques to study these processes is large, there must be limits placed on the data presented. The criteria used to define the data presented are given below.

A. The data presented will be experimental data for ionization or scattering from free atoms only. This is an important limitation since at X-ray energies matter often behaves as if it were a collection of free atoms. However, one never can be sure that molecular or solid state effects may be neglected.

B. Photon absorption without ionization will not be considered. Basically, this is the subject of atomic spectroscopy and detailed tabulations of the wavelengths of spectral lines and of the probabilities of transitions between various atomic levels are available elsewhere [58Mo1, 69We1].

C. For photoionization, the data presented will be limited to the range of incident photon energies from the threshold for ionization (between 5 and 30 eV for neutral atoms) to 10 keV.

D. Although there have been a number of sophisticated theoretical calculations of photoionization and of elastic and inelastic photon scattering, with some exceptions, no data based on computed cross sections will be given.

E. Processes in which two or more photons interact simultaneously with a single atom will not be considered.

With the above criteria in mind, the data presented is arranged in three sections. Section 1.2 is concerned with total ionization cross sections for free atoms in their ground states in the energy range from threshold to 10 keV. The material is arranged in the following way. First, a brief discussion of the experimental techniques used in obtaining the data presented. Next, data are given for atomic hydrogen, for which few experiments have been done but theory is expected to be accurate. This is followed by data on the rare gases which, since they exist in free form comprise the bulk of the experimental data on free atoms. This is followed by data on the atmospheric gases oxygen and nitrogen, by data on the easily vaporized alkalis and finally by data on other atoms for which measurements have been made.

For all of the above elements there exists a large body of relative cross section measurements. These are not presented unless they can with reasonable certainty be normalized via other absolute measurements.

The data presented in Section 1.2 omits those energy ranges where autoionization or Auger processes occur which result in rapidly varying resonant cross sections. Such processes as well as simultaneous ionization and excitation and direct double ionization have been studied by a variety of experimental techniques and the data obtained is presented in Section 1.3. As in Section 1.2, there is a brief discussion of the experimental techniques used. The section also contains some data on the branching ratios; i.e., the ratios of alternative final states of the rest of the atom when a single electron is emitted and on the angular distribution of emitted electrons.

Finally, Section 1.4 is devoted to the experimental data on elastic and inelastic scattering. Here the energy range has been expanded and some data are given at high energies which was obtained from atoms not in their free state.

A number of alternative sources of the data presented here are available either in printed form or via on-line computer access. In general, these sources are intended for a particular application, are based either entirely or in part on theoretical calculations and often include data obtained via measurements on molecular gases or solids. Alternative sources of data including a brief description of each are listed in an appendix.

1.2 Total photoionization cross sections

1.2.1 Measurement techniques

If we assume that the photon source is weak enough so that only single photon-atom processes are possible and further that the energy of the photon beam is low enough that scattering may be neglected, but monochromatic with an energy above the first atomic ionization potential, then the cross section for total ionization may be obtained simply by measuring the attenuation of the photon beam as it passes through a gas of atoms. The cross section for total ionization in this case is given simply by Beer's law:

$$\sigma = \ln(I_o/I)/nl$$

Here I_o and I are the initial and final fluxes of the photon beam, l the length of path the beam passes through and n the gas density. If l is measured in cm and n is in atoms/cm^3 the cross section will be in units of cm^2. The units commonly used for photoionization cross sections are 10^{-18} cm^2 (megabarns), 10^{-21} cm^2 (kilobarns) and 10^{-24} cm^2 (barns). All of these units will be used here. Experimental data are sometimes expressed in units of reciprocal path length $k = n\sigma$ (cm^{-1}). When this is the case the results will be converted to cross sections using known density (n) values.

Alternatively, assuming again a monochromatic photon beam of known intensity, the photoionization cross section may be obtained by measuring the number and charge of the ions produced by absorption in a given path length or by measuring the number and energy of electrons. These methods have the added advantage that they allow one to separate single from double or multiple ionization and also make it possible to obtain cross sections differential in the direction and/or energy of the ejected electrons.

By far the bulk of the data on photoionization cross sections in this section has been obtained via straightforward photon attenuation measurements as described above. When this is not the case; i.e., when the data were obtained via collection of ions or electrons this will be noted.

The measurements reported in this section refer only to those energy ranges where the photoionization cross sections are expected to be slowly varying as a function of energy and hence

the energy distribution of the photon source (linewidth for discrete sources or spectral resolution for continuous sources such as synchrotron radiation using a monochromator) is relatively unimportant. However, some information on the experimental arrangement used will be given in some cases.

In a large part of the earlier literature which used photon line sources wavelengths rather than photon energies are reported. Although these measurements have the disadvantage of only being available at sometimes widely spaced energies, they have proven to be remarkably consistent since there is good agreement between experiments by different investigators. Most of the data obtained in the last several decades were obtained using synchrotron light sources which although they have the advantage of being continuous sources over a broad energy range require careful measurements to account for the detection of light not at the wavelength of the measurement.

Often, data are reported as a function of wavelength rather than of energy. When this is the case wavelengths have been converted to electron volts using the formula:

$$E\ (\text{eV}) = 1.2398 \cdot 10^{-4}/\lambda\ (\text{cm})$$

1.2.2 Cross sections for atomic hydrogen

In the energy range between the ionization threshold (13.598 eV) and 10 keV the cross section for atomic hydrogen can be calculated to high accuracy for the following reasons. Hydrogen is an atom with a single electron moving in a known central field. Thus the ground electronic state of the atom is known analytically as are the final continuum states corresponding to photoionization. This makes it possible to calculate the cross section accurately either by evaluating analytical formulas or by direct numerical solution of a one electron Schrodinger equation.

In Table 1 the calculated cross section for atomic hydrogen is shown over the range from threshold to 10 keV. The data in the range below 100 eV has been obtained by evaluating a simple formula for the cross section within dipole approximation [57Be1], and that at higher energies taken from the tabulations of Veigele [73Ve1] and Scofield [73Sc1].The calculated values are expected to be accurate to better than 1 %.

Although the photoionization cross section of atomic hydrogen can be calculated with high accuracy, measurements are difficult and serve only to provide a check on the theoretical results. The measurements are difficult since molecular hydrogen must be dissociated and some assumptions made concerning the relative absorption of molecular hydrogen since dissociation is incomplete. Absolute measurements of the cross section have been made at three energies near threshold [65Be1, 66Be2] and the results are compared with the theoretical results in Table 2. The agreement is good only at the lowest energy. The most definitive measurement for hydrogen was made by Palenius et al. [76Pa1] using a shock tube which resulted in almost 100 % dissociation of H_2. Their results extended from threshold to 20.36 eV and are also compared with theory in Table 2.

Although it is extremely difficult to measure the atomic hydrogen photoionization cross section measurements of molecular hydrogen are relatively simple to perform and a number of them have been performed. Tabulations of data of cross sections often use measurements on molecular gases or solids to infer cross sections for individual atoms assuming that molecular binding or solid state effects do not affect the cross sections. While this may be a good approximation at moderately high photon energies for some substances it is not for molecular hydrogen [74Co1].

Table 1. Cross sections for photoionization of atomic hydrogen as obtained from the formula described in the text and from the numerical calculations of Veigele and Scofield.

Energy [eV]	Cross section [10^{-21} cm^2]		
	Formula	73Ve1	73Sc1
1.360E+01 (I.P.)	6.303E+03		
2.000E+01	2.212E+03		
4.000E+01	3.059E+02		
6.000E+01	9.178E+01		
8.000E+01	3.838E+01		
1.000E+02	1.933E+01	1.93E+01	
2.000E+02	2.195E+00	2.20E+00	
4.000E+02	2.348E–01	2.32E–01	
6.000E+02	6.208E–02	6.15E–02	
8.000E+02	2.394E–02	2.36E–02	
1.000E+03	1.139E–02	1.12E–02	1.141E–02
2.000E+03		1.10E–03	1.111E–03
4.000E+03		1.05E–04	1.053E–04
6.000E+03		2.63E–05	2.627E–05
8.000E+03		9.79E–06	9.816E–06
1.000E+04		4.55E–06	4.558E–06

Table 2. Photoionization cross sections for atomic hydrogen as measured in [1]) [65Be1], [2]) [66Be2] and [76Pa1] and as computed by the analytic formula discussed in the text.

Energy [eV]	Cross section [10^{-18} cm^2]		Energy [eV]	Cross section [10^{-18} cm^2]	
	Measured	Formula		Measured	Formula
13.62	6.25	6.28	15.34	4.40	4.57
13.73	6.16	6.15	15.96	4.09	4.11
14.01	5.62	5.83	16.49	3.89	3.75
14.22	5.98	5.60	17.41	3.93	3.23
14.38	4.85	5.43	17.94	3.22	2.98
14.57	5.15 ± 0.18 [1])	5.25	18.70	2.99	2.63
14.59	4.83	5.24	19.10	2.82	2.51
14.70	2.90 ± 0.50 [2])	5.12	19.49	2.81	2.37
14.79	4.60	5.04	19.90	2.57	2.24
15.00	3.80 ± 0.80 [2])	4.85	20.36	2.23	2.11
15.08	4.19	4.78			

1.2.3 Cross sections for helium

Unlike hydrogen, exact calculations for helium cannot be made although much theoretical effort has been expended on such calculations and there is relatively good agreement with measurements. In contrast to hydrogen, measurements (at least at low energies) are fairly straightforward and the accuracy of the measurements is believed to be of the order of 1…2 %.

Since helium, unlike hydrogen is a two electron system, double as well as single ionization is possible at photon energies above the second ionization potential (79 eV) and measurements indicate that double ionization is of the order of 1…2 % of the total. All of the data reported here is for total ionization although there have been a number of measurements for the ratio of double to single ionization which will be discussed in Section 1.3.

The cross sections for photoionization are expected to be relatively smooth functions of photon energy except in the energy range below the double ionization threshold (79 eV) and extending to a region about 1 eV below the lowest energy resonance at 60.12 eV. For this reason data here is given only for the energy range below 59 eV and above 79 eV. Data in the resonance region will be reported in Section 1.3.

At energies above (1 keV for helium, measurements of the removal of photons from a beam cannot be used to infer photoionization cross sections since photon scattering becomes important. In the energy range considered here (the ionization threshold to 10 keV) helium is the only atom for which data is available in which scattering becomes important. In order to indicate the importance of scattering for helium, the percentage of the total attenuation cross section estimated [73Ve1] to be due to photoionization is shown in Table 3.

There have been a number of critical reviews of photoionization cross sections (or alternatively attenuation cross sections) for both helium and the other rare gases and they will be briefly described here. Samson [66Sa1] provided a set of data for all of the rare gases based on new measurements and existing theoretical and experimental data. Somewhat later Henke, as part of broader study of attenuation coefficients in materials included the rare gases helium, neon and argon [82He1].

West and Marr [76We1] gave a set of cross sections for helium, neon, argon and krypton based on new measurements by them between 36 and 310 eV and a review of earlier work and tables of their results were published [76Ma1]. Samson et al. [94Sa1] have recently made new measurements of helium from threshold to 120 eV and have provided a recommended set of data up to energies of 10 keV. Samson et al. [91Sa1] have also provided a new set of recommended values for the other rare gases based on highly accurate measurements made at low energies [89Sa1]. Finally Cooper [96Co1] has reviewed both the theoretical and experimental evidence on both photoionization and scattering cross sections for helium.

In the energy range below the autoionization region there is good agreement between the recent work of Samson et al. [94Sa1] and the earlier tabulation of Marr and West [76Ma1] as shown in Table 4 (the numbers shown for Marr and West were obtained from the published results via linear interpolation). The work of Samson et al. is based on new measurements whereas the work of Marr and West is based on a critical review of all of the measurements available to them at the time. Note that all of the results shown in Table 4 agree to within 3 %.

In the energy range between 80 and 300 eV there appears to be good agreement between the measurements of a number of investigators. Fig. 1 shows a comparison of the measurements of Henke [67He1], Denne [70De1], Watson [72Wa1] and an earlier measurement at 278 eV [31De1] with the recommended values of Samson et al. [94Sa1] Earlier measurements as well as those reported by Marr and West [76Ma1] appear to be somewhat higher than those shown.

In Table 5 the recommended values of Samson are given at 10 eV intervals in the energy range from 80 to 280 eV. Since the cross section is smoothly varying in this energy range this spacing should be adequate for interpolation. The expected accuracy of the data is better than 3 % for these data at energies below 150 eV and of the order of 5 % at higher energies.

Between 280 eV and 2.95 keV there are no measurements with the exception of a single measurement by Denne [70De1] at 523 eV. The quoted value $1.8 \cdot 10^{-21}$ cm^2 is so much lower than

any reasonable extrapolation to higher energies that it must be discounted. Table 6 gives a theoretical estimate of the photoionization cross section in this range based on the calculations of Railman and Manson [79Re1] and Scofield [73Sc1].

In the 1…10 keV range there are two measurements of photon attenuation, an old but careful measurement by Bearden [66Be1] and a recent measurement by Azuma et al. [95Az1]. Bearden's measurements were done with line sources at definite energies. His data which is only given to 2 place accuracy is shown in Table 7 and compared with the linearly interpolated values obtained from the work of Azuma et al. The results appear to agree to better than 10 %. Finally, a complete set of results of photon attenuation obtained by Azuma et al. is shown in Table 8. These authors have attempted to estimate the photoionization cross sections by subtracting theoretical scattering cross sections from their data but here only the total attenuation cross section is given. An estimate of the photoionization cross section may be obtained using the ratios given in Table 3.

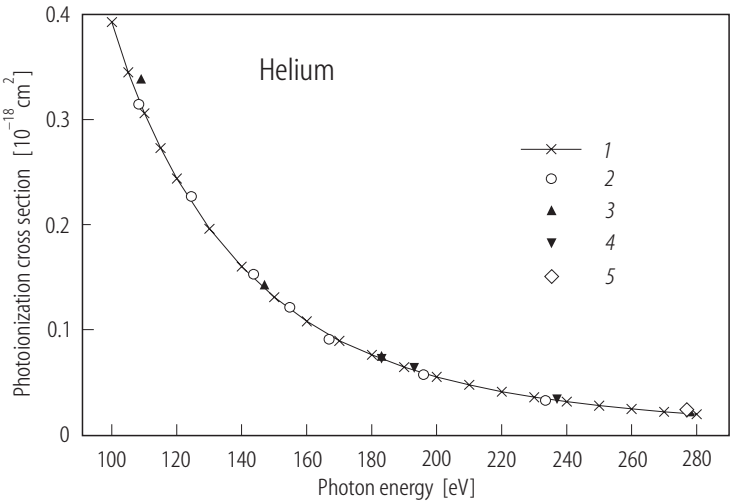

Fig. 1. Helium cross sections from 100 to 280 eV from various sources: *1* [94Sa1], *2* [72Wa1], *3* [67He1], *4* [70De1], *5* [31De1].

Table 3. Percentage of total attenuation due to photoionization for helium and neon for incident energies between 1 and 15 keV [73Ve1].

Energy [keV]	Helium [%]	Neon [%]
1.0	100	100
1.5	98	100
2.0	95	100
3.0	83	100
4.0	68	100
5.0	52	99
6.0	38	98
8.0	21	97
10.0	11	95
15.0	3	89

Table 4. A comparison of the cross sections for helium between threshold (24.59 eV) and 55 eV from [76Ma1] and [94Sa1].

Energy [eV]	Cross section [10^{-18} cm^2]	
	94Sa1	76Ma1
24.58	7.40	7.52
25.0	7.21	7.36
30.0	5.38	5.29
35.0	4.09	3.98
40.0	3.16	3.08
45.0	2.48	2.45
50.0	2.02	1.99
55.0	1.67	1.64

Table 5. Photoionization cross sections of helium at energies between 80 and 280 eV from [94Sa1].

Energy [eV]	Cross section [10^{-21} cm^2]
80.0	693.0
90.0	516.0
100.0	393.0
110.0	306.0
120.0	244.0
130.0	196.0
140.0	160.0
150.0	131.0
160.0	108.0
170.0	89.4
180.0	76.0
190.0	64.3
200.0	55.0
210.0	47.4
220.0	40.9
230.0	35.6
240.0	31.5
250.0	27.7
260.0	24.5
270.0	21.8
280.0	19.4

Table 6. Theoretical photoionization Cross sections of helium at energies between 300 eV and 3000 eV. From [73Sc1] and [79Re1].

Energy [eV]	Cross section [10^{-21} cm^2]
300.0	17.6000
450.0	5.1900
600.0	2.1000
750.0	1.0300
1000.0	0.4020
1500.0	0.1090
2000.0	0.0432
2500.0	0.0207
3000.0	0.0112

Table 7. A comparison of the measured photon attenuation cross sections of helium by Beardon [66Be1] and Azuma et al. [95Az1]. *) from [70Mc1].

Energy [keV]	Cross section [10^{-24} cm^2]		Ratio
	66Be1	95Az1	
2.98	13.3		
3.44	8.8	8.96	0.99
4.51	4.6	4.78	0.95
5.41	3.3	3.09	1.06
5.89 *)	2.8	2.66	1.04
6.40	2.3	2.44	0.94
8.15	1.9	1.82	1.04

Table 8. Measured photo attenuation cross sections of helium at energies between 3.35 and 14.0 keV from [95Az1].

Energy [keV]	Cross section [10^{-24} cm^2]
3.35	9.75
3.55	8.07
3.75	6.93
3.95	6.05
4.15	5.26
4.35	4.66
4.55	4.16
4.75	3.79
4.95	3.55
5.15	3.30
5.35	3.11
5.50	3.07
5.55	2.93
6.00	2.57
6.50	2.41
7.00	2.14
8.00	1.84
9.00	1.70
10.00	1.61
11.00	1.56
12.00	1.48
13.00	1.47
14.00	1.41

1.2.4 Cross sections for neon (Z = 10)

The experimental situation for measurements of total ionization cross sections for neon is similar to that of helium and the other rare gases. Recommended values have been given by Henke et al. [70He1], Samson [66Sa1] and Marr and West [76Ma1] based on critical reviews of the available experimental and theoretical evidence. In addition, Samson has provided an updated version of neon data based upon more recent unpublished data [91Sa1].

As in all elements there are energy ranges where resonances are expected to occur and the photoionization cross section shows rapid variations. In neon these ranges are (a) the narrow range between the two lowest states of the neon ion core (21.56…21.66 eV), (b), the range immediately below the ionization threshold for 2s electrons (L_1 edge) from 45 to 50 eV and (c), the range about the 1s ionization threshold (K edge) at 870 eV. Data in these ranges will be given in Section 1.3.

In the region below the second resonant range (threshold to 45 eV) there is good agreement between the new values of Samson and the recommended values of Marr and West as shown in Table 9. The major difference is in the range extending to about 5 eV above threshold where the new data of Samson is ≈ 3 % higher than the values of Marr and West.

In the energy range between 40 and 280 eV the neon cross section has been measured by essentially the same experimentalists as was the case for helium. Fig. 2 shows the results obtained by Marr and West [76Ma1], Henke [67He1], Denne [70De1], Watson [72Wa1], Cole et al. [78Co1] and the new results of Samson [91Sa1]. There is good agreement between all of these measurements with the exception that the results of Marr and West appear to be somewhat larger than the other measurements in the energy range from about 80 to 180 eV. Selected data from these authors is given in Table 10.

There have been few measurements in the energy range between 280 eV and 860 eV (10 eV below the K ionization threshold). The available measurements in this range from Henke [67He1], Bearden [66Be1] and Wuilleumier [69Wu1] are shown in Table 11.

In the energy range above the K ionization threshold to 10 keV there have been a number of measurements using X-ray line sources. A summary of these measurements is given in Table 12. In addition to the measurements using line sources, Wuilleumier's measurements using a continuum source are shown in Table 13. A comparison of his data with the line source data of Table 12 is shown in Fig. 3.

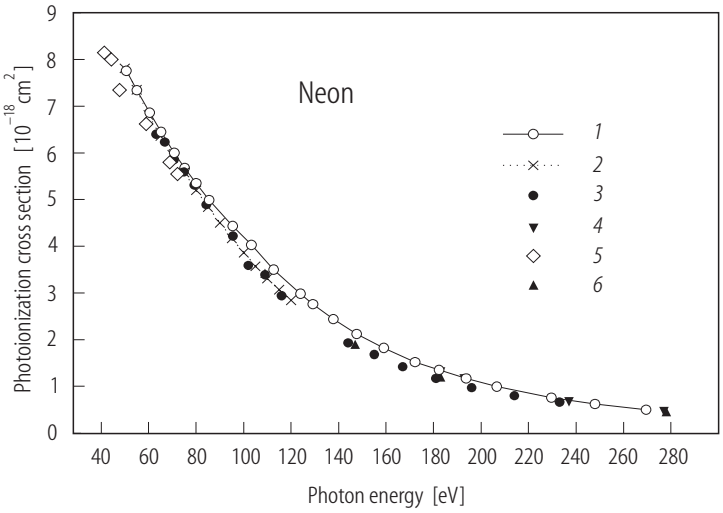

Fig. 2. Neon cross sections from 40 to 280 eV from various sources: *1* [76Ma1], *2* [91Sa1], *3* [72Wa1], *4* [70De1], *5* [78Co1], *6* [67He1].

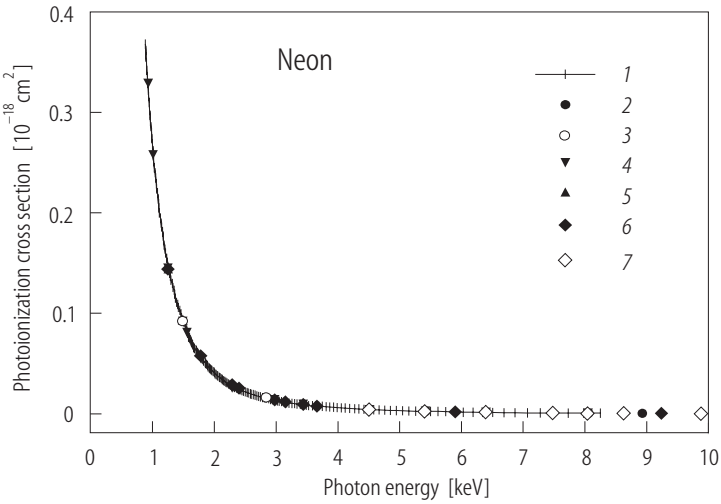

Fig. 3. Cross section for neon between 0.86 and 10 keV from various sources: *1* [69Wu1], *2* [30Co1], *3* [30Wo1], *4* [66Be1], *5* [67He1], *6* [70Mc2], *7* [74Mi1].

Overall, with the exception of the energy range from 50 to 280 eV mentioned above and the omitted resonance regions the good agreement between different experiments means that the total photoionization cross section for neon is known to an accuracy of about 3% over the entire energy range from threshold to 12 keV. Although most of the measurements were of photon attenuation rather than of the total photoionization cross section corrections for scattering are much smaller than for helium as shown in Table 3.

Table 9. Photo attenuation cross sections for neon at incident energies between 22 and 44 eV. Data from [91Sa1] and [76Ma1] (interpolated).

Energy [eV]	Cross section [10^{-18} cm^2]		Ratio
	91Sa1	76Ma1	
22.0	6.68	6.50	0.972
24.0	7.73	7.53	0.974
26.0	8.40	8.20	0.976
28.0	8.82	8.59	0.974
30.0	9.00	8.84	0.982
32.0	9.10	8.95	0.983
34.0	9.11	8.96	0.984
36.0	8.90	8.90	1.000
38.0	8.72	8.80	1.009
40.0	8.55	8.68	1.015
42.0	8.41	8.53	1.014
44.0	8.27	8.37	1.012

Table 10. Photo attenuation cross sections for neon at incident energies between 50 and 280 eV. [1]) from [72Wa1], [2]) [67He1], [3]) [70De1], [4]) [31De1].

Energy [eV]	Cross section [10^{-18} cm^2]			
	91Sa1	76Ma1	70De1	Other
50.00	7.81			
50.60		7.76		
55.00	7.35			
55.10		7.34		
60.00	6.81			
60.48		6.86		
63.10			6.40	
65.00	6.36			
65.25		6.45		
66.80			6.23	
70.00	5.96			
70.70			5.86	
70.85		6.00		
74.90			5.59	
75.00	5.58			
75.14		5.68		
79.30			5.31	
79.99		5.35		
80.00	5.20			
84.30			4.89	
85.00	4.84			
85.50		4.99		
90.00	4.50			
95.00	4.17			
95.37		4.43		
95.50			4.22	
100.00	3.86			
102.00			3.59	
103.30		4.03		
105.00	3.57			
109.00			3.39	
109.00				3.42 [1])
110.00	3.31			
112.70		3.50		
115.00	3.07			
116.00			2.94	
120.00	2.84			
124.00		2.98		
129.20		2.76		
137.80		2.44		
144.00			1.93	
147.00				1.90 [1])
147.60		2.12		
155.00			1.68	

Energy [eV]	Cross section [10^{-18} cm^2]			
	91Sa1	76Ma1	70De1	Other
159.00		1.82		
167.00			1.42	
172.20		1.52		
181.00			1.17	
182.30		1.35		
183.00				1.31 [2])
183.00				1.20 [1])
193.00				1.16 [1])
193.70		1.17		
196.00			0.968	
206.60		0.992		
214.00			0.796	
229.60		0.756		
233.00			0.662	
237.00				0.667 [2])
248.00		0.620		
269.50		0.500		
278.00				0459 [3])
278.00				0.457 [2])
278.00				0.439 [4])

Table 11. Photo attenuation cross sections for neon at incident energies between 280 and 860 eV.

Energy [eV]	Cross section [10^{-21} cm^2]	Ref.
391.0	185.0	67He1
526.0	87.1	67He1
676.0	43.9	67He1
774.0	30.1	67He1
825.0	25.9	69Wu1
830.0	25.6	69Wu1
836.0	25.3	69Wu1
842.0	24.9	69Wu1
847.0	24.7	69Wu1
852.0	25.0	66Be1
853.0	24.4	69Wu1
859.0	24.2	69Wu1

Table 12. Photo attenuation cross sections for neon at energies between 0.9 and 10 keV from various sources.

Energy [eV]	Cross section [10^{-21} cm^2]					
	30Wo1	66Be1	30Co1	67He1	70Mc2	74Mi1
930.0		329.000				
1012.0		258.000				
1254.0	144.000	145.000		144.000		
1487.0	92.160	92.300		93.000		
1557.0		81.000				
1778.0	57.880					
2293.0	25.990	25.800				
2395.0	25.570					
2838.0	16.020					
2984.0	13.940	14.100				
3151.0	11.930					
3444.0	9.350	9.450				
3662.0	7.740					
4508.0		4.360			4.190	4.243
5414.0	2.510	2.550				2.474
5420.0			2.520			
5895.0					1.910	
6404.0		1.500				1.507
7472.0						0.938
8041.0						0.750
8048.0		0.737				
8631.0						0.621
8930.0			0.533			
9243.0					0.503	
9876.0						0.410

Table 13. Photo attenuation cross sections for neon at energies between 0.87 and 10 keV [69Wu1].

Energy [eV]	Cross section [10^{-24} cm^2]	Energy [eV]	Cross section [10^{-24} cm^2]	Energy [eV]	Cross section [10^{-24} cm^2]
0.871E+03	0.387E+06	0.966E+03	0.291E+06	0.109E+04	0.214E+06
0.877E+03	0.373E+06	0.974E+03	0.286E+06	0.110E+04	0.209E+06
0.884E+03	0.368E+06	0.982E+03	0.280E+06	0.110E+04	0.205E+06
0.890E+03	0.362E+06	0.990E+03	0.274E+06	0.111E+04	0.200E+06
0.896E+03	0.355E+06	0.998E+03	0.268E+06	0.113E+04	0.195E+06
0.903E+03	0.349E+06	0.101E+04	0.262E+06	0.114E+04	0.190E+06
0.910E+03	0.342E+06	0.101E+04	0.257E+06	0.115E+04	0.186E+06
0.916E+03	0.335E+06	0.102E+04	0.251E+06	0.116E+04	0.181E+06
0.923E+03	0.329E+06	0.103E+04	0.245E+06	0.117E+04	0.177E+06
0.930E+03	0.322E+06	0.104E+04	0.240E+06	0.118E+04	0.173E+06
0.937E+03	0.316E+06	0.105E+04	0.235E+06	0.119E+04	0.168E+06
0.944E+03	0.310E+06	0.106E+04	0.229E+06	0.120E+04	0.164E+06
0.952E+03	0.303E+06	0.107E+04	0.224E+06	0.121E+04	0.160E+06
0.959E+03	0.297E+06	0.108E+04	0.220E+06	0.123E+04	0.155E+06

Energy [eV]	Cross section [10^{-24} cm^2]	Energy [eV]	Cross section [10^{-24} cm^2]	Energy [eV]	Cross section [10^{-24} cm^2]
0.124E+04	0.151E+06	0.192E+04	0.456E+05	0.317E+04	0.113E+05
0.125E+04	0.147E+06	0.193E+04	0.448E+05	0.321E+04	0.107E+05
0.126E+04	0.144E+06	0.195E+04	0.440E+05	0.326E+04	0.104E+05
0.128E+04	0.140E+06	0.196E+04	0.431E+05	0.330E+04	0.101E+05
0.129E+04	0.137E+06	0.198E+04	0.422E+05	0.334E+04	0.985E+04
0.130E+04	0.133E+06	0.200E+04	0.414E+05	0.339E+04	0.948E+04
0.132E+04	0.130E+06	0.201E+04	0.399E+05	0.344E+04	0.905E+04
0.133E+04	0.126E+06	0.203E+04	0.391E+05	0.349E+04	0.865E+04
0.135E+04	0.123E+06	0.205E+04	0.381E+05	0.353E+04	0.838E+04
0.136E+04	0.119E+06	0.206E+04	0.375E+05	0.359E+04	0.814E+04
0.137E+04	0.115E+06	0.208E+04	0.365E+05	0.364E+04	0.791E+04
0.139E+04	0.111E+06	0.210E+04	0.359E+05	0.369E+04	0.771E+04
0.141E+04	0.109E+06	0.212E+04	0.349E+05	0.375E+04	0.747E+04
0.142E+04	0.106E+06	0.213E+04	0.340E+05	0.381E+04	0.710E+04
0.144E+04	0.103E+06	0.215E+04	0.331E+05	0.387E+04	0.684E+04
0.146E+04	0.995E+05	0.217E+04	0.324E+05	0.393E+04	0.654E+04
0.147E+04	0.952E+05	0.219E+04	0.315E+05	0.399E+04	0.623E+04
0.149E+04	0.937E+05	0.221E+04	0.308E+05	0.406E+04	0.603E+04
0.151E+04	0.910E+05	0.223E+04	0.297E+05	0.412E+04	0.570E+04
0.153E+04	0.878E+05	0.225E+04	0.291E+05	0.419E+04	0.540E+04
0.155E+04	0.848E+05	0.227E+04	0.285E+05	0.427E+04	0.509E+04
0.156E+04	0.823E+05	0.229E+04	0.278E+05	0.434E+04	0.486E+04
0.157E+04	0.802E+05	0.231E+04	0.271E+05	0.442E+04	0.456E+04
0.158E+04	0.765E+05	0.233E+04	0.264E+05	0.450E+04	0.426E+04
0.159E+04	0.761E+05	0.236E+04	0.257E+05	0.458E+04	0.402E+04
0.160E+04	0.755E+05	0.238E+04	0.253E+05	0.467E+04	0.382E+04
0.161E+04	0.740E+05	0.240E+04	0.245E+05	0.476E+04	0.362E+04
0.162E+04	0.727E+05	0.243E+04	0.239E+05	0.485E+04	0.342E+04
0.163E+04	0.713E+05	0.245E+04	0.231E+05	0.495E+04	0.323E+04
0.164E+04	0.700E+05	0.247E+04	0.226E+05	0.505E+04	0.307E+04
0.165E+04	0.687E+05	0.250E+04	0.220E+05	0.515E+04	0.286E+04
0.166E+04	0.667E+05	0.253E+04	0.214E+05	0.526E+04	0.272E+04
0.167E+04	0.659E+05	0.255E+04	0.206E+05	0.538E+04	0.267E+04
0.168E+04	0.650E+05	0.258E+04	0.201E+05	0.550E+04	0.250E+04
0.170E+04	0.639E+05	0.260E+04	0.195E+05	0.562E+04	0.234E+04
0.171E+04	0.627E+05	0.263E+04	0.192E+05	0.575E+04	0.212E+04
0.172E+04	0.618E+05	0.266E+04	0.185E+05	0.589E+04	0.194E+04
0.173E+04	0.609E+05	0.269E+04	0.180E+05	0.603E+04	0.165E+04
0.174E+04	0.597E+05	0.272E+04	0.174E+05	0.619E+04	0.152E+04
0.176E+04	0.582E+05	0.275E+04	0.170E+05	0.634E+04	0.143E+04
0.177E+04	0.574E+05	0.278E+04	0.163E+05	0.651E+04	0.132E+04
0.178E+04	0.560E+05	0.281E+04	0.159E+05	0.669E+04	0.121E+04
0.179E+04	0.551E+05	0.284E+04	0.154E+05	0.687E+04	0.112E+04
0.181E+04	0.542E+05	0.288E+04	0.150E+05	0.707E+04	0.104E+04
0.182E+04	0.533E+05	0.291E+04	0.144E+05	0.728E+04	0.948E+03
0.183E+04	0.524E+05	0.295E+04	0.140E+05	0.750E+04	0.868E+03
0.185E+04	0.512E+05	0.298E+04	0.134E+05	0.773E+04	0.791E+03
0.186E+04	0.502E+05	0.302E+04	0.129E+05	0.798E+04	0.717E+03
0.187E+04	0.493E+05	0.305E+04	0.125E+05	0.825E+04	0.654E+03
0.189E+04	0.481E+05	0.309E+04	0.123E+05		
0.190E+04	0.467E+05	0.313E+04	0.118E+05		

1.2.5 Cross sections for argon (Z = 18)

For argon there have been a number of measurements in the energy range immediately above the first ionization potential (15.76 eV). As is the case in all of the heavier rare gases there is a resonance region between the ionization threshold and the first excited level of the ionic core (15.93 eV). Measurements in this energy range will be discussed in Section 1.3 as will the resonance regions near the inner subshell ionization potentials (26…30 eV, 245…255 eV and 3190…3220 eV).

In the energy range between 16 and 26 eV there have been a number of measurements of ionization cross sections. The recommended values of Samson [91Sa1]and the tabulation given by Marr and West [76Ma1] are given in Table 14 and are also shown in Fig. 4 along with data from Lee and Weissler [55Le1],Rustgi [64Ru1] and Carlson et al. [73Ca1]. The data of Carlson et al. was only presented in graphical form which means that a comparison to any better than 3 % is unwarranted. The figure shows that although there is good deal of scatter in the earlier data, there is essential agreement between the recommended data of Samson and the compilation of Marr and West to with about 3 %. Samson et al. [89Sa1] have made careful measurements of the rare gases with an expected accuracy of 1% at selected wavelengths. The results for argon at energies of 16.67,16.85 and 21.22 which form the basis of their recommended values are also shown in Fig. 4.

At energies above the resonance region between 30 and 100 eV the cross section drops rapidly to a minimum at approximately 48 eV and then rises to a maximum at approximately 70 eV. Data from various sources in this energy range are shown in Fig. 5. Owing to the rapid variation with energy the cross section is not known accurately to better than 10 % in this energy range. Values of the cross section obtained by various authors are shown in Table 15.

In the energy range between 100 and 240 eV data are shown in Table 16 from Marr and West [76Ma1], Lukirskii et al. [63Lu1], Watson [72Wa1], Henke [67He1] and Denne [70De1]. In general there is good agreement between the various data sets.

The available data in the energy range from 255 to 1000 eV is shown in Table 17. All of these measurements are of total attenuation and with the exception of the recent measurement by Yang et al. [87Ya1] and that of Wuilleumiur [69Wu1] were done using line sources. With the exception of a few points the agreement is better than 10 % over the entire energy range. At energies between 1 keV and the K ionization threshold the agreement between various sources is even better as is shown in Table 18. All of these measurements used line sources and all of the measurements were of total attenuation with the exception of the work of Woernle [30Wo1] who used a double ion chamber. The measurements of Wuilleumier [69Wu1] done at closely spaced energies are shown in Table 19 and are in good agreement with the line source data. The same type of data for energies above the K ionization threshold is shown in Tables 20 and 21. In general, there is agreement to better than 10 % in this energy range also.

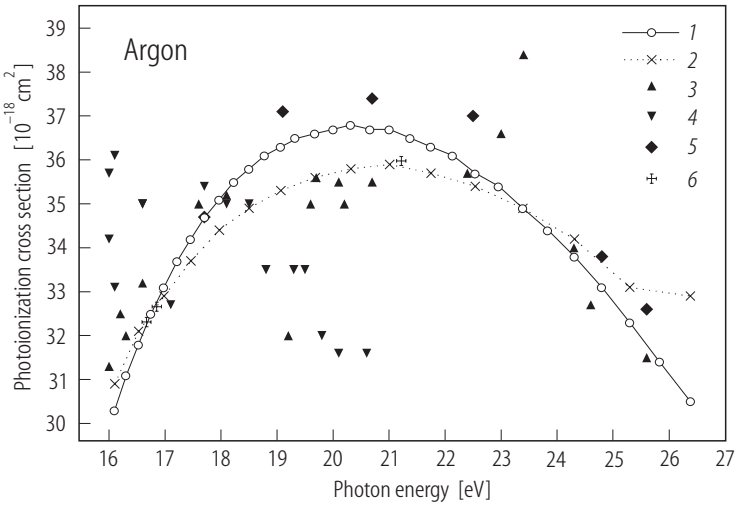

Fig. 4. Argon cross sections between 16 and 26 eV from various sources: *1* [76Ma1], *2* [91Sa1], *3* [64Ru1], *4* [55Le1], *5* [73Ca1], *6* [89Sa1].

Table 14. Photon attenuation cross sections for argon in the energy range between 16 and 26 eV.

Energy [eV]	Cross section [10^{-18} cm^2]			Energy [eV]	Cross section [10^{-18} cm^2]	
	76Ma1	91Sa1	89Sa1		76Ma1	91Sa1
16.10	30.3	30.9		19.68	36.6	35.6
16.67			32.3	20.00	36.7	35.7
16.31	31.1	31.7		20.32	36.8	35.8
16.53	31.8	32.1		20.66	36.7	35.9
16.75	32.5	32.5		21.01	36.7	35.9
16.85			32.7	21.38	36.5	35.8
16.98	33.1	32.9		21.75	36.3	35.7
17.22	33.7	33.3		22.14	36.1	35.6
17.46	34.2	33.7		22.54	35.7	35.4
17.71	34.7	34.1		22.96	35.4	35.2
17.97	35.1	34.4		23.39	34.9	34.9
18.23	35.5	34.6		23.84	34.4	34.4
18.50	35.8	34.9		24.31	33.8	34.2
18.78	36.1	35.1		24.80	33.1	33.7
19.07	36.3	35.3		25.30	32.3	33.1
19.37	36.5	35.5		25.83	31.4	32.6

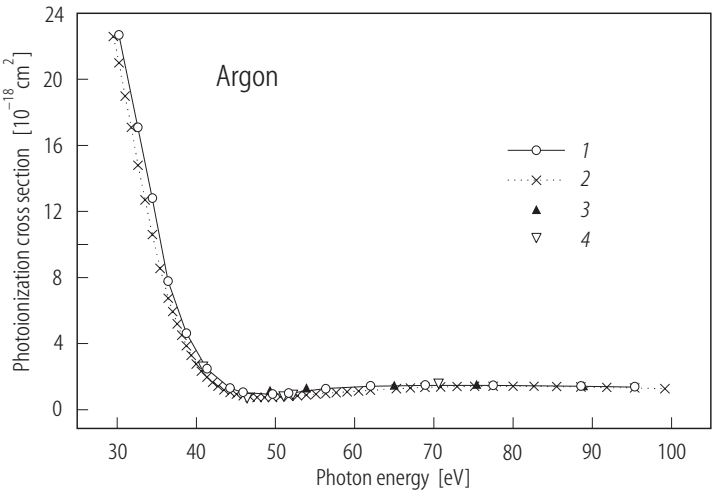

Fig. 5. Argon cross sections between 30 and 100 eV from various sources: *1* [76Ma1], *2* [63Lu1], *3* [91Sa1], *4* [64Al1].

Table 15. Photon attenuation cross sections for argon in the energy range between 30 and 100 eV.

Energy [eV]	Cross section [10^{-18} cm^2]				
	91Sa1	76Ma1	63Lu1	64Al1	72Wa1
30.24	21.0	22.7			
30.99	19.0	21.0			
31.79	17.1	19.1			
32.63	14.8	17.1			
34.44	10.6	12.8			
35.42	8.55	10.3			
36.46	6.75	7.77			
37.57	5.19	6.10			
38.15	4.51				
38.74	3.87	4.62			
39.99	2.77	3.41			
40.65	2.33				
40.80				2.6	
41.33	1.97	2.47			
42.03	1.66				
42.75	1.75	1.77			
43.50	1.20				
44.28	1.05	1.30			
45.08	0.94				
45.92	0.85	1.03			
46.40				0.7	
47.68	0.74	0.914			
48.62	0.74				
49.30			1.18		
49.59	0.75	0.916			
50.60	0.78				
51.00				0.8	
51.66	0.81	1.00			

Energy [eV]	Cross section [10^{-18} cm^2]				
	91Sa1	76Ma1	63Lu1	64Al1	72Wa1
52.20				0.9	
52.76	0.85				
53.90	0.89		1.32		
55.10	0.94				
56.35	0.99	1.28			
60.48	1.13				
61.99	1.18	1.42			
63.10					1.26
65.00			1.49		
65.25	1.27				
66.80					1.33
67.02	1.31				
68.88	1.35		1.48		
70.60				1.57	
70.70					1.38
70.85	1.38				
72.93	1.40				
74.90					1.40
75.14	1.41				
75.40			1.54		
77.49	1.42	1.47			
79.30					1.44
79.99	1.42				
82.65	1.41				
84.30					1.41
85.50	1.40				
85.56	1.38	1.41			
88.90			1.45		
91.84	1.35				
95.37	1.32	1.36			
95.50					1.33
99.18	1.28				

Table 16. Photon attenuation cross sections for argon in the energy range from 100 to 240 eV.

Energy [eV]	Cross section [10^{-18} cm^2]				
	72Wa1	63Lu1	67He1	70De1	76Ma1
101.7	1.262				
103.3					1.29
108.6	1.202				
108.9			1.293		
112.7					1.20
114.3		1.166			
116.3	1.105				

Energy [eV]	Cross section [10^{-18} cm^2]				
	72Wa1	63Lu1	67He1	70De1	76Ma1
124.0					1.10
124.5	1.049				
128.0	1.012				
130.5					1.05
133.5	0.938				
137.8					0.987
143.5	0.863				
145.9					0.923
147.2			0.842		
151.0				0.781	
151.2		0.736			
154.9	0.737				
155.0					0.856
165.3					0.785
166.9	0.666				
171.0		0.598			
171.7				0.660	
172.5	0.625				
177.1					0.709
180.8	0.584				
182.6			0.608		
183.4				0.592	
190.7					0.630
192.2		0.486			
192.6				0.543	
196.2	0.521				
217.2	0.443				
234.0		0.344			
236.9				0.360	

Table 17. Photon attenuation cross sections for argon in the energy range from 255 to 1000 eV. [1]) from [31De1], [2]) from [66Be1].

Energy [eV]	Cross section [10^{-18} cm^2]				
	87Ya1	63Lu1	67He1	69Wu1	Other
256.0		3.52			
267.0		3.10			
277.0					3.03 [1])
278.0			3.03		
282.0		2.70			
354.0		2.40			
391.4			2.00		
413.0		1.65			
442.0	1.53				
477.0	1.31				

Energy [eV]	Cross section [10^{-18} cm^2]				
	87Ya1	63Lu1	67He1	69Wu1	Other
496.0		1.08			
517.0	1.12				
526.0			1.06		
539.0	1.02				
564.0	0.933				
590.0	0.830				
620.0	0.737				
620.0		0.656			
651.0	0.668				
676.8			0.593		
687.0	0.580				
728.0	0.505				
773.0	0.432				
774.9			0.424		
824.0	0.365				
826.5		0.314			
852.0					0.305 [2])
865.0				0.324	
871.0				0.318	
877.0				0.312	
883.0	0.315				
884.0				0.305	
890.0				0.301	
896.0				0.295	
903.0				0.289	
910.0				0.284	
916.0				0.278	
923.0				0.272	
928.7			0.270		
930.0				0.267	0.268 [2])
937.0				0.262	
944.0				0.256	
950.0	0.262				
952.0				0.252	
959.0				0.246	
966.0	0.240				
974.0				0.236	
982.0				0.231	
990.0				0.226	
998.0				0.221	

Table 18. Photon attenuation cross sections for argon in the energy range between 1000 and 3190 eV. *) from [31Sp1].

Energy [eV]	Cross section [10^{-21} cm^2]				
	30Wo1	63Lu1	67He1	66Be1	75Lo1
1012.0				212.0	
1033.0		180.7			
1254.0	123.7		123.0	117.0	
1378.0		87.4			
1487.0	76.7		78.3	76.2	
1557.0				69.0	
1771.0		45.4			
1778.0	49.6				50.5 *)
2293.0	23.9			20.9	
2395.0	21.5				
2480.0		18.9			
2622.0					16.2
2838.0	13.4				
2839.0					12.9
2984.0	11.6			11.5	
2991.0					11.3 *)
3100.0		10.0			
3134.0	9.77				
3142.0					10.0 *)
3151.0	10.13				

Table 19. Photon attenuation cross sections for argon in the energy range from 1000 to 3190 eV from [69Wu1].

Energy [eV]	Cross section [10^{-21} cm^2]	Energy [eV]	Cross section [10^{-21} cm^2]	Energy [eV]	Cross section [10^{-21} cm^2]
1006.0	216.0	1167.0	146.0	1390.0	90.2
1014.0	211.0	1178.0	142.0	1406.0	87.0
1022.0	207.0	1190.0	138.0	1422.0	84.8
1031.0	202.0	1201.0	134.0	1438.0	82.1
1040.0	197.0	1213.0	131.0	1455.0	79.8
1048.0	192.0	1225.0	128.0	1473.0	77.1
1057.0	189.0	1237.0	124.0	1490.0	75.6
1066.0	185.0	1250.0	121.0	1509.0	73.3
1076.0	181.0	1262.0	118.0	1527.0	70.4
1085.0	177.0	1275.0	114.0	1546.0	68.3
1095.0	173.0	1289.0	111.0	1556.0	67.7
1104.0	168.0	1302.0	108.0	1566.0	67.1
1114.0	165.0	1316.0	105.0	1576.0	66.6
1125.0	161.0	1330.0	102.0	1586.0	64.4
1135.0	157.0	1345.0	99.7	1596.0	63.7
1145.0	153.0	1359.0	96.5	1607.0	63.3
1156.0	150.0	1374.0	93.1	1617.0	61.9

Energy [eV]	Cross section [10^{-21} cm^2]	Energy [eV]	Cross section [10^{-21} cm^2]	Energy [eV]	Cross section [10^{-21} cm^2]
1628.0	61.1	1933.0	36.9	2499.0	18.0
1638.0	60.3	1948.0	35.9	2525.0	17.5
1649.0	59.0	1964.0	34.8	2551.0	17.0
1660.0	57.0	1979.0	34.4	2577.0	16.6
1672.0	55.7	1995.0	33.4	2604.0	16.4
1683.0	55.1	2012.0	32.2	2632.0	16.3
1695.0	53.9	2028.0	31.3	2660.0	15.8
1706.0	52.7	2045.0	30.4	2689.0	15.4
1718.0	51.8	2062.0	29.5	2719.0	15.1
1730.0	50.8	2079.0	29.1	2749.0	14.5
1742.0	49.7	2097.0	28.8	2780.0	14.1
1755.0	49.0	2115.0	28.3	2812.0	13.7
1767.0	48.2	2133.0	27.0	2844.0	13.5
1780.0	47.2	2151.0	25.9	2877.0	13.1
1793.0	46.2	2170.0	24.8	2911.0	12.7
1806.0	44.4	2190.0	23.9	2945.0	12.1
1819.0	43.6	2209.0	23.4	2981.0	11.9
1833.0	41.9	2229.0	22.8	3017.0	11.4
1846.0	41.8	2249.0	22.5	3054.0	10.6
1860.0	40.3	2270.0	21.8	3093.0	10.3
1874.0	39.1	2291.0	21.2	3132.0	10.1
1889.0	38.1	2402.0	20.3	3172.0	10.0
1903.0	37.7	2450.0	19.6		
1918.0	37.4	2474.0	19.0		

Table 20. Photon attenuation cross sections for argon in the energy range from 3.25 to 10 keV from selected sources.

Energy [eV]	Cross section [10^{-21} cm^2]	Ref.	Energy [eV]	Cross section [10^{-21} cm^2]	Ref.
3336.0	87.560	31Sp1	6404.0	18.200	66Be1
3444.0	80.260	30Wo1	6925.0	11.690	75Lo1
3444.0	97.400	66Be1	7472.0	9.518	74Mi1
3662.0	67.990	30Wo1	8000.0	8.16	62Bu1
4089.0	48.050	75Lo1	8041.0	7.462	32Cr1
4508.0	37.000	70Mc2	8041.0	7.811	74Mi1
4508.0	37.210	74Mi1	8048.0	7.830	66Be1
5411.0	24.200	66Be1	8060.0	7.500	30Co1
5411.0	23.340	74Mi1	8067.0	7.429	31Sp1
5412.0	22.890	75Lo1	8631.0	6.353	74Mi1
5414.0	23.480	30Wo1	8631.0	6.324	75Lo1
5414.0	28.000	66Be1	8930.0	5.640	30Co1
5420.0	22.330	30Co1	9000.0	5.57	62Bu1
5428.0	22.820	31Sp1	9243.0	5.290	70Mc2
5895.0	18.200	70Mc2	9876.0	4.341	74Mi1
5946.0	18.700	30Co1	10000.0	4.18	62Bu1
6400.0	14.700	74Mi1			

Table 21. Photon attenuation cross sections for argon in the energy range from 3.25 to 8.5 keV from [69Wu1].

Energy [eV]	Cross section [10^{-21} cm^2]	Energy [eV]	Cross section [10^{-21} cm^2]
3255.0	91.0	4758.0	33.8
3299.0	88.9	4851.0	31.8
3343.0	85.9	4948.0	29.7
3389.0	83.7	5049.0	28.7
3436.0	79.1	5154.0	27.1
3485.0	77.3	5264.0	24.8
3534.0	74.2	5378.0	24.0
3586.0	72.2	5498.0	23.0
3638.0	69.6	5623.0	21.2
3693.0	66.9	5754.0	20.0
3749.0	64.5	5891.0	19.2
3806.0	62.2	6034.0	17.1
3866.0	58.2	6185.0	16.5
3927.0	55.1	6344.0	15.6
3990.0	53.9	6511.0	14.7
4056.0	52.4	6687.0	13.7
4124.0	48.8	6872.0	12.8
4193.0	45.6	7069.0	11.9
4266.0	43.9	7277.0	10.8
4340.0	42.4	7497.0	9.88
4418.0	40.9	7732.0	8.95
4498.0	39.3	7981.0	8.16
4582.0	37.1	8247.0	7.36
4668.0	36.2		

1.2.6 Cross sections for krypton (Z = 36)

There is a resonance range in krypton between the ionization potential (14.00 eV) and 14.7 eV and another one between 25 and 30 eV. The cross section in the range from 15 to 25 eV is shown in Fig. 6. The two curves show the recommended values of Marr and West [76Ma1] and Samson [91Sa1]. Earlier results of Pery-Thorne and Garton [60Pe1] and Rustgi et al. [64Ru2] show a good deal of scatter but the recommended values have the same general shape with the values of Samson being approximately 6 % higher than those of Marr and West. Their results are shown in tabular form in Table 22 along with the highly accurate values of Samson et al. [89Sa1] at three selected wavelengths.

The same is true in the energy range between 30 and 90 eV as shown in Fig. 7. The discrepancy is about 15 % at the minimum of the cross section. Both sets are much lower than the measured values of Lang and Watson [75La1]. All of these results are given in Table 23.

Between 100 and 200 eV there have been a number of measurements made in addition to the recommended values of Marr and West as shown in Fig. 8 and in Table 24. The earlier results of Lukirskii et al. [64Lu1] seem to scatter and those of Haensel et al. [69Ha2] seem too low at 150 eV. There is good agreement between the recommended values of Marr and West and the data of Henke [67He1] but the values of Lang et al. [75La1] are higher as they are at lower energies. In view of the

disagreement between these sources one must conclude that the cross section in this energy range is not known to better than 10 %.

In the energy range between 300 and 800 eV there are only a few measurements as shown in Table 25. The values of Henke in this energy range are probably the most reliable since they agree with the tabulation of Marr and West at lower energies and with the data of Wuilleumier [69Wu1] at higher energies as shown in Table 25.

The energy range between 1.6 and 2.0 keV contains the L edges and will be treated in Section 1.3. In the energy range from 2 to 10 keV the only measurements are those of Wuilleumier [69Wu1] and those of McCrary et al. [70Mc2]. Their data are shown in Table 26 and the agreement is excellent.

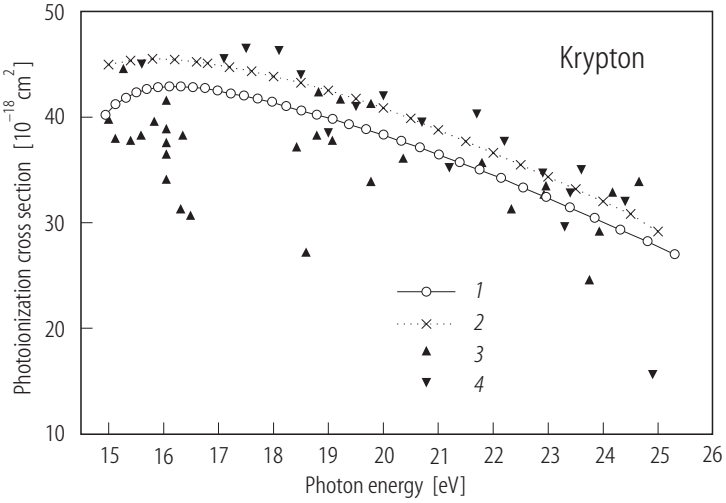

Fig. 6. Krypton cross sections from 15 to 26 eV from various sources: *1* [76Ma1], *2* [91Sa1], *3* [60Pe1], *4* [64Ru2].

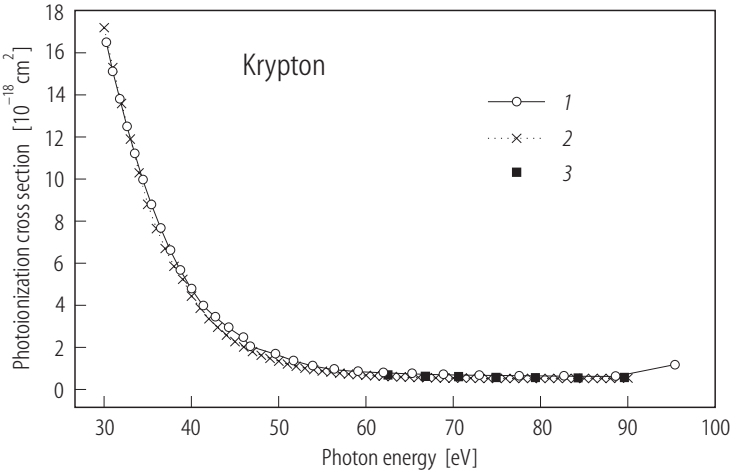

Fig. 7. Krypton cross sections from 30 and 90 eV from various sources: *1* [76Ma1], *2* [91Sa1], *3* [75La1].

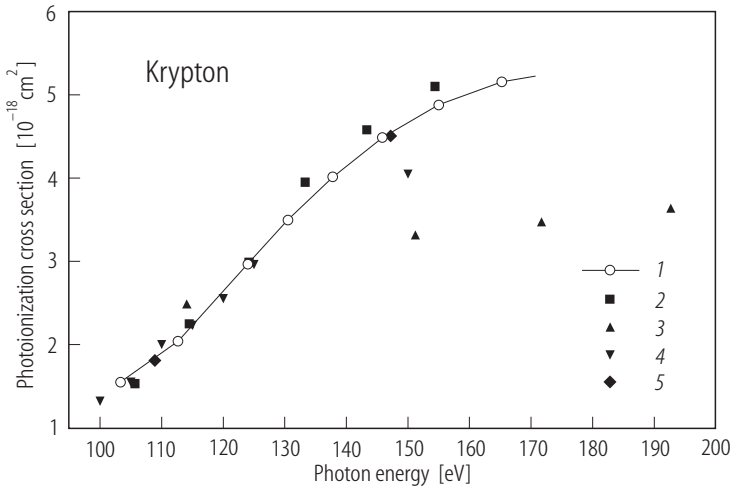

Fig. 8. Krypton cross sections from 100 to 200 eV from various sources: *1* [76Ma1], *2* [75La1], *3* [64Lu1], *4* [69Ha2], *5* [67He1].

Table 22. Photon attenuation cross sections for krypton in the energy range between 15 and 25 eV.

Energy [eV]	Cross section [10^{-18} cm^2]			Energy [eV]	Cross section [10^{-18} cm^2]		
	76Ma1	91Sa1	89Sa1		76Ma1	91Sa1	89Sa1
15.0		44.96		18.78	40.2		
15.12	41.2			19.0		42.53	
15.31	41.8			19.07	39.8		
15.4		45.34		19.37	39.3		
15.50	42.3			19.5		41.74	
15.69	42.6			19.68	38.8		
15.8		45.50		20.00	38.3	40.85	
15.89	42.8			20.32	37.7		
16.1	42.9			20.5		39.86	
16.2		45.44		20.66	37.1		
16.31	42.9			21.00	36.4	38.78	
16.40		45.36		21.22			38.31
16.53	42.8			21.38	35.7		
16.60		45.23		21.50		37.70	
16.67			44.90	21.75	35.0		
16.75	42.7			22.00		36.60	
16.80		45.08		22.14	34.2		
16.85			44.87	22.50		35.48	
16.98	42.5			22.54	33.3		
17.00		44.92		22.96	32.4		
17.20		44.73		23.00		34.34	
17.22	42.2			23.39	31.4		
17.40		44.54		23.50		33.19	
17.46	42.0			23.84	30.4		
17.60		44.34		24.00		32.02	
17.71	41.7			24.31	29.3		
17.80		44.12		24.50		30.82	
17.97	41.4			24.80	28.2		
18.00		43.84		25.00		29.15	
18.23	41.0			25.30	27.0		
18.50	40.6	43.25					

Table 23. Photon attenuation cross section of krypton in the energy range from 30 to 90 eV.

Energy [eV]	Cross section [10^{-18} cm^2]			Energy [eV]	Cross section [10^{-18} cm^2]		
	76Ma1	91Sa1	75La1		76Ma1	91Sa1	75La1
30.00		17.2		59.00		0.703	
30.24	16.5			59.04	0.838		
31.00	15.1	15.3		60.00		0.674	
31.79	13.8			61.00		0.650	
32.00		13.6		62.00	0.789	0.628	
32.63	12.5			62.50			0.692
33.00		11.9		63.00		0.610	
33.51	11.2			64.00		0.595	
34.00		10.3		65.00		0.582	
34.44	9.96			65.25	0.737		
35.00		8.80		66.00		0.570	
35.42	8.78			66.80			0.618
36.00		7.64		67.00		0.560	
36.46	7.67			68.00		0.552	
37.00		6.70		68.88	0.697		
37.57	6.62			69.00		0.544	
38.00		5.85		70.00		0.537	
38.74	5.66			70.60			0.610
39.00		5.24		71.00		0.534	
40.00	4.78	4.43		72.00		0.530	
41.00		3.86		72.93	0.671		
41.33	3.98			73.00		0.527	
42.00		3.36		74.00		0.525	
42.75	3.43			74.90			0.573
43.00		2.95		75.00		0.524	
44.00		2.58		76.00		0.523	
44.28	2.93			77.00		0.522	
45.00		2.28		77.49	0.652		
45.92	2.47			78.00		0.521	
46.00		2.02		79.00		0.520	
46.68	2.05			79.40			0.558
47.00		1.80		80.00		0.519	
48.00		1.62		81.00		0.518	
49.00		1.47		82.00		0.518	
49.59	1.68			82.65	0.633		
50.00		1.34		83.00		0.518	
51.00		1.21		84.00		0.519	
51.66	1.36			84.30			0.551
52.00		1.10		85.00		0.520	
53.00		1.01		86.00		0.522	
53.90	1.11			87.00		0.523	
54.00		0.934		88.00		0.525	
55.00		0.865		88.56	0.607		
56.00		0.817		89.00		0.528	
56.35	0.943			89.60			0.577
57.00		0.773		90.00		0.530	
58.00		0.735					

Table 24. Photon attenuation cross section for krypton in the energy range between 100 and 200 eV.

Energy [eV]	Cross section [10^{-18} cm^2]				
	76Ma1	75La1	69Ha2	67He1	64Lu1
100.0			1.32		
101.6		1.35			
103.3	1.55				
105.0			1.55		
105.7		1.53			
108.9				1.81	
110.0			2.00		
112.7	2.04				
114.1					2.49
114.5		2.25			
115.0			2.23		
120.0			2.55		
124.0	2.97				
124.2		2.99			
125.0			2.96		
130.5	3.50				
133.3		3.95			
137.8	4.01				
143.3		4.58			
145.9	4.49				
147.2				4.51	
150.0			4.05		
151.2					3.32
154.4		5.10			
155.0	4.88				
165.3	5.16				
171.7					3.47
177.1	5.31				
180.2		5.21			
182.6				4.98	
190.7	5.31				
192.7					3.64
195.6		5.32			

Table 25. Photon attenuation cross sections for krypton in the energy range between 300 and 1600 eV.

Energy [eV]	Cross section [10^{-18} cm^2]			
	67He1	69Ha2	64Lu1	76Ma1
300.0		3.90		
310.0				3.41
391.0	2.99			
394.0			2.00	
400.0	2.60			
525.0			1.32	
526.0	1.71			
677.0	1.01			
775.0	0.76			

Energy [eV]	Cross section [10^{-18} cm^2]		Energy [eV]	Cross section [10^{-18} cm^2]	
	69Wu1	67He1		69Wu1	67He1
825.0	0.666		1014.0	0.395	
830.0	0.650		1022.0	0.387	
836.0	0.640		1031.0	0.379	
842.0	0.631		1040.0	0.370	
847.0	0.623		1048.0	0.362	
853.0	0.610		1057.0	0.354	
859.0	0.600		1066.0	0.346	
865.0	0.589		1076.0	0.339	
871.0	0.579		1085.0	0.331	
877.0	0.568		1095.0	0.323	
884.0	0.557		1104.0	0.317	
890.0	0.550		1114.0	0.309	
896.0	0.538		1125.0	0.302	
903.0	0.527		1135.0	0.296	
910.0	0.518		1145.0	0.289	
916.0	0.508		1156.0	0.281	
923.0	0.498		1167.0	0.275	
928.0		0.494	1178.0	0.268	
930.0	0.491		1190.0	0.262	
937.0	0.484		1201.0	0.257	
944.0	0.474		1213.0	0.250	
952.0	0.463		1225.0	0.243	
959.0	0.454		1237.0	0.237	
966.0	0.444		1250.0	0.232	
974.0	0.436		1254.0		0.238
982.0	0.428		1262.0	0.226	
990.0	0.419		1275.0	0.220	
998.0	0.411		1289.0	0.215	
1006.0	0.402		1302.0	0.210	

Energy [eV]	Cross section [10^{-18} cm^2]		Energy [eV]	Cross section [10^{-18} cm^2]	
	69Wu1	67He01		69Wu1	67He01
1316.0	0.204		1487.0		0.152
1330.0	0.196		1490.0	0.148	
1345.0	0.193		1509.0	0.144	
1359.0	0.184		1527.0	0.140	
1374.0	0.182		1546.0	0.135	
1390.0	0.177		1556.0	0.133	
1406.0	0.172		1566.0	0.131	
1422.0	0.167		1576.0	0.129	
1438.0	0.162		1586.0	0.127	
1455.0	0.157		1596.0	0.125	
1473.0	0.152				

Table 26. Photon attenuation cross sections for krypton in the energy range between 1,600 and 10,000 eV from [69Wu1], *) values are from [70Mc2].

Energy [eV]	Cross section [10^{-21} cm^2]	Energy [eV]	Cross section [10^{-21} cm^2]	Energy [eV]	Cross section [10^{-21} cm^2]
1607.0	123.0	1925.0	582.0	2474.0	314.0
1617.0	121.0	1933.0	576.0	2499.0	306.0
1628.0	118.0	1948.0	565.0	2525.0	298.0
1638.0	116.0	1964.0	554.0	2551.0	289.0
1649.0	114.0	1979.0	543.0	2577.0	280.0
1660.0	113.0	1995.0	534.0	2604.0	274.0
1672.0	111.0	2012.0	522.0	2632.0	266.0
1680.0	462.0	2028.0	513.0	2660.0	259.0
1683.0	456.0	2045.0	504.0	2689.0	251.0
1695.0	483.0	2062.0	494.0	2719.0	243.0
1706.0	441.0	2079.0	484.0	2749.0	236.0
1718.0	433.0	2097.0	475.0	2780.0	229.0
1723.0	431.0	2115.0	465.0	2812.0	222.0
1732.0	623.0	2133.0	455.0	2844.0	215.0
1742.0	613.0	2151.0	447.0	2877.0	208.0
1755.0	603.0	2170.0	437.0	2911.0	202.0
1767.0	592.0	2190.0	429.0	2945.0	196.0
1780.0	582.0	2209.0	419.0	2981.0	189.0
1793.0	573.0	2229.0	410.0	3017.0	182.0
1806.0	564.0	2249.0	401.0	3054.0	177.0
1819.0	556.0	2270.0	391.0	3093.0	172.0
1833.0	548.0	2291.0	383.0	3132.0	166.0
1846.0	540.0	2312.0	373.0	3172.0	160.0
1860.0	533.0	2334.0	363.0	3213.0	155.0
1874.0	526.0	2356.0	356.0	3255.0	149.0
1889.0	520.0	2379.0	348.0	3299.0	144.0
1903.0	515.0	2402.0	339.0	3343.0	139.0
1917.0	507.0	2426.0	330.0	3389.0	134.0
1918.0	508.0	2450.0	323.0	3436.0	130.0

Energy [eV]	Cross section [10^{-21} cm^2]	Energy [eV]	Cross section [10^{-21} cm^2]	Energy [eV]	Cross section [10^{-21} cm^2]
3485.0	126.0	4418.0	69.7	5891.0	32.8
3534.0	121.0	4498.0	66.4	5895.0	31.6 *)
3586.0	117.0	4508.0	64.8 *)	6034.0	30.5
3638.0	113.0	4582.0	63.2	6185.0	28.1
3693.0	109.0	4668.0	60.5	6344.0	26.2
3749.0	106.0	4758.0	57.2	6511.0	24.6
3806.0	103.0	4851.0	54.5	6687.0	22.8
3866.0	99.1	4948.0	51.8	6872.0	21.3
3927.0	94.9	5049.0	49.3	7069.0	19.8
3990.0	90.9	5154.0	46.6	7277.0	17.8
4056.0	87.4	5264.0	44.0	7497.0	16.8
4124.0	83.5	5378.0	41.5	7732.0	15.3
4193.0	79.9	5498.0	39.2	7981.0	14.2
4266.0	76.2	5623.0	36.6	8247.0	13.5
4340.0	72.8	5754.0	34.6	9243.0	9.1 *)

1.2.7 Cross sections for xenon (Z = 54)

Xenon has resonance regions similar to those in krypton below 14 eV and in the energy range between 20 and 25 eV. Recommended values of the cross sections have been given by West and Morton [78We1] and by Samson [91Sa1] and are shown in Table 27 for the energy range between 14 and 20 eV and are shown along with earlier data by Rustgi et al. [64Ru2] in Fig. 9. As in krypton, the data of Rustgi et al. is scattered but there is good agreement between the two recommended data sets. As in krypton, the two highly accurate data points measured by Samson et al. [89Sa1] are also shown. The cross section is known in this energy range to better than 3 %.

Between 25 and 60 eV the cross section decreases rapidly as shown in Fig. 10. which gives data from the same sources as Fig. 9. As in Fig. 9, the data of Rustgi et al. is scattered, but there is good agreement between the two recommended data sets at the lower energies. At higher energies where the cross section is low Samson's results are 10…15 % lower than those of West and Morton as is shown in Table 28.

The cross section goes through a maximum at 100 eV and there have been a number of measurements of the cross section in the energy range between 70 and 140 eV as shown in Fig. 11. Data from a variety of sources is shown in Fig. 11 and tabulated in Table 29. There is good agreement between the recommended values of West and Morton and of Samson over the entire energy range.

There have also been a number of measurements in the energy range between 140 and 680 eV as shown in Fig. 12 and listed in Table 30. There is much better agreement between the various sets for energies up to about 300 eV. At higher energies there is moderately good agreement between the results of Henke [67He1] and Lukirskii [66Lu1].

The results of Wuilleumier [69Wu1] between 955 eV and 4770 eV are shown in Table 31. These data agree extremely well with the results made at various energies using line source sources. Data are also shown for Xenon in the energy range above the L thresholds from 5500 eV to 8247 eV [69Wu1] along with a single measurement made at 9243 eV [70Mc2] in Table 32.

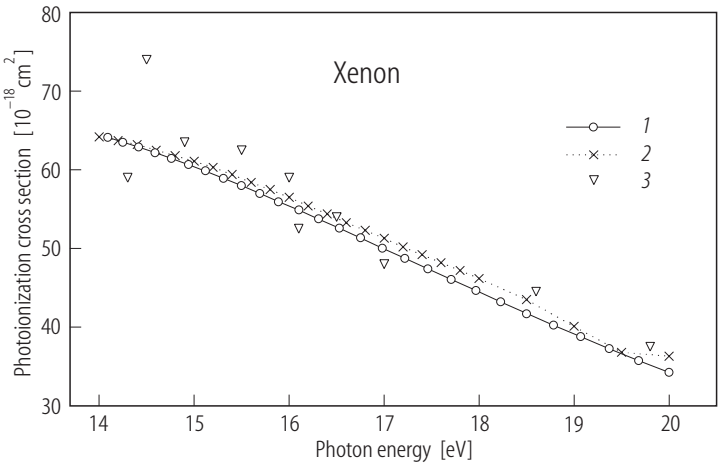

Fig. 9. Cross sections for xenon from 14 to 20 eV from various sources: *1* [78We1], *2* [91Sa1], *3* [64Ru2].

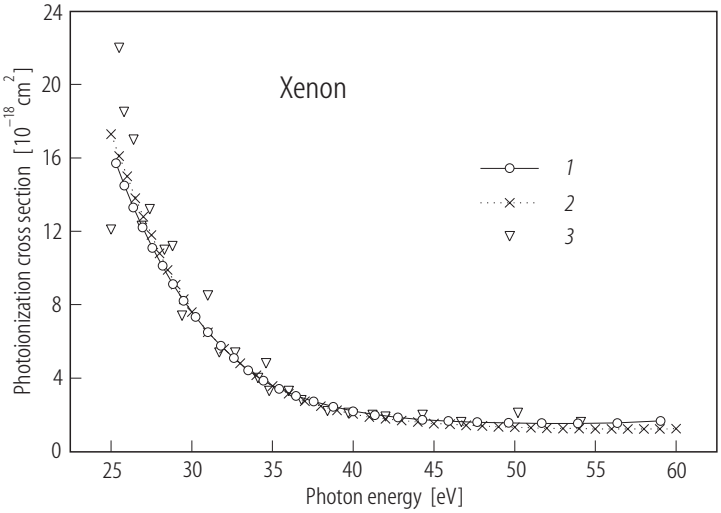

Fig. 10. Cross sections for xenon from 25 to 60 eV from various sources: *1* [78We1], *2* [91Sa1], *3* [64Ru2].

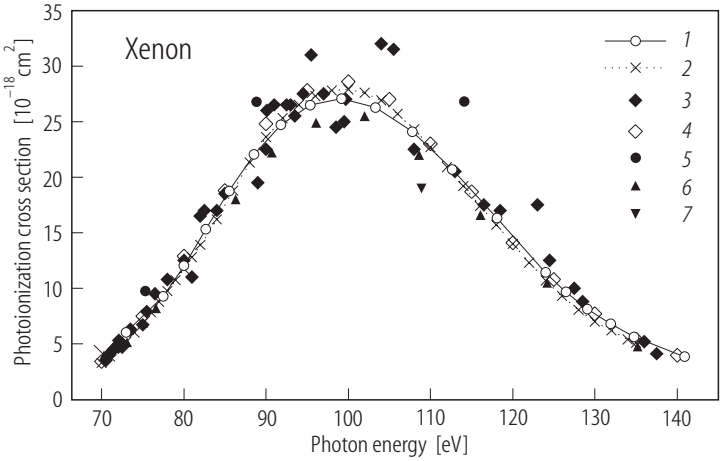

Fig. 11. Cross sections for xenon from 70 to 140 eV from various sources: *1* [78We1], *2* [91Sa1], *3* [64Ed1], *4* [69Ha2], *5* [64Lu1], *6* [75La1], *7* [67He1].

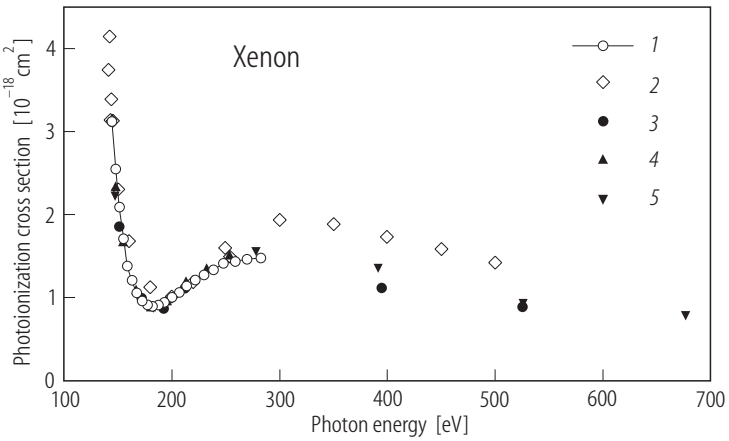

Fig. 12. Cross sections for xenon from 140 to 680 eV from various sources: *1* [78We1], *2* [69Ma2], *3* [66Lu1], *4* [64Lu1], *5* [67He1].

Table 27. Photon attenuation cross sections for xenon in the energy range from 14 to 20 eV.

Energy [eV]	Cross section [10^{-18} cm^2]			Energy [eV]	Cross section [10^{-18} cm^2]		
	78We1	91Sa1	89Sa1		78We1	91Sa1	89Sa1
14.00		64.2		16.53	52.55		
14.09	64.13			16.60		53.3	
14.20		63.7		16.67			52.65
14.25	63.53			16.75	51.32		
14.40		63.2		16.80		52.3	
14.42	62.88			16.85			51.88
14.59	62.19			16.98	50.05		
14.60		62.5		17.00		51.3	
14.76	61.45			17.20		50.2	
14.80		61.8		17.22	48.75		
14.94	60.67			17.40		49.2	
15.00		61.1		17.46	47.4		
15.12	59.83			17.60		48.2	
15.20		60.3		17.71	46.03		
15.31	58.94			17.80		47.2	
15.40		59.4		17.97	44.62		
15.50	58.00			18.00		46.2	
16.60		56.5		18.23	43.19		
15.69	57.01			18.50	41.73	43.5	
15.80		57.5		18.78	40.25		
15.89	55.96			19.00		40.1	
16.00		56.5		19.07	38.76		
16.10	54.87			19.37	37.26		
16.20		55.4		19.50		38.6	
16.31	53.74			19.68	35.75		
16.40		54.4		20.00	34.23	36.3	

Table 28. Photon attenuation cross section for xenon in the energy range from 25 to 60 eV.

Energy [eV]	Cross section [10^{-18} cm^2]		Energy [eV]	Cross section [10^{-18} cm^2]	
	78We1	91Sa1		78We1	91Sa1
25.00		17.3	38.00		2.47
25.30	15.72		38.74	2.44	
25.50		16.1	39.00		2.24
25.83	14.51		40.00	2.21	2.04
26.00		15.0	41.00		1.88
26.38	13.33		41.33	2.00	
26.50		13.8	42.00		1.77
26.95	12.21		42.75	1.86	
27.00		12.8	43.00		1.68
27.50		11.8	44.00		1.60
27.55	11.13		44.28	1.73	
28.00		10.8	45.00		1.52
28.18	10.10		45.92	1.66	
28.50		9.90	46.00		1.48
28.83	9.12		47.00		1.43
29.00		9.10	47.68	1.59	
29.50		8.30	48.00		1.39
29.52	8.20		49.00		1.35
30.00		7.60	49.59	1.56	
30.24	7.33		50.00		1.32
31.00	6.52	6.50	51.00		1.29
31.79	5.76		51.66	1.52	
32.00		5.60	52.00		1.26
32.63	5.06		53.00		1.25
33.00		4.80	53.90	1.52	
33.51	4.43		54.00		1.24
34.00		4.15	55.00		1.23
34.44	3.85		56.00		1.23
35.00		3.56	56.35	1.55	
35.42	3.41		57.00		1.23
36.00		3.11	58.00		1.23
36.46	3.04		59.00		1.23
37.00		2.74	59.04	1.67	
37.57	2.73		60.00		1.24

Table 29. Photon attenuation cross sections for xenon in the energy range from 70 to 140 eV. [1]) [64Lu1], [2]) [67He1].

Energy [eV]	Cross section [10^{-18} cm^2]					
	78We1	91Sa1	75La1	69Ha2	64Ed1	Other
68.88	3.89					
70.00		3.29			3.4	
70.30	3.95					
70.50					3.5	
71.00		3.86			4.0	
71.20					4.3	
71.40					4.5	
72.00		4.46			4.7	
72.00					4.9	
72.10					5.3	
72.50					4.7	
72.50					5.0	
72.93	6.01					
73.00		5.20				
73.10			5.14			
73.50					6.3	
74.00		6.00				
75.00		6.88		7.5	6.7	
75.32						9.74 [1])
75.50					7.9	
76.00		7.83				
76.50					9.5	
76.60			8.19			
77.00		8.78				
77.49	9.27					
78.00		9.74			10.8	
80.00	11.97	11.75		12.9	12.5	
81.00		12.78			11.0	
82.00		13.9			16.5	
82.50					17.0	
82.65	15.27					
83.00		15.0				
84.00		16.2			17.0	
85.00		17.5		18.8	18.5	
85.50	18.75					
86.00		18.8				
86.30			18.0			
87.00		20.1				
88.00		21.3				
88.56	22.04					
88.88						26.81 [1])
89.00		22.5			19.5	
90.00		23.6		24.8	22.5	
90.10					26.0	
90.70			22.2			

Energy [eV]	Cross section [10^{-18} cm^2]					
	78We1	91Sa1	75La1	69Ha2	64Ed1	Other
91.00		24.5			26.5	
91.84	24.7					
92.00		25.3				
92.50					26.5	
93.00		25.9			26.5	
93.50					25.5	
94.00		26.5				
94.50					27.5	
95.00		27.0		27.8		
95.37	26.5					
95.50					31.0	
96.00		27.3				
96.10			24.9			
97.00		27.6			27.5	
98.00		27.8				
98.50					24.5	
99.00		27.9				
99.18	27.1					
99.50					25.0	
99.70	27.0					
100.00		27.9		28.6		
101.00		27.8				
102.00		27.6	25.5			
103.30	26.3	27.3				
104.00		26.9			32.0	
105.00		26.4		27.0		
105.50					31.5	
106.00		25.7				
107.00		25.1				
107.80	24.1					
108.00		24.3			22.5	
108.60			22.0			
108.90						18.97 [2])
109.00		23.5				
110.00		22.7		23.0		
111.00		21.8				
112.00		20.9				
112.70	20.7					
113.00		20.0			20.5	
114.00		19.2				
114.10						26.81 [1])
115.00		18.3	18.7			
116.00		17.4				
116.10			16.6			
116.50					17.5	
117.00		16.5				
118.00		15.7				
118.10	16.3					
118.50					17.0	

Energy [eV]	Cross section [10^{-18} cm^2]					
	78We1	91Sa1	75La1	69Ha2	64Ed1	Other
119.00		14.8				
120.00		14.0		14.1		
121.00		13.2				
122.00		12.3				
123.00		11.5			17.5	
124.00	11.4	10.7				
124.20			10.5			
124.50					12.5	
125.00		10.0		10.8		
126.00		9.30				
126.50	9.64					
127.00		8.65				
127.50					10.0	
128.00		8.05				
128.50					8.8	
129.00		7.50				
129.10	8.11					
130.00		7.00		7.7		
131.00		6.60				
131.90	6.78					
132.00		6.20				
133.00		5.80				
134.00		5.40				
134.80	5.64					
135.00		5.10		5.4		
135.20			4.76			
136.00					5.2	
137.50					4.1	
140.00				3.96		

Table 30. Photon attenuation cross sections for xenon in the energy range from 140 to 680 eV. [1]) from [64Ed1], [2]) from [31De1], [3]) from [69De1].

Energy [eV]	Cross section [10^{-18} cm^2]				
	78We1	75La1	69Ha2	64Lu1, 66Lu1	67He1
140.9	3.82				
141.0			3.8		
141.8			4.2		
143.0			3.2		
143.7			3.4		
144.2	3.13				
145.0			3.2		
145.5					2.9 [1])
147.2					2.2

Energy [eV]	Cross section [10^{-18} cm^2]				
	78We1	75La1	69Ha2	64Lu1, 66Lu1	67He1
147.6	2.55	2.32			
149.0					2.6 [1])
150.0			2.3		
151.2	2.08			1.86	
154.0					2.3 [1])
154.4		1.66			
155.0	1.71				
158.9	1.42				
160.0			1.7		
163.1	1.21				
166.6		1.08			
167.5	1.06				
171.7				1.00	
172.2	0.96				
177.2	0.91				
180.0			1.1		
180.2		0.88			
182.3	0.89				
182.6					0.87
187.8	0.91				
192.7				0.87	
193.7	0.94				
195.6		0.95			
200.0	1.00		1.0		
206.6	1.06				
211.9				1.12	
213.0		1.18			
213.8	1.13				
220.0			1.2		
221.4	1.20				
229.6	1.27				
232.0		1.34			
238.4	1.33				
248.0	1.39				
250.0			1.6		
254.0		1.49			
258.3	1.43				
269.5	1.46				
278.0					1.56
278.0				1.38	1.47 [2])
281.8	1.48				
300.0			1.9		
350.0			1.9		
391.4					1.35
394.8				1.12	
395.0				1.32	
400.0			1.7		
450.0			1.6		

Energy [eV]	Cross section [10^{-18} cm^2]				
	78We1	75La1	69Ha2	64Lu1, 66Lu1	67He1
453.0				1.17	
500.0			1.4		
525.0				0.89	
526.0					0.93
557.0				0.65	
572.0				0.97	
637.0				0.65	
672.0	0.70 [3])				
675.0	0.80 [3])				
676.8					0.78
678.0	0.85 [3])				
680.0	1.00 [3])				

Table 31. Photon attenuation cross sections for xenon in the energy range from 950 to 4,750 eV. from [69Wu1], [1]) from [67He1], [2]) from [66Lu1], [3]) from [70Mc2].

Energy [eV]	Cross section [10^{-18} cm^2]	Energy [eV]	Cross section [10^{-18} cm^2]	Energy [eV]	Cross section [10^{-18} cm^2]
952.00	1.820	1190.00	1.330	1527.00	0.830
955.00	1.810	1201.00	1.310	1546.00	0.809
959.00	1.790	1213.00	1.290	1556.00	0.798
966.00	1.770	1225.00	1.270	1566.00	0.786
974.00	1.740	1237.00	1.250	1576.00	0.775
982.00	1.730	1250.00	1.220	1586.00	0.764
990.00	1.720	1254.00	1.35 [1])	1596.00	0.754
998.00	1.700	1254.00	1.17 [2])	1607.00	0.742
1006.00	1.680	1262.00	1.200	1617.00	0.732
1014.00	1.670	1275.00	1.180	1628.00	0.720
1022.00	1.650	1289.00	1.160	1638.00	0.710
1031.00	1.640	1302.00	1.130	1649.00	0.698
1040.00	1.620	1316.00	1.110	1660.00	0.691
1048.00	1.600	1330.00	1.090	1672.00	0.680
1057.00	1.590	1345.00	1.070	1683.00	0.670
1066.00	1.570	1359.00	1.050	1695.00	0.658
1076.00	1.560	1374.00	1.030	1706.00	0.646
1085.00	1.540	1390.00	1.040	1718.00	0.637
1095.00	1.520	1406.00	0.983	1730.00	0.628
1104.00	1.500	1422.00	0.962	1742.00	0.618
1114.00	1.480	1438.00	0.938	1755.00	0.607
1125.00	1.460	1455.00	0.917	1767.00	0.596
1135.00	1.440	1473.00	0.897	1776.00	0.600 [2])
1145.00	1.420	1487.00	0.98 [1])	1780.00	0.588
1156.00	1.400	1487.00	0.83 [2])	1793.00	0.577
1167.00	1.380	1490.00	0.873	1806.00	0.563
1178.00	1.360	1509.00	0.853	1819.00	0.554

Energy [eV]	Cross section [10^{-18} cm^2]	Energy [eV]	Cross section [10^{-18} cm^2]	Energy [eV]	Cross section [10^{-18} cm^2]
1833.00	0.546	2312.00	0.306	3132.00	0.147
1846.00	0.535	2334.00	0.300	3172.00	0.142
1860.00	0.523	2356.00	0.293	3213.00	0.138
1874.00	0.515	2379.00	0.286	3255.00	0.133
1889.00	0.506	2402.00	0.279	3299.00	0.128
1903.00	0.497	2426.00	0.274	3343.00	0.124
1918.00	0.488	2450.00	0.267	3389.00	0.119
1933.00	0.476	2474.00	0.258	3436.00	0.115
1948.00	0.468	2499.00	0.255	3485.00	0.111
1964.00	0.457	2525.00	0.249	3534.00	0.107
1979.00	0.448	2551.00	0.244	3586.00	0.103
1995.00	0.438	2577.00	0.239	3638.00	0.099
2012.00	0.429	2604.00	0.230	3693.00	0.095
2028.00	0.420	2632.00	0.226	3749.00	0.092
2045.00	0.411	2660.00	0.220	3806.00	0.088
2062.00	0.404	2689.00	0.216	3866.00	0.085
2079.00	0.394	2719.00	0.209	3927.00	0.081
2097.00	0.386	2749.00	0.203	3990.00	0.078
2115.00	0.379	2780.00	0.199	4056.00	0.075
2133.00	0.372	2812.00	0.193	4124.00	0.072
2151.00	0.365	2844.00	0.188	4193.00	0.068
2170.00	0.356	2877.00	0.184	4266.00	0.066
2190.00	0.349	2911.00	0.177	4340.00	0.064
2209.00	0.340	2945.00	0.172	4418.00	0.060
2229.00	0.333	2981.00	0.167	4498.00	0.058
2249.00	0.328	3017.00	0.163	4508.00	0.061 [3])
2270.00	0.321	3054.00	0.157	4582.00	0.056
2291.00	0.313	3093.00	0.151	4668.00	0.053

Table 32. Photon attenuation cross sections for xenon in the energy range between 4,850 and 10,000 eV. From [69Wu1]. *) from [70Mc2].

Energy [eV]	Cross section [10^{-18} cm^2]	Energy [eV]	Cross section [10^{-18} cm^2]	Energy [eV]	Cross section [10^{-18} cm^2]
4758.0	0.051	5378.0	0.158	6511.0	0.113
4791.0	0.144	5442.0	0.154	6687.0	0.105
4794.0	0.140	5461.0	0.182	6872.0	0.097
4851.0	0.138	5473.0	0.181	7069.0	0.090
4948.0	0.136	5498.0	0.178	7277.0	0.083
5049.0	0.134	5623.0	0.166	7497.0	0.077
5090.0	0.131	5754.0	0.156	7732.0	0.071
5114.0	0.179	5891.0	0.147	7981.0	0.065
5154.0	0.173	6034.0	0.138	8247.0	0.060
5208.0	0.169	6185.0	0.129	9243.0	0.046 *)
5264.0	0.160	6344.0	0.121		

1.2.8 Cross sections for atomic oxygen and nitrogen (Z = 8, 7)

Because they are important components of the earth's atmosphere the cross sections for absorption and ionization of both atomic and molecular oxygen and nitrogen have been the subject of numerous experimental and theoretical investigations and a recent compilation of data from both experimental and theoretical sources is available [92Fe1]. Here we list only the experimental data for the absolute photoionization cross sections of atomic oxygen and nitrogen in those energy ranges where there are no resonances. In these ranges the cross sections are expected to be smoothly varying functions of the energy. For atomic oxygen absolute measurements were made by Samson and Pareek [85Sa1] and van der Meer el al. [88Me1]. These measurements at 21.22 eV differed by about 40 % and it has been pointed out via a sum rule analysis [97Be1] that Samson and Pareek's value probably is more nearly correct. Earlier measurements were made by Comes [68Co1] and at lower energies by Kohl et al. [78Ko1]. Angel and Samson [88An1] extended the earlier measurements to higher energies and normalized the new data to that of Samson and Pareek at 21.22 eV. In Table 33 we show the cross sections from both of these sources from 28.8 eV; i.e., just above the energy where resonances occur, to 280 eV. The accuracy of these data is probably better than 10 %.

For atomic nitrogen absolute measurements have been made by Ehler et al. [55Eh1] by Comes [68Co2] at energies between threshold and 30 eV and by Samson and Angel [90Sa1] from threshold to 400 eV. Data from [90Sa1] from 44 eV, just above the range where resonant structure occurs, to 400 eV are given in Table 34.

There have been a number of measurements of relative cross sections and branching ratios for both nitrogen and oxygen at lower energies and these will be discussed in Section 1.3.

For Table 33 see p. 1-40.

Table 34. Photoionization cross sections for nitrogen in the energy range between 44 and 400 eV. From [90Sa1].

Energy [eV]	Cross section [10^{-18} cm^2]	Energy [eV]	Cross section [10^{-18} cm^2]	Energy [eV]	Cross section [10^{-18} cm^2]
44.1	5.65	80.0	1.57	160.0	0.313
46.0	5.30	85.0	1.34	170.0	0.272
48.0	4.94	90.0	1.17	180.0	0.238
50.0	4.60	95.0	1.04	190.0	0.211
52.0	4.30	100.0	0.92	200.0	0.187
54.0	4.00	105.0	0.82	220.0	0.150
56.0	3.80	110.0	0.740	240.0	0.123
58.0	3.55	115.0	0.668	260.0	0.102
60.0	3.33	120.0	0.606	280.0	0.086
65.0	2.80	130.0	0.504	300.0	0.074
70.0	2.34	140.0	0.425	350.0	0.052
75.0	1.96	150.0	0.363	400.0	0.038

Table 33. Total photoionization cross sections for oxygen in the energy range between 28 and 280 eV.

Energy [eV]	Cross section [10^{-18} cm^2]		Energy [eV]	Cross section [10^{-18} cm^2]	
	88An1	85Sa1		88An1	85Sa1
28.8	11.5		57.6		4.47
29.5	11.3		60.0	4.44	
29.8		11.2	61.1		3.97
30.2	11.0		62.1		3.94
30.3		11.0	64.3		3.58
30.6		11.1	67.3		3.41
31.0	11.8		68.8		2.88
31.3		10.0	70.0	3.43	
31.4		12.1	70.2		2.63
31.8	10.5		74.9		2.61
32.6	10.2		78.0		2.09
33.1		9.95	80.0	2.60	
33.5	9.90		80.3		1.93
34.4	9.57		81.6		2.30
35.3		9.37	89.6		1.81
35.4	9.25		90.0	2.06	
36.5	8.92		94.9		1.95
36.8		8.46	100.0	1.65	
37.6	8.60		103.2		1.34
37.7		8.70	110.0	1.39	
38.7	8.25		120.0	1.17	
40.0	7.90	7.97	130.0	1.00	
40.8	7.70	7.70	140.0	0.84	
41.3	7.55		150.0	0.73	
41.6		7.49	160.0	0.61	
42.1		7.20	170.0	0.52	
42.8	7.40		180.0	0.45	
44.3	6.85		190.0	0.38	
44.4		7.10	200.0	0.33	
45.9	6.50		210.0	0.28	
47.6		6.25	220.0	0.25	
47.7	6.15		230.0	0.22	
48.1		6.03	240.0	0.20	
48.7	6.00		250.0	0.18	
49.5		6.09	260.0	0.17	
50.0	5.77		270.0	0.17	
53.7		5.47	280.0	0.16	
56.1		4.91			

1.2.9 Cross sections for the alkalis (Z = 3, 11, 19, 37, 55)

Due to their low ionization potentials there have been a number of measurements of photoionization cross sections in the energy range below 25 eV. A summary of the earlier work has been given by Marr and Creek [68Ma1]. Measurements of absolute cross sections are difficult for two reasons. First, the cross sections in this energy range with the exception of lithium, are quite small (<< 1 Mb) and second, the measurements are always made on a species that contains some fraction of molecules and thus it is difficult to estimate the number of atoms that contribute to the absorption. As a result there are wide differences in both the absolute values of the cross sections reported as well as the variation of the cross section with energy.

At higher energies there have been measurements for lithium [82Me1], sodium [77Co1] and potassium [76Dr1] and a relative measurement for Cs [75Pe1].

For lithium, the results of Hudson and Carter [67Hu2] are shown in Fig. 13 between the ionization threshold, 5.39 eV and 22 eV. At higher energies the results of Mehlman et al. [82Me1] are shown along with an earlier measurement made on solid lithium [62Ba1] which illustrates that there is considerable difference in atomic and solid state cross sections at these energies. The results of Hudson and Carter are about 10 % lower than those of Marr and Creek [68Ma1] (not shown) but have the same dependence on energy. The results of Hudson and Carter and of Mehlman et al. are also shown in Table 35. There have been no measurements for lithium between 22 and 60 eV. However, there have been a number of measurements in the resonance region between 60 and 75 eV and between 140 and 175 eV which will be discussed in Section 1.3.

For sodium, Fig. 14 shows the low energy results of Hudson and Carter [67Hu2, 68Hu1] which are in agreement with an earlier measurement by Ditchburn et al. [53Di1] and a measurement at higher energies by Codling et al. [77Co1]. As with lithium, these data are also shown in Tables 36 and 37. Relative data in the resonance range between 30 and 70 eV [72Wo1] will be discussed in Section 1.3.

Table 38 gives the results of the measurements of Hudson and Carter [67Hu1] for potassium from the ionization threshold 4.34 eV to 18 eV and measurements at higher energies [76Dr1]. Also shown are results derived by Marr and Creek [68Ma1] from an analysis of their own results and previous measurements.

For rubidium and cesium measurements have only been made in the energy range from threshold (4.18 eV for rubidium, 3.89 eV for caesium) up to 11 eV. Results from various authors are shown in Table 39. For cesium the table shows that there is relatively good agreement between the results of Cook et al. [77Co2] and the relative measurements of Suemitsu and Samson [83Su1] concerning the energy dependence of the cross section. The results of Cook et al. are approximately a factor of 2 lower than the results of Marr and Creek [68Ma1]. In view of the small size of these cross sections and the difficulties of the measurements it is not surprising that there are large discrepancies.

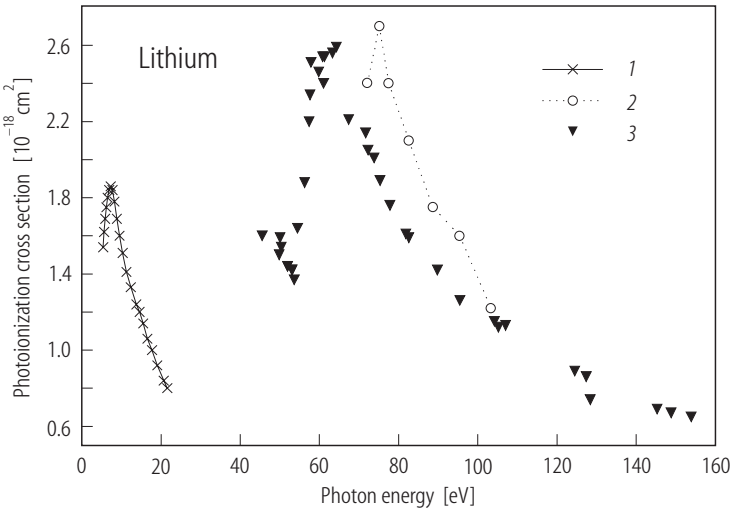

Fig. 13. Cross section for lithium between threshold and 160 eV from *1* [67Hu2] and *2* [82Me1]. The solid state measurements of *3* [62Ba1] are shown for comparison.

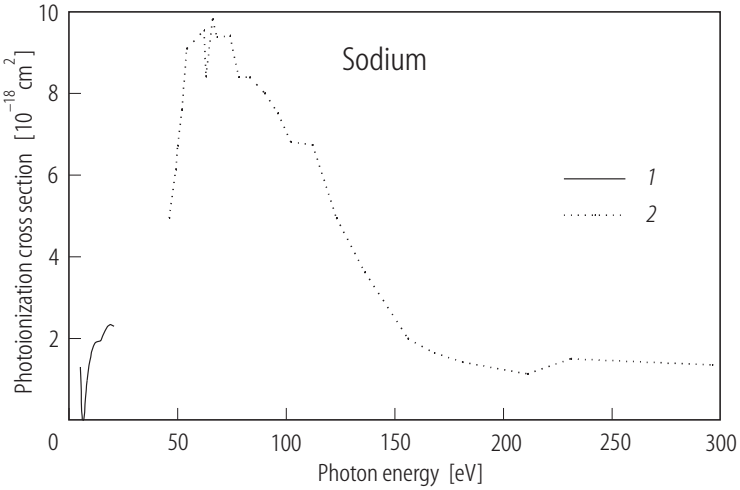

Fig. 14. Cross section for sodium from threshold to 300 eV from *1* [67Hu1, 68Hu1] and *2* [77Co1]. Note that the low energy data is shown multiplied by 10.

Table 35. Attenuation cross section for lithium in the energy ranges from 5.39 to 22.0 eV [67Hu2] and from 75 to 104 eV [82Me1].

Energy [eV]	Cross section [10^{-18} cm^2]	Energy [eV]	Cross section [10^{-18} cm^2]	Energy [eV]	Cross section [10^{-18} cm^2]
5.39	1.54	9.54	1.60	20.66	0.84
5.64	1.62	10.33	1.51	21.56	0.80
5.90	1.69	11.27	1.41	75.1	2.70
6.20	1.75	12.40	1.33	77.5	2.40
6.53	1.80	13.78	1.24	82.6	2.10
6.89	1.84	14.59	1.20	88.6	1.75
7.29	1.86	15.50	1.14	95.4	1.60
7.75	1.84	16.53	1.06	103.3	1.22
8.27	1.78	17.71	1.00		
8.85	1.69	19.07	0.92		

Table 36. Photon attenuation cross section for sodium in the energy range from 5 to 25 eV. From [67Hu2] and [68Hu1].

Energy [eV]	Cross section [10^{-18} cm^2]	Energy [eV]	Cross section [10^{-18} cm^2]	Energy [eV]	Cross section [10^{-18} cm^2]
5.14	0.130	7.29	0.038	13.05	0.192
5.17	0.126	7.51	0.057	13.78	0.193
5.28	0.110	7.75	0.072	14.59	0.195
5.39	0.092	8.00	0.085	15.50	0.207
5.51	0.070	8.27	0.097	16.53	0.219
5.64	0.045	8.55	0.110	17.71	0.230
5.77	0.022	8.86	0.122	19.07	0.240
5.91	0.008	9.18	0.134	20.66	0.230
6.05	0.001	9.54	0.145	20.66	0.250
6.20	0.000	9.92	0.155	21.56	0.240
6.36	0.000	10.33	0.166	22.54	0.230
6.53	0.000	10.78	0.175	23.62	0.220
6.70	0.001	11.27	0.182	24.80	0.190
6.89	0.006	11.81	0.189		
7.08	0.019	12.40	0.191		

Table 37. Photon attenuation cross section for sodium in the energy range between 46 and 290 eV. From [77Co1].

Energy [eV]	Cross section [10^{-18} cm^2]	Energy [eV]	Cross section [10^{-18} cm^2]	Energy [eV]	Cross section [10^{-18} cm^2]
46.00	4.95	68.00	9.38	123.00	4.95
49.00	6.14	74.00	9.42	136.00	3.63
50.00	6.72	78.00	8.40	156.00	2.00
52.00	7.61	83.00	8.40	168.00	1.65
54.00	9.10	90.00	8.01	181.00	1.42
62.00	9.55	96.00	7.52	211.00	1.13
63.00	8.42	102.00	6.81	231.00	1.50
66.00	9.82	112.00	6.75	246.00	1.35

Table 38. Photon attenuation cross section for potassium in the energy range between 5 and 18 eV. and between 25 and 35 eV.

Energy [eV]	Cross section [10^{-18} cm^2]		Energy [eV]	Cross section [10^{-18} cm^2]	
	67Hu1	68Ma1		67Hu1	68Ma1
4.96		0.065 ± 0.005	10.33	0.395	0.21 ± 0.02
5.39	0.060		11.27	0.413	
5.63	0.092		12.40	0.430	
5.90	0.125		13.78	0.460	
6.20	0.157		15.50	0.532	
6.53	0.188		17.71	0.700	
6.89	0.218				76Dr1
7.29	0.250	0.15 ± 0.01			
7.75	0.280		26.3		47.0 ± 9
8.27	0.313		32.5		31.0 ± 7
8.86	0.340		38.0		20.0 ± 4
9.54	0.370				

Table 39. Photoionization cross sections for rubidium and cesium in the energy range below 11 eV. *) value from [80Gr1].

Energy [eV]	Rb cross section [10^{-18} cm^2]		Cs cross section [10^{-18} cm^2]		
	68Ma1	83Su1	68Ma1	77Co2	83Su1
3.89			0.20 ± 0.01		0.10
3.90				0.086 ± 0.02	
3.92					0.095
3.96					0.077
4.00				0.068 ± 0.02	0.076
4.11					0.056
4.13				0.051 ± 0.02	0.054
4.18	0.1 ± 0.005				0.046
4.19		0.105			
4.28		0.062		0.037 ± 0.01	0.037
4.35		0.049			0.034
4.42		0.038			0.028
4.51		0.027			0.025
4.59		0.018			0.025
4.67		0.001	0.06 ± 0.01		0.028
4.76				0.023 ± 0.01	
5.00	0.008 ± 0.003	0.004			0.041
5.06		0.004			0.047
5.16				0.047 ± 0.02	
5.21		0.006			0.060
5.39		0.010			0.080
7.20				0.09 ± 0.027*	
7.28	0.10 ± 0.01		0.23 ± 0.015		
10.20	0.15 ± 0.02		0.33 ± 0.04		

1.2.10 Cross sections for other elements

While there have been a number of measurements of absolute cross sections for other elements made at low energies (below 25 eV) almost invariably these measurements are made in energy ranges where resonant structure dominates the cross section. The only exceptions are higher energy measurements of zinc, cadmium, mercury and chlorine. Data in the resonance ranges for these elements as well as selected data for other elements will be given in Section 1.3.

Harrison et al. [69Ha1] obtained relative data of single ionization of zinc in the energy range from threshold to 50 eV. In a later publication [69Ca1] these data were put on an absolute scale using the low energy measurements of Marr and Austin [69Ma2] and data on the formation of doubly charged ions was obtained. An estimate of the total attenuation cross section obtained from these data are shown in Table 40 in the structure-less range from 20 to 44 eV along with the rms deviance of the measurements.

A complicated structure exists in cadmium in the energy range below 20 eV [68Be1]. At higher energies cross sections for both single and double ionization have been measured [69Ca1] at energies up to 80 eV. Total attenuation has been measured from 20 to 250 eV by Codling et al. [78Co2]. The results of this measurement for energies between 40 and 250 eV are shown in Table 41.

Relative cross sections for the production of singly and doubly charged mercury were measured by Cairns et al. [70Ca1] and these data were normalized by Dehmer and Berkowitz [74De1] to previous data on oscillator strengths. The results in the energy range from 20 to 72 eV of these measurements are given in Table 42.

The cross section for atomic chlorine has been measured from threshold (13 eV) up to 80 eV by Samson et al. [86Sa1]. The results in the energy range from 30 to 80 eV, the range where no structure is expected are shown in Table 43.

Table 40. Photon attenuation cross section for zinc in the energy range between 18 and 51 eV. From [69Ha1] and [69Ca1].

Energy [eV]	Cross section [10^{-18} cm^2]
18.78	3.6 ± 1.2
19.68	4.6 ± 2.4
20.35	5.3 ± 1.3
20.69	4.6 ± 0.7
21.67	6.8 ± 0.8
22.38	6.1 ± 1.7
22.87	7.0 ± 0.4
24.40	7.0 ± 0.7
25.66	9.1 ± 0.9
26.37	8.2 ± 0.8
28.56	9.1 ± 0.9
29.80	12.1 ± 1.1
33.14	9.3 ± 2.0
43.80	12.4 ± 2.3

Table 43. Photoionization cross section for chlorine in the energy range from 30 to 80 eV. From [86Sa1].

Energy [eV]	Cross section [10^{-18} cm^2]
30.99	7.50
33.06	4.60
35.43	2.50
38.15	1.40
41.33	0.94
45.08	0.90
49.59	1.02
55.10	1.19
61.99	1.30
70.85	1.32
78.47	1.29

Table 41. Photon attenuation cross section for cadmium in the energy range between 41 and 250 eV. From [78Co2].

Energy [eV]	Cross section [10^{-18} cm^2]
41.92	12.64
44.23	14.52
50.13	15.76
56.54	16.27
62.56	14.69
66.15	14.44
69.49	14.42
73.08	14.42
78.21	13.88
83.33	12.69
89.36	11.44
95.00	9.81
103.80	7.35
113.80	4.58
124.70	3.78
135.60	1.98
155.10	0.58
167.95	0.51
179.50	0.66
189.70	0.71
193.80	0.99
210.40	1.22
228.70	1.53
247.70	1.83

Table 42. Photon attenuation cross section for mercury in the energy range from 20 to 72 eV. From [70Ca1].

Energy [eV]	Cross section [10^{-18} cm^2]
20.09	13.9
20.36	14.1
20.66	15.8
20.73	16.1
20.80	13.5
21.27	15.1
21.67	14.1
21.79	13.5
22.34	13.9
23.13	13.7
23.61	15.4
24.41	16.4
25.30	15.6
26.66	17.3
27.43	18.5
28.57	19.0
29.52	22.1
33.15	21.2
35.94	22.4
37.01	20.9
38.38	23.4
44.28	22.3
45.58	23.6
50.19	19.6
57.66	19.7
64.57	15.9
71.66	13.2

1.3 Cross sections due to resonances, branching ratios, multiple ionization and angular distributions

In the previous section data were presented for atomic photoionization or absorption in those energy ranges where the cross sections were expected to be slowly varying and consequently some energy ranges were omitted. Here data in those ranges will be given, but will for the most part not be presented in the form of tables, since in resonance regions the observed cross sections are strongly dependent on the instrumental bandpass used in making the measurements.

When single ionization occurs as a result of photoabsorption, the ions left behind may not be in their ground state. This is especially true at higher energies where most of the single ionization is from inner subshells of the atom. When this happens, the ions then decay via a complicated set of decay processes which emit both Auger electrons and fluorescence radiation and the end result is a

distribution of multiply charged ions. When ions and/or electrons are observed following photoabsorption it is possible to obtain information on both the intermediate and final states of the decay process and express the results in terms of branching ratios. Some data of this type will be presented.

Finally, when electrons are observed as a result of photoionizaton, in general their angular distributions will not be isotropic. At low energies the angular distribution of photoelectrons has a simple form and some data on angular distributions will be given.

1.3.1 Cross sections due to resonances

For the rare gases, which form the bulk of the data presented in the previous section, the spectral regions where resonances are expected to occur are well known. For helium, the range is from 60 eV, just below the position of the lowest doubly excited resonance, up to 79 eV., the threshold for direct double ionization. For the heavier rare gases, there will be resonances between the two lowest $^2P_{3/2}$-$^2P_{1/2}$ energy states of the singly charged ion in each case and resonance regions extending from about 10…12 eV below each inner shell ionization potential up to an energy corresponding to removal of both an inner shell and a valence shell electron. The ranges for He, Ne, Ar, Kr and Xe where resonances are expected are shown in Table 44.

For other atoms, the ranges corresponding to inner shell ionization are essentially the same as the rare gases; i.e., from about 10…12 eV below each inner shell ionization potential up to an energy corresponding to double ionization involving an inner shell electron. However, at lower energies resonances occur frequently and must be considered atom by atom.

Table 44. Energy ranges for photoionization in the rare gases where resonant structure is expected to occur.

Gas	Energy range [eV]					
	$^2P_{3/2}$-$^2P_{1/2}$	Inner subshells				
Helium		65-69				
Neon	21.56-21.66	44.0-43.4	860-910			
Argon	15.76-15.93	25.0-38.6	240-310	3200-3250		
Krypton	14.00-14.66	25.0-38.6	90-140	200-310	1650-1950	
Xenon	12.13-13.43	20.0-33.3	60-110	140-250	670-720	930-1200
Xenon						4780-5600

1.3.2 Resonances in helium

Resonances in helium were first discovered by Madden and Codling [63Ma1] in the energy range between 59 and 79 eV via an absorption measurement using synchrotron light and since that time there have been a number of measurements of helium resonances using alternative techniques. Since cross sections are rapidly varying near resonances the normal procedure has been to present graphs of cross sections or of transmitted intensity or observed ion or electron yields rather than try to give values of the cross section in tabular form. An example is shown in Fig. 15 in the resonance range between 59 and 66 eV [91Ch1]. The measurement here was an electron impact experiment at low

momentum transfer, but the results are expected to be equivalent to an absorption measurement. The results shown are in very good agreement with the recommended values of Samson et al. [94Sa1] as is shown in Table 45 which compares the results at energies between the resonances where the cross section is slowly varying.

It is important to note that the cross sections reported as in Fig. 15 are not "true" cross sections, but depend on the spectral resolution used in making the measurements. Due to the finite resolution the "true" cross section will always be larger than that reported at the peak of resonance and smaller at its minimum.

Higher resolution studies (see Fig. 16) have shown that unresolved structure exists at higher energies than is evident in Fig. 15. This means that if resonances are present the results only indicate the average cross section over the bandwidth of the measurement.

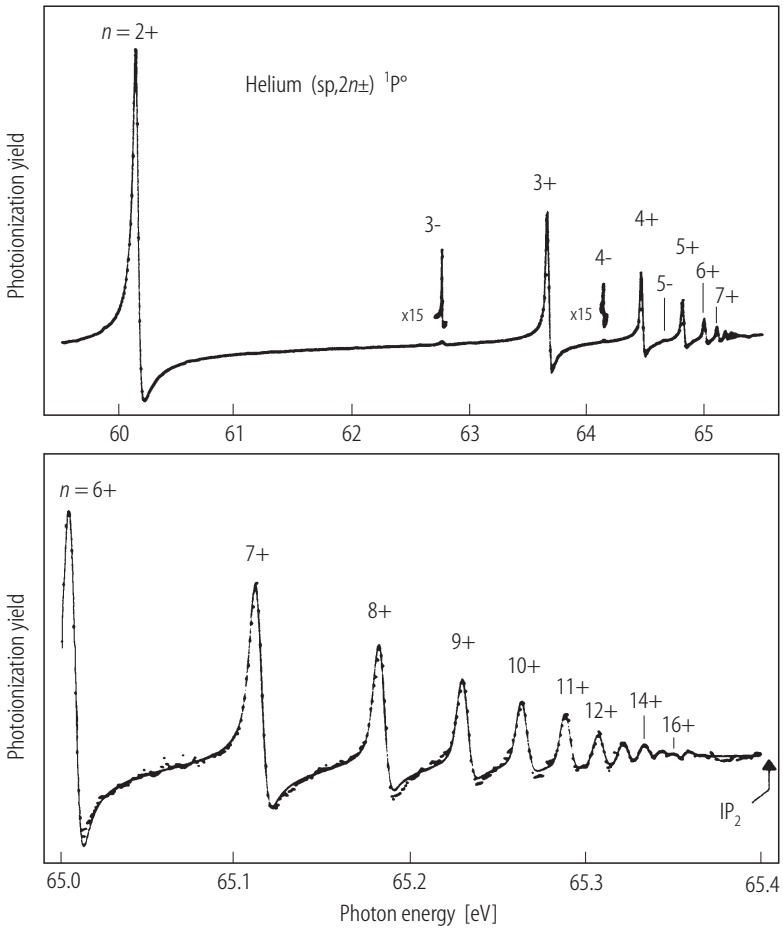

Fig. 16. Cross section for helium in the resonance region between 60 and 65.4 eV from [91Do1].

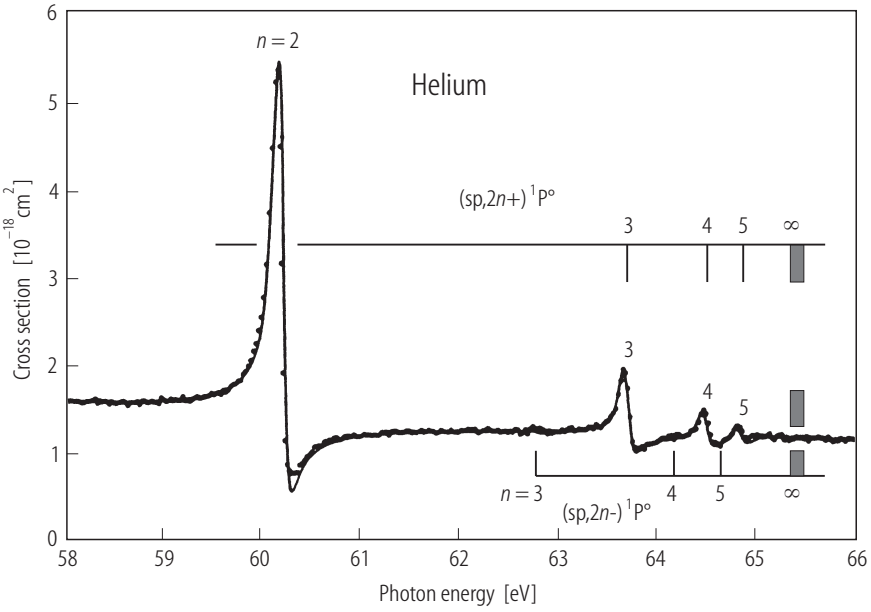

Fig. 15. Cross section for helium in the resonance region between 59 and 66 eV from [91Ch1].

Table 45. A comparison of measured cross sections of helium in the non-resonance range from 66 to 69 eV.

Energy [eV]	Cross section [10^{-18} cm^2]	
	94Sa1	91Ch1
66.0	1.15	1.15
67.0	1.11	1.10
68.0	1.06	1.06
69.0	1.02	1.02

1.3.3 Resonances between the two lowest ionization thresholds of the rare gases

For neon, argon, krypton and xenon removal of an outer subshell electron can leave the ion core in two possible states with a slight energy difference. Consequently, there will be two series of resonances in each case converging to the limit of higher energy as discovered by Beutler [35Be1].

For neon, the interval between the two limits is small (0.1 eV) and the structure has been observed by a number of techniques. Fig. 17 shows a measurement of the apparent cross section for neon taken with a band pass of 0.045 Å [79Ra1] and observing ions produced. Similar measurements were made at higher resolution observing both ions and electron for the lower energy part of the resonant region [90Ca1].

Since the early work of Beutler there have been a number of measurements of the resonances between the two lowest limits for argon, krypton and xenon. For these resonances, a careful measurement and an analysis of previous work have been carried out by Maeda et al. [93Ma1]. For the low energy resonances they obtained resonance parameters for each pair of resonances using the following formulas:

$$\sigma = \frac{\sigma_{as}(\varepsilon_s + q_s)^2}{1+\varepsilon_s^2} + \frac{\sigma_{ad}(\varepsilon_d + q_d)^2}{1+\varepsilon_d^2} + \sigma_b \quad (1)$$

$$\varepsilon_l = \frac{\tan[\pi(\nu_{1/2} + \mu_l)]}{W_l} \qquad \text{for } l = \text{s, d} \quad (2)$$

where the parameters σ_{as}, σ_{ad} and σ_b are partial cross sections, q_s and q_d are shape parameters, ε_l (l = s, d) are reduced energies and the parameters μ_l and W_l determine the energy position of the resonance relative to $\nu_{1/2}$, the energy (in cm^{-1}) of the upper series limit. The parameters for the lower resonances in each case along with estimates from other recent measurements are shown in Table 46.

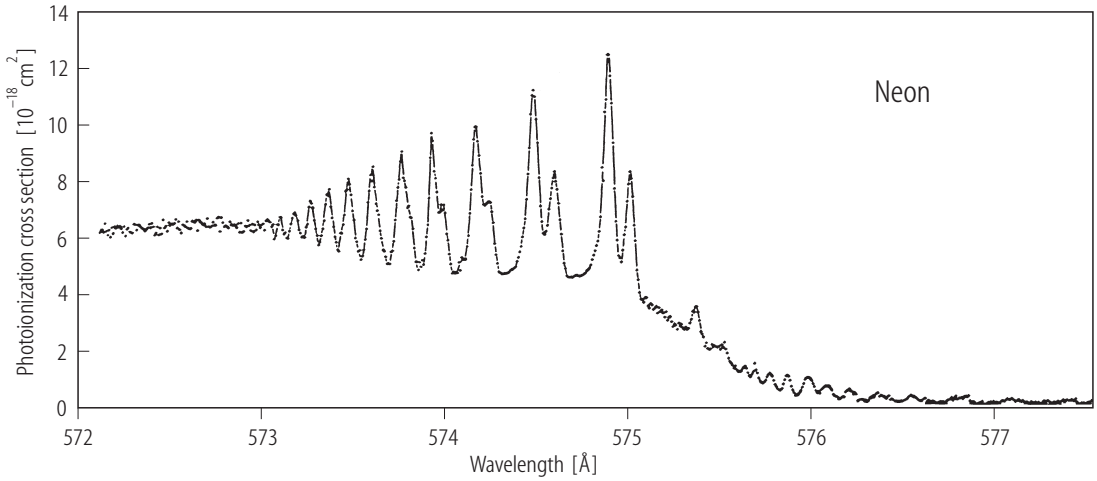

Fig. 17. Ionization yield for neon in the resonance region between 577 and 572 Å (21.5-21.7 eV) [79Ra1].

Table 46a. Energy width parameters W_s and W_d for argon, krypton and xenon resonances [93Ma1].

Atom	n	W_s	W_d	Atom	n	W_s	W_d
Argon	11	0.00544(65)	0.2122(70)		13	0.00911(85)	0.2070(55)
	12	0.00524(80)	0.2245(80)		14	0.00967(120)	0.2089(55)
	13	0.00438(100)	0.2296(90)	Xenon	8	0.00732(35)	0.2505(60)
	14	0.00461(130)	0.2258(90)		9	0.00657(40)	0.2465(65)
Krypton	8	0.00989(50)	0.1561(55)		10	0.00657(35)	0.2499(65)
	9	0.00952(55)	0.1741(55)		11	0.00642(50)	0.2499(65)
	10	0.00949(55)	0.1894(55)		12	0.00651(60)	0.2448(65)
	11	0.00938(60)	0.2040(50)		13	0.00645(80)	0.2505(65)
	12	0.00942(65)	0.1946(50)		14	0.00653(105)	0.2608(65)

Table 46b. Line shape parameters μ_1, q_1, σ_{al} and σ_1 for argon, krypton and xenon resonances [93Ma1].

Atom	n	μ_s	μ_d	q_s	q_d	σ_{as}	σ_{ad}	σ_b
Argon	11	0.138(1)	0.199(4)	14.8(5.1)	2.14(15)	1.28(80)	9.9(1.5)	9.5(1.5)
	12	0.137(1)	0.202(3)	16.5(6.8)	2.06(20)	0.96(75)	10.1(1.0)	10.7(2.0)
	13	0.139(1)	0.202(2)	14.8(6.5)	2.02(20)	1.21(85)	9.9(2.0)	11.1(2.0)
	14	0.136(1)	0.198(2)	15.9(6.5)	2.29(25)	0.91(75)	8.3(2.0)	11.9(3.0)
Krypton	8	0.099(1)	0.223(3)	36.9(6.5)	1.94(10)	0.20[10)	20.5(2.0)	11.7(1.5)
	8	0.097(1)	0.223(3)	23.2(5.0)	1.90(10)	0.45(20)	20.9(2.0)	12.8(2.0)
	10	0.096(1)	0.227(3)	26.0(5.0)	1.84(10)	0.34(15)	21.6(2.5)	11.2(1.5)
	11	0.095(1)	0.235(3)	19.2(3.5)	1.66(20)	0.61(20)	25.5(4.0)	9.1(3.5)
	12	0.094(1)	0.240(2)	25.5(5.5)	1.76(15)	0.31(15)	22.3(2.5)	11.1(2.0)
	13	0.094(1)	0.241(2)	21.4(4.0)	1.74(15)	0.46(15)	22.5(3.0)	11.0(2.0)
	14	0.094(1)	0.243(1)	25.5(5.5)	1.71(15)	0.27(15)	22.0(2.5)	11.2(2.0)
Xenon	8	0.025(1)	0.323(3)	22.7(6.0)	1.49(5)	0.66(35)	43.3(3.0)	6.8(3.0)
	9	0.021(1)	0.328(3)	15.8(2.5)	1.47(10)	1.33(45)	44.9(3.0)	6.3(3.0)
	10	0.019(1)	0.332(2)	13.9(2.5)	1.45(10)	1.65(55)	45.4(2.5)	5.3(2.0)
	11	0.017(1)	0.335(2)	13.2(2.5)	1.40(10)	1.97(65)	46.4(3.0)	5.9(2.0)
	12	0.016(1)	0.331(1)	15.3(3.0)	1.53(10)	1.32(55)	42.4(4.0)	8.7(1.5)
	13	0.014(1)	0.332(1)	14.7(2.5)	1.47(10)	1.35(55)	42.8(3.5)	7.1(2.0)
	14	0.014(1)	0.332(2)	17.6(3.0)	1.41(10)	0.90(35)	43.6(3.0)	7.7(2.0)

1.3.4 ns and doubly excited resonances in neon, argon, krypton and xenon

For the heavier rare gases a single series of autoionizing resonances converge to the inner *n*s subshell limits (n = 2, L_1 for neon, n = 3, M_1 for argon, etc.) which lie between 20 and 30 eV above the neutral ground state. In addition there are doubly excited resonances in each case which are intermingled with the series of s subshell resonances.

As example of a measurement of the photoionization cross section in the resonance region of neon between 40 and 55 eV is shown in Fig. 18 [92Ch1]. Here, as Fig. 15, the measurement was done by electron impact at low momentum transfer, but the results agree reasonably well with photoionization data obtained by direct measurement [65Sa1] as shown in the figure.

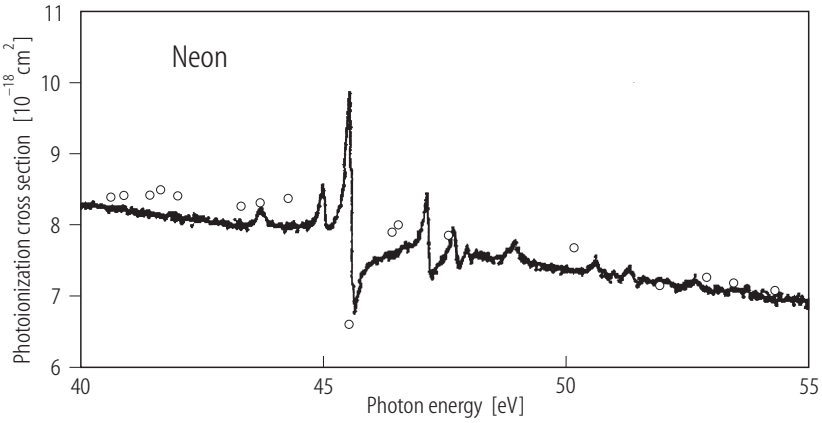

Fig. 18. Cross section for neon in the resonance region between 40 and 55 eV [92Ch1]. Circles are from [65Sa1].

As in the previous sections, the figure shows only an "apparent" cross section since the true cross section will be considerably larger (or smaller) in the vicinity of the resonances. Similar data for argon and krypton in the energy ranges from 25…31 and 22…31 eV is shown in Fig. 19 [63Sa1].

Although there have been few attempts to obtain absolute photoionization cross sections near resonances, the wavelengths (and therefore energies) of a number of the rare gas ns-np and doubly excited resonances are known (neon [67Co1]; argon [69Ma1]; krypton and xenon [72Co1]). Ederer [71Ed1] has obtained resonance parameters for some of the lower lying resonances in krypton and xenon and his analysis has been extended by Flemming et al. [91Fl1]. The analysis is similar to that of Maeda et al. and makes possible a representation of the true cross section in resonance regions.

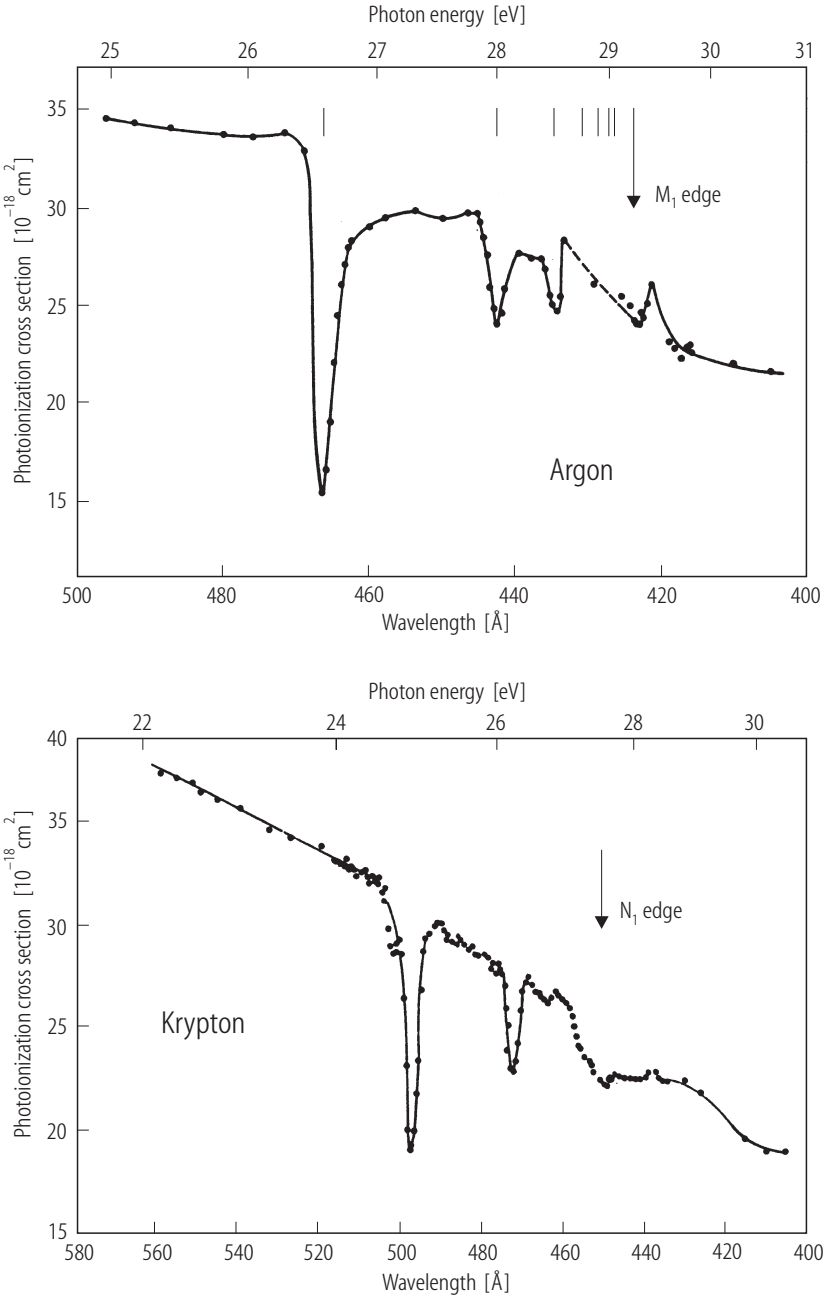

Fig. 19. Cross sections for argon and krypton in the resonance regions between 25-31 and 22-31 eV [63Sa1].

1.3.5 Deep inner shell resonance regions

In the vicinity of each inner shell ionization threshold in the rare gases, there will be a series of singly excited resonances below the limit and possibly doubly excited resonances in the energy range up to approximately 50 eV above the threshold. Typically these resonances are much weaker than those discussed in the previous sections and have larger widths due to the fact that the resonances can decay via a number of radiative and autoionization processes. As a result, measurements of total cross sections in the vicinity of inner shell thresholds are probably a more accurate estimate of the true cross section than those made at lower energies. A typical example is data near the K ionization threshold of neon, shown in Fig. 20 [69Wu1]. The resonances represent a series of single electron 1s-*n*p transitions (P3-P6) lying below the 1s ionization potential (870.1 eV). There is evidence for a double excitation resonance at higher energy (35 eV above the P3 peak in Fig. 20) but the resonance is less than 2 % of the observed apparent cross section. Values of the total absorption cross section in the vicinity of the ionization limit are given in Table 47.

The situation is similar for the energy ranges near the $L_{2,3}$ (240…260 eV) and K (3206 eV) thresholds of argon. Fig. 21 shows a high resolution measurement of the cross section just below the $L_{2,3}$ thresholds [81Gi1] and Table 48 gives data taken at lower resolution [69De1]. Evidence of the resonant structure near the K threshold of argon [83De1] is shown in Fig. 22 and cross section data in this energy range [Wu6901] are given in Table 49.

For the inner subshells of the heavier rare gases there is little evidence of structure near absorption thresholds since any discrete levels that exist are broadened by the many Auger and radiative decay processes that can occur. Thus the data shown in Tables 24 and 25 for krypton probably represents true cross sections at the energies listed. The same is true of the data for xenon shown in Tables 29 and 30. Arcon et al. [95Ar1) have made a detailed measurement of the attenuation cross section of xenon from 4700 to 6200 eV. They find that resonances never produce deviations larger than 3 % from a smooth energy dependence of the cross section.

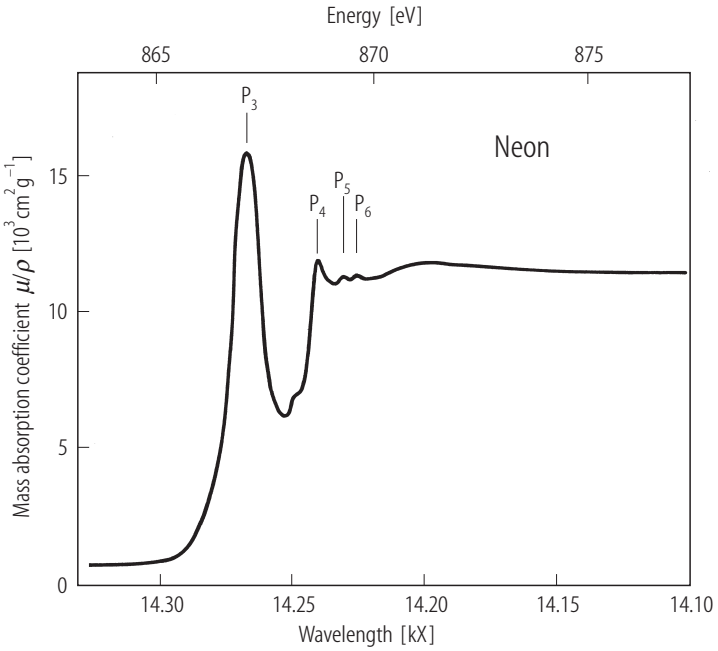

Fig. 20. Cross section for neon near the 1s ionization potential (870.1 eV) from [69Wu1].

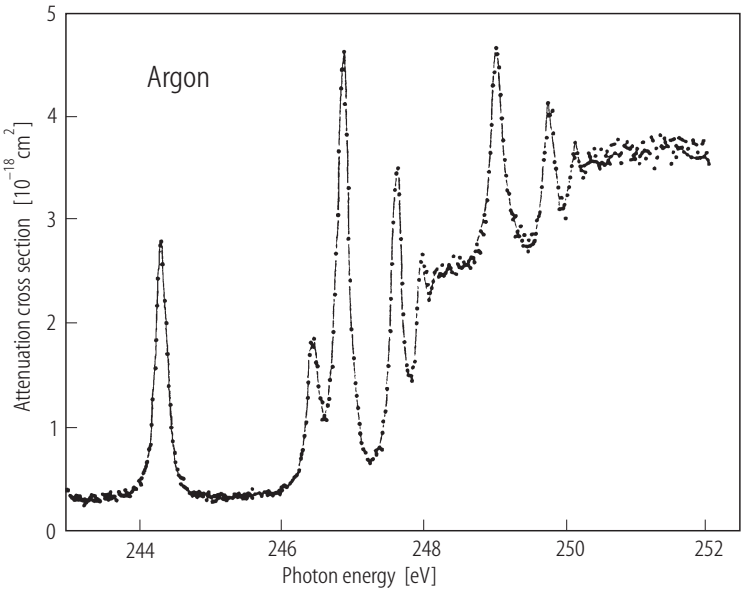

Fig. 21. Cross section for argon near the $L_{2,3}$ edges [81Gi1].

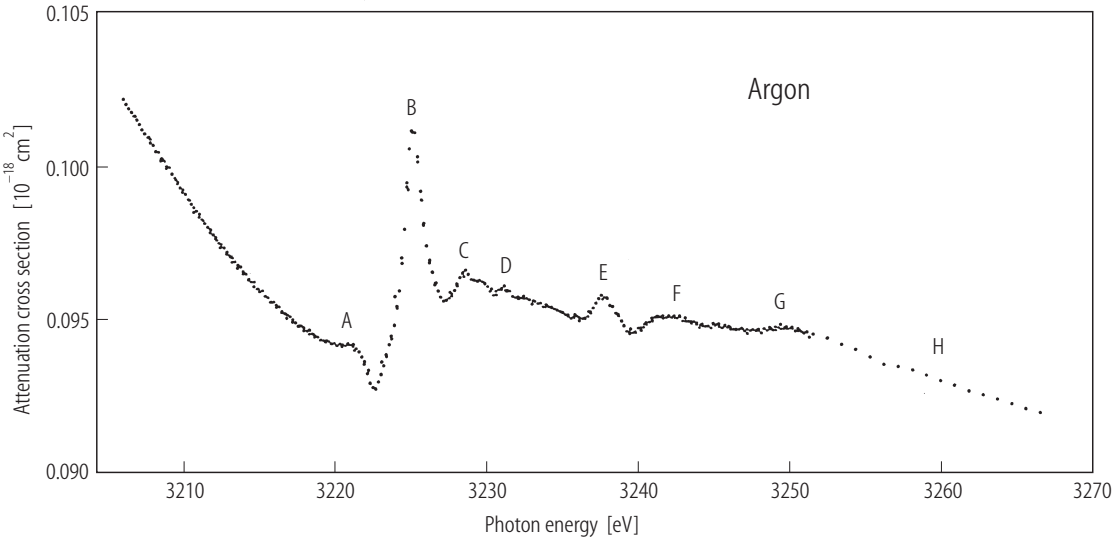

Fig. 22. Cross section for argon in the resonance range between 3205 and 3250 eV [83De1].

Table 47. Apparent photon attenuation cross sections for neon near the K absorption threshold [69Wu1].

Energy [eV]	Cross section [10^{-21} cm^2]	Energy [eV]	Cross section [10^{-21} cm^2]	Energy [eV]	Cross section [10^{-21} cm^2]
830.0	25.9	859.0	24.2	890.0	362.0
836.0	25.3	865.0	23.8	896.0	355.0
842.0	24.9	871.0	387.0	903.0	349.0
847.0	24.7	877.0	373.0	910.0	342.0
853.0	24.4	884.0	368.0		

Table 48. Apparent photon attenuation cross sections for argon near the $L_{2,3}$ absorption thresholds [69De1].

Energy [eV]	Cross section [10^{-18} cm^2]
240.0	0.31
241.0	0.35
242.0	0.35
243.0	0.39
244.0	0.44
245.0	1.11
246.0	0.72
247.0	1.18
248.0	1.86
249.0	1.73
250.0	3.81
251.0	4.27
252.0	4.59
253.0	4.68
254.0	4.62
255.0	4.58
256.0	4.48
257.0	4.37
258.0	4.29
259.0	4.20
260.0	4,14
261.0	4.07
262.0	4.03
263.0	4.03

Table 49. Apparent photon attenuation cross sections for argon near the K absorption threshold [69Wu1].

Energy [keV]	Cross section [10^{-21} cm^2]
3.017	11.4
3.054	10.6
3.093	10.3
3.132	10.1
3.172	10.0
3.196	9.7
3.205	98.8
3.213	93.7
3.255	91.0
3.299	88.9
3.343	85.9
3.389	83.7
3.436	79.1
3.485	77.3
3.534	74.2
3.586	72.2
3.638	69.6
3.693	66.9
3.749	64.5

1.3.6 Resonance regions in oxygen and nitrogen

Since these are open shell atoms, when ionization occurs the ion core can be left in a number of states and there will be resonant structure at energies lying just below the higher ionization thresholds. For oxygen the lowest ionization threshold is 13.61 eV but higher thresholds are at 16.93, 18.63 and 18.49 eV. The resonance structure below the 16.93 and 18.63 eV thresholds has been observed [67Hu3] and relative cross sections near these thresholds have been obtained [73De1]. For nitrogen the lowest ionization threshold is 14.54 eV and higher thresholds are at 16, 44, 18.59 and 20.4 eV. However, due to selection rules, no structure is expected below the 16.44 and 18.59 eV thresholds and none has been observed, but a single series of resonances has been observed between 17.7 and 20.4 eV and relative cross sections obtained the resonance region [74De2]. Cross sections for both oxygen [85Sa1, 88An1] and nitrogen [90Sa1] have been measured in the energy ranges where resonances are present and are shown in Table 50 and 51, respectively. The measurements shown are at energy values which do not correspond to known resonance positions and thus the values shown are expected to be true cross sections.

Table 50. Total photoionization cross sections for oxygen in the energy range between 13.7 and 25.4 eV. From [88An1].

Energy [eV]	Cross section [10^{-18} cm^2]
13.78	2.85
14.25	3.10
14.50	3.10
14.93	3.30
15.02	3.30
15.79	3.70
15.89	3.70
16.20	4.00
16.31	3.90
16.98	8.03
17.04	8.90
17.32	9.24
17.48	9.71
17.87	9.00
17.95	9.47
18.30	10.0
18.78	12.6
19.68	13.4
20.66	13.3
21.37	13.0
22.14	12.7
22.54	12.5
23.00	12.3
23.40	12.1
23.80	12.0
24.31	11.9
24.80	11.9
25.30	12.0

Table 51. Photoionization cross sections for nitrogen in the energy range between 14 and 44 eV. From [90Sa1].

Energy [eV]	Cross section [10^{-18} cm^2]
14.6	9.5
14.8	10.2
15.1	10.6
15.5	10.8
15.9	11.1
16.3	11.4
16.8	11.6
17.2	12.1
17.7	13.5
20.3	11.6
20.7	11.7
21.7	11.8
22.1	11.8
23.0	11.7
23.8	11.5
24.8	11.2
25.8	10.8
27.0	10.5
28.2	10.0
29.5	9.6
31.0	9.1
32.6	8.6
34.4	8.1
36.5	7.5
38.7	6.9
41.3	6.3

1.3.7 Resonances in the alkalis

Resonances have been observed near inner subshell ionization thresholds in lithium, sodium and potassium. In lithium there are autoionization resonances due to excitation of a single K shell electron which were first observed by Ederer et. al. [70Ed1]. Absolute measurements of the apparent cross sections in the resonant range between 58.91 eV (the position of the lowest resonance) and 81 eV. (the double ionization threshold were made by Mehlman et al. [78Me1, 82Me1]. The results in the energy range from 62 to 72 eV (200…172 Å) are shown in Fig. 23. More recently the resonance structure has been studied in detail in the energy range between 64.5 and 68 eV [96Ki1] and the results were found to agree closely with theoretical calculations [97Ch1].

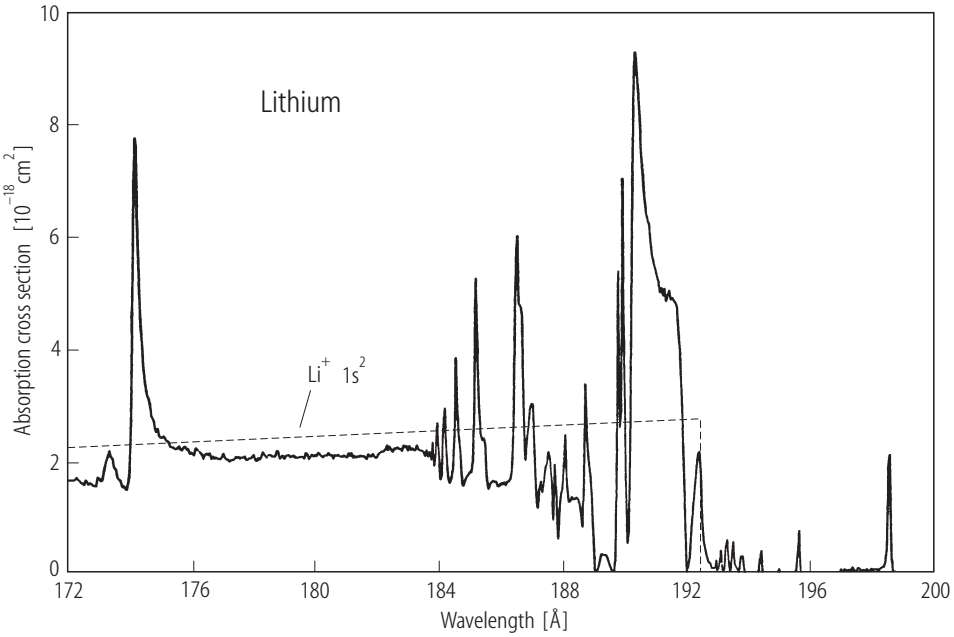

Fig. 23. Cross section for lithium in the resonance region between 200 and 172 Å (62-72 eV) from [78Me1]. The line labeled Li^+ $1s^2$ is from theory [79Re1].

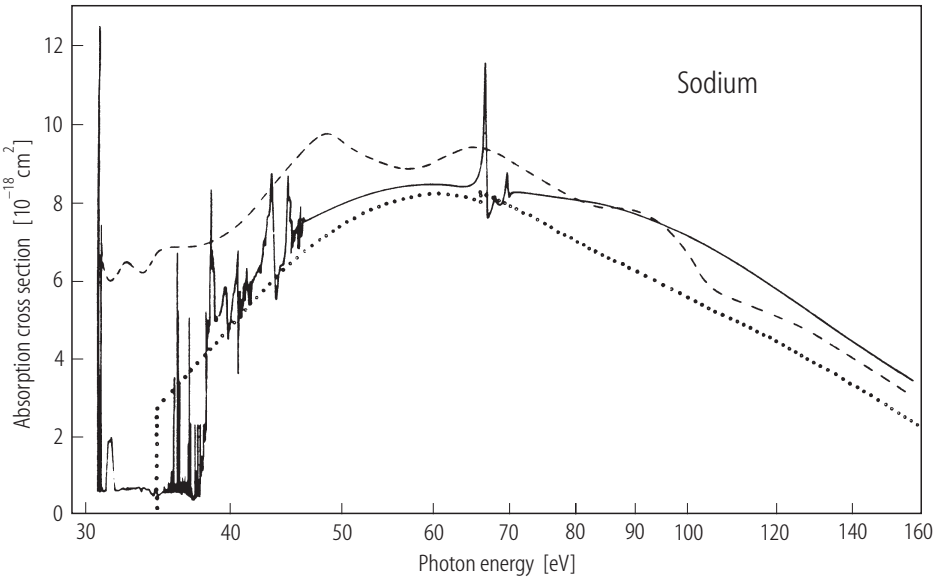

Fig. 24. Cross section for sodium in vapor (solid line) and solid (dashed line) phases compared with an atomic calculation (dotted line) from [72Wo1].

There is also a resonance region corresponding to excitation of two K shell electron which has been studied recently by a number of theoretical and experimental groups [96Wu1]. Resonances have been observed between 142.3 eV (the position of the lowest resonance [94Ki1] and 175.3 eV [97Az1]. Although it is possible that other resonances exist below the double ionization potential (203.4 eV), none have been observed.

Wolff et al. [72Wo1] have observed resonant structure for Na in the energy range between 35 and 75 eV in a relative measurement and a comparison of their results with solid state absorption and theory is shown in Fig. 24. Note that the normalized scale of the figure yield results approximately a factor of two higher than the results of Codling et. al. [77Co1] shown in Table 37.

Structure similar to this has been observed photographically in both potassium [34Be1] and rubidium [34Be2]. Hudson and Carter [67Hu1] have measured the apparent cross sections at the peaks of several of the resonances in potassium in the energy range between 18 and 21 eV.

For cesium Peterson et. al. [75Pe1] made a measurement of the relative cross section between 80 and 180 eV and found structure between 80 and 100 eV and between 160 and 180 eV.

1.3.8 Resonance regions in other elements

There have been a number of measurements of relative cross sections for elements other than those discussed above. Most of the earlier work was directed towards identifying resonances and was done with absorption measurements using photographic plates for detection with little or no attempt to derive relative cross sections. Later work involved ion and/or electron collection as well as attempts to obtain absolute cross sections from absorption measurements. A summary of this type of work for selected elements is given below.

Resonance structure was first observed in zinc by Beutler [33Be1]. A measurement of the absorption cross section in the energy range from threshold (9.39 eV) to 16.6 eV was made by Marr and Austin [69Ma2]. They find that the cross section at threshold is $(1.1 \pm 0.2)\cdot 10^{-18}$cm^2 and falls to a near zero minimum at 10.33 eV and there is a detailed resonance structure at higher energies. They report apparent cross sections over the entire energy range.

Ross and Marr [65Ro1] measured the absorption cross section for cadmium from threshold (9 eV) to 10.8 eV and found a threshold value of $(0.32 \pm 0.03)\cdot 10^{-18}$cm^2 and a decreasing cross section. The relative photoionization cross section from threshold to 19 eV was measured by collecting ions by Berkowitz and Lifshitz [68Be1] and the relative strengths of the resonances in the energy range from 10 to 18 eV previously identified by Beutler [33Be2] were reported. The work of Ross and Marr was extended by Marr and Austin [69Ma3] who measured the absorption cross section from threshold to 23.6 eV. They report apparent cross sections in the energy range between 13 and 23.63 eV.

Berkowitz and Lifshitz [68Be1]also obtained relative photoionization cross sections for mercury in the range between threshold (10.5 eV)and 18 eV and have identified a number of resonances in that range but no attempt was made to obtain absolute cross sections.

Chlorine is similar to atomic oxygen in that although the first ionization potential is at 13.01 eV., the ion can be left in excited states corresponding to higher thresholds of 14.45, 16.47 and 24.57 eV. Consequently there will be a complex resonant structure at energies immediately below these thresholds and structure has been observed via absorption measurements between 13 and 16.3 eV [83Ru1] and in photoelectron measurements in the energy ranges between 21.5 and 25 eV [92Me1]. Samson et al. [86Sa1] have measured the cross section at selected points in this energy range and at higher energies as shown in Table 43 and have assumed that the cross section is smoothly varying to obtain cross sections at specific energies. Their results are shown in Table 52.

The ionization threshold of barium is at 5.21 eV but there are a number of thresholds for ionization plus excitation extending up to 10.5 eV. Consequently, there is a complex resonant structure in this energy range which has been observed photographically [59Ga1, 73Br1]. Absolute cross sections were measured by Hudson et al. [70Hu1] between threshold and 7.3 eV and relative measurements were made by Saloman et al. [85Sa2] and the range was extended to 10.5 eV. Barium has a resonance at threshold and consequently the cross section is quite large in the threshold region. Carlsten and McIlrath [73Ca2] obtained a value at threshold of $5.6\cdot 10^{-17}$cm^2 which agrees with an estimate made by Armstrong and Wynn [79Ar1] based on their oscillator strength measurements but indicates that the absolute measurements of the cross sections by Hudson et al. are probably too low.

At higher energies relative photoabsorption and photoionizaton cross sections have been determined in the energy range from 85 to 140 eV. These data have recently been placed on an absolute basis by a careful measurement by van dem Borne et al. [95Bo1]. The results are shown in Fig. 25.

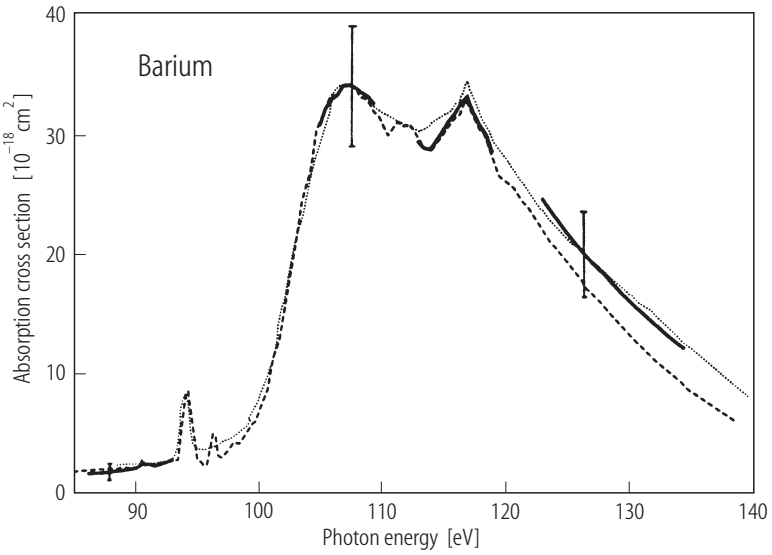

Fig. 25. Absolute cross section of barium from 90 to 130 eV from [95Bo1].

Table 52. Apparent photoionizaton cross section for chlorine in the energy range from 13.0 to 30 eV. From [86Sa1].

Energy [eV]	Cross section [10^{-18} cm^2]	Energy [eV]	Cross section [10^{-18} cm^2]
16.42	43.6	21.56	38.0
17.10	43.4	22.54	35.7
17.71	43.0	23.01	32.2
18.37	42.4	24.79	25.8
19.07	41.6	26.10	20.2
19.83	40.6	27.55	15.3
20.66	39.4	29.17	11.0

1.3.9 Branching ratios and angular distributions

The data presented in the preceding sections is, for the most part, cross sections for photo absorption in energy ranges where photoionization is the most important process. If measurements are made with monochromatic photon sources and either ions or electrons collected, it is possible to break down the total absorption cross section into a number of partial cross sections. With ion collection it is possible to measure cross sections for single,double and in general *n*-fold ionization and the total photoionization cross section will be the sum of these partial cross sections. When electrons are collected and their energy is specified, it is possible to obtain an alternative partitioning of the total photoionization cross section. Since energy is conserved, the difference between photon and electron

energy completely specifies the final state of the ion when a single electron is emitted. Thus by observing "main lines" in the photoelectron spectrum as photon energy is scanned, cross sections for single ionization of individual atomic subshells may be obtained. Alternatively, by observing "satellite lines" cross sections for ionization plus excitation or for double ionization may be measured. However, it is more difficult to obtain total photoionization cross sections via this technique for the following reasons. First, if multiple ionization occurs electrons must be collected over all energies allowed by conservation of energy. Second, typically electrons are collected at fixed angles with respect to the photon beam and its principal axis of polarization. Although at low energies the angular distribution of electrons ejected via photoionization relative to the photon beams polarization direction may be described by a single energy dependent parameter or, if the photon beam is unpolarized, to its direction, in general the photon polarization must be specified in order for cross sections measured at a "magic angle" to represent true partial cross sections. At higher energies corresponding to inner shell ionization measurements in general depend on both the direction and polarization of the photon beam and obtaining true partial cross sections is more difficult.

Although there has been a great deal of experimental work during the past several decades devoted to obtaining partial cross sections and electron angular distributions, most of the results have been presented in graphical form. Some of these results will be presented here and some references to alternative sources of data will be given in the appendix.

1.3.9.1 The ratio of double to single ionization for helium

Helium is the simplest atom which can be doubly ionized and the ratio of double to single ionization has been studied extensively by a number of groups and has been reviewed for both photon and charged particle impact recently [95MG1]. Helium is unusual in that at photon energies above 1 keV most of the cross section is due to scattering rather than absorption and there is considerable theoretical interest in the ratio at high energies.

A summary of experimental work on the ratio in the energy ranges between the double ionization threshold (79 eV) and 350 eV where photoionization is the dominant process and between 2 and 20 keV where ionization is due mainly to Compton scattering is given by Figs. 26 [98Sa1] and 27 [96Le1]. The ratio is less than 5 % at all energies and is between 1 and 2 % at high energies. More recent work [96Do1] and [96Sp1] indicates that the maximum of the ratio at low energies is less than 4 % and of the order of 1 % at higher energies.

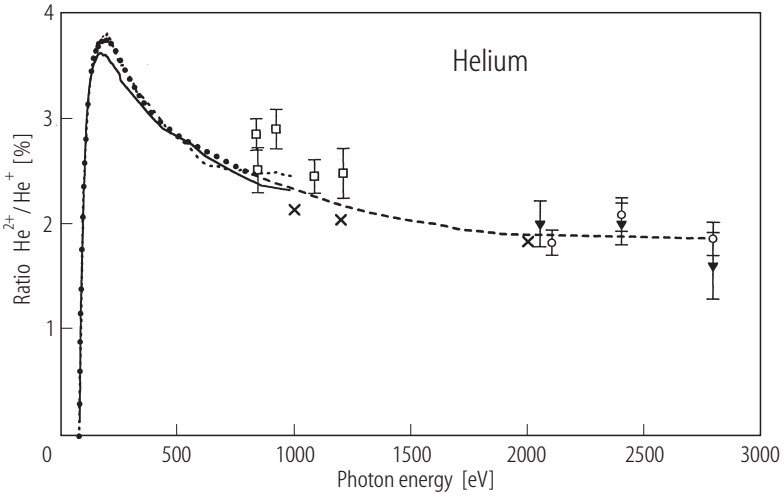

Fig. 26. Ratio of helium double to single ionization threshold (79 eV) to 3 keV from various sources [98Sa1].

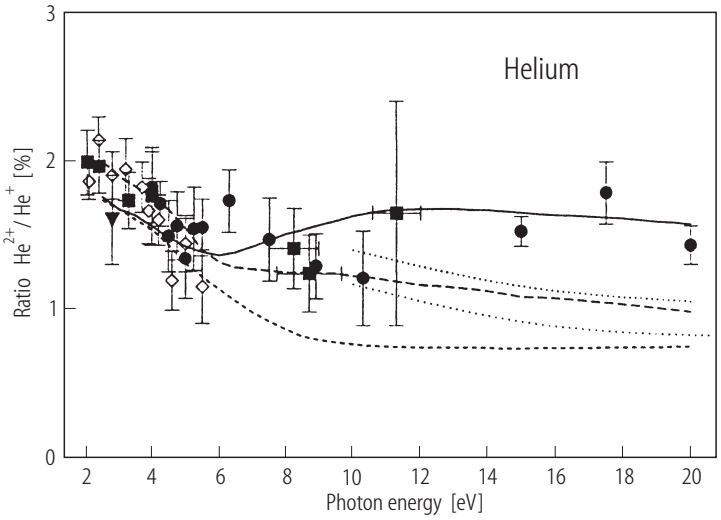

Fig. 27. Ratio of helium double to single ionization from 2 to 20 keV from various sources [96Le1].

1.3.9.2 Branching ratios for light elements

Although branching ratios between single, double and multiple ionization have been obtained by measuring the charge state of ions collected following photoionization for a number of elements, only for the light elements at low energies do the measurements reflect simple direct ionization processes. This is because at higher energies inner subshell ionization occurs followed by a cascade of radiative and Auger processes. Consequently the measured branching ratios must be interpreted in terms of cross sections for initial subshell ionization and relative probabilities for Auger and radiative decay processes. For neon, oxygen and nitrogen Auger processes cannot occur at energies below the 1s (K) shell ionizaton thresholds (865, 538 and 403 eV, respectively) and radiative processes are negligible. Consequently for these atoms measurements of the ratios of ions produced is a measure of direct multiple ionization.

There have been a number of measurements of the cross section for double ionization of neon between the threshold for double ionization (62.63 eV) and 280 eV and the results of various authors are shown in Fig. 28. Typically branching ratios of singly and doubly charged ions are measured and the results are put on an absolute scale by assuming that the total absorption cross section is the sum of single and double ionization cross sections. Samson and Angel [90Sa2] and Holland et al. [79Ho1] have made estimates of the double ionization cross section and their data is shown in Table 53 based on alternative values of the total cross section. Samson and Angel [88An1, 90Sa1,90Sa2] have measured the branching ratios for oxygen and nitrogen from their double ionization thresholds (48.76 and 44.15eV, respectively) to 280 eV. Using their total cross sections given in Tables 33 and 34 and their branching ratios, they have obtained cross sections for double ionization of oxygen and nitrogen and triple ionization of oxygen. Their results are given in Table 54.

Although the cross sections for double ionization of these elements are small near threshold they account for approximately 10 % of the total cross section at energies greater than 50 eV above the double ionization threshold.

Branching ratios for argon have been measured by a number of investigators and some of the earlier results for double ionization are shown in Fig. 29. For argon double ionization via Auger processes cannot take place at energies below 250 eV so the results shown in Fig. 29 represent direct double ionization. Cross sections for single, double and triple ionization in the energy range from 55 to 280 eV have been obtained by Holland et al. [79Ho1] by normalizing measured branching ratios to the total cross sections of Marr and West [76Ma1] and their results are given in Table 55. Although the double ionization cross sections are small they represent a large fraction of the total

cross sections at energies greater than 50 eV above the threshold. The double ionization cross section increases rapidly at 250 eV due to L sub shell ionization followed by Auger decay.

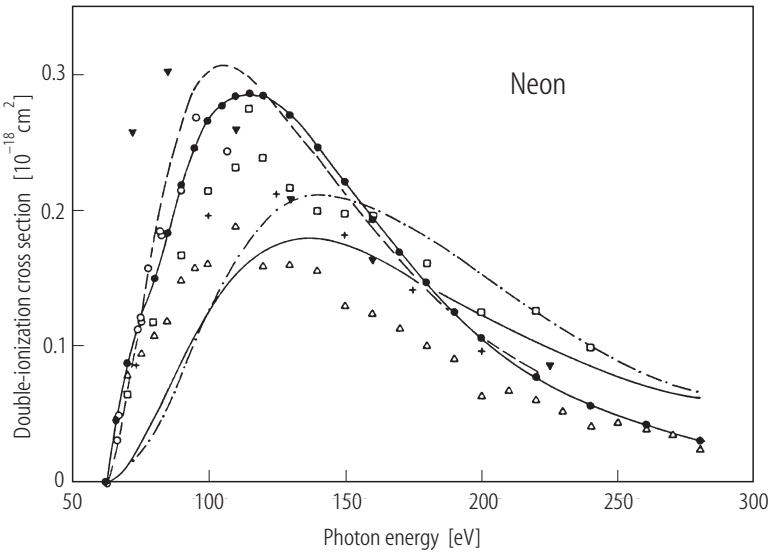

Fig. 28. Measurements of the cross section for neon double ionization from threshold (62.63 eV) to 280 eV from various sources [90Sa2].

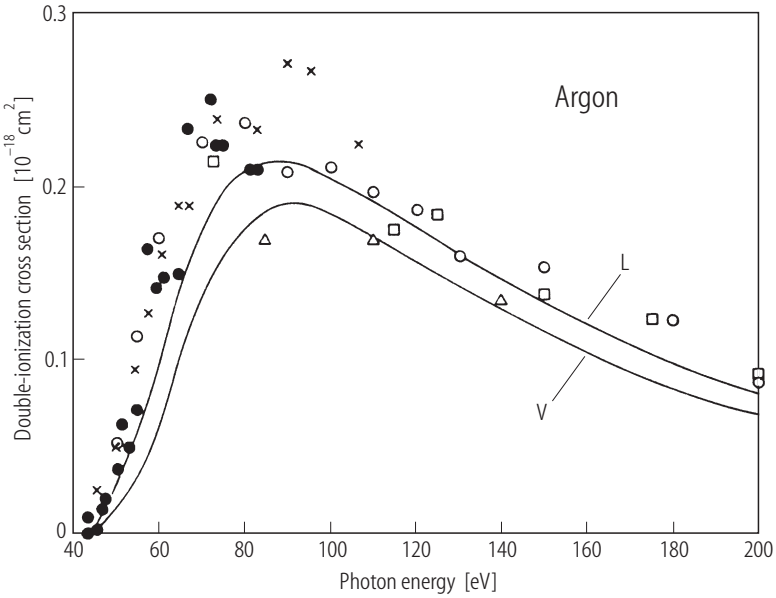

Fig. 29. Double ionization cross section for argon from various sources [A5]. Solid lines represent calculations: dipole-length (*L*) and velocity (*V*) approximation.

Table 53. Double ionization cross sections for neon at incident energies between 70 and 280 eV.

Energy [eV]	Cross section [10^{-18} cm^2]		Energy [eV]	Cross section [10^{-18} cm^2]	
	90Sa2	79Ho1		90Sa2	79Ho1
70.0	0.087	0.081	150.0	0.221	0.149
75.0	0.118	0.098	160.0	0.194	0.142
80.0	0.149	0.112	170.0	0.169	0.129
85.0	0.183	0.126	180.0	0.147	0.115
90.0	0.219	0.158	190.0	0.125	0.104
95.0	0.246	0.170	200.0	0.106	0.076
100.0	0.266	0.177	220.0	0.077	0.070
110.0	0.284	0.210	240.0	0.056	0.046
120.0	0.283	0.178	260.0	0.043	0.043
130.0	0.270	0.183	280.0	0.031	0.027
140.0	0.247	0.178			

Table 54. Double ionization cross sections for nitrogen and oxygen and triple ionization cross sections for oxygen at incident energies between 50 and 280 eV. From [90Sa1] and [88An1].

Energy [eV]	Cross section [10^{-18} cm^2]		
	σ_N^{++}	σ_O^{++}	σ_O^{+++}
50.0	0.117	0.002	
60.0	0.200	0.187	
70.0	0.186	0.225	
75.0	0.173		
80.0	0.159	0.230	
85.0	0.147		
90.0	0.135	0.221	
95.0	0.125		
100.0	0.115	0.205	
110.0	0.098	0.185	0.00028
120.0	0.084	0.164	0.00101
130.0	0.072	0.142	0.00165
140.0	0.062	0.121	0.00202
150.0	0.052	0.103	0.00220
160.0	0.043	0.084	0.00212
170.0	0.035	0.069	0.00195
180.0	0.028	0.058	0.00175
190.0	0.023	0.048	0.00151
200.0	0.019	0.039	0.00128
220.0	0.013	0.026	0.00087
240.0	0.010	0.018	0.00054
260.0	0.008	0.013	0.00037
280.0	0.008	0.011	0.00027

Table 55. Single, double and triple photoionization cross sections for argon in the energy range between 55 and 280 eV. From [79Ho1].

Energy [eV]	Cross section [10^{-18} cm^2]		
	σ^{+++}	σ^{++}	σ^{+}
55.0		0.136	1.06
60.0		0.194	1.20
65.0		0.201	1.25
70.0		0.220	1.26
80.0		0.224	1.24
90.0		0.227	1.17
100.0		0.198	1.12
110.0		0.200	1.02
120.0		0.184	0.96
130.0	0.010	0.161	0.88
140.0	0.017	0.155	0.80
150.0	0.008	0.134	0.75
160.0	0.007	0.119	0.69
170.0	0.010	0.119	0.63
180.0	0.014	0.103	0.59
190.0	0.006	0.098	0.53
200.0	0.018	0.086	0.48
210.0	0.013	0.087	0.43
220.0	0.010	0.098	0.37
230.0	0.015	0.104	0.32
240.0	0.015	0.147	0.25
250.0	0.378	3.77	0.41
260.0	0.398	3.45	0.30
270.0	0.506	3.04	0.28
280.0	0.529	2.69	0.28

1.3.9.3 Ionization plus excitation, partial subshell cross sections and angular distributions

For helium, results have already been presented for total ionization cross sections in both non resonant and resonant regions and for the ratios of double to single ionization. If electrons are collected following photoionization it is possible to obtain cross sections corresponding to ionization plus excitation, to obtain angular distributions of emitted electrons and to study the angular correlations between electrons emitted in double ionization by collecting two electrons in coincidence. Although these topics are currently being actively investigated most of the data is in the form of graphs. An example is given in Fig. 30 which shows the breakdown of the total cross section into partial cross sections corresponding to leaving the ion in various excited states obtained from various sources. Similar results for ionization plus excitation have been obtained for specific states for a number of atoms (see [A3, A8]).

For other atoms which have subshells it is possible to break down the total photoionization cross section into partial cross sections for single ionization or ionization plus excitation from various subshells. This was first done for neon by Wuilleumier and Krause [74Wu1]. Fig. 31 shows their breakdown of the total cross section from threshold to 2 keV into components which represent 1s, 2s or 2p single ionization and either ionization plus excitation or double ionization from these subshells.

Similar results are available for limited spectral ranges in all of the rare gases as well as in other elements (see [A3, A8]).

For low energy photoionization the angular distribution of any electron produced by photoabsorption will have the simple form

$$\frac{d\sigma}{d\Omega} = \frac{\sigma_n}{4\pi}[1+\frac{\beta}{2}(3\cos^2\theta - 1)] \quad (3)$$

where σ_n is the partial cross section for a particular process (single ionization or ionization plus excitation) and θ is the angle between photon polarization and electron ejection. At the "magic angle" 57.3° the differential cross section does not depend on the value of the angular distribution parameter β_n and measurements of partial cross sections are often made at this angle. However, using photoelectron spectroscopy it is possible to obtain both σ_n and β_n as functions of photon energy and such measurements have been made for a number of atoms. An example of this type of data [79Wu1] is given in Table 56 which gives the cross section for single 2p ionization and the β parameter for this process as a function of energy. Similar results are available for most of the subshells of the rare gases as well as for various excitation processes in other atoms (see [A3, A8]).

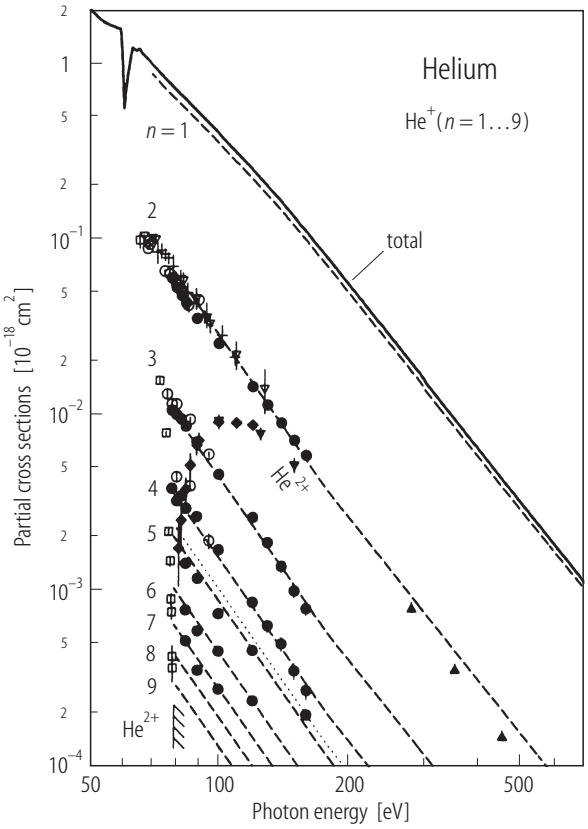

Fig. 30. Cross sections for ionization plus excitation of helium from various sources [A8].

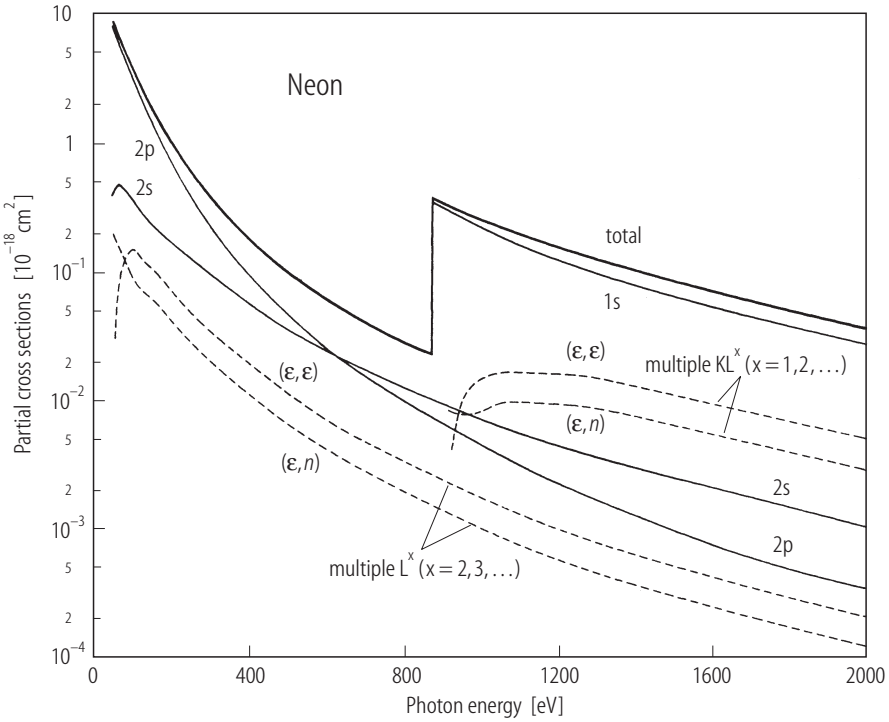

Fig. 31. Cross sections for ionization of neon inner shells and for ionization plus excitation [74Wu1].

Table 56. Photoionization cross sections and β parameters for neon 2p subshell ionization from 30 to 300 eV [79Wu1].

Energy [eV]	σ_{2p} [10^{-18} cm^2]	β	Energy [eV]	σ_{2p} [10^{-18} cm^2]
30.0	8.86	0.42	170.0	1.06
40.0	8.69	0.79	180.0	0.93
50.0	7.92	1.03	190.0	0.81
60.0	6.85	1.18	200.0	0.70
70.0	5.40	1.27	210.0	0.62
80.0	4.57	1.31	220.0	0.54
90.0	3.85	1.33	230.0	0.48
100.0	3.30		240.0	0.43
110.0	2.80		250.0	0.38
120.0	2.34		260.0	0.33
130.0	1.96		270.0	0.29
140.0	1.67		280.0	0.26
150.0	1.44		290.0	0.23
160.0	1.24		300.0	0.21

1.4 Elastic and inelastic scattering

1.4.1 Relationship of cross sections to the index of refraction and scattering factors

In contrast to the material presented in the previous two sections, there is comparatively little data on the scattering of photons from single atoms. There are two reasons for this. First, except at extremely high photon energies, the cross sections for photon scattering are much smaller than those for photon attenuation or ionization. As a result, experiments of single scattering from free atoms are more difficult and those that have been performed have been done mainly as a check on theoretical calculations rather than as a source of data to be used directly for applications. Second, while scattering from free atoms is an important process in applied fields, most of the experimental work has been performed within the basic context of scattering from aggregates of atoms. As a result, the experimental work attempts to provide information on optical constants at low energies or on scattering factors over an extended energy range which essentially provide a correction to the scattering from free electrons for each atom as a function of incident photon energy. A knowledge of the relationships between these quantities and scattering cross sections is essential to understand the experimental data and is given briefly below.

Basically, scattering from free atoms is of three types, namely:

a) Elastic scattering, where the photon transfers no energy to the atom.

b) Inelastic scattering, where there is a transfer of energy.

c) Resonant scattering, where the photon excites an atomic level which then re-emits a photon of the same energy, or the atom decays by emitting photons (or electrons) of different energies.

At low energies; i.e., below all ionization potentials inelastic scattering does not occur and the elastic scattering cross section for free atoms is simply related to the index of refraction. Resonant scattering occurs only for energies near atomic levels and results in an increase in cross sections and variations of the index of refraction known as anomalous dispersion. At higher energies inelastic scattering can occur but occurs mainly in the backward direction. Elastic and inelastic scattering are referred to as coherent or incoherent scattering or alternatively as Rayleigh (or Thomson) and Compton scattering. At higher energies resonant scattering can occur at energies near absorption edges and is termed resonant anomalous scattering. Although this is a subject of interest in molecules and solids, there have been few scattering measurements of this type for free atoms.

Since at low energies nuclear scattering and relativistic effects are negligible scattering from free atoms is assumed to be only from bound electrons. To the extent that the electrons in an atom are unbound, only elastic scattering can occur and the differential and total cross section for scattering will be given by the expressions:

$$\frac{\mathrm{d}\sigma}{\mathrm{d}\Omega} = \frac{1}{2} r_\mathrm{e}^2 (1 + \cos^2 \theta) \tag{4}$$

$$\sigma_\mathrm{tot} = \frac{8\pi}{3} r_\mathrm{e}^2 = 6.65 \cdot 10^{-25} \tag{5}$$

where $\mathrm{d}\sigma/\mathrm{d}\Omega$ is the differential cross section for scattering into angle θ, σ_tot is the total cross section and r_e is the electron radius. Coherent scattering from free atoms is modeled by defining correction factors that must be multiplied by the differential cross sections to account for the fact that the electrons are bound. Eq. 4 now becomes:

$$\frac{d\sigma}{d\Omega} = \frac{1}{2} r_e^2 (1+\cos^2\theta) f_1^2(q, Z) \tag{6}$$

where the momentum transfer q is defined in terms of the incident energy E_0 and scattering angle θ as

$$q = 2E_0 \sin\frac{\theta}{2} \tag{7}$$

and $f_1(q, Z)$ is a scattering factor which depends on the momentum transfer q (and hence the scattering angle θ)

When absorption can occur an imaginary component must be added to the scattering factor $f_2(0, Z)$ to indicate a loss of intensity in the forward direction. Both $f_1(0, Z)$ and $f_2(0, Z)$ depend on the incident photon energy and are related to one another and to the total absorption cross section. $f_2(0, Z)$ is proportional to the absorption cross section:

$$f_2(0, Z) = \frac{\pi}{2} CE\sigma(E, Z) \tag{8}$$

where $\sigma(E)$ is the absorption cross section. The constant C is 9.11 when the energy E is in eV and the cross section in barns (10^{-24}cm^2).

The forward scattering amplitude $f_1(0, Z)$ can be obtained from the absorption cross section via a dispersion relation:

$$f_1(0, Z) = Z + C\int_0^\infty \frac{\varepsilon^2 \sigma(\varepsilon, Z)}{E^2 - \varepsilon^2} d\varepsilon \tag{9}$$

The scattering factors described above depend on the atomic number Z and on photon energy E_0. One of the most important applications of the data described in the previous sections is the estimation of the scattering factor $f_1(0, Z)$ using Eq. 9. This requires a knowledge of the absorption cross section for each element over those energy ranges which make appreciable contributions to the integral in Eq. 9.

The forward scattering factor $f_1(0, Z)$ is also related to the index of refraction. The relationship is:

$$n = 1 - \delta\,;\ \delta = 2.72\cdot 10^{10}\ \lambda^2 f_1(0, Z) \tag{10}$$

where n is the index of refraction and λ the wavelength in Å.

Although inelastic scattering is important in molecules and solids at low energies; e.g., below 100 eV, the cross sections are negligible for all atoms compared to those for photoabsorption and elastic scattering. At higher energies the Compton effect has been studied mainly at large angles where it is possible to resolve photons elastically and inelastically scattered. In analogy to elastic scattering, inelastic scattering from free atoms is modeled by defining a correction factor which multiplies the free electron differential cross section for Compton scattering given by the Klein-Nishima formula:

$$\frac{d\sigma_{KN}}{d\Omega} = \frac{r_e^2}{2}[1+k(1-\cos\theta)]^{-2}\left[1+\cos^2\theta + \frac{k^2(1-\cos\theta)^2}{1+k(1-\cos\theta)}\right] \tag{11}$$

where θ is the scattering angle and k is the photon energy in mc^2 units (511 keV).

As for elastic scattering, atomic effects are modeled by multiplying by an incoherent scattering factor $S(q, Z)$ which depends on q, the momentum transferred in the collision and atomic number Z. The differential cross section is then:

$$\frac{d\sigma}{d\Omega} = \frac{d\sigma_{KN}}{d\Omega} S(q, Z) \tag{12}$$

and the total cross section can be obtained by integrating over all angles.

As stated previously, there has been little experimental work on scattering from free atoms although there have been theoretical calculations of form factors as described above and direct calculations of scattering cross sections for both elastic and inelastic scattering. The available experimental data falls into the following categories which will be described below:

A. Measurements of the index of refraction at energies below all excitation thresholds.

B. Measurements of elastic scattering cross sections at specific wavelengths both at low energies and in the X-ray range.

C. Measurements of inelastic scattering at high energies on solids where it is assumed that the atoms in the solid scatter as free atoms.

In order to show the relative importance of scattering and absorption, Table 57 gives theoretical estimates of the total cross sections for absorption,elastic and inelastic scattering from rare gases and hydrogen at various energies. Note that scattering is orders of magnitude smaller than absorption for all elements at energies below 100 eV, but becomes important for light elements in the energy range between 1 and 10 keV. For heavier elements scattering is negligible for energies below 10 keV but becomes important for all elements at energies above 100 keV.

Table 57. Cross sections for photoabsorption, coherent and incoherent scattering from [73Ve1].

Element	Energy [keV]	Cross section [10^{-24} cm^2]		
		Absorption	Coherent	Incoherent
Hydrogen	0.1	19300	0.664	0.001
Helium	0.1	359000	2.66	0.0008
Neon	0.1	4110000.0	66.5	0.0021
Argon	0.1	1310000.0	215.0	0.006
Hydrogen	1.0	10.9	0.579	0.085
Helium	1.0	413.0	2.52	0.072
Neon	1.0	266000.0	63.6	0.186
Argon	1.0	210000	202.0	0.471
Hydrogen	10	0.0046	0.0416	0.599
Helium	10	0.191	0.395	1.08
Neon	10	380	13.4	3.96
Argon	0	4120.0	49.2	6.18
Argon	100	3.7	1.4	8.5
Krypton	100	74.0	8.2	16.2
Xenon	100	383.0	23.0	23.7

1.4.2 Measurements of the index of refraction

The indices of refraction of the rare gases were measured by Cuthbertson and Cuthbertson in 1910 [10Cu1] at a number of wavelengths in the visible spectrum and much later the measurements for helium and neon were extended to shorter wavelengths [32Cu1].
This and other early work was found to be well represented by the simple formula:

$$n-1=\frac{C}{\nu_0^2-\nu^2} \tag{13}$$

Tables of the constants ν_0 and C for all of the rare gases and the ranges of wavelengths where the formula is valid are given in a review article by Korft and Breit [32Ko1]. A table of the values of $n - 1$ for wavelengths between 6200 and 2300 Å is given by Larsen [62La1]. Actually, all of the earlier measurements of the index of refraction made by various authors where there is no anomalous dispersion agree very well. This is demonstrated in Fig. 32 where the measurements of Cuthbertson and Cuthbertson are compared with the tabulated data of Larsen. The agreement is better than 1 %. Table 58 gives the index of refraction for neon as measured by Cuthbertson and Cuthbertson [32Cu1]. This table along with the tabulation given in [62La1] provided a compete set of experimental data in the normal dispersion range for all of the rare gases.

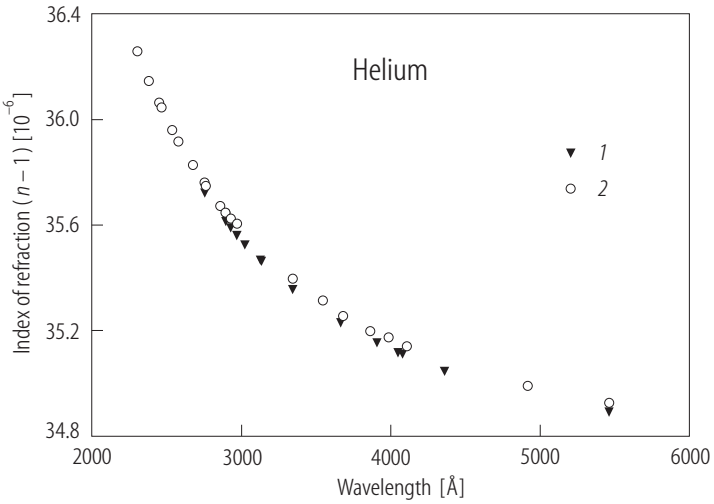

Fig. 32. Index of refraction of helium from *1* [10Cu1] and *2* [62La1].

Table 58. Refractive index of neon [32Cu1].

Wavelength [Å]	$(n-1)\cdot 10^6$	Wavelength [Å]	$(n-1)\cdot 10^6$
5462.23	67.250	3664.10	67.891
4917.40	67.372	3342.42	68.129
4359.54	67.540	3132.59	68.324
4078.97	67.662	3022.37	68.447
4047.68	67.675	2968.13	68.516
3907.56	67.744	2894.44	68.612

1.4.3 Measurements of elastic scattering

Although there were some earlier measurements of elastic scattering cross sections to compare with refractive indices [21Ca1, 25Da1, 51Va1], the major emphasis of this type of work was the study of polarization upon scattering in an attempt to obtain the polarizability of molecules. Definitive measurements on the rare gases were not done until the 1960's using ruby laser light (6943 Å) or Lyman α (1216 Å). The elastic differential cross section in these measurements is expressed as:

$$\frac{d\sigma}{d\Omega} = \sigma_R\left[(1-\rho)\cos^2\theta + \rho\right] \qquad (14)$$

where ρ is a depolarization ratio. For both atoms and molecules one expects a $\cos^2\theta$ distribution ($\rho = 0$) for horizontal polarization and an isotropic distribution ($\rho = 1$) for vertical polarization since the angular distribution depends only on the direction relative to the polarization of the incident beam. George et al. [63Ge1, 65Ge1] obtained a $\cos^2\theta$ distribution for horizontal polarization of 6943 Å light on argon and xenon but did not obtain a isotropic distribution for vertically polarized light. Subsequent experiments made on nitrogen molecules using 6943 Å [65Wa2, 68Ru1] gave an isotropic distribution for vertically polarized light in agreement with theory. The Rayleigh cross section σ_R is related to the index of refraction by:

$$\sigma_R = \frac{4\pi^2 (n-1)^2}{N^2 \lambda^4} \tag{15}$$

where N is Loschmidt's number $2.687 \cdot 10^{19}$ cm^{-3}; i.e., the number of atoms/cm^3 in an ideal gas at standard temperature and pressure and λ is the wavelength in cm. Table 59 gives the measured values obtained for σ_R for the rare gases and some molecular gases [65Ge1, 68Ru1] as well as the cross section obtained from the measured values of the index of refraction [62La1]. The results of 68Ru1 agree very well with the refractive index data. Both measurements were absolute.

Measurements of the refractive index or σ_R at 1216 Å for argon, krypton xenon and molecular hydrogen and nitrogen were made by Gill and Heddle [63Gi1] and of helium, neon, argon and molecular hydrogen and nitrogen by Shardanand and Mikawa [67Sh1]. Neither of these measurements were absolute, but they normalized using previous refractive index measurements [62He1] for nitrogen or theory [65Ch1] for helium. Table 60 gives the results of all of these measurements using the theoretical normalization.

In the X-ray range of energies (1…30 keV) there were a number of experiments performed before 1932 which measured the total scattering cross sections for various gases and both theoretical [31Wo1] and experimental work during that period has been summarized by Wollin [32Wo1]. Experiments were performed on helium,neon, argon and mercury and as well as hydrogen,oxygen and nitrogen in molecular form and the results compared with theoretical calculations. Practically all of the work was presented in graphical form and compared with theory. In these early experiments it was impossible to separate coherent and incoherent scattering, but the agreement with theory was remarkably good in most cases. Since it was assumed that the cross sections depended only on momentum transfer what was plotted was the scattering per electron as a function of momentum transfer, $\sin(\theta/2)/\lambda$ where θ is the scattering angle and λ the wavelength in Å (10^{-8} cm). An example of this type of experiment is shown in Fig. 33 for helium. The measurements were made at wavelengths of 0.39 [28Ba1] and 0.71 Å [31Wo2], (31.8 and 17.4 keV). The theoretical calculations are by Waller and Hartree [29Wa1].

A careful set of measurements were made by Chipman and Jennings [63Ch1] using 17.4 keV radiation for neon, argon, krypton and xenon. Their results are shown in Table 61. Their results for neon and argon are in good agreement with the earlier work of Wollin [31Wo2]. In order to estimate the elastic scattering form factor $f(q, Z)$ they estimated the cross sections due to inelastic scattering from theory and used measured values of the absorption cross section to correct their measured results. The results for all gases showed good agreement with theoretical calculations as shown in Table 62. The calculated form factors are from various sources (see [63Ch1]).

Ice et al. [78Ic1] measured cross sections for helium and molecular hydrogen at several energies and two angles using synchrotron light. Their results, when normalized to theory showed good agreement with theoretical calculations as shown in Table 63 for both gases. They also made absolute measurements at several energies and found that the measured cross sections were somewhat lower than theory, but within their estimated error.

Smend and Czerwinski [86Sm1] made measurements of the elastic scattering of 59.54 keV photons from krypton and xenon at angles between 20 and 120°. The measurements were compared with calculations of the scattering cross sections which included a small contribution for nuclear scattering. The results are shown in Table 64. The calculations in this case [80Ki1] are direct

calculations of the differential cross sections for elastic scattering which do not make the approximations inherent in using form factors.

There have been no measurements of inelastic scattering cross sections for free atoms or, alternatively measurements of the incoherent scattering factor $S(q, Z)$ for free atoms. However, there have been a number of measurements of this type for solids at energies where it is reasonable to expect the atoms in the solid to scatter as free atoms. An example of this type of data is given in Table 65 which compares the measured differential cross sections for a number of elements for scattering of 59.5 keV radiation at 120° [94Ku1] to those obtained via theory [75Hu1]. At this value of momentum transfer peaks due to inelastic and elastic scattering can be resolved so that only inelastic scattering is measured. The measurement in this case was normalized to the theoretical differential cross section for aluminum.

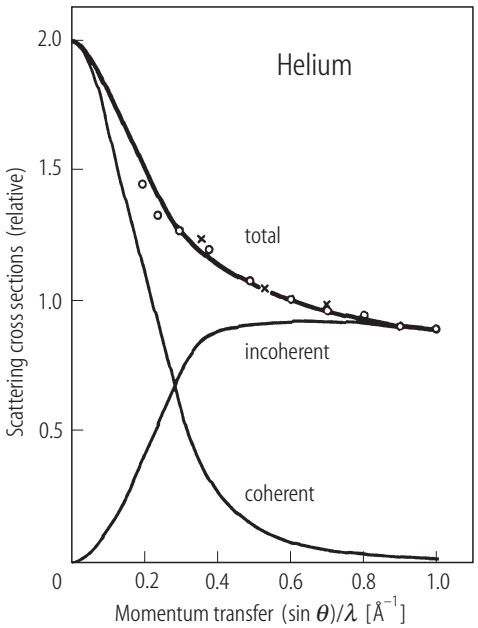

Fig. 33. Cross sections for scattering of 17.4 and 31.8 keV photons by helium from various sources [32Wo1].

Table 60. Rayleigh cross sections for scattering by 1216 Å light. From [63Gi1] and [67Sh1], theory [65Ch1].

Gas	Cross section [10^{-26} cm^2]	
	Experiment	Theory
He	0.41	0.41
Ne	1.8	1.7
Ar	76.0	76.0
Kr	714.0	
Xe	$2.3 \cdot 10^4$	
N_2	77.0	
H_2	26.0	

Table 59. Cross sections for elastic scattering by 6943 Å light.

Gas	Cross section [10^{-28} cm^2]		
	65Ge1	68Ru1	62La1
He	-	0.0296 ± 0.0014	0.0284
Ne	0.228	-	0.108
Ar	4.04	1.88 ± 0.09	1.85
Xe	27.4	11.55 ± 0.55	11.38
N_2	5.0	2.12 ± 0.09	2.10
H_2		0.438 ± 0.026	0.449
D_2		0.431 ± 0.021	0.449
N_2O		6.40 ± 0.31	6.40
CH_4		4.56 ± 0.22	4.49

Table 61. Measured values of $f_1^2(q, Z)$ (see eqs. 6 and 7) for the rare gases [63Ch1] before making corrections for absorption and inelastic scattering.

Neon		Argon		Krypton		Xenon	
θ	f_1^2	θ	f_1^2	θ	f_1^2	θ	f_1^2
3.76°	9.88	3.69°	17.72	3.73°	34.7	3.74°	52.8
4.59°	9.79	4.53°	17.54	4.57°	34.5	4.56°	52.4
7.33°	9.49	7.28°	16.77	7.31°	33.2	7.31°	50.5
10.22°	9.03	10.18°	15.71	10.20°	31.6	10.21°	48.2
14.13°	8.37	14.09°	14.14	14.13°	29.2	14.14°	44.7
22.05°	6.79	22.03°	11.40	22.08°	25.1	22.09°	38.7
27.02°	5.94	27.03°	10.20	27.07°	22.9	27.07°	35.8
32.01°	5.24	32.03°	9.36	32.06°	21.0	32.06°	33.0

Table 62. Estimated contributions of inelastic scattering f_{in} and absorption f_2 to the measurements shown in Table 60 and comparison of corrected f_1 (eqs. 6 and 7) with theory (f_{th}).

Gas	θ	f_{in}	f_2	f_1	f_{th}
Neon	3.76°	0.2	0.02	9.87	9.86
	4.59°	0.3	0.02	9.78	9.79
	7.33°	0.7	0.02	9.46	9.47
	10.22°	1.2	0.02	8.97	9.01
	14.13°	2.0	0.02	8.26	8.26
	22.05°	3.7	0.02	6.51	6.59
	27.02°	4.6	0.02	5.54	5.61
	32.01°	5.4	0.02	4.70	4.76
Argon	3.69°	0.6	0.20	17.71	17.62
	4.53°	0.8	0.20	17.52	17.43
	7.27°	1.7	0.20	16.72	16.61
	10.18°	2.7	0.20	15.63	15.50
	14.09°	4.3	0.20	13.99	13.85
	22.03°	6.7	0.20	11.10	10.92
	27.03°	7.8	0.20	9.81	9.61
	32.03°	8.8	0.20	8.88	8.68
Krypton	3.73°	1.0	2.8	34.61	35.41
	4.57°	1.0	2.8	34.34	35.12
	7.31°	2.0	2.8	33.05	33.88
	10.20°	4.0	2.8	31.43	32.24
	14.13°	6.0	2.8	29.00	29.83
	22.08°	9.0	2.8	24.80	25.50
	27.07°	11.0	2.8	22.43	23.40
	32.06°	12.0	2.8	20.54	21.63
Xenon	3.73°	1.0	2.2	52.70	53.06
	4.56°	1.0	2.2	52.30	52.62
	7.31°	4.0	2.2	50.38	50.71

Gas	θ	f_{in}	f_2	f_1	f_{th}
Xenon	10.21°	6.0	2.2	48.07	48.24
	14.14°	8.0	2.2	44.58	44.76
	22.09°	14.0	2.2	38.48	38.69
	27.07°	16.0	2.2	35.41	35.67
	32.06°	18.0	2.2	32.68	33.03

Table 63. Deviations of the measured relative differential cross sections of H_2 and helium from theoretical predictions ([75Be1] for H_2 and [73Br1] for helium).From [78Ic1]. [1]) Normalization point.

Gas	θ	Energy [keV]	$\frac{(d\sigma/d\Omega)_{exp}}{(d\sigma/d\Omega)_{theor}}$
He	60.9°	6.0	1.001
	135.6°	6.0	0.987
	60.9°	2.0	0.987
	135.6°	12.0	1.00 [1])
H_2	60.9°	5.0	0.996
	60.9°	6.0	1.007
	60.9°	7.0	0.986
	135.6°	5.0	1.001
	135.6°	6.0	1.005
	135.6°	7.0	1.00 [1])

Table 64. Experimental and theoretical differential cross sections for elastic scattering of 59.54 keV photons from krypton and xenon. Cross sections are in units of 10^{-24} cm^2 sr^{-1}. Theoretical values are from [80Ki1]. From [86Sm1].

θ	Krypton		Xenon	
	Experiment	Theory	Experiment	Theory
20°	11.86(20)	11.17	32.00(71)	30.24
30°	4.43(11)	4.190	16.62(32)	15.71
40°	2.38(5)	2.317	9.18(19)	8.067
50°	1.44(3)	1.467	4.74(11)	4.058
60°	0.888(22)	0.924	2.56(6)	2.292
70°	0.524(14)	0.579	1.67(4)	1.519
80°	0.350(6)	0.380	1.24(3)	1.149
90°	0.273(8)	0.272	1.07(3)	0.960
100°	0.221(7)	0.217	0.904(20)	0.867
110°	0.200(7)	0.191	0.873(23)	0.831
120°	0.179(6)	0.182	0.847(22)	0.830

Table 65. Experimental and theoretical differential cross sections for inelastic scattering of 59.54 keV photons at 120° from various elements. Cross sections are in units of 10^{-24} cm^2 sr^{-1}. Theoretical values are from [75Hu1]. Experimental values from [94Ku1].

Element (Z)	Cross section	
	Experiment	Theory
Ti (22)	0.8271	0.8306
Ni (28)	1.0336	1.0441
Zn (30)	1.1049	1.1159
Se (34)	1.2048	1.2558
Mo (42)	1.4326	1.5326
Ru (44)	1.4214	1.6019
Cd (48)	1.6615	1.7340
Sn (50)	1.6416	1.7898
Te (52)	1.6916	1.8662
Yt (70)	1.8813	2.4056
W (74)	1.9985	2.5467
Pb (82)	2.1043	2.7928

Appendix: Alternative sources of data

The aim of the present chapter has been to present critically evaluated experimental data on photon ionization and scattering from free atoms. This data base is necessarily incomplete since measurements covering the whole spectral range from the ionization threshold to 10 keV have only been made for rare gas atoms. However there are additional sources of data that may be used which are not covered in this report. Basically, these sources are of four different types, namely:

A. Other review articles which include data or references not presented here
B. Measurements made of molecules and/or solids
C. Theoretical calculations
D. Data bases which have been assembled for specific applications
E. On line data

Brief descriptions of these sources will be given here.

A. Other review articles

There have been a number of reviews which contain material similar to that reported here [A1-A8]. The entire subject of atomic photoionization was reviewed in 1982 by J. A. R. Samson [A5]. and the experimental techniques used discussed [A4] and these references are still useful, since they contain a comprehensive history of the subject, a discussion of experimental techniques and attempts to reference all of the experimental data available at that time. This work is complimented by the book by J. Berkowitz [A3] which, in addition to presenting much of the available data on both atoms and

molecules surveys the theory of the various processes. The chapters on partial cross sections and the angular distribution of photo electrons are especially useful.

More recently, Schmidt [A6] has provided a comprehensive review of the more recent work on rare gas photoionization using synchrotron radiation. He discusses recent theoretical and experimental developments and provides a detailed bibliography. Sonntag and Zimmermann [A7] have reviewed the recent work on relative measurements of metallic vapors using synchrotron sources. Finally, a recent book [A8] contains much useful information about recent photoionization measurements in atoms molecules and solids principally using synchrotron sources. The chapter on partial cross sections and angular distributions is particularly useful and provides much more detailed information than is contained in Section 1.3.

B. Measurements made on molecules and solids

Although photon processes on molecules and solids are not the subject of this report information of them particularly at higher energies where most of the photoionization comes from inner shells and is expected to be approximately the same as for free atoms. At lower energies information on the photoionization of molecules can be found in [A3, A8]. For oxygen and nitrogen a useful source is the compilation of Fennelly and Torr [92Fe1]. In the energy range above 100 eV most of the experimental data on photon attenuation has been tabulated by Saloman et. al. [A9, A10] for all elements and compared with theoretical calculations. The tabulation is extremely useful since the data is presented in both graphical and tabulated form. This data base in fact served as a starting point for the present tabulation.

C. Theoretical calculations

Since there is little or no data for most atoms, one must rely on theoretical calculations for those cases where no data exits. Such calculations have been carried out for photoionizaton, elastic and inelastic scattering over the entire energy range considered here and for all elements [A11-A16]. Early tabulations based on theory have been quoted previously, namely [73Ve1] which gives photoionization, elastic and inelastic scattering cross sections from 100 eV to 1 MeV for all elements based mostly on theoretical calculations, [73Sc1] which gives photoionization cross sections for all elements from 1 keV to 1.5 MeV, [79Re1] which gives photoionization cross sections for atoms and charged ions from 5 eV to 5 keV and for $Z < 31$, and [75Hu1] which gives elastic and inelastic scattering cross sections from 100 eV to 10 MeV for all elements. Other similar tabulations [A11-A14] have been made and may be useful for specific applications.

D. Data bases that have been assembled for specific purposes

While there are a number of data bases that contain data on photoionization and scattering cross sections we list here only those that are based largely on experimental information which has been supplemented by theoretical calculations. Photoionization cross sections for all elements are available in the energy range from 100 eV to 100 keV [A10] which are based on theoretical calculations [73Sc1]. The tabulation lists also experimental results for each element and compares both graphically and in tabular form the experimental results with theory. References to all of the experimental papers quoted are given. Similar data over a broader energy range is available in [A17, A18]. Data for photoionization, and elastic and inelastic form factors for all elements in the energy range from 50 eV to 30 keV which are based on a careful analysis of all of the available experimental and theoretical data available is given in [A19]. The data for photoionization given in this reference is compared with that of [A10] in some detail in [A9]. A tabulation similar to that of [A19] based solely on theoretical cross sections is also available [A16].

E. On line data

It is possible to obtain data on photoionization via the world-wide web from a number of sources. One of the easiest ways at present to obtain access to these sources is to contact directly one of two

addresses, namely ORNL (Oak Ridge National Laboratory; http://www-cfadc.phy.ornl.gov/) or the Weizmann Institute (http://plasma-gate.weizmann.ac.il/). Both of these sources maintain links to data bases which contain both numerical and bibliographic information on photoionization and scattering processes.

Currently the main links to data bases from ORNL which contain data on photon processes are the atomic data base for astrophysics at the University of Kentucky, which contains theoretical cross sections for photoionization; the Corex Data base at McMaster University, which provides data on inner shell excitation processes for atoms and molecules and Topbase, the data base for opacity at the University of Strasbourg which provides theoretical photoionization cross sections for atoms and ions for light elements. The most useful links that can be reached from the Weizmann address are the Interactive Elastic-Atom Scattering Database at Lawrence Livermore Laboratories, which provides theoretical cross sections for elastic photon scattering for all elements and DABAX, the data base for X-rays of the European Synchrotron Radiation Facility, which provides on lie X-ray scattering factors and photoabsorption cross sections from various tabulations, and the Henke Scattering Factors data base, maintained by Uppsala University which provides the scattering factors of [A19] online.

References for 1

10Cu1 Cuthbertson, C., Cuthbertson, M.: Proc R. Soc. London A **84** (1910) 13.

21Ca1 Cabannes, J.: Ann. Phys. **15** (1921) 5.

25Da1 Daure, P.: C. R. **180** (1925) 2032.

28Ba1 Barrett, C.S.: Phys. Rev. **32** (1928) 223.

29Wa1 Waller, I., Hartree, D.R.: Proc. R. Soc. A **124** (1929) 119.

30Co1 Colvert, W.W.: Phys. Rev. **36** (1930) 1619-1624. (5.42-25.0 keV: Ne, Ar)

30Wo1 Woernle, B.: Ann. Phys. (Leipzig) **5** (1930) 475-506. (1.254-5.946 keV: Ne, Ar)

31De1 Dershem, E., Schein, M.: Phys. Rev. **37** (1931) 1238-1245. (0.277 keV: He, Ne, Ar, Kr, Xe)

31Sp1 Spencer, R.G.: Phys. Rev. **39** (1932) 178 (see also: Phys. Rev. **38** (1931) 1932). (1.778-8.066 keV: Ar)

31Wo1 Woo, Y.H.: Proc Nat. Acad. Sci **17** (1931) 467.

31Wo2 Wollan, E.O.: Phys. Rev **37** (1931)862.

32Cu1 Cuthbertson, C., Cuthbertson, M.: Proc R. Soc. London A **135** (1932) 44.

32Cr1 Crowther, J.A., Orton, L.H.H.: Philos. Mag. **13** (1932) 505-523 (see also: Philos. Mag. **10** (1930) 329-342). (6.407-8.056 keV: Ar)

32Ko1 Korft, S.A., Breit, G.: Rev. Mod. Phys. **4** (1932) 471.

32Wo1 Wollan, E.O.: Rev. Mod Phys. **4** (1932) 205.

33Be1 Beutler, H., Guggenheimer, K.: Z. Phys. **87** (1933) 176.

33Be2 Beutler, H.: Z. Phys. **85** (1933) 710.

34Be1 Beutler, H., Guggenheimer, K.: Z. Phys. **88** (1934) 25.

34Be2 Beutler, H., Guggenheimer, K.: Z. Phys. **88** (1934) 141.

35Be1 Beutler, H.: Z. Phys. **93** (1935) 177.

51Va1 Vaucouleurs, G.: Ann. Phys. **6** (1951) 211.

53Di1 Ditchburn, R.W., Jutsum, P.J., Marr, G.V.: Proc. R. Soc. London A **219** (1953) 89.

55Eh1 Ehler, A.W., Weissler, G.L.: J. Opt. Soc. Am. B **6** (1955) 2326-2330. (18-30 eV: N)

55Le1 Lee, P., Weissler, G.L.: Phys. Rev. **99** (1955) 540-542. (0.0147-0.0517 keV: He, Ar)

57Be1 Bethe, H.A., Salpeter, E.E.: Quantum Mechanics of one- and two-electron atoms, New York: Academic Press (1957), p. 304.

58Mo1 Moore, C.E.: Atomic Energy levels NBS Circular **467** (1958).

59Ga1 Garton, W.R.S., Codling, K.: Proc. Phys. Soc. London A **75** (1959) 87.
60Pe1 Pery-Thorne, A., Garton, W.R.S.: Proc. Phys. Soc. London **76** (1960) 833-843. (0.01463-0.02465 keV: Kr)
62Ba1 Baker, D. J., Tombouulian, D.U.: Phys. Rev. **128** (1962) 677-680. (45.5-153.87 eV: Li)
62Bu1 Buckman, W.G.: Thesis, Vanderbilt Univ., Tenn. (1962). (6.-24. keV: Ar)
62He1 Heddle,D.W.O.: JQSRT **2** (1962) 349.
62La1 Larsen, R., in: Zahlenwerte and Funktionen aus Physik, Chemie, Astronomie, Geophysik und Technik, Vol. II, part 8, Berlin: Springer (1962), p. 6-82.
63Ch1 Chipman, D.R., Jennings, L.D.: Phys. Rev. **37** (1963) 862.
63Ge1 George, T.V., Slama, L., Yokoyama, M., Goldstein, L.: Phys. Rev. Lett. **11** (1963) 403.
63Gi1 Gill, P., Heddle, D.W.O.: J. Opt. Soc. Am. **53** (1963) 847.
63Ma1 Madden, R.P., Codling, K.: Phys. Rev. Lett. **10** (1963) 516.
63Lu1 Lukirskii, A.P., Zimkina, T.M.: Izv. Akad. Nauk SSSR **27** (1963) 808-811; Engl. Transl. in: Bull. Acad. Sci. USSR, Phys. Ser. **27** (1963) 817-820. (0.0493-3.10 keV: Ar)
63Sa1 Samson, J.A.R.: Phys. Rev. **132** (1963) 2122.
64Al1 Alexander, R.W., Ederer, D.L., Tomboulian, D.H.: Bull. Am. Phys. Soc. (Ser. 2) **9** (1964) 626. (40.8-117.7 eV: Ar)
64Ed1 Ederer, D.L.: Phys. Rev. Lett. **13** (1964) 760-762. (0.0455-0.154 keV: Xe)
64Lu1 Lukirskii, A.P., Brytov, I.A., Zimkina, T.M.: Opt. Spectrosc. **17** (1964) 234-237. (0.04949-0.5253 keV: He, Kr, Xe)
64Ru1 Rustgi, O.P.: J. Opt. Soc. Am. **54** (1964) 464-466. (0.0125-0.0742 keV: Ar)
64Ru2 Rustgi, O.P., Fisher, E.I., Fuller, C.H.: J. Opt. Soc. Am. **54** (1964) 745-746. (0.0135-0.0541 keV: Kr, Xe)
65Be1 Beynon, J.D.E., Cairns,R.B.: Proc. Phys. Soc. **86** (1965) 1343-1349. (0.014576 keV: H)
65Ch1 Chan, Y.M., Dalgarno, A.: Proc. Phys. Soc. London **85** (1965) 227.
65Ge1 George, T.V., Goldstein, L, Yokoyama, M.: Phys. Rev. **137** (1965) 369.
65Ro1 Ross, K.J., Marr, G.V.: Proc.Phys. Soc. London **85** (1965) 193. (9-10.8 eV: Cd)
65Sa1 Samson, J.A.R.: J. Opt. Soc. Am. **55** (1965) 935-937. (0.02156-0.04379 keV: Ne)
65Wa2 Watson, R.D., Clark, M.D.: Phys. Rev. Lett. **14** (1965) 1057.
66Be1 Bearden, A.J.: J. Appl. Phys. **37** (1966) 1681-1692. (0.852-40. keV: He, Ne, Ar)
66Be2 Beynon, J.D.E.: Proc. Phys. Soc. **89** (1966) 59-61. (0.01476-0.015 keV: H)
66Lu1 Lukirskii, A.P., Brytov, I.A., Gribovskii, S.A.: Opt. Spektrosk. **20** (1966) 368-369; Engl. Transl. in: Opt. Spectrosc. **20** (1966) 203-204. (0.279-1.776 keV: Xe)
66Sa1 Samson, J.A.R.: Adv. At. Mol. Phys. **2** (1966) 177-261. (0.0122-0.0592 keV: He, Ne, Ar, Kr, Xe)
67Co1 Codling, K., Madden, R.P., Ederer, D.L.: Phys. Rev. **155** (1967) 26.
67He1 Henke, B.L., Elgin, R.L., Lent, R.E., Ledingham,R.B.: Norelco Rep. **14** (1967) 112-131. (0.1089-1.487 keV: He, Ne, Ar, Kr, Xe)
67Hu1 Hudson, R.D., Carter, V.L.: J. Opt. Soc. Am. **57** (1967) 1471-1474. (0.00434-0.02021 keV: K)
67Hu2 Hudson, R.D., Carter, V.L.: J. Opt. Soc. Am. **57** (1967) 651-654. (0.00514-0.02156 keV: Li, Na)
67Hu3 Huffman, R.E., Larrabee, J.C., Tanaka,Y.: J. Chem. Phys. **46** (1967) 2213.
67Sh1 Shardanand, Mikawa, Y.: JQSRT **7** (1967) 605.
68Be1 Berkowitz, J., Lifshitz, C.: J. Phys. B **1** (1968) 438-44. (8.99-18 eV:Cd, Hg).
68Co1 Comes, F.J., Speier, F., Elzer, A.: Z. Naturforsch. A **3** (1968) 125-133. (13-28 eV: O)
68Co2 Comes, F.J., Elzer, A.: Z. Naturforsch. A **23** (1968) 133-136. (14-30 eV: N)
68Hu1 Hudson, R.D., Carter, V.L.: J. Opt. Soc. Am. **58** (1968) 430-431. (17.711-24.796 eV: Na)
68Ma1 Marr, G.V., Creek, D.M.: Proc. R. Soc. A **304** (1968) 233.

68Ru1 Rudder, R.R., Bach, P.R.: J. Opt. Soc. Am. **58** (1968) 1260.

69Ca1 Cairns, R.B., Harrison, H., Schoen, R.I.: J. Chem. Phys. **53** (1969) 5440-5443. (9- 83 eV: Cd, 27- 65 eV: Zn)

69De1 Deslattes, R.D.: Phys. Rev. **186** (1969) 1.

69Ha1 Harrison, H., Schoen, R.I., Cairns, R.B., Schubert, K.E.: J. Chem. Phys. **50** (1969) 3930-3936. (9.97 -50.19 eV: Zn)

69Ha2 Haensel, R., Keitel, G., Schreiber, P., Kunz, C.: Phys. Rev. **188** (1969) 1375-1380 (see also: Schreiber, P.: Internal Report DESY-F41-69/6 (1970)). (0.064-0.500 keV: Kr, Xe)

69Ma1 Madden, R.P., Ederer, D.L., Codling, K.: Phys. Rev. **177** (1969) 136.

69Ma2 Marr, G.V., Austin, J.M.: J. Phys. B **2** (1969) 107-114. (9.47-16.6 eV: Zn)

69Ma3 Marr, G.V., Austin, J.M.: Proc. R. Soc. A **310** (1969) 137. (9-23 eV: Cd)

69We1 Wiese, W.L., Smith, M.W., Glennon, B.M.: Atomic Transition Probabilities Vol. I.II NRSDS-NBS-4,22 (1966,1969).

69Wu1 Wuilleumier, F.: Thesis, Lab. Chim. Phys., Paris (1969) (see also: C. R. Acad. Sci. **257** (1963) 855-858; ibid **269** (1969) 968-971; J. Phys. (Paris) **26** (1965) 776-784; Phys. Rev. A **6** (1972) 2067-2077). 0.825-8.247 keV: Ne, Ar, Kr, Xe)

70Ca1 Cairns, R.B., Harrison, H., Schoen, R.I.: J. Chem. Phys. **53** (1970) 96-101. (10-72 eV: Hg)

70De1 Denne, D.R.: J. Phys. D **3** (1970) 1392-1398. (0.151-0.523 keV: He, Ne, Ar)

70Ed1 Ederer, D.L., Lucatorto, T., Madden, R.P.: Phys. Rev. Lett. **25** (1970) 1537.

70He1 Henke, B.L., Elgin, R.L.: X-Ray Absorption Tables for the 2- to 200 Å Region, Adv. X-Ray Anal. **13** (1970) 639-664.

70Mc1 McCrary, J.H., Looney, L.D., Atwater, H.F.: J. Appl. Phys. **41** (1970) 3570-3572. (5.895 keV: He)

70Mc2 McCrary, J.H., Looney, L.D., Constanten, C.P., Atwater, H.F.:Phys. Rev.A **2** (1970) 2489-2497 (see also: McCrary, J.H., Ziegler, L.H., Looney, L.D.: J. Appl. Phys. **40** (1969) 2690-2693. (4.508-145.43 keV: Ne, Ar, Kr, Xe)

70Hu1 Hudson, R.D., Carter, V.L., Young, P.A.: Phys. Rev. A **2** (1970) 643. (5.2-7.3 eV:Ba)

71Ed1 Ederer, D.L.: Phys. Rev. A **4** (1971) 2263.

72Co1 Codling, K., Madden, R.P.: J. Res. Natl. Bur. Stand. A **76** (1972) 1.

72Wa1 Watson, W.S.: J. Phys. B **5** (1972) 2292-2303. (0.0631-.2335 keV: He, Ne, Ar)

72Wo1 Wolff, H.W., Radler, K., Sonntag, B., Haensel, R.: Z. Phys. **257** (1972) 353-368. (30- 160 eV: Na)

73Br1 Brown, C.M., Tilford, S.G., Ginter, M.L.: J. Opt. Soc. **63** (1973) 1454.

73Ca1 Carlson, R.W., Judge, D.L., Ogawa, M., Lee, L. C.: Appl. Opt. **12** (1973) 409-412. (0.0177-0.0681 keV: Ar)

73Ca2 Carlsten, J.L., McIlrath, T.C.: J. Phys. B **6** (1973) L284.

73De1 Dehmer, P.M., Berkowitz, J., Chupka,W.A.: J. Chem. Phys. **59** (1973) 5777.

73Sc1 Scofield, J.H.: Theoretical Photoionization Cross Sections from 1 to 1500 keV, Lawrence Livermore National Laboratory Report UCRL-51326 (1973).

73Ve1 Veigele, Wm.J.: Photon Cross Sections from 0.1 keV to 1 MeV for Elements $Z = 1$ to $Z = 94$, At. Data **5** (1973) 51-111.

74Co1 Cooper, J.W.: Phys. Rev. A **9** (1974) 2236.

74De1 Dehmer, J.L., Berkowitz, J.: Phys. Rev. A **10** (1974) 484-490. (15-70 eV: Hg)

74De2 Dehmer, P.M., Berkowitz, J., Chupka, W.A.: J. Chem. Phys. **60** (1974) 2676.

74Mi1 Millar, R.H., Greening, J.R.: J. Phys. B **7** (1974) 2332-2344. (4.508-25.192 keV: Ne, Ar)

74Wu1 Wuilleumier, F., Krause, M. O.: Phys. Rev. A **10** (1974) 242.

75Be1 Bentley, J.J., Stewart, R.F.: J. Chem. Phys. **62** (1975) 875.

75Hu1 Hubbell, J.W., Veigele, W.J., Briggs, E.A., Brown, R.T., Cromer, D.T., Howerton, R.J.: J. Phys. Chem. Ref. Data **4** (1975) 471-538.

75La1 Lang, J., Watson, W.S.: J. Phys. B **8** (1975) L339-L343. (0.0611-0.254 keV: Kr, Xe)

75Lo1 Loomis, T.C., Keith, H.D.: Appl. Spectrosc. **29** (1975) 316-322. (2.622-11.209 keV: Ar)

75Pe1 Peterson, H., Radler, K., Sonntag, B., Haensel, R.: J. Phys. B **8** (1975) 31. (80-180 eV: Cs)

76Dr1 Driver, R.D. J. Phys. B **9** (1976) 817-827. (24- 40 eV: K)

76Ma1 Marr, G.V., West, J.B.: At. Data Nucl. Data Tables **18** (1976) 497.

76Pa1 Palenius, H.P., Kohl, J.L., Parkinson, W.H.: Phys. Rev. A **13** (1976) 1805-1816. (13.6-20.36 eV: H)

76We1 West, J.B., Marr, G.V.: Proc. R. Soc. London A **349** (1976) 397-421 (36.46-306.6 eV: He, Ne, Ar, Kr)

77Co1 Codling, K., Hamley, J.R., West, J.B.: J. Phys. B **10** (1977) 2797-2807 (0.046-0.296 keV: Na)

77Co2 Cook, T.B., Dunning, F.B., Foltz, G.W., Stebbings, R.F.: Phys. Rev A **15** (1977) 1526-1529. (3.8-5.2 eV:Cs)

78Co1 Cole, B.E., Dexter, R.N.: JQSRT **19** (1978) 467-471. (0.0365-0.248 keV: He, C, N, O, F, Ne, Cl)

78Co2 Codling, K., Hamley, J.R., West, J.B.: J. Phys. B **11** (1978) 1713-1716. (41.92-247.7 eV: Cd)

78Ic1 Ice, G.E., Chen, M.H., Crasemann, B.: Phys. Rev. A **17** (1978) 650.

78Ko1 Kohl, J.L., Lafyatis, G.P., Palenius, H.P., Parkinson, W.H.: Phys. Rev. A **18** (1978) 571-574. (13.1-10.5 eV: O)

78Me1 Mehlman, G., Ederer, D.L., Saloman, E.B., Cooper, J.W.: J.Phys.B **11** (1978) L689.

78We1 West, J.B., Morton, J.: At. Data Nucl. Data Tables **22** (1978) 103-107. (13.45- 14,530 eV: Xe compilation)

79Ar1 Armstrong, J.A., Wynne, J.J.: J. Opt. Soc. **69** (1979) 211.

79Ho1 Holland, D.M.P., Codling, K., West, J.B., Marr, G.V.: J. Phys. B **12** (1979) 2465.

79Ra1 Radler, K., Berkowitz, J.: J. Chem. Phys. **70** (1979) 216.

79Re1 Reilman, R.F., Manson, S.T.: Photoabsorption Cross Sections for Positive Atomic Ions with $Z \leq 30$, Astrophys. J. Suppl. **40** (1979) 815-880.

79Wu1 Wuilleumier, F., Krause, M.O.: J. Electron. Spectros. Relat. Phenom. **15** (1979) 15.

80Gr1 Grattan, K.T.V., Hutchinson, M.H.R., Theocharous, E.S.: J. Phys. B **13** (1980) 2931-2935. (7.2 eV: Cs)

80Ki1 Kissel, L., Pratt, R.H., Roy, S.C.: Phys. Rev. A **22** (1980) 1970.

81Gi1 Gilberg, E., Hanus, M.J., Folz, B.: Rev. Sci. Instr. **52** (1981) 662.

82He1 Henke, B.L., Lee, P., Tahaka, T.J., Shimabukuro, R.L., Fujikawa, B.K.: At. Data Nucl. Data Tables **27** (1982) 1.

82Me1 Mehlman, G., Cooper, J.W., Saloman, E.B.: Phys. Rev. A **25** (1982) 2113-2122. (71-107 eV: Li)

83De1 Deslattes, R.D., LaVilla, R.E., Cowan, P.L., Henins, A.: Phys. Rev. A **27** (1983) 923.

83Ru1 Rusic, B., Berkowitz, J.: Phys. Rev. Lett. **50** (1983) 675.

83Su1 Suemitsu, H., Samson J.A.R.: Phys. Rev. A **28** (1983) 2752. (3.66-4.42 eV: Rb, Cs)

85Sa1 Samson, J.A.R., Pareek, P.N.: Phys. Rev. A **31** (1985) 1470-1476. (14.86-103.2 eV: O)

85Sa2 Saloman, E.B., Cooper, J.W., Mehlman, G.: Phys. Rev. A **32** (1985) 1878. (5.2-10.5 eV: Ba)

86Sa1 Samson, J. A. R., Shefer,Y., Angel, G. C. Phys. Rev. Lett. **56** (1986) 2020-2022. (13.0-70 eV:Cl)

86Sm1 Smend, F., Czerwinski, H.: Z. Phys. D **1** (1986) 139.

87Ya1 Yang, B.X., Kirz, J.: Appl. Opt. **26** (1987) 3823-3826. (0.326-1.01 keV: Ar)

88An1 Angel, G.C., Samson, J.A.R.: Phys. Rev. A **38** (1988) 5578-5585. (13.6-280 eV: O)

88Me1 van der Meer, W.J., van der Meulen, P., Volmer, M., de Lange, C.A.: Chem. Phys. **126** (1988) 385-93. (21.22 eV: O)
89Sa1 Samson, J.A.R., Yin, L.: J. Opt. Soc. Am. B **6** (1989) 2326- 2333. (16.7-21.2 eV: Ar, Kr, Xe)
90Ca1 Caldwell, C.D., Krause, M.O.: J. Phys. B **23** (1990) 2233.
90Sa1 Samson, J.A.R., Angel, G.C.: Phys. Rev. A **42** (1990) 1307-1312. (44-400 eV: N)
90Sa2 Samson, J.A.R., Angel, G.C.: Phys. Rev. A **42** (1990) 5328.
91Ch1 Chan, W.F. Cooper, G, Brion, C.E.: Phys. Rev. A **44** (1991) 186.
91Do1 Domke, M., Xue, A., Puschmann, T., Mandel, E., Hudson, E., Shirley, D.A., Kaindl, G., Greene, C.H., Sadeghpour, H.R., Peterson, H.: Phys. Rev. Lett. **66** (1991) 1306.
91Fl1 Flemming, M.G., Wu, J-Z., Caldwell, C.D.: Phys. Rev. A **44** (1991) 1733.
91Sa1 Samson, J.A.R., Yin, L., Haddad, G.N., Angel, G.C.: J. Phys. (Paris) IV suppl. Vol **1** (1991) Cl99-107 and private communication. (Ne: 21-705 eV, Ar: 16-248 eV, Kr: 15-125 eV, Xe:13.6-135 eV) (recommended data)
92Ch1 Chan, W.F., Cooper, G., Guo, X., Brion, C.E.: Phys. Rev. A **45** (1992) 1420.
92Fe1 Fennelly, J.A., Torr, D.G.: At. Data Nucl. Data Tables, **51** (1992) 321.
92Me1 Meulen, P., Krause, M.O., Caldwell, C.D., Whitfield, S.B., Lange, C.A.: Phys. Rev. A **46** (1992) 2468. (21.5-25 eV: Cl)
93Ma1 Maeda, K., Ueda, K., Ito, K.: J. Phys. B **26** (1993) 1541.
94Ki1 Kiernan, L.M., Mosnier, J-P., Kennedy, E.T., Costello, J.T., Sonntag, B.F.: Phys. Rev. Lett. **72** (1994) 2359.
94Ku1 Kurucu, Y., Erzeneoglu, S., Sahin,Y., Durak, R.: Nuovo Cimento **16** (1994) 555.
94Sa1 Samson, J.A.R., He, Z.X., Yin, L., Haddad, G.N.: J. Phys. B **27** (1994) 887.
95Ar1 Arcon, I., Kodre, A., Stuhec, M., Glavic-Cindro, D.: Phys. Rev. A **51** (1995) 147.
95Bo1 Borne, A. Federmann, F., Lee, M.K., Sonntag, B.: J. Phys. B **28** (1995) 2591.
95Az1 Azuma, Y., Berry, H.G, Gemmell, D.S., Suleiman, J., Westerlind, M., Sellin, I.A., Woicik, J.C., Kirkland, J.P.: Phys. Rev. A **51** (1995) 447, 453.
95MG1 McGuire, J.H., Berrah, N., Bartlett, R.J., Samson, J.A.R., Tanis, J.A., Cocke, C.L., Schlachter, A.S.: J. Phys. B **28** (1995) 913.
96Co1 Cooper, J.W.: Radiat. Phys. Chem. **47** (1996) 927-934.
96Do1 Doerner, R. et al.: Phys. Rev. Lett. **76** (1996) 2654.
96Ki1 Kiernan, L.M.: J. Phys. B **29** (1996) L181.
96Le1 Levin, J.C., Armen, B., Sellin, I.A.: Phys. Rev. Lett. **76** (1996) 1220.
96Sp1 Spielberger, L. et al.: Phys. Rev. Lett. **76** (1996) 4685.
96Wu1 Wuilleumier, F.J., Diehl, S., Cubaynes, D., Bizau, J-M., in: X-Ray and Inner Shell Processes, AIP Press, New York: Woodbury (1996), p 625.
97Ch1 Chung, K.T.: Phys. Rev. Lett. **78** (1997) 1416.
97Az1 Azuma, Y. et al.: Phys. Rev. Lett. **79** (1997) 2419.
97Be1 Berkowitz, J.: J. Phys. B **30** (1997) 583.
98Sa1 Samson, J.A.R., Stolte, W.C., He, Z.X., Cutler, J.N., Lu, Y., Bartlett, R.J.: Phys. Rev. A **57** (1998) 1906.

A1 Hudson, R.D., Kieffer, L.J.: Compilation of Atomic Ultraviolet Photoabsorption Cross Sections for Wavelengths between 3000 and 10 Å, At. Data **2** (1971) 205-262.
A2 Kieffer, L.J.: Bibliograpy of Low Energy Electron and Photon Cross Section Data, NBS Special Pub. **426** (1976) and NBS Special Pub. **426**, Suppl. 1 (1979).
A3 Berkowitz, J.: Photoabsorption, Photoionization, and Photoelectron Spectroscopy, New York: Academic Press (1979).
A4 Samson, J.A.R.: Techniques of Vacuum Ultraviolet Spectroscopy, New York: Wiley (1967).

A5 Samson, J.A.R.: Atomic Photoionization (p. 123-213), Encyclopedia of Physics (W. Mehlhorn, ed.), Berlin: Springer (1982).
A6 Schmidt, V.: Photoionization of Atoms Using Synchrotron Radiation, Rep. Prog. Phys. **55** (1992) 1483.
A7 Sonntag, B., Zimmermann, P.: Rep. Prog. Phys. **55** (1992) 911.
A8 VUV and Soft X-Ray Photoionization (U. Becker, D.A. Shirley, eds.), New York: Plenum Press (1996).
A9 Saloman, E.B., Hubbell, J.H.: X-Ray Attenuation Coefficients (Total Cross Sections): Comparison of the Experimental Data Base with the Recommended Values of Henke and the Theoretical Values of Scofield for Energies Between 0.1-100 keV, Natl. Bur. Stand. Int. Rep. NBSIR 86-3431 (1986).
A10 Saloman, E.B., Hubbell, J.H., Scofield, J.H.: X-Ray Attenuation Cross Sections for Energies 100 eV to 100 keV and Elements Z = 1 to Z = 92, Atomic Data and Nuclear Data Tables **38** (1988) 1-197.
A11 Band, I.M., Yu, I.K., Trzhaskovskaya: Photoionization Cross Sections and Photoelectron Angular Distributions for X-Ray Lines Energies in the Range 0.132-4.509 keV. Targets:$1 \le Z \le 100$, At. Data Nucl. Data Tables **23** (1979) 443.
A12 Huang, K.N., Johnson, W.R., Cheng, K.T.: Theoretical Photoionization Parameters for the Noble Gases Argon, Krypton and Xenon, At. Data Nucl. Data Tables, **26** (1981) 33.
A13 Yeh, J.J., Lindau, I.: Atomic Subshell Photoionization Cross Sections and Asymmetry Parameters: $1 \le Z \le 103$, At. Data Nucl. Data Tables **32** (1985) 1.
A14 Verner, D.A., Yakovlevd, G., Band, I.M., Trzhakovskaya, M.B.: Subshell Photoioniza tion Cross Sections and Ionization Energies of Atoms and Ions from He to Zn, At. Data Nucl. Data Tables **55** (1993) 233.
A15 Wang, J., Sagar, R.P., Schmider, H., Smith, V.H.: X-Ray Elastic and Inelastic Scattering Factors for Neutral Atoms Z = 2-92, At. Data Nucl. Data Tables **53** (1993) 233.
A16 Chantler, C.T.: Theoretical Form Factor, Attenuation and Scattering Tabulation for Z = 1-92 from E = 1-10 eV to E = 0.4-1.0 MeV, J. Phys. Chem. Ref. Data **24** (1995) 71.
A17 Saloman, E.B., Hubbell, J.H., Berger, M.J.: Natl. Bur. Stand. Data Base of Photon Absorption Cross Sections from 10 eV to 100 GeV, Proc. SPIE **911** (1988) 100-106.
A18 Cullen, D.E., Chen, M.H., Hubbell, J.H., Perkins, S.T., Plechaty, E.F., Rathkopf, J.A., Scofield, J.H.: Tables and Graphs of Photon-Interaction Cross Sections from 10 eV to 100 GeV, Derived from the LLNL Evaluated Photon Data Library. Part A: Z = 1-50. Part B: Z = 51-100, Lawrence Livermore Lab. Rep. UCRL-50400, Vol. **6**, Rev. 4 (1989).
A19 Henke, B.L., Gullikson, E.M., Davis, J.C.: X-Ray Interactions: Photoabsorption, Scattering, Transmission, and Reflection at E = 50-30,000 eV, Z = 1-92, At. Data Nucl. Data Tables **54** (1993) 181-342.

Acknowledgements

The author is indebted to J.H. Hubbell who not only made his collection of photon attenuation cross section reprints available to him, but provided much useful information on data sources, to E.B. Saloman, who made available the information contained in the NIST X-ray attenuation data base and to J.A.R. Samson who read preliminary versions of this work and provided in useful form some of the data contained here.

2 Electron collisions with atoms

2.1 Introduction

2.1.1 Generalities

An idealized experiment for studying electron collisions with atoms may be described as follows. A beam of n electrons of a fixed momentum $\boldsymbol{p}$ impinges on a gas per unit time per unit area perpendicular to $\boldsymbol{p}$; then one says that the electron beam is characterized by fluence rate (or flux) n. The gas consists of N atoms of a given species A per unit volume; then one says that the gas is characterized by (number) density N of atoms A. Suppose that a detector registers the number of electrons emerging per unit time into an infinitesimal solid-angle element $\mathrm{d}\omega_0$ around the direction given by the polar angles θ_0, φ_0 (called scattering angles) with respect to $\boldsymbol{p}$. The registered number should be proportional to n, N, and $\mathrm{d}\omega_0$, if n and N are small enough to ensure the conditions that (i) no appreciable interactions occur among electrons; (ii) each collision of an electron with an atom occurs independently, i.e., without interference by other atoms; (iii) no appreciable reduction of atoms occur as a result of electron collisions, e.g., by recoil. Under these conditions (which may be called single-collision conditions), the registered number of collisions per unit time is small, and can be expressed as $N[\mathrm{d}\sigma(\theta_0, \varphi_0)/\mathrm{d}\omega_0]\mathrm{d}\omega_0$, where the proportionality factor $\mathrm{d}\sigma(\theta_0, \varphi_0)/\mathrm{d}\omega_0$ has the dimension of area, and is called the differential cross section. The integral

$$\sigma = \int \frac{\mathrm{d}\sigma(\theta_0, \varphi_0)}{\mathrm{d}\omega_0} \mathrm{d}\omega_0 \tag{1}$$

also has the dimension of area, is called the integrated (or total) cross section, and is an index of the probability of collisions regardless of the scattering angles. We shall use the term "cross section" in this sense, and put the adjective "integrated" when it is necessary to prevent misunderstanding; the adjective "total" will be used in a different sense to be described in Section 2.2.

Atoms in a gas are in thermal motion, and we need to consider the influence of the translational motion of atoms. In another experimental setup, atoms in a beam interact with an electron beam. In general, the physics of an individual collision is determined by the relative motion of an electron and an atom, the translational motion of the combined system of the two being irrelevant. This consideration leads to the distinction between the laboratory frame of reference and the center-of-mass frame of reference. Let us assume that all speeds are nonrelativistic. Suppose that, in the laboratory frame, an electron of mass m and velocity $\boldsymbol{v}_\mathrm{e}$ collides with an atom of mass M_A and velocity $\boldsymbol{v}_\mathrm{A}$. The center of mass moves throughout at constant momentum $M_\mathrm{A}\boldsymbol{v}_\mathrm{A} + m\boldsymbol{v}_\mathrm{e}$, and hence at constant velocity $\boldsymbol{v}_\mathrm{c} = (M_\mathrm{A}\boldsymbol{v}_\mathrm{A} + m\boldsymbol{v}_\mathrm{e})/(M_\mathrm{A} + m_\mathrm{e})$. Seen in the center-of-mass frame, the electron velocity is $\boldsymbol{v}_\mathrm{e} - \boldsymbol{v}_\mathrm{c}$, and the atom velocity is $\boldsymbol{v}_\mathrm{A} - \boldsymbol{v}_\mathrm{c}$. The differential cross section $\mathrm{d}\sigma(\theta, \varphi)/\mathrm{d}\omega$ in the center-of-mass frame is defined by stating that the number of electrons emerging into the solid angle element $\mathrm{d}\omega$ around the direction given by the polar angles θ, ϕ is $n\mathrm{d}\sigma(\theta, \varphi)/\mathrm{d}\omega$. Considering the transformation of the variables, one has the relation [68Sch1]

$$\frac{d\sigma_0(\theta_0,\phi_0)}{d\omega_0} = \frac{(1+\gamma^2+2\gamma\cos\theta)^{3/2}}{|1+\gamma\cos\theta|}\frac{d\sigma(\theta,\phi)}{d\omega} \quad , \tag{2}$$

where $\gamma = m/M_A$. Because γ is 1/1836 = $5.4\cdot10^{-4}$ for electron collision with atomic hydrogen, and is smaller with other atoms, the distinction between the center-of-mass frame and the laboratory frame is inappreciable for most purposes, and also compared to the precision of presently available cross-section data. An exception arises when one considers the energy loss of subexcitation electrons, viz., electrons at kinetic energies below the first electronic threshold, passing through a gas [90Ino1, 93Kim1]. Then, the recoil that an atom receives upon elastic scattering is the sole mechanism for the energy loss, and is determined by the momentum-transfer cross section, discussed extensively in Section 2.5.

For more detailed discussion, one must consider the state of the atom left after a collision. Suppose for simplicity that the atom was initially in the ground state. If the atom is left in the ground state, one says that the collision is elastic; then, the scattered electron has a kinetic energy that equals the initial kinetic energy minus the recoil energy, which is generally small as discussed in the preceding paragraph. The (integrated) cross section for elastic scattering is denoted by σ_{el}, which is treated in Section 2.3.

If the atom is left in a state other than the ground state, then one says that the collision is inelastic; then, the scattered electron has a kinetic energy that equals the initial kinetic energy minus the energy transferred to the atom, which includes the excitation energy of the atom and the recoil energy. Suppose that the state is characterized by a set of quantum numbers, s, the (integrated) cross section is called the cross section for the excitation of s, and is denoted by σ_s.

More specifically, when the state s belongs to a discrete spectrum, it is called the discrete-excitation cross section, which is the subject of Section 2.4. When the state s belongs to a continuous spectrum, one or more of the atomic electrons will depart from the atom, leaving an atomic ion; one calls this process ionization. The (integrated) cross section is called the ionization cross section, which is the subject of Section 2.6.

Finally, if an atom was in an excited state before a collision, it is possible that the atom is left in a state with lower energy, for instance, in the ground state; then, the scattered electron will have a kinetic energy higher than the initial kinetic energy. One calls this process a super-elastic collision. If the state of the atom remains the same after a collision, one says that the collision is elastic.

2.1.2 Scope and policy of the present treatment

The present article will presume basic knowledge of atomic physics; whenever the reader is uncertain about a point in atomic physics, he may consult with "Atomic, Molecular, and Optical Physics Handbook" [96Dra1], which presents concise treatments of many topics related to atomic collisions and spectroscopy. We shall focus on electrons of kinetic energies up to a few keV, chiefly for two reasons. First, most of applications of cross-section data concern primarily electrons of those kinetic energies, as summarized in Chapters 78-88 of the Handbook [96Dra1]. Second, when cross sections are needed for electrons at higher kinetic energies, it is generally possible to estimate their values on the basis of cross sections at lower kinetic energies, using elements of the Bethe theory [30Bet1, 71Ino1, 86Bet1].

We shall treat only neutral atoms initially in their ground state. For neutral atoms initially in an excited state, the electron scattering cross section is in general completely different from that for the ground state. Our knowledge about this topic is so severely limited both experimentally and theoretically that a survey of data for atoms in general is unwarranted at present. However, cross sections for atoms in metastable states, required in certain applications, are indeed a topic of extensive studies, as seen in a review of cross sections of metastable states of helium by de Heer et al. [95deH1]. Electron collisions with atomic ions are treated extensively in Chapter 3.

The quality of data for neutral atoms depends very much on their species. More precisely, it depends especially on whether the electronic structure is a closed shell (as in a rare-gas atom) or an open shell. Closed-shell atoms are readily prepared as targets, and simpler to treat theoretically. Open-shell atoms, in contrast, are not straightforward to prepare as target, because they are formed in fine-structure states differing only slightly in binding energies and are also chemically reactive; even in a chemically pure gas, they readily produce dimers, trimers, and other atomic clusters. As a result, the cross section data presented below are in general more trustworthy for closed-shell atoms than for open-shell atoms.

The differing quality of data for different atoms makes it not only impractical to present cross-section data for all atoms in a unified and systematic format, but also seriously misleading to the reader. Sections 2.2-2.5 thus present data only for selected atomic species for which our knowledge is better than for others. Even among the selected atoms, the data quality differs greatly. Therefore, data are presented sometimes in graphs, sometimes in tables, together with a commentary indicating the status of our knowledge.

The present article is intended to serve as a guide for rapid access to cross-section data, rather than for studying cross sections from a basic point of view. Therefore, only a single set of data is presented for each cross section.

2.1.3 Methods for the determination of cross sections

Experimental methods for measuring electron-collision cross sections have been extensively discussed in the literature. Here we remark only on their most salient features. Basically, one can determine cross sections either through an experiment under single-collision conditions ("beam method"as sketched in Subsection 2.1.1) or through analysis of the transport of macroscopic "electron swarms" in a gas, which involves a large number and variety of collision processes. The two approaches are often viewed as competitive, but are really complementary. The beam method, applicable to a wide range of the electron kinetic energy, yields results of successful measurements conceptually clear and straightforward to interpret, but it suffers from the great technical difficulty in the preparation of an electron beam with finely resolved momentum and in the momentum-analysis of scattered electrons; in general, it is also difficult to determine the absolute value of cross sections. The swarm method is experimentally easier in principle, yields absolute measurements of transport properties leading to absolute values of cross sections, but requires a numerical analysis, using either a Boltzmann transport equation or a Monte Carlo simulation. (See Section 2.5 for further discussion.) Its application is also limited to low electron kinetic energies, i.e., in practice to energies not far exceeding the lowest ionization threshold. In summary, the two methods are complementary to each other.

Theoretical methods for evaluating electron-collision cross sections have been a subject of discussion for many decades, as seen in recent representative textbooks [86Fan1, 95McC1, 95Bur1]. Trustworthy ab initio calculations are feasible only in exceptional cases concerning atoms with the simplest electronic structure such as hydrogen, helium, and, to a lesser extent, other rare gases or alkali atoms. More importantly, theory provides general constraints on certain aspects of cross-section data. An example is the Bethe expression for the energy dependence of the (integrated) cross section [71Ino1], applicable at sufficiently high energy. Another example concerns the threshold behavior for the cross section for a specific inelastic process, discussed for instance by Fano and Rau [86Fan1].

Further constraints on the cross section data are provided by what one might call systematics, e.g., by trends of the data on related species, such as those along a row or a column of the periodic table. Physically, the plausibility of the systematics can be understood in terms of the atomic size, the binding energy, and other properties of the electronic structure. However, it is in general difficult to derive the systematics on a rigorous theoretical basis. Many approaches have been made to the evaluation of the systematics using a simplified scheme and usually also some empirical parameters,

as seen for instance in [94Mar1]. Although these approaches are generally subject to questions from a basic point of view, their results often provide an educated guess in the absence of measurements or better theoretical results.

2.1.4 Data sources and data centers

Since the cross-section data for electron-atom collisions are important to many applications including the physics of discharges and plasmas, atmospheric physics, astrophysics, fusion research, and radiation physics, there have been considerable efforts toward compilation and critical analysis of the data. An early survey appears in the treatise by Massey and Burhop [69Mas1]. Recent surveys are Janev [95Jan1], Crompton et al. [91Cro1], and IAEA [95Int1]. The treatment in each of these references focuses on single applied area: Janev [95Jan1] on fusion plasma research, Crompton et al. [91Cro1] on gaseous electronics, i.e., discharges and low-temperature plasmas, and IAEA [95Int1] on radiological physics.

More general surveys occur in Inokuti [94Ino1], including discussions on various aspects of the cross-section determination, both experimental and theoretical, rather than on the data themselves. Perhaps the most general introduction to the literature is seen in McDaniel et al. [85McD1], which presents an extensive bibliography of data collections, bibliographies, review articles, and monographs (but not individual research articles) up to mid-1984 updated by McDaniel and Mansky [94McD1] to cover work up to mid-1992.

Documents presenting data collections are too numerous to be cited, but are readily found in the bibliographies [85McD1] and [94McD1]. The most recent survey of cross-section data for atoms (and also of diatomic molecules) is published by Zecca et al. [96Zec1].

To access data it is valuable to use data centers, as explained by Gallagher [94Gal1]. One of the most active data centers is the Atomic and Molecular Data Unit, Nuclear Data Section, International Atomic Energy Agency, which publishes the International Bulletin on Atomic and Molecular Data for Fusion, and maintains AMDIS (Atomic and Molecular Data Information System) accessible via the Internet at http://www.iaea.org/programmes/amdis/.

2.2 Total scattering cross sections

2.2.1 Generalities

By the term "total scattering cross section" σ_{tot} one means the sum of the (integrated) cross section σ_{el} for elastic scattering and the total inelastic-scattering cross section σ_{inel}, which is in turn the sum of the (total) excitation cross section σ_{ex} and the (total) ionization cross section σ_i. Here σ_{ex} means again the sum of cross sections for all the individual discrete excitation processes possible at the electron kinetic energy. Further, σ_i means the cross section for all possible ionization processes possible at the electron kinetic energy, including every multiplicity and the final state of the resulting ion. More precisely, σ_i here means the sum of the cross sections for single ionization, double ionization, triple ionization, and so forth with the same unit weight; it is sometimes called the *counting* ionization cross section, and is determined in principle in an experiment that scores the number of all ionization events. Another kind of experiments measure the current produced by ionization, and lead to the *gross* ionization cross section, or the *apparent total* ionization cross section, which is the sum of the cross sections for single ionization, double ionization, triple ionization, and so forth with the weights 1, 2, 3, … (The adjective "total" signifying "all

energetically possible" is necessary for precise expression; however, it is cumbersome, and therefore is often omitted when the meaning is clear from the context.) In summary,

$$\sigma_{tot} = \sigma_{el} + \sigma_{inel}, \quad (1)$$

and

$$\sigma_{inel} = \sigma_{ex} + \sigma_{i}. \quad (2)$$

To emphasize the idea of including both elastic and inelastic scattering, some authors use the term "grand total scattering cross section" for σ_{tot}.

Experimentally, the total scattering cross section is in principle measurable through attenuation of an electron beam passing through a gas, or through recoil of atoms in a beam target. Measurements of this kind and resulting data are discussed by Bederson and Kieffer [71Bed1]. In general, the quality of data thus obtained should be good for those atoms that can be readily prepared in a gas target, for instance, rare gases, owing to the simplicity of the measurements at least in principle. An example of recent work is seen in the article by Szmytkiwski et al. [96Szm1], who measured σ_{tot} of rare gases (and several molecules) and also reviewed the recent literature.

Alternatively, the total scattering cross section may be evaluated from data for individual cross sections by summation expressed by eqs. (1) and (2). In a lower part of the energy range treated in the present article, the total elastic-scattering cross section usually dominates. At higher electron energies, and certainly at relativistic kinetic energies, i.e., comparable to, or exceeding 511 keV, the total inelastic-scattering cross section will dominate. The latter may be in turn evaluated from individual inelastic-scattering cross sections, as seen for instance in the study by de Heer and co-workers [77deH1, 77deH2, 79deH1], or are under certain circumstances amenable to theoretical evaluation, as seen for instance in [67Ino1, 81Ino1, 94Jai1]. The total scattering cross section is also important in the analysis of cross-section data with the use of dispersion relations, as seen in the work by de Heer and co-workers [76deH1, 77deH1].

2.2.2 Individual atoms

2.2.2.1 Hydrogen

An early survey of data is seen in the work by de Heer et al. [77deH1]. Trajmar and Kanik [95Tra1] reviewed various experimental and theoretical data. We adopt here their recommendations (Fig. 2.2.1 and Table 2.2.1). Recent measurements by Zhou et al. [97Zho1] confirm the data to several percent.

Below the first excitation threshold (10.2 eV), the total scattering cross section σ_{tot} is the same as the elastic-scattering cross section σ_{el}. Generally, σ_{el} decreases with increasing kinetic energy E, and eventually behaves as E^{-1} at high E. The total inelastic-scattering cross section σ_{inel} increases with increasing E with the successive opening of excitation and ionization channels, reaches a maximum around 50 eV, decreases at higher E. However, because of its asymptotic behavior of the form $E^{-1} \ln E$, σ_{inel} dominates over σ_{el} at high E; then, σ_{tot} is nearly the same as σ_{inel}. Consequently, σ_{tot} is a decreasing function of E in general, with a mild modulation around 50-100 eV.

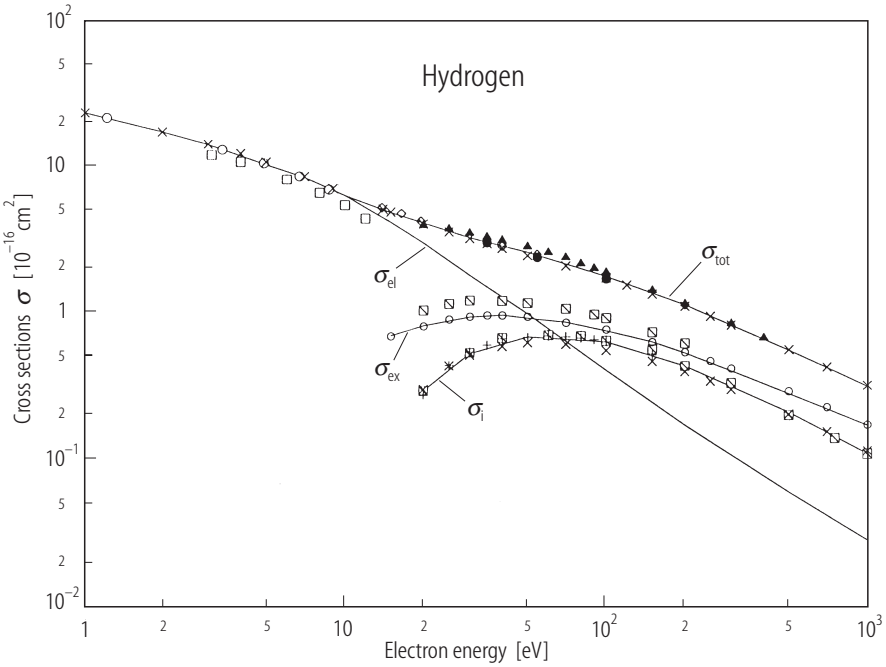

Fig. 2.2.1. Overview of cross sections for H, reproduced with permission from [95Tra1].

Table 2.2.1. Overview of cross sections for H. Data are taken primarily from Trajmar and Kanik [95Tra1]. Janev and Smith [93Jan1] give more detailed tabulations.

Energy [eV]	Cross sections [10^{-16} cm^2]				
	σ_{el}	σ_{ex}	σ_i	σ_{inel}	σ_{tot}
1	23.0				23.0
2	17.1				17.1
3	14.0				14.0
5	10.2				10.2
7	8.40				8.40
10	6.30				6.30
15	4.15	0.69		0.69	4.84
20	3.00	0.81	0.31	1.12	4.12
30	1.80	0.93	0.53	1.46	3.26
50	0.98	0.93	0.64	1.57	2.55
100	0.40	0.73	0.54	1.27	1.67
200	0.172	0.53	0.38	0.91	1.08
500	0.061	0.28	0.21	0.49	0.55
1000	0.029	0.17	0.11	0.28	0.31

2.2.2.2 Helium

de Heer and Jansen [77deH2] critically examined data on individual cross sections and evaluated σ_{el} and σ_{inel}. Hayashi [81Hay1] also presented recommended values of cross sections. More recently, Trajmar and Kanik [95Tra1], as well as Szmytkowski et al. [96Szm1] and Zecca et al. [96Zec1], reviewed extensive data, both experimental and theoretical. We adopt here the recommendation of Trajmar and Kanik [95Tra1] (Fig. 2.2.2 and Table 2.2.2). The general trend of σ_{tot} is similar to that for atomic hydrogen.

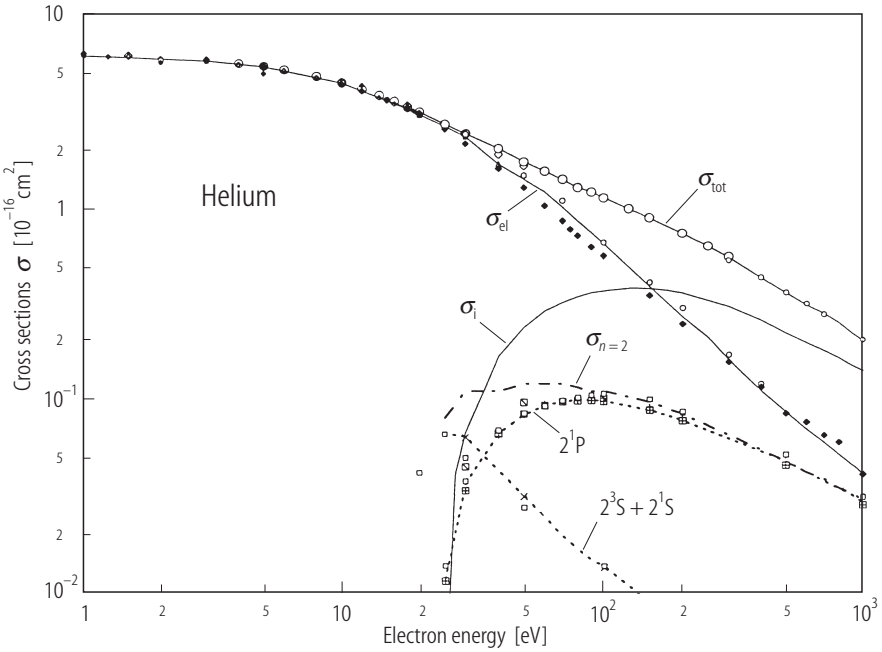

Fig. 2.2.2. Overview of cross sections for He, reproduced with permission from [95Tra1].

Table 2.2.2. Overview of cross sections for He. Data are taken primarily from Trajmar and Kanik [95Tra1], and are augmented by values given by de Heer et al [77deH2] and by Hayashi [81Hay1].

Energy [eV]	Cross sections [10^{-16} cm^2]				
	σ_{el}	σ_{ex}	σ_i	σ_{inel}	σ_{tot}
1	6.08				6.08
3	5.70				5.70
5	5.30				5.30
10	4.36				4.36
15	3.55				3.55
20	3.00				3.00
25	2.60	0.08		0.08	2.68
30	2.30	0.08	0.07	0.15	2.45
40	1.67	0.17	0.18	0.35	2.02
50	1.40	0.14	0.23	0.37	1.77
60	1.20	0.14	0.29	0.43	1.63

Energy [eV]	Cross sections [10^{-16} cm^2]				
	σ_{el}	σ_{ex}	σ_i	σ_{inel}	σ_{tot}
80	0.85	0.15	0.35	0.50	1.35
100	0.65	0.16	0.37	0.53	1.18
150	0.39	0.16	0.37	0.53	0.92
200	0.27	0.15	0.35	0.50	0.77
250	0.21	0.14	0.28	0.42	0.63
300	0.16	0.12	0.28	0.40	0.56
400	0.11	0.10	0.24	0.34	0.45
500	0.086	0.074	0.20	0.27	0.36
600	0.070	0.070	0.18	0.25	0.32
700	0.060	0.067	0.16	0.23	0.29
800	0.052	0.061	0.15	0.21	0.26
900	0.046	0.056	0.13	0.18	0.23
1000	0.042	0.050	0.12	0.17	0.21

2.2.2.3 Lithium

As the survey by Zecca et al. [96Zec1] indicates, source data are not only limited in scope and volume, but discordant. The paucity of the data chiefly stems from the difficulty of preparing atomic lithium, in high-temperature vapor, under controlled conditions including a known number density. In particular, current data for σ_{tot} from direct measurements are inconsistent with the sum of individual cross sections. Merely to show the trend of data, we adopt here values of Table 2.2.3, primarily based on the survey by Zecca et al. [96Zec1], with augmentations with the use of the excitation and ionization cross sections given by Wutte et al. [97Wut1] and with extrapolations of σ_{el}. The reliability of the presented data is much less than the data for H and He.

All cross sections are large, i.e., much larger than those for He, and are similar in trends to those of H. This is understandable from the shell structure $1s^2 2s$, with a single electron outside the inner core. However, σ_{inel} dominates over σ_{el} at all electron kinetic energies above 10 eV; the main contributor to σ_{inel} is σ_{ex}, in particular, the cross section for the lowest discrete excitation, viz., the 2s - 2p excitation.

Table 2.2.3. Overview of cross sections for Li. Data are taken primarily from Zecca et al. [96Zec1], and have been augmented by values given by Wutte et al [97Wut1] and by extrapolation.

Energy [eV]	Cross sections [10^{-16} cm^2]				
	σ_{el}	σ_{ex}	σ_i	σ_{inel}	σ_{tot}
5.4	49	49		49	98
10	40	43	3.9	47	87
20	19	36	4.1	40	59
60	4.5	21	2.2	23	28
100	2.0	13	1.5	15	17
150	1.0	10	1.0	11	12
200	0.5	8.2	0.8	9	9.5

2.2.2.4 Oxygen

According to Itikawa [94Iti1], the only experimental source of σ_{tot} is the measurement by Sunshine et al. [67Sun1]. Their data scatter widely, and are not quite consistent with the sum of individual cross sections adopted by Itikawa and Ichimura [90Iti1]. Note that values of individual cross sections are given also by Laher and Gilmore [90Lah1]. We adopt here values shown in Table 2.2.4, based on the compilations by Laher and Gilmore [90Lah1], Itikawa and Ichimura [90Iti1], Itikawa [94Iti1], and Zecca et al. [96Zec1].

Figure 2.2.3, taken from Itikawa [94Iti], shows σ_{el} and major contributors to σ_{inel} including discrete-excitation cross sections, which are complex in their behavior owing to the multiplet structure of the open shell $2s^2 2p^4$.

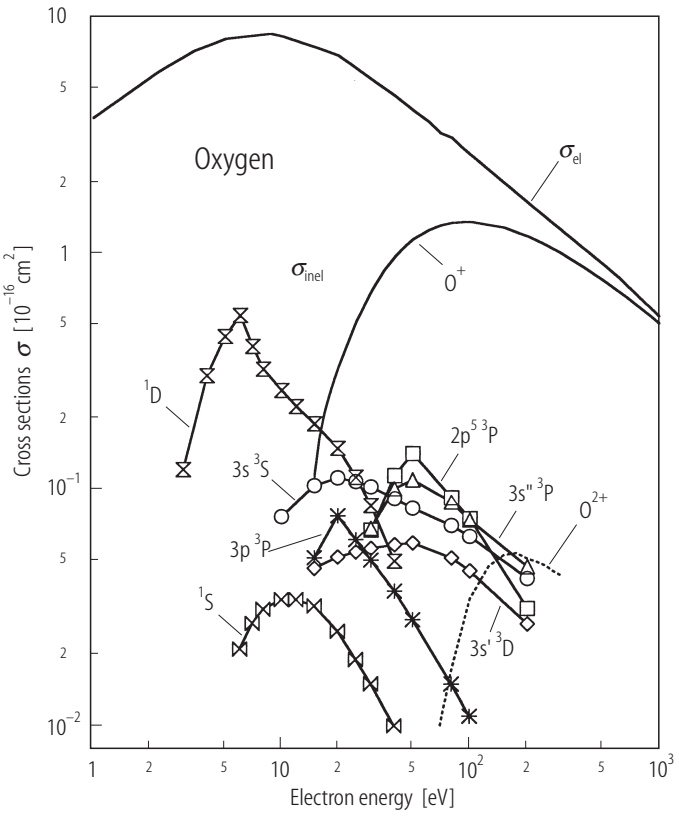

Fig. 2.2.3. Overview of cross sections for O, reproduced with permission from [94Iti1].

Table 2.2.4. Overview of cross sections for O. Data are taken primarily from Laher and Gilmore [90Lah1], Itikawa and Ichimura [90Iti], Itikawa [94Iti1], and Zecca et al. [96Zec1].

Energy [eV]	Cross sections [10^{-16} cm^2]				
	σ_{el}	σ_{ex}	σ_i	σ_{inel}	σ_{tot}
3.4	7.1	0.2		0.2	7.3
5	7.5	0.3		0.3	7.8
10	8.1	0.3		0.3	8.4
20	6.6	0.7	0.3	1.0	7.6

Energy [eV]	Cross sections [10^{-16} cm^2]				
	σ_{el}	σ_{ex}	σ_i	σ_{inel}	σ_{tot}
45	4.4	1.1	1.1	2.2	6.6
100	2.6	0.64	1.5	2.1	4.7
200	1.6	0.45	1.3	1.8	3.4
500	0.88	0.19	0.79	0.98	1.8

2.2.2.5 Neon

Soong [76Soo1, 76Soo2] reviewed data on individual cross sections, tested consistency with other information including the oscillator-strength spectrum, and adopted a complete set of inelastic-scattering cross sections, with emphasis on high electron energies. de Heer, Jansen, and van der Kaay [79deH1] also critically examined data of a broader class including σ_{el}, and evaluated σ_{inel}. Notice in particular that de Heer et al. [79deH1] determined the counting ionization cross section σ_i through full consideration of multiple ionization, which is about 5 percent at electron kinetic energies above 200 eV. Hayashi [81Hay1] also presented recommended values. Table 2.2.5 has been prepared after consideration of these earlier recommendations, and represents our adoption. The data should be good to several percent, especially in view of the compatibility of directly measured σ_{tot} with the summed value of individual cross sections within ten percent, except at electron kinetic energies below 100 eV.

Table 2.2.5. Overview of cross sections for Ne. Data are based primarily on de Heer et al. [79deH1] and Zecca et al. [96Zec1].

Energy [eV]	Cross sections [10^{-16} cm^2]				
	σ_{el}	σ_{ex}	σ_i	σ_{inel}	σ_{tot}
5	2.7				2.7
10	3.3				3.3
15	3.5	0.1		0.1	3.6
20	3.4	0.1	0.1	0.2	3.7
30	3.6	0.1	0.1	0.2	3.8
40	3.4	0.20	0.23	0.43	3.8
50	3.1	0.21	0.30	0.51	3.6
60	2.9	0.17	0.43	0.60	3.5
80	2.6	0.17	0.58	0.75	3.4
100	2.3	0.16	0.68	0.84	3.1
150	1.7	0.14	0.75	0.89	2.6
200	1.4	0.12	0.74	0.86	2.3
300	1.1	0.10	0.72	0.82	1.9
400	0.91	0.083	0.65	0.73	1.6
500	0.77	0.071	0.58	0.65	1.4
700	0.62	0.055	0.41	0.46	1.1
800	0.49	0.051	0.44	0.49	1.0
1000	0.46	0.043	0.33	0.37	0.82
2000	0.29	0.025	0.19	0.21	0.50
3000	0.21	0.018	0.14	0.16	0.37

The composition of the total scattering cross section σ_{tot} considerably differs from that for He; σ_{el} for Ne continues to be appreciable on going to higher electron kinetic energies E, and indeed dominates over σ_{inel} up to 3000 eV, basically owing to the presence of the atomic inner core $1s^2 2s^2$. (On the basis of the Bethe theory one expects that σ_{inel} should dominate over σ_{el} at a sufficiently high E, owing to the behavior of the form $E^{-1} \ln E$, with relativistic modifications.) Yet the outermost subshell $2p^6$, containing six electrons, makes σ_{inel} appreciably larger than that for He.

2.2.2.6 Sodium

Sodium, Na, has been studied more extensively than Li, even though it is also difficult to prepare as atomic vapor. As a result, the data are probably more trustworthy than those for Li, but yet at a level far inferior to those for rare gases. Table 2.2.6 shows our adoption, based on Zecca et al. [96Zec1] and the recent literature cited there.

The general trend of the cross sections of Na is similar to those of Li, reflecting the structure $1s^2 2s^2 2p^6 3s$, containing one electron outside the inner core.

Table 2.2.6. Overview of cross sections for Na. Data are based primarily on Zecca et al. [96Zec1].

Energy [eV]	Cross sections [10^{-16} cm^2]				
	σ_{el}	σ_{ex}	σ_i	σ_{inel}	σ_{tot}
10	14	37	4.4	41	55
20	10	39	4.6	44	54
50	5	21	3.2	24	29
100	2.4	16	2.1	18	21
150	2.2	12	1.7	14	16

2.2.2.7 Argon

Eggarter [75Egg1, 80Egg1] critically reviewed data in view of criteria including the compatibility with the oscillator-strength spectrum, and produced a complete set of individual cross sections for inelastic scattering, with emphasis on high electron energies. de Heer, Jansen, and van der Kaay [79deH1] also critically examined data of a broader class including σ_{el}, and evaluated σ_{inel}. Upon evaluating σ_{inel}, they determined specifically the counting ionization cross section σ_i; multiple ionization amounts to 7 % or higher at electron kinetic energies above 200 eV. Hayashi [81Hay1] also presented recommended values. Table 2.2.7, prepared after consideration of these compilations, represents our adoption. The quality of the data should be good in view of many tests of criteria, including the compatibility of directly measured stot with the summation of individual cross sections, except at electron kinetic energies below 100 eV, and the consistency of inelastic-scattering cross sections with the oscillator-strength spectrum, and other theoretical constraints [75Egg1]. Uncertainties of cross-section values at 100 eV and below even for this repeatedly studied case represent a major challenge for future work.

The dominant component of σ_{tot} is σ_{el} throughout the energy range, up to 3000 eV, for which the data are shown, because of the presence of the substantial atomic inner core $1s^2 2s^2 2p^6$. At the same time σ_{inel} has an appreciable magnitude, indeed much greater than that for Ne, chiefly attributable to the sizable outer shell $3s^2 3p^6$.

Table 2.2.7. Overview of cross sections for Ar. Data are based primarily on de Heer et al. [79deH1] and Zecca et al. [96Zec1].

Energy [eV]	Cross sections [10^{-16} cm^2]				
	σ_{el}	σ_{ex}	σ_i	σ_{inel}	σ_{tot}
5	9				9
10	19				19
15	23				23
20	19	0.5	0.6	1.1	20
30	13	0.7	1.8	2.5	15
40	9.5	0.8	2.3	3.1	13
50	7.2	0.7	2.4	3.1	10
100	4.8	0.7	2.50	3.2	8.0
150	3.8	0.65	2.35	3.00	6.8
200	3.2	0.54	2.25	2.78	6.0
300	2.5	0.41	1.83	2.24	4.7
400	2.1	0.33	1.55	1.88	4.0
500	2.0	0.28	1.35	1.63	3.6
800	1.4	0.20	0.91	1.11	2.6
1000	1.3	0.17	0.79	0.96	2.2
2000	0.80	0.09	0.45	0.54	1.35
3000	0.57	0.055	0.35	0.40	0.97

2.2.2.8 Krypton

Table 2.2.8. Overview of cross sections for Kr. Data are based primarily on de Heer et al. [79deH1] and Zecca et al. [96Zec1].

Energy [eV]	Cross sections [10^{-16} cm^2]				
	σ_{el}	σ_{ex}	σ_i	σ_{inel}	σ_{tot}
5	15				15
10	13				13
20	20	1.3	1.2	2.5	23
30	13	0.9	2.6	3.5	17
40	11	1.0	3.2	4.2	15
50	9	0.98	3.4	4.4	13
100	5.9	0.88	3.4	4.3	10.2
150	4.5	0.76	3.2	4.0	8.5
200	3.7	0.62	3.1	3.7	7.5
300	3.2	0.48	2.4	2.9	6.1
400	2.8	0.40	2.1	2.5	5.3
500	2.4	0.33	1.8	2.2	4.6
1000	1.8	0.20	1.2	1.4	3.2
2000	1.1	0.11	0.67	0.79	1.9
3000	0.98	0.08	0.47	0.55	1.5

Table 2.2.8 represents our adoption primarily based on the surveys by de Heer et al. [79deH1] and by Zecca et al. [96Zec1]. The degree of compatibility of directly measured σ_{tot} with the summation of individual cross sections is comparable with the data for Ar.

The composition of σ_{tot} shows a feature different from that for Ar. Over a wide range, 150-1000 eV, σ_{el} and σ_{inel} contribute comparably to σ_{tot}. The greater importance of σ_{inel} than in Ar is understandable from the outer subshells $3d^{10}4s^{2}4p^{6}$, which give rise to successively greater contributions to inelasticity with the opening of many excitation channels at higher and higher E. Yet at 2000 eV and 3000 eV, σ_{el} remains to dominate, as that for Ar.

2.2.2.9 Xenon

Table 2.2.9 shows our adoption primarily based on de Heer et al. [79deH1] and Zecca et al. [96Zec1]. The degree of compatibility of directly measured σ_{tot} with the summation of individual cross sections is more modest than for the data for Ar.

The composition of σ_{tot} is roughly similar to that for Kr. However, as Zecca et al. [96Zec1] point out, the trend of σ_{inel} as a function of the electron kinetic energy E is more complicated upon closer examination (not readily discernible in Table 2.2.8 because of the coarse grid for E).

Table 2.2.9. Overview of cross sections for Xe. Data are based primarily on de Heer et al. [79deH1] and Zecca et al. [96Zec1].

Energy [eV]	Cross sections [10^{-16} cm^2]				
	σ_{el}	σ_{ex}	σ_{i}	σ_{inel}	σ_{tot}
5	34				34
10	38	0.2		0.2	38
15	38	0.2	1.0	1.2	39
20	29	3.7	2.5	6.2	35
30	13	3.8	4.2	8.0	21
40	9.6	2.9	4.6	7.5	17
50	8.8	2.4	4.8	7.2	16
60	6.3	2.1	4.9	7.0	13
80	6.2	1.7	5.0	6.7	13
100	5.5	1.4	5.0	6.4	12
150	4.4	0.9	4.6	5.5	10
200	4.9	0.8	4.0	4.8	9.6
300	3.8	0.6	2.9	3.5	7.3
400	4.0	0.47	2.86	3.3	7.3
500	3.5	0.40	2.53	2.93	6.4
700	2.8	0.30	2.01	2.31	5.1
1000	2.5	0.23	1.50	1.73	4.2
2000	1.7	0.13	0.91	1.04	2.7
3000	1.44	0.095	0.63	0.73	2.17

2.2.2.10 Mercury

Unlike Li and Na, mercury, Hg, has an appreciable vapor pressure even at room temperature. Therefore, it has been an object of extensive studies with respect to electron scattering since the celebrated experiment by Franck and Hertz [14Fra1], who demonstrated the presence of discrete energy levels through observation of electron transmission through mercury vapor. As a consequence, the electron-scattering cross sections of Hg are reasonably well established up to about 300 eV. Table 2.2.10 shows our adoption, which is based on the survey by Zecca et al. [96Zec1] and the recent literature cited therein.

The composition of σ_{tot} is roughly similar to that for Xe, but is more complicated in detail, and depending on the electron kinetic energy. This is attributable to the presence of as many as 80 electrons, the large dipole polarizability (which makes σ_{el} sizable), the outer electronic structure $4f^{14}5d^{10}6s^2$, which includes 2 valence electrons moving outside a not very rigid inner core.

Table 2.2.10. Overview of cross sections for Hg. Data are based primarily on Zecca et al. [96Zec1].

Energy [eV]	Cross sections [10^{-16} cm^2]				
	σ_{el}	σ_{ex}	σ_i	σ_{inel}	σ_{tot}
15	12	5	1.8	7	19
25	10	7	4.4	11	20
50	10	6	5.8	12	22
100	9	3.6	5.0	8.6	18
150	8	2.0	4.2	6.2	14
300	5	1.3	3.1	4.4	9

2.2.3 Additional remarks

For the other atoms in general, data found in the current literature are uncertain at least to the same level as those for the atoms explicitly discussed above. The survey by Zecca et al. [96Zec1] mentions to some data on Mn, K, Rb, Cs, Mg, Cu, Bi, and Pb, but not to the other some 80 atoms.

If the reader needs some values for an application, he may refer to some of the theoretical results. For instance, Inokuti et al. [81Ino1] give values of σ_{inel} for all atoms up to strontium (Z = 38), evaluated with the Bethe theory and thus applicable to sufficiently high electron kinetic energies.

2.3 Elastic scattering cross section

2.3.1 Generalities

Modern quantitative study of elastic scattering of electrons by atoms was pioneered by Westin [46Wes1], who systematized data with the use of the partial-wave analysis, as explained in many textbooks, for instance, [86Beth1] and [95Bur1]. To the extent that one may describe electron-atom interactions in terms of a central (i.e., spherically symmetric) potential, the elastic scattering is fully characterized by the phase shift, which is a function of the kinetic energy and the angular momentum of the electron, and may be readily evaluated for a given potential or may be determined to through a fit of measured data for the differential cross section. A key point of this analysis is that each partial wave, corresponding to a fixed angular momentum, is determined independently of the other partial waves. At sufficiently low energies, only a modest number of lower partial waves have appreciable values of the phase shifts, because higher partial waves cannot penetrate the inner region of the atom owing to the centrifugal potential. The partial-wave analysis is fully justified for electron kinetic energies below the lowest electronic-excitation threshold. (As a qualification, considerations of the electron spin necessitates a more elaborate treatment.)

The use of a central potential is an approximation when the electron kinetic energy exceeds the lowest electronic-excitation threshold for any atom, because any inelasticity means a loss of electron flux from the elastic channel and should affect the elastic-scattering cross section. Influence of inelastic scattering on elastic scattering can be formally incorporated by use of a complex-valued potential, as discussed by Burke and Joachain [95Bur1]. More importantly, when the target atom has an open electronic structure, the central-potential approach is a schematization in general. Nevertheless, the phase-shift data evaluated with a central potential are useful for estimating elastic-scattering cross sections when no other data source is available, and also for interpreting their systematics. (Further discussion on this topic is given in Subsection 2.3.3 below.)

It is customary to consider a central potential as consisting of several contributions. First, an electrostatic potential is produced by the nuclear charge Ze and the charge distribution of atomic electrons in the ground state, and is usually the dominant contribution. This potential approaches that of the bare nuclear charge, $-Ze^2/r$, at short distances r from the nucleus, and progressively weakens by the shielding by atomic electrons at larger distances, and eventually falls off exponentially at very large distances. Second, the electric polarization of the charge distribution of atomic electrons by a slowly approaching electron gives rise to a polarization potential, which behaves as $-\alpha e^4/(2r^4)$ at very large distances, where α represents the dipole polarizability of the atom. As the electron becomes faster, the electric polarization becomes less, and the polarization potential diminishes. Third, effects of the indistinguishability of the approaching electron from atomic electrons may be approximately represented by a potential, which is appreciable at distances comparable to the atomic size and shorter. (These effects are often referred to as electron-exchange effects. The term "exchange" historically originates from a presumed labeling of interacting electrons, which is in principle impossible, and is unfortunate, but is now too well established to be purged.) In general, a short-range part of a central potential primarily affects large-angle scattering, and a long-range part small-angle scattering; however, there is often an interplay of different parts of the potential, which defies straightforward interpretation.

If the potential for a particular partial wave, viz., the central potential plus the centrifugal potential has a sufficiently deep minimum at some distance, an incoming electron of a certain kinetic energy can be temporarily trapped, and stay near the atom for a period much longer than the ordinary transit time r_a/v before eventually leaving away, where r_a is the atomic radius and v is the electron speed. This phenomenon is called a (shape) resonance, and manifests itself as an abrupt change of the phase shift for the partial wave at the particular electron energy, Sometimes it leads to a drastic change in the differential cross section, or even in the (integrated) cross section near that particular electron energy.

2.3.2 Individual atoms

Many of the remarks made in Subsection 2.2.2 pertain to the total elastic-scattering cross section, and its relation with other cross sections, for each atom treated.

2.3.2.1 Hydrogen

Trajmar and Kanik [95Tra1] thoroughly reviewed theoretical and experimental data. One finds excellent agreement among recent results as well as consensus among recent recommendations. See Fig. 2.2.1 and Table 2.2.1.

2.3.2.2 Helium

Trajmar and Kanik [95Tra1] and Zecca et al. [96Zec1] reviewed extensive data, both theoretical and experimental. We adopt here the recommendation of [95Tra1] (Fig. 2.2.2 and Table 2.2.2). A resonance at 19.3 eV is most conspicuous in σ_{el}.

2.3.2.3 Lithium

As the survey by Zecca et al. [96Zec1] indicates, source data are limited in both scope and volume. See Table 2.2.3.

2.3.2.4 Oxygen

Itikawa and Ichimura [90Iti1], as well as Laher and Gilmore [90Lah1], reviewed data, Later Itikawa [94Iti1] present additional discussion. See Table 2.2.4, and also Fig. 2.2.3, taken from Itikawa [94Iti1].

2.3.2.5 Neon

Data up to 1978 were reviewed by de Heer et al. [79deH1]. More recent data were reviewed by Zecca et al. [96Zec1]. See Table 2.2.5. Values of σ_{el} are well established, to precision of a few percent. The total elastic-scattering cross section σ_{el} has a very broad maximum around 20…30 eV. Resonances at 16.11 eV and 16.30 eV are prominent in σ_{el}.

2.3.2.6 Sodium

Table 2.2.6 gives our adoption primarily based on the survey by Zecca et al. [96Zec1].

2.3.2.7 Argon

Data were reviewed by de Heer et al. [79deH1], and recently by Zecca et al. [96Zec1]. See Table 2.2.7. Values of σ_{el} are established, to precision of a few percent. There is a fairly sharp maximum around 16 eV. Resonances at 11.1 eV and 11.3 eV are also notable in high-resolution data.

At 0.235 eV, σ_{el} shows a conspicuous minimum. called the Ramsauer-Townsend minimum, as discussed in greater detail in Section 2.5.

2.3.2.8 Krypton

Data were reviewed by de Heer et al. [79deH1], and recently by Zecca et al. [96Zec1]. See Table 2.2.8. Around 10 eV, σ_{el} shows a maximum. A Ramsauer-Townsend minimum occurs at 0.55 eV.

2.3.2.9 Xenon

Data were reviewed by de Heer et al. [79deH1], and recently by Zecca et al. [96Zec1]. See Table 2.2.9. Around 7-8 eV, σ_{el} shows a broad maximum. A Ramsauer-Townsend minimum occurs at 0.65 eV.

2.3.2.10 Mercury

See Table 2.2.10.

2.3.3 Additional remarks

When no reliable experimental results are available for an application, one may wish to use theoretical results on electron elastic scattering by atoms. Recent sources of theoretical results for many atoms include Salvat et al. [85Sal1], Tilinin [88Til1], Browning [91Bro1], and Mayol and Salvat [97May1]. Tilinin [88Til1] discusses the momentum-transfer cross section, and presents a scaling relation claimed to be applicable to electron kinetic energies of $3 \cdot 10^2$-$1 \cdot 10^4$ eV and to all atoms. Browning [91Bro1] presents an analytic expression for the total elastic-scattering cross section as a function of the electron kinetic energy E and the atomic number Z, which is based on a survey of calculations with the phase-shift method and is claimed to be useful for E = 1-100 keV. Mayol and Salvat [97May1] have recently carried out extensive calculations of the phase shift using the Dirac equation with a central potential, and present total and momentum-transfer cross sections for all neutral atoms up to uranium for $E = 10^2$-10^9 eV. (The use of the Dirac equation is essential at E appreciable compared with mc^2 = 511 keV or higher.)

Table 2.3.1 presents comparison of the values given by Mayol and Salvat and by Browning with the values of the total elastic-scattering cross section we adopted as realistic in Tables 2.2.1-10. The values by Mayol and Salvat are reasonably close to our adopted values in general, and very close for Hg and rare gases except for He. The sizable discrepancies for H, Li, and Na might be indicative of the extent of applicability of a central potential to the electron scattering by an open-shell atom. The analytic expression of Browning is a low-precision approximation for heavier atoms at best.

Table 2.3.1. Calculated values of the total elastic-scattering cross section. Values given by Mayol and Savat [97May1] are indicated by *MS*. Values computed from a fitting equation, Eq. (4) of Browning [91Bro1], are indicated by *Br*. They are compared here with the values we adopted as realistic, and are indicated by *Ad*.

Atom	Cross section [10^{-16}cm^2]									
	E = 100 eV		E = 500 eV		E = 1000 eV			E = 2000 eV		
	MS	Ad	MS	Ad	MS	Br	Ad	MS	Br	Ad
H	0.33	0.40	0.058	0.061	0.029	0.048	0.029	0.014	0.024	
He	0.55	0.65	0.092	0.086	0.044	0.12	0.042	0.022	0.061	0.021
Li	2.43	2.0	0.55		0.28	0.21		0.14	0.11	
O	2.54	2.6	0.90	0.88	0.54	0.71		0.31	0.38	
Ne	2.15	2.3	0.81	0.77	0.51	0.92	0.46	0.30	0.50	0.29
Na	3.68	2.4	1.33		0.81	1.01		0.48	0.56	
Ar	4.92	4.8	2.05	2.0	1.38	1.63	1.3	0.88	0.95	0.80
Kr	5.90	5.9	2.69	2.4	1.90	2.73	1.8	1.30	1.73	1.1
Xe	3.90	3.9	3.86	3.5	2.83	3.43	2.5	2.02	2.26	1.7
Hg	9.21	9.0	7.01		3.71	4.14		2.59	2.80	

2.4 Excitation

2.4.1 Generalities

The present section treats the cross section for the excitation of lower discrete excited states. The term "lower" here means more precisely the excitation of an electron from the valence shell (technically from the outermost subshell) of atoms. The inner-shell excitation of atoms by electron collisions is certainly a subject rich in basic physics involved and is important in certain applications, but is beyond the scope of the present Chapter.

The following brief summary of general characteristics of the discrete-excitation cross section should serve as a preliminary to the presentation of cross-section data.

2.4.1.1 Dipole allowed and forbidden transitions

An important result of the Bethe theory [30Bet1, 71Ino1, 86Bet1] concerns the dependence of the cross section σ_s for the discrete excitation to state s on the electron kinetic energy E. When the transition from the ground state to state s is dipole allowed, i.e., when it has a nonvanishing dipole oscillator strength f_s, then σ_s behaves as

$$\sigma_s = 4\pi\, a_0^2\, \mathrm{Ry}^2\, E^{-1}\, [(f_s/W_s) \ln E + B_s], \tag{1}$$

for sufficiently high (but nonrelativistic) E, more precisely, at E exceeding many multiples of the excitation energy W_s of state s measured from the ground state, where B_s is a parameter that depends on s, a_0 represents the Bohr radius, $\hbar^2/me^2$ = 0.05292 nm, and Ry the Rydberg energy, $me^4/(2\hbar^2)$ = 13.606 eV. This result arises from the dominance of the dipole interaction of a fast incident electron

passing at a large distance with atomic electrons, whose action on the atom is equivalent to that of the absorption of photons characterized by a broad energy spectrum, over other modes of interactions effective at shorter distances. Indeed, the contribution of the dipole interaction is represented by the term proportional to $(f_s/W_s)\, E^{-1} \ln E$. The other contributions are represented by the term proportional to E^{-1} at high E. (At relativistic E, i.e., at kinetic energies comparable to, or higher than, mc^2 = 511 keV, Eq. (1) needs to be modified, as fully explained in [71Ino1].)

The above observation leads to the idea of plotting the product $E\sigma_s$ against $\ln E$, as first pointed out by Fano [54Fan1]. One should then obtain a curve that approaches at sufficiently high E a straight line with a slope given by f_s/W_s, apart from a universal constant. (At relativistic E, it is appropriate to plot $\beta^2\sigma_s$ against $\ln(\beta^2/(1-\beta^2))-\beta^2$, where $\beta c = v$ is the speed of an incident electron, as explained in [71Ino1].) Incidentally, the product $E\sigma_s$, apart from a universal factor, is significant also in the theory of electron collisions at low energies, and is called in this context the collision strength [96Bur1].

For a dipole-forbidden transition, for which f_s vanishes by definition, the $E^{-1} \ln E$ term is missing in Eq. (1). The distinction between a dipole-allowed transition and a dipole-forbidden transition is crucial at high E; in other words, σ_s for a dipole-forbidden transition decreases much more rapidly than σ_s for a dipole-allowed transition. More importantly, this trend of the E-dependence generally persists at considerably lower kinetic energies, i.e., down to E comparable to only a few multiples of W_s.

Furthermore, one should note differences among different kinds of forbidden transitions. When a transition is dipole-forbidden by the spatial symmetry, for instance, when it is an s-s or s-d transition, the excitation cross section σ_s is usually appreciable at fairly high kinetic energies. In contrast, when a transition is more strongly forbidden, for instance, when it involves a change in the spin quantum number, the excitation cross section σ_s decreases with electron kinetic energy more rapidly, for atoms of lower atomic numbers.

All the above-described general characteristics of the discrete-excitation cross section are useful on judging the correctness of experimental data.

2.4.1.2 Collision strength

Suppose that an atom A initially in a state i is excited to a state j by collision of an electron with momentum $\hbar k_i$, and let us write the (integrated) cross section for this process as σ_{fi}. After the collision the electron will have momentum $\hbar k_f$, which can be readily computed from the conservation of the total energy of the electron plus the atom. Similarly, we may consider the de-excitation of the atom in the state j back to the state i by collision of an electron with momentum $\hbar k_f$, and write the (integrated) cross section for this process as σ_{if}. Symbolically we may write

$$e(\hbar k_i) + A_i \leftrightarrow e(\hbar k_f) + A_f. \tag{2}$$

Then, there is a relation, called the principle of detailed balancing,

$$\omega_i\, k_i^2\, \sigma_{fi} = \omega_f\, k_f^2\, \sigma_{if}\,, \tag{3}$$

where ω_i represents the statistical weight of the state i, and ω_f that of the state f. The quantity on either side of Eq. (3) is called the collision strength and is usually denoted by symbol Ω_{fi}; obviously it is symmetric with respect to the interchange of i and f. (See p. 538 of [96Dra1].)

The collision strength is dimensionless, and is more closely connected with basic elements of the quantum theory of scattering than the cross section. It is convenient for data presentation because its dependence on the electron kinetic energy is often mild, milder than the dependence of the corresponding cross section itself. In addition, the collision strength is the same quantity used in the Fano plot, apart from a constant factor.

2.4.1.3 Resonance

The discrete-excitation cross section is often a smooth function of the electron kinetic energy E for a broad range of E. Exceptions arise in certain ranges of E owing to a temporary formation of a combined state of an electron plus an atom, which persists for a period much longer than the period of ordinary orbital motion of an atomic electron (which is of the order of $\hbar^3/me^4 = 2.419 \cdot 10^{-17}$ s). Such a state is called a resonance [86Fan1, 95McC1, 95Bur1]. For a resonance to occur, an electron must have a certain energy and angular momentum. The occurrence of a resonance is often interpreted in terms of an unoccupied atomic orbital in the Hartree-Fock approximation. A resonance manifests itself often conspicuously in the differential cross section for elastic or inelastic scattering, and sometimes cause sharp variations of the (integrated) cross section as a function of E, which can be characterized by a set of parameters as fully explained in [86Fan1].

2.4.1.4 Threshold behavior

The behavior of the excitation cross section σ_s near the threshold W_s, i.e., at E slightly above W_s, is determined by the motion of the scattered electron, which has a minute kinetic energy and is governed by long-range interactions with the atom left behind [84Rau1, 86Fan1]. In the simplest case where long-range interactions are negligible, σ_s should behave as in $(E - W_s)^{l+1/2}$, where $E - W_s$ is the excess energy and l is the orbital angular momentum of the scattered electron; usually the contribution from $l = 0$ should dominate near the threshold. When long-range interactions are appreciable (as is the case for instance for atomic hydrogen left in any of its discrete excited states, which are degenerate and thus give rise to strong dipole interactions), the threshold behavior is more complicated.

2.4.1.5 Relation to the ionization cross section

At a fixed electron kinetic energy, the cross section for the excitation to higher discrete states should be connected with the cross section for ionization resulting in ejection of an electron with zero kinetic energy, because the final states of higher and higher discrete excitations should converge to the continuum state of zero kinetic energy [86Fan1]. Consider for instance a Rydberg series of states characterized by the principal quantum number n and the orbital angular-momentum quantum number l of a single electron moving around a closed-shell ion core. The energy E_{nl} of the state n, l measured from the relevant ionization threshold is $\mathrm{Ry}/(n - \mu_l)^2$, where Ry represents the Rydberg energy (13.606 eV) and μ_l is the quantum defect characteristic of the series. Let the cross section for the excitation of state n, l be $\sigma_{n,l}$. Then, the product $(2\mathrm{Ry})^{-1}(n - \mu_l)^3\sigma_{n,l}$ should approach in the limit of large n the cross section $\mathrm{d}\sigma_l/\mathrm{d}w$ for ionization resulting in the ejection of an electron with kinetic energy w and angular momentum number l, in the limit of w approaching zero. Notice that $\mathrm{d}\sigma_l/\mathrm{d}w$ represents the cross section per unit range of w; the factor $(2\mathrm{Ry})^{-1}\ (n - \mu_l)^3$ represents the density of states per unit range of the excitation energy in the discrete spectrum. This relation is useful for estimating the cross sections for higher excitations from data on lower excitations, or for testing consistency of data [73Kim1].

As a consequence of the above consideration, one expects that $\sigma_{n,l}$ at a fixed electron kinetic energy can be fitted to the form $K_1/n^3 + K_2/n^4 + K_3/n^5 + \ldots$, K_1, K_2, K_3 ... being constant, which is often used in practice.

2.4.1.6 Photo-emission cross section

It is important to distinguish the discrete-excitation cross section from the cross section for the emission of photons corresponding to a particular spectral line. (The latter cross section is often referred to as the optical-excitation cross section when it is presented in an absolute value, and as the optical-excitation function when relative values are presented as a function of the electron kinetic energy.)

Suppose one considers a state s that emits a photon of interest. However, the state s in general may emit also a photon of different energy or may decay nonradiatively (e.g., by thermal collision with another atom or molecule, or by an Auger effect). Therefore, the probability of emission of a photon of interest (often called the branching ratio) is less than unity in general. Furthermore, the state s may be formed either directly by electron collision or indirectly by the excitation of a higher discrete state s' followed by a radiative or nonradiative transition, or even by a succession of such transitions; this indirect process is called a cascade.

The light emitted by an atom after electron collision is in general polarized and has an angular distribution. Thus, a quantitative treatment must account for the polarization and the angular distribution.

An extensive review of the topic up to 1988 is given by Heddle and Gallagher [89Hed1], and a survey of data by van der Burgt et al. [89van1]. A more recent review is given by Filippelli et al. [94Fil1].

2.4.2 Individual atoms

Subsection 2.2.2 presents adopted values of the total discrete-excitation cross sections for ten atoms. Many of the remarks given there are basic to discrete excitation in general. Following are additional discussions on selected data and topics.

2.4.2.1 Hydrogen

Janev and Smith [93Jan1] present recommended cross sections for the excitation to the 2s, 2p, 3s, 3p, and 3d states individually for the electron kinetic energy E up to 10 keV, with estimated accuracy of 10 % or better at E > 100 eV, and more modest at lower E. They also give the sum of the excitation cross sections for to n = 4 and n =5 states. See Tables 2.4.1-6. More recent recommendations for the 2s and 2p excitations by Trajmar and Kanik [95Tra1] are similar.

More significantly, the recent measurements by James et al. [97Jam1] of the 2p excitation cross section agree with the recent calculations with the convergent close-coupling method within 7 % for the electron kinetic energy from 14 eV to 1.8 keV. These authors carried out not only elaborate measurements, but also conducted extremely detailed evaluation of errors and a critical analysis of results in comparison with theory. An element of the analysis is the Fano plot, reproduced here as Fig. 2.4.1.

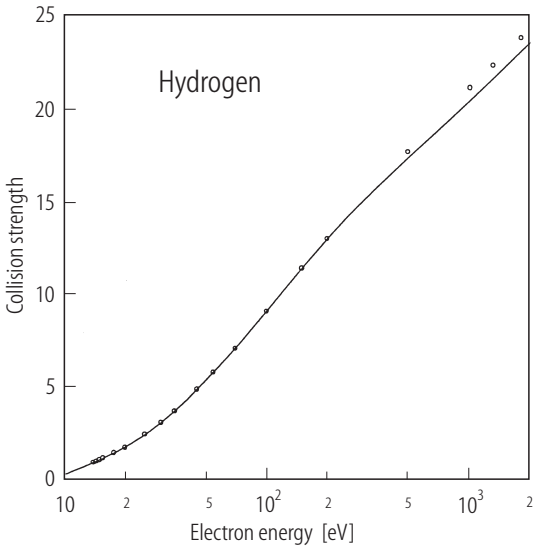

Fig 2.4.1 The Fano plot for the cross section for the 2p excitation of H, reproduced with permission from [97Jam1]. The vertical axis represents the collision strength, which is defined as $\omega_i(E/\mathrm{Ry})(\sigma_n/\pi a_0^2)$, where ω_i is the statistical weight of the initial state, E/Ry is the electron kinetic energy measured in units of the Rydberg energy, and $\sigma_n/\pi a_0^2$ is the cross section measured in $\pi a_0^2 = 0.280 \cdot 10^{-16}$ cm^2. (See p. 538 of [96Dra1].) The horizontal axis represents E on a logarithmic scale. The Bethe theory tells that the plot should approach a straight line at high enough E, as seen from Eq. (1).

Table 2.4.1. Cross sections for discrete excitations to the 2s and 2p states of H, as recommended by Janev and Smith.

E [eV]	σ [10^{-18}cm^2]	
	2s	2p
10.2	11.4	14.1
20	8.46	44.9
40	6.73	64.4
60	5.46	64.6
80	4.57	60.5
100	3.92	55.9
200	2.27	39.2
400	1.22	24.8
600	0.838	18.5
800	0.637	14.9
1000	0.513	12.5
2000	0.261	7.22
4000	0.131	4.08
6000	0.0879	2.90
8000	0.0660	2.27
10000	0.0528	1.88

Table 2.4.2. Cross sections for discrete excitations to the n = 2 states of H, as recommended by Janev and Smith.

E [eV]	σ [10^{-18}cm^2]
	n = 2
10.2	25.5
20	53.3
40	71.2
60	70.1
80	65.1
100	60.0
200	41.5
400	26.1
600	19.4
800	15.5
1000	13.1
2000	7.5
4000	4.22
6000	3.00
8000	2.35
10000	1.94

Table 2.4.3. Cross sections for discrete excitations to the 3s, 3p and 3d states of H, as recommended by Janev and Smith.

E [eV]	σ [10^{-18}cm^2]		
	3s	3p	3d
12.4	2.25	5.71	2.92
20	3.12	9.91	4.58
40	1.04	12.4	2.42
60	0.893	11.7	1.58
80	0.799	10.7	1.17
100	0.712	9.68	0.923
200	0.441	6.55	0.432
400	0.244	4.08	0.206
600	0.168	3.03	0.134
800	0.127	2.44	0.100
1000	0.103	2.05	0.0812
2000	0.0517	1.19	0.0412
4000	0.0258	0.676	0.0204
6000	0.0172	0.479	0.0136
8000	0.0129	0.375	0.0102
10000	0.0103	0.310	0.00822

Table 2.4.4. Cross sections for discrete excitations to the n = 3 states of H, as recommended by Janev and Smith.

E [eV]	σ [10^{-18}cm^2]
12.4	10.8
20	17.9
40	15.8
60	14.3
80	12.7
100	11.3
200	7.42
400	4.55
600	3.34
800	2.67
1000	2.23
2000	1.27
4000	0.718
6000	0.512
8000	0.398
10000	0.331

Table 2.4.5. Cross sections for discrete excitations to the n = 4 states of H, as recommended by Janev and Smith.

E [eV]	σ [10^{-18}cm^2]
14	7.02
20	9.44
40	7.46
60	5.98
80	5.03
100	4.37
200	2.72
400	1.62
600	1.17
800	0.936
1000	0.783
2000	0.441
4000	0.246
6000	0.173
8000	0.135
10000	0.111

Table 2.4.6. Cross sections for discrete excitations to the n = 5 states of H, as recommended by Janev and Smith.

E [eV]	σ [10^{-18}cm^2]
14	4.62
20	5.99
40	4.36
60	3.21
80	2.58
100	2.20
200	1.33
400	0.777
600	0.569
800	0.456
1000	0.379
2000	0.212
4000	0.119
6000	0.0837
8000	0.0652
10000	0.0537

2.4.2.2 Helium

de Heer et al. [92deH1] present recommended cross-section values for the excitation to the n^1S ($n = 2…6$), n^1P ($n = 2…6$), and n^1D ($n = 3…6$) states, as well as to the n^3S ($n = 2…6$), n^3P ($n = 2…6$), and n^3D ($n = 3…6$) states, for the electron kinetic energy up to 2 keV. Kato and Janev [92Kat1] gave analytic representation of the cross-section values recommended by de Heer et al. [92deH1].

A recent update by de Heer [98deH1] indicates that the recommended values are accurate to better than 10 % for the singlet excitations as well as the 2^3S and 2^3P excitations, but are less certain for the other triplet excitations. Tables 2.4.7-14 present the results of this update [98deH1], which should be even more accurate.

Table 2.4.7. Cross sections for discrete excitations to the 2^1S and 2^1P states of He, as recommended by de Heer.

E [eV]	σ [10^{-18}cm^2]	
	2^1S	2^1P
25	2.31	2.11
26.5	2.34	2.64
30.0	2.25	3.75
33.882	2.18	
35.160	2.15	5.41
40.0	2.07	6.43
45.0	1.95	7.71
50.0	1.85	8.21
60.0	1.70	9.51
80.0	1.42	10.14
100	1.30	10.10
150		9.17
200	0.794	8.31
250		7.61
300		6.94
350		6.39
400		5.95
500	0.380	5.67
600		5.02
800		3.75
900	0.238	
1000		3.13
1500		2.34
2000		1.85

Table 2.4.9. Cross sections for discrete excitations to the 4^1S and 4^1P states of He, as recommended by de Heer.

E [eV]	σ [10^{-18}cm^2]	
	4^1S	4^1P
25	0.129	0.170
26.5	0.114	0.201
30	0.162	0.310
35	0.165	
40	0.152	0.586
45	0.143	
50	0.133	0.833
60	0.113	0.943
80	0.0951	1.150
100	0.0906	1.069
150	0.0699	1.021
200	0.0592	0.891
250	0.0522	
300	0.0451	0.722
350	0.0403	
400	0.0362	0.613
500	0.0326	0.529
600	0.0263	0.476
800	0.0226	0.378
1000	0.0176	0.319
1500	0.0118	0.232
2000	0.00903	0.190

Table 2.4.8. Cross sections for discrete excitations to the 3^1S, 3^1P, and 3^1D states of He, as recommended by de Heer.

E [eV]	σ [10^{-18}cm^2]		
	3^1S	3^1P	3^1D
25	0.364	0.377	0.192
26.5	0.405	0.454	
30	0.437	0.738	0.228
35		1.11	0.248
35.16	0.413		
40	0.378	1.38	0.259
45		1.66	0.264
50	0.337	1.84	0.261
60		2.15	0.227
80	0.260	2.42	0.185
100	0.233	2.44	0.144
150	0.172	2.26	0.0933
200	0.146	2.08	0.0706
250	0.131	1.88	0.0579
300	0.119	1.77	0.0447
350	0.103	1.63	
400	0.0915	1.51	0.0320
500	0.0845	1.29	0.0242
600	0.0676	1.11	0.0199
800	0.0571	0.915	0.0156
1000	0.0463	0.793	0.0124
1500	0.0314	0.588	0.00780
2000	0.0245	0.468	0.00582

Table 2.4.10. Cross sections for discrete excitations to the 4^1D, and 4^1F states of He, as recommended by de Heer.

E [eV]	σ [10^{-18}cm^2]		E [eV]	σ [10^{-18}cm^2]	
	4^1D	4^1F		4^1D	4^1F
23.45		0.0158	150	0.0514	
25	0.105	0.0163	200	0.0388	0.000368
26.5		0.0158	250	0.0318	
30	0.122	0.0105	300	0.0246	
35	0.133		400	0.0176	
35.16		0.00889	500	0.0133	0.000105
40	0.139	0.00740	600	0.0110	
45	0.139		800	0.00855	
50	0.138	0.00513	900		0.0000564
60	0.120		1000	0.00685	
80	0.0984	0.00206	1500	0.00429	
100	0.0791	0.00136	2000	0.00320	

Table 2.4.11. Cross sections for discrete excitations to the 2^3S and 2^3P states of He, as recommended by de Heer.

E [eV]	σ [10^{-18}cm^2]	
	2^3S	2^3P
25	2.64	2.26
26.5	2.35	2.30
30	1.96	2.19
35.16	1.52	1.96
40	1.12	1.63
50	0.754	1.11
80	0.245	0.370
100	0.150	0.194
200	0.0287	0.0244
500	0.00240	0.00145
900	0.000494	0.000231

Table 2.4.13. Cross sections for discrete excitations to the 4^3S and 4^3P states of He, as recommended by de Heer.

E [eV]	σ [10^{-18}cm^2]	
	4^3S	4^3P
25	0.224	0.168
26.5	0.259	0.225
30	0.224	0.206
35.16	0.156	0.192
40	0.121	0.170
50	0.0781	0.130
80	0.0212	0.0473
100	0.0126	0.0267
200	0.00235	0.00335
500	0.000195	0.000203
900	0.0000389	0.0000303

Table 2.4.12. Cross sections for discrete excitations to the 3^3S, 3^3P, and 3^3D states of He, as recommended by de Heer.

E [eV]	σ [10^{-18}cm^2]		
	3^3S	3^3P	3^3D
25	0.708	0.462	0.124
26.5	0.677	0.477	0.112
30	0.571	0.541	0.112
35			0.0860
35.16	0.414	0.495	0.0603
40	0.303	0.426	
50	0.194	0.318	0.0365
80	0.0553	0.112	0.00778
100	0.0325	0.0603	0.00355
200	0.00615	0.00757	0.000325
500	0.000510	0.000460	0.0000132
900	0.000107	0.0000733	0.00000198

2.4.2.3 Lithium

Wutte et al. [97Wut1] reviewed experimental and theoretical data, and presented analytic representation of the cross sections for the excitation of the 2p, 3s, 3p, and 3d states. See Tables 2.4.15 and 2.4.16.

Table 2.4.14. Cross sections for discrete excitations to the 4^3D and 4^3F states of He, as recommended by de Heer.

E [eV]	σ [10^{-18}cm^2]	
	4^3D	4^3F
25	0.0782	0.00884
26.5	0.0614	0.0104
30	0.0584	0.00746
35.16	0.0487	0.00368
40	0.0373	0.00219
50	0.0218	0.00101
80	0.00461	0.000137
100	0.00227	0.0000389
200	0.000191	0.00000197
500	0.00000756	0.0000000717
900	0.00000115	0.0000000117

Table 2.4.15. Cross section for discrete excitation to the 2^2P state of Li, as recommended by Wutte et al.

E [eV]	σ [10^{-15}cm^2]
1.848	0.002631
2	0.8183
3	2.973
4	3.663
6	4.265
8	4.371
10	4.281
20	3.415
30	2.773
40	2.339
60	1.798
80	1.473
100	1.255
200	0.7434
300	0.5400
400	0.4284
600	0.3074
800	0.2421
1000	0.2009

Table 2.4.16. Cross section for discrete excitations to the 3^2S, 3^2P and 3^2D states of Li, as recommended by Wutte et al.

E [eV]	σ [10^{-17}cm^2]		
	3^2S	3^2P	3^2D
3.373	2.248		
3.834		0.7729	
3.878			0.004137
4	30.95	10.6	3.163
6	20.28	16.86	32.15
8	17.09	13.35	34.16
10	15.52	10.77	33.13
20	10.55	5.378	22.86
30	7.787	3.609	16.28
40	6.134	2.731	12.46
60	4.289	1.852	8.385
80	3.291	1.409	6.290
100	2.669	1.141	5.023
200	1.371	0.5934	2.493
300	0.9218	0.4052	1.656
400	0.6944	0.3091	1.239
600	0.4649	0.2110	0.8241
800	0.3494	0.1610	0.6173
1000	0.2799	0.1304	0.4934

2.4.2.4 Other atoms

The current knowledge of discrete-excitation cross sections of other atoms is often fragmentary, incomplete, and uncertain in many respects, and is therefore unsuitable for a simple systematic presentation. Nevertheless, the total amount of data in the recent literature, though fragmentary, is considerable, as seen in Table 2.4.17. Some of the data in the cited literature should be useful for the reader in need of cross-section values. The coverage is limited to articles that report experimentally measured values, rather than theoretically calculated values, and were published in 1980-1997.

For a broader coverage of the current literature, including articles reporting theoretical results, see the International Bulletin on Atomic and Molecular Data for Fusion, published by the International Atomic Energy Agency (IAEA), or access http://www.iaea.org/programme/amdis/ on the Internet. In particular, the relevant papers published before 1980 are listed in CIAMDA (an index to the literature on atomic and molecular collision data relevant to fusion research) publised by IAEA in 1980.

Table 2.4.17 shows different degrees of research activities on different classes of atoms. Many measurements have been reported on rare gases, viz., Ne, Ar, Kr, and Xe. Therefore, it may be timely to conduct a comprehensive survey of data and to update in effect the classic work by de Heer et al. [79deH1], although the total discrete-excitation cross sections given by them should not be drastically revised.

It is gratifying to see a considerable number of new reports on O and N, i.e. the two most important atomic species relevant to many applications such as aeronomy and combustion. A comprehensive analysis of cross-section data for N, similar to the work on O by Itikawa and Ichimura [90Iti1] and by Laher and Gilmore [90Lah1], might be appropriate in the near future. For Na and Hg also, an appreciable number of measurements have been carried out.

On the rest of the atoms cited in Table 2.4.17 only a few measurements have been performed, and only by a few groups of workers. A principal reason for this is the need of very high temperatures to vaporize those atoms.

Table 2.4.17. Recent literature on the discrete-excitation cross sections of other atoms (by courtesy of Y. Itikawa). Following is a list of articles reporting experimental results on discrete-excitation cross sections of each atom, published since 1980. For articles reporting theoretical results, see the International Bulletin on Atomic and Molecular Data published by the International Atomic Energy Agency, or access the Internet at http://www.iaea.org/programme/amdis/.

Atom	References
B	81Kuc1
N	80Spe1, 91Doe1, 92Doe3, 96Yan1
O	85Shy1, 85Zip1, 86Doe1, 86Shy1, 86Shy2, 86Vau1, 86Zip1, 86Zip2, 87Gul1, 87Vau1, 88Ger1, 88Gul1, 88Gul2, 88Vau1, 89Doe1, 89Doe2, 89Tei1, 90Lah1, 92Doe1, 92Doe2, 92Wan1
Ne	81Zav1, 82Mie1, 84Reg1, 84Sha1, 84Shp1, 84Tac1, 85McC1, 85Phi1, 85Teu1, 85Zav1,86Zet1, 87Bog3, 87Kha1, 87Mas1, 87Sch1, 87Tac1, 91Mar1, 91Peu1, 92Kha1, 92Zhe1, 93Mit1, 94Kha1, 96Kan2, 97Jan1
Na	80Sri1, 81Phe1, 82Fol1, 84Jad1, 84Jit1, 85Ril1, 85Stu1, 86Teu1, 88Teu1, 90Han1, 90Jia1, 92Mar1, 92Mar2, 93Yin1
Mg	88Bru1, 94Hou1
Ar	81Chu1, 81Zav1, 83Fer1, 84Shp1, 85Mit1, 85Zav1, 86Mit2, 86Tac1, 87Bog1, 87Kha1, 87Mas1, 87Sch1, 88For1, 88Li1, 88Nis1, 90Aje1, 90Bog1, 91Mar1, 91Mor1, 92Bla1, 92Cor1, 92Kha1, 92Zhe1, 93Mit1, 93Zhe1, 94Kha1, 94Mit1, 94Wan2, 96Tsu1, 97Jan1
K	80Vus1, 93Par1

Atom	References
Ca	82Dob1, 95Kuc1
Ti	88Smi1, 96Smi1
V	82Mel2
Cr	82Mel1
Mn	81Mel1, 81Mel2, 95Smi2
Fe	83Kol2
Co	83Kol1, 83Kol3
Cu	82Kra1, 95Ism1
Zn	81Bog1
Ge	82Kol1
Kr	81Tra1, 81Zav1, 82Phi1, 84Shp1, 85Kin1, 86Mit1, 87Bog2, 87Kha1, 87Mas1, 87Sch1, 88Ham1, 90Mur1, 90Tak1, 91Mar1, 91Zec1, 93Mit1, 93Zhe1, 94Gou1, 94Kha1, 94Mit1, 97Jan1
Rb	84Vus1, 93Par1, 93Wei1
Sr	94Bey1
Y	84Kuc1
Zr	83Kuc1, 96Smi1
Mo	82Bog1, 95Smi2
Rh	92Kol1
Pd	89Kol1
Ag	83Kra1
Sn	86Kol1
Xe	84Shp1, 86Pen1, 86Ver1, 87Mas1, 87Sch1, 88Fil1, 88Ham1, 88Kor1, 90DeJ1, 91Peu1, 91Suz1, 91Zec1, 92Kha1, 94Est1, 94Kha1, 94Mit1, 96Kan1, 96Kha1, 96Kha2, 96LeC1, 96Suz1, 97Jan1
Ba	93Zet1, 94Li1, 94Li2, 94Wan1
Sm	95Smi1
Dy	92Vas1, 94Smi1
Ho	92Vas1
Tm	92Vas1
Hf	93Kuc1, 96Smi1
Ir	91Smi1
Au	81Sha1, 90Hol1
Hg	84Pos1, 85New1, 90Pei1, 90Pei2, 93Pan1, 94Mul1, 96Zub1
Tl	91Ges1
Pb	91Ges1
Bi	97Smi1

References for 2.1 to 2.4

14Fra1 Franck, J., Hertz, G.: Verh. Dtsch. Phys. Ges. **16** (1914) 457.

30Bet1 Bethe, H.: Ann. Phys. (Leipzig) **5** (1930) 325.

46Wes1 Westin, N.: K. Nor. Vidensk. Selsk. Skr. No. **2** (1946) 1.

54Fan1 Fano, U.: Phys. Rev. **95** (1954) 1198.

67Ino1 Inokuti, M., Kim, Y.-K., Platzman, R.L.: Phys. Rev. **164** (1967) 55.

67Sun1 Sunshine, G. Aubrey, B.B., Bederson, B.: Phys. Rev. **154** (1967) 1.

68Sch1 Schiff, L.I.: Quantum Mechanics, Third Edition, New York: McGraw-Hill (1968), p. 113.

69Mas1 Massey, H.S.W., Burhop, E.H.S.: Electronic and Ionic Impact Phenomena, Second Edition, Volume I. Collisions of Electrons with Atoms, Oxford: Clarendon Press 1969.
71Bed1 Bederson, B., Kieffer, L.J.: Rev. Mod. Phys. **43** (1971) 601.
71Ino1 Inokuti, M.: Rev. Mod. Phys. **43** (1971) 297.
73Kim1 Kim, Y.-K., Inokuti, M.: Phys. Rev. A **7** (1973) 1257.
75Egg1 Eggarter, E.: J. Chem. Phys. **62** (1975) 833.
76deH1 de Heer, F. J., Wagenaar, R.W., Blaauw, H. J., Tip, A.: J. Phys. B **9** (1976) L269.
76Soo1 Soong, S.C.: Radiat. Res. **67** (1976) 187.
76Soo2 Soong, S.C., Kim, Y.-K.: Inelastic-collision cross sections for Ne, Argonne National Laboratory Report No. ANL-76-66 (1976).
77deH1 de Heer, F.J., McDowell, M. R. C., Wagenaar, R. W.: J. Phys. B **10** (1977) 1945.
77deH2 de Heer, F.J., Jansen, R.H.: J. Phys. B **10** (1977) 3741.
79deH1 de Heer, F.J., Jansen, R.H., van der Kaay: J. Phys. B **12** (1979) 979.
80Egg1 Eggarter, E., Inokuti, M.: Cross sections for electron inelastic collisions with argon, Argonne National Laboratory Report ANL-80-58 (1980).
80Spe1 Spence, D., Burrow, P.D.: J. Phys. B **13** (1980) 2809.
80Sri1 Srivastava, S.K., Vuskovic, L.: J. Phys. B. **13** (1980) 2633.
80Vus1 Vuskovic, L., Srivastava, S.K.: J. Phys. B **13** (1980) 4849.
81Bog1 Bogdanova, I.P., Ryazantseva, S.V., Yakhontova, V.E.: Opt. Spectrosc. **41** (1981) 244.
81Chu1 Chutjian, A., Cartwright, D.C.: Phys. Rev. A **23** (1981) 2178.
81Hay1 Hayashi, M.: Recommended values of transport cross sections for elastic collision and total collision cross section for electrons in atomic and molecular gases, Report IPP-AM-19, Institute of Plasma Physics, Nagoya University, 1981.
81Ino1 Inokuti, M., Dehmer, J.L., Baer, T., Hanson, J.D.: Phys. Rev. A **23** (1981) 95.
81Kuc1 Kuchenev, A.N., Smirnov, Y.M.: Opt. Spectrosc. **51** (1981) 116.
81Mel1 Melnikov, V.V., Smirnov, Y.M., Sharonov, Y.D.: Opt. Spectrosc. **50** (1981) 357.
81Mel2 Melnikov, V.V., Smirnov, Y.M., Sharonov, Y.D.: Opt. Spectrosc. **51** (1981) 423.
81Phe1 Phelps, J.O., Lin, C.C.: Phys. Rev. A **24** (1981) 1299.
81Sha1 Shafranosh, I.I., Shishova, T.A., Aleksakhin, I.S.: Opt. Spectrosc. **50** (1981) 210.
81Tra1 Trajmar, S., Srivastava, S.K., Tanaka, H., Nishimura, H., Cartwright, D.C.: Phys. Rev. A **23** (1981) 2167.
81Zav1 Zavilopulo, A.N., Snegursky, A.V., Shpenik, O.B., Kutsuina, N.N.: Sov. Phys. JETP **54** (1981) 449.
82Bog1 Bogdanov, S.N., Bodiev, A.Y., Kuchenev, A.N., Smirnov, Y.M.: Zh. Prikl. Spektrosk. **37** (1982) 364.
82Dob1 Dobryshin, V.E., Rakhovskij, V.I., Shustryakov, V.M.: Opt. Spectrosc. **52** (1982) 364.
82Fol1 Foltz, G.W., Beiting, E.J., Smith, T.H., Dunning, F.B., Stebbings, R.F.: Phys. Rev. A **25** (1982) 187.
82Kol1 Kolosov, P.A., Smirnov, Y.M.: Opt. Spectrosc. **53** (1982) 243.
82Kra1 Krasavin, A.Y., Kuchenov, A.N., Smirnov, Y.M.: Zh. Prikl. Spektrosk. **36** (1982) 912.
82Mel1 Melnikov, V.V., Smirnov, Y.M.: Opt. Spectrosc. **52** (1982) 362.
82Mel2 Melnikov, V.V., Smirnov, Y.M.: Opt. Spectrosc. **53** (1982) 15.
82Mie1 Miers, R.E., Gastineau, J.E., Phillips, M.H., Anderson, L.W., Lin, C.C.: Phys. Rev. A **25** (1982) 1185.
82Phi1 Phillips, J.M.: J. Phys. B **15** (1982) 4259.
83Fer1 Ferreira, C.M., Loureiro, J.: J. Phys. D **16** (1983) 1611.
83Kol1 Kolsov, P.A., Smirnov, Y.M.: J. Appl. Spectrosc. **39** (1983) 880.
83Kol2 Kolsov, P.A., Smirnov, Y.M.: Sov. Astron. - AJ **27** (1983) 304.
83Kol3 Kolsov, P.A., Smirnov, Y.M.: Zh. Prikl. Spektrosk. **39** (1983) 200.
83Kra1 Krasavin, A.Y. , Kuchenov, A.N., Smirnov, Y.M.: Opt . Spectrosc. **54** (1983) 11.
83Kuc1 Kuchenev, A.N., Smirnov, Y.M.: J. Appl. Spectrosc. **39** (1983) 751.
84Jad1 Jaduszliwer, B., Weiss, P., Tino, A, Bederson, B.: Phys. Rev. A **30** (1984) 1255.

84Jit1 Jitschin, W., Osimitsch, Reihl, H., Kleinpoppen, H., Lutz, H.O.: J. Phys. B **17** (1984) 1899.
84Kuc1 Kuchenev, A.N., Smirnov, Y.M.: J. Appl. Spectrosc. **40** (1984) 368.
84Pos1 Post, H.A.: J. Phys. B **17** (1984) 3193.
84Rau1 Rau, A.R.P.: Comments At. Mol. Phys. **14** (1984) 285.
84Reg1 Register, D.F., Trajmar, S., Steffensen, G., Cartwright, D.C.: Phys. Rev. A **29** (1984) 1793.
84Sha1 Shaw, M., Borge, M.J.G., Campos, J.: J. Chem. Phys. **80** (1984) 1882.
84Shp1 Shpenik, O.B., Zavilopulo, A.N., Snegursky, A.V., Fabrikant, I.I.: J. Phys. B **17** (1984) 887.
84Tac1 Tachibana, K., Harima, H., Urano, Y.: J. Phys. B **17** (1984) 879.
84Vus1 Vuskovic, L., Maleki, L., Trajmar, S.:J. Phys. B **17** (1984) 2519.
85Kin1 King, S.J., Neill, P.A., Crowe, A.: J. Phys. B **18** (1985) L589.
85McC1 McClelland, J.J., Fink, M.: Phys. Rev. A **31** (1985) 1328.
85McD1 McDaniel, E.W., Flannery, M.R., Thomas, E.W., Manson, S.T.: At. Data Nucl. Data Tables **33** (1985) 1.
85Mit1 Mityureva, A.A., Smirnov, V.V.: Opt. Spectrosc. **59** (1985) 303.
85New1 Newman, D.S., Zubek, M., King, G.C.: J. Phys. B **18** (1985) 985.
85Phi1 Phillips, M.H., Andersen, L.W., Lin, C.C.: Phys. Rev. A **32** (1985) 2117.
85Ril1 Riley, J.L., Teubner, P.J.O., Brunger, M.J.: Phys. Rev. A **31** (1985) 1959.
85Sal1 Salvat, F., Mayol, R., Parellada, J.: J. Phys. D **18** (1985) 1401.
85Shy1 Shyn, T.W., Sharp, W.E.: Geophys. Res. Lett. **12** (1985) 171.
85Stu1 Stumpf, B., Gallagher, A.: Phys. Rev. A **32** (1985) 3344.
85Teu1 Teubner, P.J.O., Riley, J.L., Tonkin, M.C., Furst, J.E., Buckman, S.J.: J. Phys. B **18** (1985) 3641.
85Zav1 Zavilopulo, A.N., Snegursky, A.V., Shpenik, O.B.: J. Appl. Spectrosc. **42** (1985) 125.
85Zip1 Zipf, E.C., Erdman, P.W.: J. Geophys. Res. **90** (1985) 11087.
86Bet1 Bethe, H.A., Jackiw, R.: Intermediate Quantum Mechanics, Third Edition, New York: Benjamin Cummings, 1986.
86Doe1 Doering, J.P., Vaughan, S.O.: J. Geophys. Res. **91** (1986) 3279.
86Fan1 Fano, U., Rau, A.R.P.: Atomic Collisions and Spectra, Orlando: Academic Press, 1986.
86Kol1 Kolsov, P.A., Smirnov, Y.M.: Opt. Spectrosc. **61** (1986) 146.
86Mit1 Mityureva, A.A., Penkin, N.P., Smirnov, V.V.: Opt. Spectrosc. **60** (1986) 144.
86Mit2 Mityureva, A.A., Smirnov, V.V.: Opt. Spectrosc. **61** (1986) 413.
86Pen1 Penkin, N.P., Smirnov, V.V.: Opt. Spectrosc. **61** (1986) 412.
86Shy1 Shyn, T.W., Cho, S.Y., Sharp, W.E.: J. Geophys. Res. **91A** (1986) 13751.
86Shy2 Shyn, T.W., Sharp, W.E.: J. Geophys. Res. **91** (1986) 1691.
86Tac1 Tachibana, K.: Phys. Rev. A **34** (1986) 1007.
86Teu1 Teubner, P.J.O., Riley, J.L., Brunger, M.J., Buckman, S.J.: J. Phys. **19** (1986) 3313.
86Vau1 Vaughan, S.O., Doering, J.P.. J. Geophys. Res. **91** (1986) 13755.
86Ver1 Verkhovtseva, E.T., Gnatchenko, E.V., Pogrebnyak, P.S., Tkachenko, A.A.: J. Phys. B **19** (1986) 2089.
86Zet1 Zetner, P.W., Westerveld, W.B., King, G.C., McConkey, J.W.: J. Phys. **19** (1986) 4205.
86Zip1 Zipf, E.C.: J. Phys. B **19** (1986) 2199.
86Zip2 Zipf, E.C., Kao, W.W.: Chem. Phys. Lett. **125** (1986) 394.
87Bog1 Bogdanova, I.P., Yurgenson, S.V.: Opt. Spectrosc. **62** (1987) 281.
87Bog2 Bogdanova, I.P., Yurgenson, S.V.: Opt. Spectrosc. **62** (1987) 424.
87Bog3 Bogdanova, I.P., Yurgenson, S.V.: Opt. Spectrosc. **63** (1987) 815.
87Gul1 Gulcicek, E.E., Doering, J.P.: J. Geophys. Res. **92** (1987) 3445.
87Kha1 Khakoo, M.A., McConkey, J.W.: J. Phys. B **20** (1987) 5541.
87Mas1 Mason, N.J., Newell, W.R.: J. Phys. B **20** (1987) 1357.

87Sch1 Schartner, K.H., Kraus, B., Poffel, W., Reymann: Nucl. Instr. Meth. B **27** (1987) 519.
87Tac1 Tachibana, K., Phelps, A.V.: Phys. Rev. A **36** (1987) 999.
87Vau1 Vaughan, S.O., Doering, J.P.: J. Geophys. Res. **92** (1987) 7749.
88Bru1 Brunger, M.J., Riley, J.L., Scholten, R.E., Teubner, P.J.O.: J. Phys. B **21** (1988) 1639.
88Fil1 Filipovic, D., Marinkovec, B., Pejcev, V., Vuskovic, L.: Phys. Rev. A **37** (1988) 356.
88For1 Forand, J.L., Wang, S., Woolsey, J.M., McConkey, J.W.: Can. J. Phys. **66** (1988) 349.
88Ger1 Germany, G.A., Anderson, R.J., Salamo, G.J.: J. Chem. Phys. **89** (1988) 1999.
88Gul1 Gulcicek, E.E., Doering, J.P.: J. Geophys. Res. **93A** (1988) 5879.
88Gul2 Gulcicek, E.E., Doering, J.P., Vaughan, S.O.: J. Geophys. Res. **93A** (1988) 5885.
88Ham1 Hammond, P., Read, F.H., King, G.C.: J. Phys. B **21** (1988) 3121.
88Kor1 Korotkov, A.I., Mitryukhin, L.K., Petrov, N.I., Sorokin, G.M.: Opt. Spectrosc. **64** (1988) 174.
88Li1 Li, G.P., Takayanagi, T., Wakiya, K., Suzuki, H., Ajiro, T., Yagi, S., Kano, S.S., Takuma, H.: Phys. Rev. A **38** (1988) 1240.
88Nis1 Nishimura, H., Yano, K.: J. Phys. Soc. Jpn. **57** (1988) 1951.
88Smi1 Smirnov, Y.M.: J. Appl. Spectrosc. **48** (1988) 363.
88Teu1 Teubner, P.J.O., Riley, J.L., Brunger, M.J., Furst, J.E.: Phys. Rev. A **37** (1988) 1476.
88Til1 Tilinin, I.S.: Zh. Eksp. Teor. Fiz. **94** (1988) 96. English translation: Sov. Phys. JETP **67** (1988) 1570.
88Vau1 Vaughan, S.O., Doering, J.P.: J. Geophys. Res. **93** (1988) 289.
89Doe1 Doering, J.P., Gulcicek, E.E.: J. Geophys. Res. **94A** (1989) 1541.
89Doe2 Doering, J.P., Gulcicek, E.E.: J. Geophys. Res. **94A** (1989) 2733.
89Hed1 Heddle, D.W.O., Gallagher, J.W.: Rev. Mod. Phys. **61** (1989) 221.
89Kol1 Kolosov, P.A., Kuchenev, A.N., Smirnov, Y.M.: J. Appl. Spectrosc. **51** (1989) 1241.
89Tei1 Teillet-Billy, D., Gauyacq, J.P.: J. Phys. B **22** (1989) L335.
89van1 van der Burgt, P.J.M., Westerveld, W.B., Risley, J.S.: J. Phys. Chem. Ref. Data **18** (1989) 1757.
90Aje1 Ajello, J.M., James, G.K., Franklin, B., Howell, S.: J. Phys. B **23** (1990) 4355.
90Bog1 Bogdanova, I.P., Yurgenson, S.V.: Opt. Spectrosc. **68** (1990) 730.
90DeJ1 DeJoseph, Jr., C.R., Clark, C.D.: J. Phys. B **23** (1990) 1879.
90Han1 Han, X.L., Schinn, G.W., Gallagher, A.: Phys. Rev. A **42** (1990) 1245.
90Hol1 Holst, S., Legler, W., Newjoto, R., Peters, J.: J. Phys. B **23** (1990) 2977.
90Ino1 Inokuti, M., in: Molecular Processes in Space (T. Watanabe et al., eds.), New York: Plenum Press (1990), p. 65.
90Iti1 Itikawa, Y., Ichimura, A.: J. Phys. Chem. Ref. Data **19** (1990) 637.
90Jia1 Jiang, T.Y., Ying, C.H., Vuskovic, L., Bederson, B.: Phys. Rev. A **42** (1990) 3852.
90Lah1 Laher, R.R., Gilmore, F.R.: J. Phys. Chem. Ref. Data **19** (1990) 277.
90Mur1 Murray, P.B., Gough, S.F., Neill, P.A., Crowe, A.: J. Phys. B **23** (1990) 2137.
90Pei1 Peitzmann, F.J., Kessler, J.: J. Phys. B **23** (1990) 2629.
90Pei2 Peitzmann, F.J., Kessler, J.: J. Phys. B **23** (1990) 4005.
90Tak1 Takayanagi, T., Li, G.P., Wakiya, K., Suzuki, H., Ajiro, T., Inaba, T., Kano, S.S., Takuma, H.: Phys. Rev. A **41** (1990) 5948.
91Bro1 Browning, R.: Appl. Phys. Lett. **58** (1991) 2845.
91Cro1 Crompton, R.W., Hayashi, M., Boyd, D.E., Makabe, T.: Gaseous Electronics and Its Applications, Tokyo: KTK Scientific Publishers, and Dordrecht: Kluwer Academic Publishers 1991.
91Doe1 Doering, J.P., Goembel, L.: J. Geophys. Res. **96A** (1991) 16021.
91Ges1 Gessmann, H., Bartsch, M., Hanne, G.F., Kessler, J.: J. Phys. B **24** (1991) 2817.
91Mar1 Martus, K.E., Zheng, S.H., Becker, H.: Phys. Rev. A **44** (1991) 1682.
91Mor1 Morgan, W.L.: Phys. Rev. A **44** (1991) 1677.
91Peu1 Peuch, Mizzi, S.: J. Phys. B **24** (1991) 1974.
91Smi1 Smirnov, Y.M.: J. Appl. Spectrosc. **54** (1991) 413.

91Suz1 Suzuki, T.Y., Sakai, Y., Min, B.S., Takayanagi, T., Wakiya, K., Suzuki, H., Inaba, T, Takuma, H.: Phys. Rev. A **43** (1991) 5867.
91Zec1 Zecca, A., Karwasz, G., Brusa, R.S., Grisenti, R.J.: J. Phys. B **24** (1991) 2737.
92Bla1 Blanco, F., Sanchez, J.A., Campos, J.: J. Phys. B **25** (1992) 3531.
92Cor1 Corr, T.T., Wang, S., McConkey, J.W.: J. Phys. B **25** (1992) 4929.
92deH1 de Heer, F.J., Hoekstra, R., Kingston, A.E., Summers, H.P.: Nucl. Fusion Suppl. **3** (1992) 19.
92Doe1 Doering, J.P.: Geophys. Res. Lett. **19** (1992) 449.
92Doe2 Doering, J.P.: J. Geophys. Res. **97A** (1992) 19531.
92Doe3 Doering, J.P., Goembel, L.: J. Geophys. Res. **97A** (1992) 4295.
92Kat1 Kato, T., Janev, R.K.: Suppl. Nucl. Fusion **2** (1992) 33.
92Kha1 Khakoo, M.A., Tran, T., Bordelon, D., Csanak, G.: Phys. Rev. A **45** (1992) 219.
92Kol1 Kolsov, P.A., Kuchenev, A.N., Smirnov, Y.M.: J. Appl. Spectrosc. **57** (1992) 542.
92Mar1 Marinkovic, B., Pejcev, V., Folipovic, D., Cadez, I., Vuskovic, L.: J. Phys. B **25** (1992) 5179.
92Mar2 Marinkovic, B., Wang, P., Gallagher, A.: Phys. Rev. A **46** (1992) 2553.
92Vas1 Vasilijeva, E.K., Morozov, S.N.: Nucl. Instr. Meth. B **69** (1992) 253.
92Wan1 Wang, S., McConkey, J.W.: J. Phys. B **25** (1992) 5461.
92Zhe1 Zheng, S.H., Becker, K.: Z. Phys. D **23** (1992) 137.
93Jan1 Janev, R.K., Smith, J.J.: Suppl. Nucl. Fusion **4** (1993) 1.
93Kim1 Kimura, M., Inokuti, M., Dillon, M.A., in: Advances in Chemical Physics (I. Prigogine, S. A. Rice, eds.), New York: John Wiley, Vol. **84** (1993), p. 193.
93Kuc1 Kuchenev, A.N., Smirnov, Y.M.: J. Phys. B **26** (1993) 2417.
93Mit1 Mityureva, A.A., Smirnov, V.V.: Opt. Spectrosc. **74** (1993) 6.
93Pan1 Panajtovic, R., Pejcev, V., Konstantinovic, M., Filipovic, D., Bocvarski, and Marinkovic, B.: J. Phys. B **26** (1993) 1005.
93Par1 Parikh, S.P., Kauppila, W.E., Kwan, W.E., Lukaszew, R.A., Przylbyla, D.: Phys. Rev. A **47** (1993) 1535.
93Wei1 Wei, Z., Flynn, C., Redd, A., Stumpf, B.: Phys. Rev. A **47** (1993) 1918.
93Yin1 Ying, C.H., Perales, F., Vuskovic, L., Bederson, B.: Phys. Rev. A **48** (1993) 1189.
93Zet1 Zetner, P.W., Li, Y., Trajmar, S.: Phys. Rev. A **48** (1993) 495.
93Zhe1 Zheng, S.H., Becker, K.: J. Phys. B **26** (1993) 517.
94Bey1 Beyer, H.J., Hamdy, H., Zohny, E.I.M., Mathmoud, K.R.: Z. Phys. D **30** (1994) 91.
94Est1 Ester, T., Kessler, J.: Phys. B **27** (1994) 4295.
94Fil1 Filippelli, Lin, C.C., Andersen, L.W., McConkey, J.W.: in [94Ino1], p.1.
94Gal1 Gallagher, J.W.: in [94Ino1], p. 373.
94Gou1 Gough, S.F., Crowe, A.: J. Phys. B **27** (1994) 955.
94Hou1 Houghton, R.K., Brunger, M.J., Shen, G., Teubner, P.J.O.: J. Phys. B **27** (1994) 3573.
94Ino1 Inokuti, M. (ed.): Advances in Atomic, Molecular, and Optical Physics, Vol. 33, Cross-Section Data, Boston: Academic Press 1994.
94Iti1 Itikawa, Y.: in [94Ino1], p. 253.
94Jai1 Jain, A.K., Kumar, P., Tripathi, A.N.: Z. Phys. D **32** (1994) 205.
94Kha1 Khakoo, M.A., Beckmann, C.E., Trajmar, S., Csanak, G.: J. Phys. B **27** (1994) 3159.
94Li1 Li, Y., Wang, S., Zetner, P.W., Trajmar, S.: J. Phys. B **27** (1994) 4025.
94Li2 Li, Y., Zetner, P.W.: Phys. Rev. A **49** (1994) 950.
94Mar1 Margreiter, D., Deutsch, H., Märk, T.D.: Int. J. Mass Spectrom. **139** (1994) 127.
94McD1 McDaniel, E.W., Mansky, E.J.: in [94Ino1], p. 389.
94Mit1 Mityureva, A.A., Smirnov, V.V.: J. Phys. B **27** (1994) 1869.
94Mul1 Muller, H., Kessler, J.: J. Phys. B **27** (1994) 5933.
94Smi1 Smirnov, Y.M.: Phys. Scripta **49** (1994) 689.
94Wan1 Wang, S., Trajmar, S., Zetner, P.W.: J. Phys. B **27** (1994) 1613.

94Wan2 Wang, S., van der Brugt, P.J.M., Corr, J.J., McConkey, J.W., Madison, D.H.: J. Phys. B **27** (1994) 329.

95Bur1 Burke, P.G., Joachain, C.J.: Theory of Electron-Atom Collisions. Part 1: Potential Scattering, New York: Plenum Press 1995.

95deH1 de Heer, F.J., Bray, I., Fursa, D.V., Bliek, F.W., Folkerts, H.O., Hoekstra, R., Summers, H.P.: Suppl. Nucl. Fusion **6** (1995) 7.

95Int1 International Atomic Energy Agency, Atomic and Molecular Data for Radiotherapy and Radiation Research, IAEA-TECDOC-799, Vienna 1995.

95Ism1 Ismail, M., Teubner, P.J.O.: J. Phys. B **28** (1995) 4149.

95Jan1 Janev, R.K. (ed.): Atomic and Molecular Processes in Fusion Edge Plasmas, New York: Plenum Press 1995.

95Kuc1 Kuchenev, A.N., Smirnov, Y.M.: Phys. Scripta **51** (1995) 578.

95McC1 McCarthy, I.E., Weigold, E.: Electron-Atom Collisions, Cambridge: University Press, U. K., 1995.

95Smi1 Smirnov, Y.M.: J. Appl. Spectrosc. **62** (1995) 26.

95Smi2 Smirnov, Y.M.: Opt. Spectrosc. **78** (1995) 498.

95Tra1 Trajmar, S., Kanik, I.: in [95Jan1], p. 31.

96Bur1 Burke, P.G.: in [96Dra1], p. 536.

96Dra1 Drake, G.W.F. (ed.): Atomic, Molecular, and Optical Physics Handbook, American Institute of Physics, New York: Woodbury 1996.

96Kan1 Kanik, I.: Chem. Phys. Lett. **258** (1996) 455.

96Kan2 Kanik, I., Ajello, J.M., James, G.K.: J. Phys. B **29** (1996) 2355.

96Kha1 Khakoo, M.A., Trajmar, S., LeClair, L.R., Kanik, I., Csanak, G., Fontes, C.J.: J. Phys. B **29** (1996) 3455.

96Kha2 Khakoo, M.A., Trajmar, S., Wang, S., Kanik, I., Aguirre, A, Fontes, C.J., Clark, R.E.H., Abdallah: J. Phys. B **29** (1996) 3477.

96LeC1 LeClair, L.R., Trajmar, S.: J. Phys. B **29** (1996) 5543.

96Smi1 Smirnov, Y.M.: High Temp. **34** (1996) 367.

96Suz1 Suzuki, T., Suzuki, H., Currell, F.J., Ohtani, S., Takayanagi, T., Wakiya, K.: Phys. Rev. A **53** (1996) 4138.

96Szm1 Szmykowski, Cz., Maciag, K., Karwasz, G.: Physica Scripta **54** (1996) 271.

96Tsu1 Tsurubuchi, S., Miyazaki, T., Motohashi, K.: J. Phys. B **29** (1996) 1785.

96Yan1 Yang, J., Doering, J.P.: J. Geophys. Res. **101** (1996) 21765.

96Zec1 Zecca, A., Karwasz, P., Brusa, R.S.: Riv. Nuovo Cim. **19** (1996) 1.

96Zub1 Zubec, M., Gulley, N., Danjo, A., King, G.C.: J. Phys. B **29** (1996) 5927.

97Jam1 James, G.K., Selvin, J.A., Shemansky, D.E., McConkey, J.W., Bray, I., Dziczek, D., Kanik, I., Ajello, J.M.: Phys. Rev. A **55** (1997) 1069.

97Jan1 Jans, W., Mobus, B., Kuhne, M., Ulm, G., Werner, A., Schartner, K.-H.: Phys. Rev. A **55** (1997) 1890.

97May1 Mayol, R., Salvat, F.: At. Data Nucl. Data Tables **65** (1997) 55.

97Smi1 Smirnov, Y.M.: Opt. Spectrosc. **83** (1997) 826.

97Wut1 Wutte, F., Janev, R.K., Aumayer, F., Schneider, M., Schweinzer, J., Smith, J.J., Winter, HP.: At. Data Nucl. Data Tables **65** (1997) 155.

97Zho1 Zhou, S., Li, H., Kauppila, W.E., Kwan, C.K., Stein, T.S.: Phys. Rev. A **55** (1997) 361.

98deH1 de Heer, F.J.: Critically Assessed Electron-Impact Excitation Cross Sections for He(1^1S). Report No. INDC(NDS)-385, International Atomic Energy Agency, Vienna 1998.

2.5 Momentum transfer cross sections

2.5.1 Introduction

2.5.1.1 Definition in terms of the differential cross section

The momentum transfer cross section, σ_m, for electron scattering is defined as

$$\sigma_m(E) = 2\pi \int_0^{\pi} \frac{d\sigma}{d\Omega}(1 - \frac{c'}{c}\cos\theta)\sin\theta \, d\theta \tag{1}$$

where $d\sigma/d\Omega$, the differential cross section, is defined as that fraction of a beam of electrons of energy E which are scattered at an angle θ into the element of solid angle $d\Omega = 2\pi \sin\theta \, d\theta$; c and c' are the electron velocities before and after the collision respectively. The name of this cross section arises from the fact that the term $[1 - (c'/c)\cos\theta]$ is the fractional loss of directed momentum of the electron in a collision.

In general electron collisions may be elastic, inelastic or superelastic. Relation (1) can thus be written as the sum of the momentum transfer cross sections for specific scattering processes, i.e.

$$\sigma_m(E) = \sigma_m(E)^{el} + \sum_k \sigma_m^k(E)^{in} + \sum_k \sigma_m^k(E)^{sup} \tag{2}$$

where $\sigma_m(E)^{el}$ is the elastic momentum transfer cross section and $\sigma_m^k(E)^{in}$ and $\sigma_m^k(E)^{sup}$ are the momentum transfer cross sections for the k^{th} inelastic and superelastic scattering processes, respectively. Superelastic collisions can be neglected for the scattering of electrons in atomic gases because of the relatively high energy of the thresholds for electronic excitation.

There are a number of special cases:

(a) if the scattering is isotropic (i.e. $d\sigma/d\Omega$ is independent of θ) then

$$\sigma_m(E) = \sigma(E) \tag{3}$$

where $\sigma(E)$ is the integral elastic cross section which is given by

$$\sigma(E) = 2\pi \int_0^{\pi} \frac{d\sigma}{d\Omega}\sin\theta \, d\theta \tag{4}$$

(b) if the scattering is elastic only, then

$$\sigma_m(E) = \sigma_m(E)^{el} = 2\pi \int_0^{\pi} \frac{d\sigma}{d\Omega}(1 - \cos\theta)\sin\theta \, d\theta \tag{5}$$

The entries in the accompanying tables of momentum transfer cross sections are values of $\sigma_m(E)^{el}$, i.e. the elastic component of $\sigma_m(E)$.

The momentum transfer cross section arises most often, but not exclusively, in the description of the motion of electrons in a gas at a given temperature and number density, usually in the presence of electric and/or magnetic fields. For a detailed description of the electron motion see Huxley and Crompton [74Hux1].

2.5.1.2 Definition in terms of the scattering phase shifts

In the quantum mechanical description of elastic scattering the wave function of an electron, at a distance r from a scattering centre, after being scattered at an angle θ, is given (in its simplest form) by

$$\Psi = e^{ikz} + \frac{f(\theta)}{r} e^{ikr} \tag{6}$$

where $f(\theta)$ is the amplitude of the scattered wave, k is the wave vector and the z axis is in the direction of the incoming particle. The angular part of the outgoing wave may be expressed in partial waves [27Fax1] corresponding to specific values of the angular momentum quantum number l. The differential cross section is given by

$$\frac{d\sigma}{d\Omega} = |f(\theta)|^2 \tag{7}$$

where

$$f(\theta) = \frac{1}{2ik} \sum_l (2l+1)(e^{2i\eta_l} - 1) P_l(\cos\theta) \tag{8}$$

from which it follows that

$$\sigma_m(E) = \frac{4\pi}{k^2} \sum_l (l+1) \sin^2(\eta_l - \eta_{l+1}) \tag{9}$$

where η_l is the additional shift introduced into the asymptotic phase of the l^{th} partial wave by the scattering. $P_l(\cos\theta)$ are the Legendre polynomials.

For elastic electron scattering from atoms without permanent electric dipole moments O'Malley and co-workers [62OMa1, 63OMa1] have shown that the phase shifts at low energies may be expanded in terms of the wave number (the resulting relations are known as modified effective range (MERT) formulae). These formulae have been used in fitting routines to derive the momentum transfer cross section at low energies, the scattering length, and to enable conversion from $\sigma_m(E)$ to $\sigma(E)$ and vice versa. An extended version of their formulae (see for example [95Pet1]) is as follows (atomic units are used):

$$\tan\eta_0 = -Ak[1 + (4\alpha/3a_0)k^2 \ln(ka_0)] - (\pi\alpha/3a_0)k^2 + Dk^3 + Fk^4 \tag{10}$$

$$\tan\eta_1 = (\pi\alpha/15a_0)k^2 - A_1k^3 \tag{11}$$

where A (the scattering length), A_1, D and F are fitting parameters, a_0 is the Bohr radius and α is the dipole polarizability. For higher order phaseshifts ($l \geq 2$) the Born expansion is used

$$\tan\eta_l = \frac{\pi\alpha k^2}{(2l+3)(2l+1)(2l-1)} \tag{12}$$

The scattering length is also related to the zero energy momentum transfer and integral cross sections via the relation

$$\sigma_m = \sigma = 4\pi A^2 \tag{13}$$

2.5.2 Experimental determinations

2.5.2.1 Swarm experiments

The momentum transfer cross section, $\sigma_m(E)$, can be obtained from transport coefficients measured in electron swarm experiments by using a solution of the Boltzmann equation, and an iterative procedure, to match calculated values of the transport coefficients (commonly the drift velocity, v_{dr}, and the ratio of the lateral diffusion coefficient, D_T, to the electron mobility, μ, i.e. D_T/μ) to the experimental data. Problems involving non-uniqueness of the fitted cross sections, due to the form of $\sigma_m(E)$ or the presence of inelastic processes, have been discussed by Huxley and Crompton [74Hux1]. The energy range over which $\sigma_m(E)$ can be derived from swarm data is limited by the range of values of E/N (E is the electric field strength and N the gas number density) for which transport coefficient data are available. This range is limited by the onset of electric discharge.

Two types of solution of the Boltzman equation have been used:

(a) the "two-term" solution

This is the most commonly used solution and involves the assumption that the electron velocity distribution can be expanded in spherical harmonics and truncated after two terms. If the cross section for elastic scattering is very much greater than those for inelastic collisions then the angular scattering in such collisions does not significantly affect $\sigma_m(E)$. In these circumstances the inelastic scattering may be assumed to be isotropic and thus

$$\sigma_m(E) = \sigma_m(E)^{el} + \sum_k \sigma^k(E)^{in} \qquad (14)$$

where $\sigma^k(E)^{in}$ is the integral cross sections for the k^{th} inelastic collision process.

If the present tables are used for calculations of transport coefficients in atomic gases under conditions where inelastic scattering is a significant process, the $\sigma_m(E)$ used should be the sum of the tabled values of $\sigma_m(E)^{el}$ and the sum of the integral cross sections for the specific inelastic processes.

(b) the "multiterm" solutions

In certain cases (e.g. D_T/μ calculations for argon) the two-term representation of the velocity distribution function is inadequate and a more complex representation is required. In multiterm solutions the isotropic scattering assumption for all the inelastic processes is not made and $\sigma_m(E)$ is given by relation (1).

2.5.2.2 Crossed beam and attenuation experiments

The momentum transfer cross section, $\sigma_m(E)$, can be derived from absolute measurements of $d\sigma/d\Omega$ and relation (1). The main complication with this technique is that most measurements of $d\sigma/d\Omega$ cannot cover the entire range of scattering angles between 0 and π, due to the presence of the primary beam and other geometrical constraints, and some extrapolation procedure is required to extend these measurements to 0 and π. Various techniques have been applied to enable this extrapolation and they, and the uncertainties involved have been discussed by various authors (e.g. [83Tra1]). One common technique which has been applied to many atomic species is the so-called phaseshift analysis. In this technique, the experimental differential cross sections are fitted with an expression such as (7) and (8), where the first few (perhaps 2…4) phaseshifts are treated as free parameters. Higher-order phaseshifts are obtained by the use of (12). The results of the fitting process can then be used to calculate the differential cross section over the entire angular range as well as the total and momentum transfer cross sections. This process has been applied, for instance, in electron-rare-gas atom collisions for energies up to the first inelastic threshold (see for example

[75And1, 80Reg1, 96Gib1]). It generally can enable a reasonably accurate derivation of $\sigma_m(E)$ at higher energies which may not be possible using electron swarm methods.

Momentum transfer cross sections can also be derived, in certain circumstances, from measurements of the total elastic cross section using beam attenuation techniques. In this case, a phaseshift analysis is applied at the total cross section level using equations (10)-(12) and the $\sigma_m(E)$ is derived from the resulting phaseshifts. Examples of this approach can be found in Buckman and Mitroy [89Buc1].

A previous, critical review of momentum transfer cross sections in atoms and molecules has been provided by Itikawa [74Iti1, 78Iti1].

References for 2.5.1 and 2.5.2

27Fax1 Faxén, H, Holtsmark, J.: Z.: Phys. **45** (1927) 307.

62OMa1 O'Malley, T.F., Rosenberg, L., Spruch, L.: Phys. Rev. **125** (1962) 1300.

63OMa1 O'Malley, T.F.: Phys. Rev. **130** (1963) 1020.

74Hux1 Huxley, L.G.H., Crompton, R.W.: The diffusion and drift of electrons in gases, NewYork: Wiley-Interscience 1974.

74Iti1 Itikawa, Y.: At. Data. Nucl. Data. Tables **14** (1974) 1.

75And1 Andrick, D., Bitsch, A.: J. Phys. B **8** (1975) 393.

78Iti1 Itikawa, Y.: At. Data. Nucl. Data. Tables **14** (1978) 69.

80Reg1 Register, D.F., Trajmar, S., Srivastava, S.K.: Phys. Rev. A **21** (1980) 1134.

83Tra1 Trajmar, S., Register, D.F., Chutjian, A.: Phys. Rep. **97** (1983) 219.

89Buc1 Buckman, S.J., Mitroy, J.: J. Phys. B **22** (1989) 1365.

95Pet1 Petrovic, Z.Lj., O'Malley, T.F., Crompton, R.W.: J. Phys. B **28** (1995) 3309.

96Gib1 Gibson, J.C., Gulley, R.J., Sullivan, J.P., Buckman, S.J., Chan, V., Burrow, P.D.: J. Phys. B **29** (1996) 3177.

2.5.3 Determination of preferred cross sections

The preferred momentum transfer cross section for each atom has been derived from a consideration of all available (published) experimental and theoretical work. In general, we do not consider those cases where only theoretical values exist, unless there is substantial corroboration between two or more diffferent calculations. More weight has been placed on recent measurements which have realistic and well quantified uncertainties. The uncertainty estimates on the preferred cross sections indicate the level of concurrence between the various individual measurements and calculations.

2.5.4 Units

Cross sections are given in square Ångström (1 $Å^2 = 10^{-16}$ cm^2) and electron energies in electron volt [eV]. Where applicable, scattering lengths are given in atomic units (1 $a_0 = 5.2918 \cdot 10^{-9}$ cm) as is customary.

2.5.5 The elements

2.5.5.1 Hydrogen

Whilst there have been several measurements of absolute elastic differential cross sections for atomic hydrogen, there are no published experimental values of σ_m. The preferred cross sections, listed in Table 2.5.1 and shown in Fig. 2.5.1, are theoretical values obtained using the convergent close-coupling approach [98Bra1]. This has been shown to provide excellent agreement with a range of experimental cross sections in atomic hydrogen [92Bra1].

No estimate of the uncertainty is provided in this case.

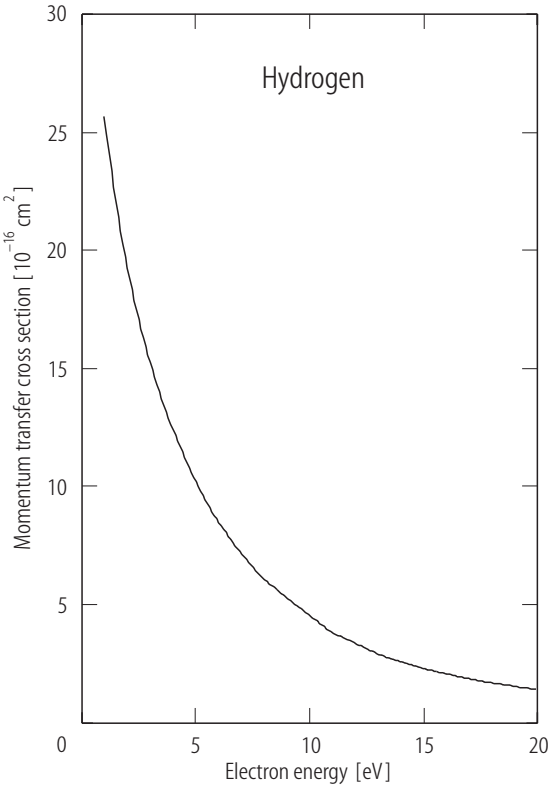

Fig. 2.5.1. Preferred values of σ_m for atomic hydrogen.

Table 2.5.1. The preferred values of the elastic momentum transfer cross section (σ_m) for electrons in atomic hydrogen.

E [eV]	σ_m [Å^2]
1	25.7
2	19.3
3	15.3
4	12.4
5	10.2
6	8.52
7	7.16
8	6.09
9	5.29
10	4.54
11	3.82
12	3.37
13	2.91
15	2.30
16	2.07
17	1.86
18	1.69
19	1.54
20	1.41
21	1.29

References for 2.5.5.1

92Bra1 Bray, I., Stelbovics, A.T.: Phys. Rev. A **46** (1992) 6995.
98Bra1 Bray, I.: Private Communication 1998.

2.5.5.2 Helium

The preferred elastic momentum transfer cross section for helium is presented over the energy range 0.008 to 100 eV. The data are tabulated in Table 2.5.2 and presented graphically in two ranges, 0.008 to 1.0 eV in Fig. 2.5.2 and 0.008 to 100 eV in Fig. 2.5.3. At lower energies (< 10 eV) the preferred cross section is based on the swarm cross sections of [67Cro1, 70Cro1, 77Mil1]; the crossed beam measurements of [80Reg1, 92Bru1], and the theoretical calculations of [79Nes1, 93Sah1, 97Fur1]. At higher energies (10…100 eV) the preferred cross section is based on the crossed beam measurements of [80Reg1, 92Bru1] and the calculation of [97Fur1].

The uncertainty is estimated to be: ± 2 % for $0.008 \leq E \leq 5$ eV, ± 3 % for $5 < E \leq 12$ eV, ± 5 % for $12 < E \leq 20$ eV and ± 10 % for $E > 20$ eV. The best estimate scattering length for helium is considered to be 1.18 ± 0.01 a_0.

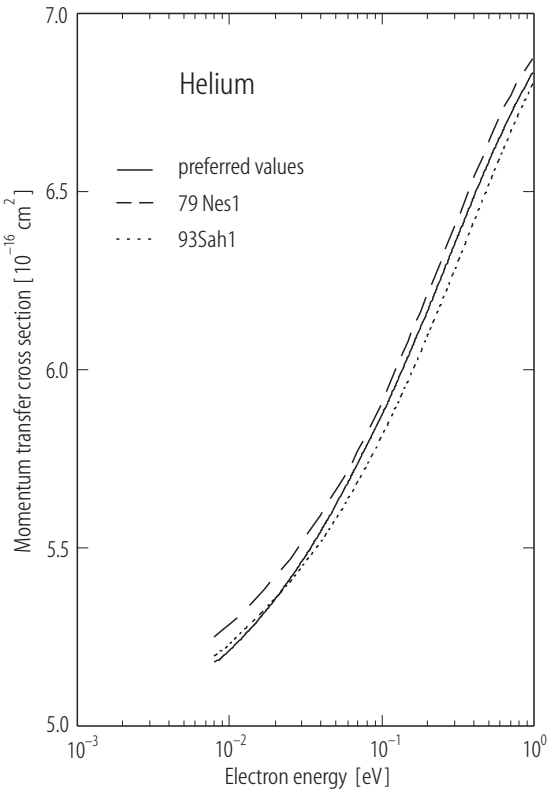

Fig. 2.5.2. Preferred values of σ_m for helium over the range 0.008 to 1 eV together with the theoretical calculations of [79Nes1] and [93Sah1].

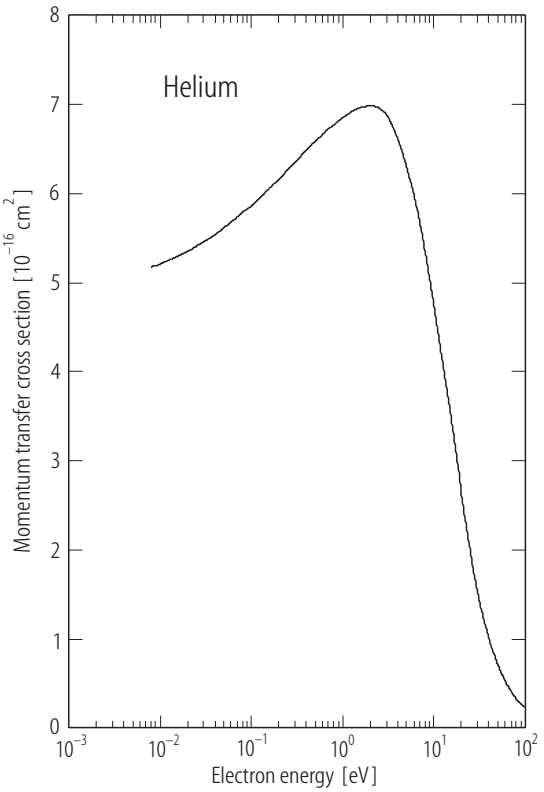

Fig. 2.5.3. Preferred values of σ_m for helium over the range 0.008 to 100 eV.

Table 2.5.2. The preferred values of the elastic momentum transfer cross section (σ_m) for electrons in helium.

E [eV]	σ_m [Å^2]	E [eV]	σ_m [Å^2]	E [eV]	σ_m [Å^2]
0.008	5.18	0.25	6.27	9	5.03
0.009	5.19	0.3	6.35	10	4.74
0.010	5.21	0.4	6.49	12	4.21
0.012	5.25	0.5	6.59	15	3.56
0.015	5.29	0.6	6.66	16	3.36
0.018	5.33	0.7	6.73	17	3.18
0.020	5.35	0.8	6.77	18	3.01
0.025	5.41	0.9	6.82	19	2.84
0.03	5.46	1.0	6.85	20	2.63
0.04	5.54	1.2	6.91	25	1.98
0.05	5.62	1.5	6.96	30	1.53
0.06	5.68	1.8	6.98	40	1.01
0.07	5.74	2.0	6.99	50	0.713
0.08	5.79	2.5	6.96	60	0.535
0.09	5.83	3	6.89	70	0.411
0.10	5.86	4	6.62	80	0.326
0.12	5.94	5	6.31	90	0.271
0.15	6.04	6	6.00	100	0.231
0.18	6.12	7	5.68		
0.20	6.16	8	5.35		

References for 2.5.5.2

64Fro1 Frost, L.S., Phelps, A.V.: Phys. Rev. **136** (1964) 1538.
67Cro1 Crompton, R.W., Elford, M.T., Jory, R.L.: Aust. J. Phys. **20** (1967) 369.
70Cro1 Crompton, R.W., Elford, M.T., Robertson, A.G.: Aust. J. Phys. **23** (1970) 667.
75And1 Andrick, D., Bitsch, A.: J. Phys. B **8** (1975) 393.
77Mil1 Milloy, H.B., Crompton, R.W.: Phys. Rev. A **15** (1977) 1847.
79Nes1 Nesbet, R.K.: Phys. Rev. A **20** (1979) 58.
80Reg1 Register, D.F., Trajmar, S., Srivastava, S.K.: Phys. Rev A **21** (1980) 1134.
92Bru1 Brunger, M.J., Buckman, S.J., Allen, L.J., McCarthy, I.E., Ratnavelu, K.: J. Phys. B **25** (1992) 1823.
93Sah1 Saha, H.P.: Phys. Rev. A **48** (1993) 1163.
97Fur1 Fursa, D.V., Bray, I.: J. Phys. B **30** (1997) 757.

2.5.5.3 Lithium

The only published experimental values for the elastic momentum transfer cross section for lithium are those of [76Wil1] and these are subject to substantial uncertainty. The preferred cross section, listed in Table 2.5.3 and shown in Fig. 2.5.4, are theoretical values obtained using the convergent close-coupling approach [98Bra1].

No estimate of the uncertainty is provided in this case.

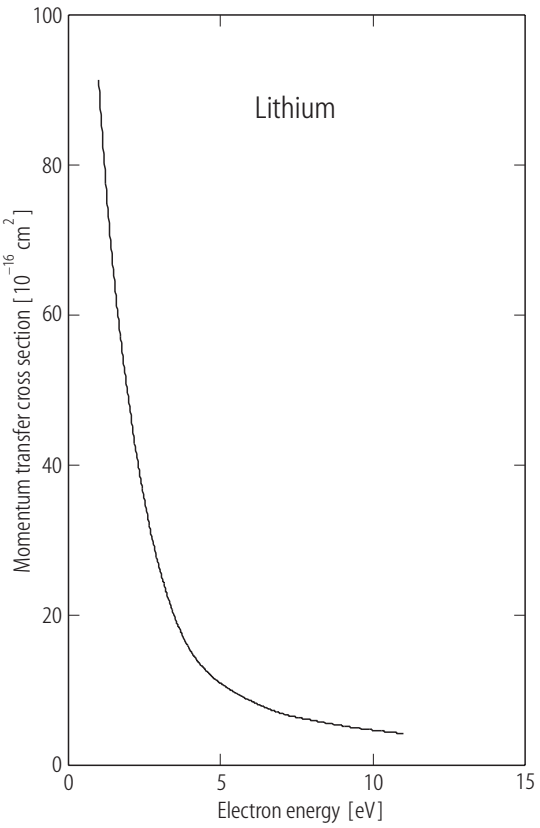

Fig. 2.5.4. Preferred values of σ_m for lithium.

Table 2.5.3. The preferred values of the elastic momentum transfer cross section (σ_m) for electrons in lithium.

E [eV]	σ_m [Å^2]
1	91.4
2	46.3
3	25.2
4	14.6
5	10.7
6	8.49
7	6.72
8	5.94
9	5.17
10	4.62
11	4.19

References for 2.5.5.3

76Wil1 Williams, W., Trajmar, S., Bozinis, D.: J. Phys. B **9** (1976) 1529.
98Bra1 Bray, I.: Private Communication 1998.

2.5.5.4 Oxygen

There appears to be only one experimental determination of the elastic momentum transfer cross section, σ_m, for atomic oxygen, that of [89Wil1]. This was obtained from a phaseshift analysis of absolute differential cross sections. The preferred cross section is listed in Table 2.5.4.

The uncertainty on the cross section is estimated to be ± 10 %.

Table 2.5.4. The preferred values of the elastic momentum transfer cross section (σ_m) for electrons in atomic oxygen.

E [eV]	σ_m [Å^2]
0.54	2.55
2.18	3.95
3.40	4.23
4.90	4.03
8.71	5.12

References for 2.5.5.4

89Wil1 Williams, J.F., Allen, L.J.: J. Phys. B **22** (1989) 3529.

2.5.5.5 Neon

The preferred cross sections for neon are presented over the energy range 0.003 to 30 eV. The data are tabulated in Table 2.5.5 and presented graphically in two ranges, 0.003 to 10 eV in Fig. 2.5.5 and 0.003 to 30 eV in Fig. 2.5.6. The upper limit on the energy range has been limited to 30 eV as there are serious discrepancies between the available experimental and theoretical cross sections above this energy. At lower energies (< 4 eV) the preferred cross section is based on the swarm cross sections of [72Rob1, 80OMa1], together with the theoretical calculations of [90Sah1]. Between 4 and 30 eV, the preferred cross section is based on the crossed beam measurements of [84Reg1, 94Gul1], and the theoretical calculations of [89Sah1, 90Sah1].

The uncertainty is estimated to be: ± 2 % for $0.003 \le E < 1$ eV, ± 5 % for $1 \le E < 10$ eV, ± 8 % for $E \ge 10$ eV. The best estimate scattering length for neon is considered to be $0.215 \pm 0.015\ a_0$ and is based on the values of [80OMa1, 85McE1, 89Buc1, 90Sah1, 94Gul1].

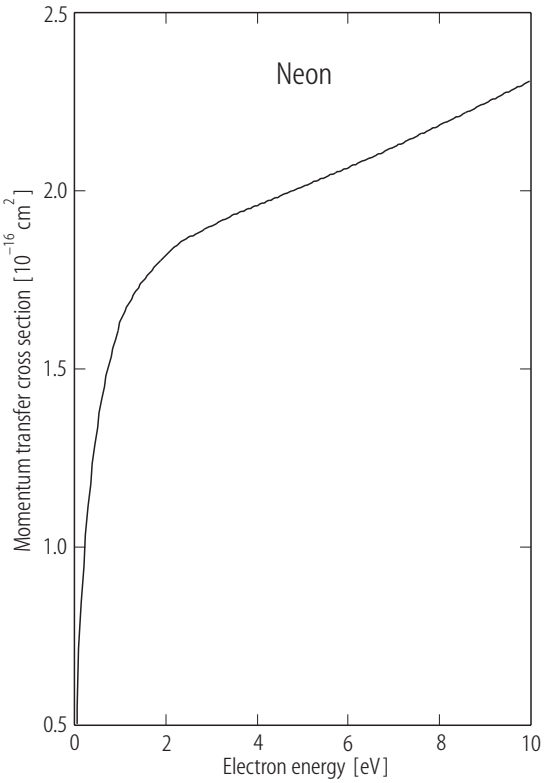

Fig. 2.5.5. Preferred values of σ_m for neon over the range 0.003 to 10 eV.

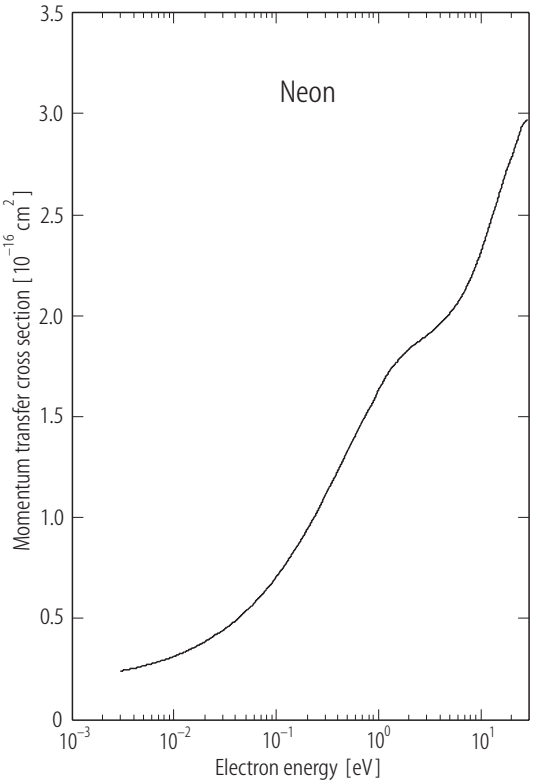

Fig. 2.5.6. Preferred values of σ_m for neon over the range 0.003 to 30 eV.

Table 2.5.5. The preferred values of the elastic momentum transfer cross section (σ_m) for electrons in neon.

E [eV]	σ_m [Å^2]	E [eV]	σ_m [Å^2]	E [eV]	σ_m [Å^2]
0.000	0.163	0.07	0.611	1.5	1.75
0.003	0.241	0.08	0.645	1.8	1.80
0.004	0.254	0.09	0.675	2.0	1.82
0.005	0.266	0.10	0.707	2.5	1.86
0.006	0.277	0.12	0.762	3	1.90
0.007	0.287	0.15	0.837	4	1.96
0.008	0.296	0.18	0.901	5	2.01
0.009	0.305	0.20	0.94	6	2.07
0.010	0.314	0.25	1.03	7	2.12
0.012	0.33	0.3	1.11	8	2.19
0.015	0.352	0.4	1.23	9	2.25
0.018	0.373	0.5	1.33	10	2.31
0.020	0.386	0.6	1.41	12	2.44
0.025	0.417	0.7	1.48	15	2.59
0.03	0.442	0.8	1.53	18	2.72
0.04	0.491	0.9	1.58	20	2.78
0.05	0.535	1.0	1.62	25	2.93
0.06	0.574	1.2	1.69	30	2.98

References for 2.5.5.5

72Rob1 Robertson, A.G.: J. Phys. B **5** (1972) 648.
80OMa1 O'Malley, T.F., Crompton, R.W.: J. Phys. B **13** (1980) 3451.
84Reg1 Register, D.F., Trajmar, S.: Phys. Rev. A **29** (1984) 1785.
85McE1 McEachran, R.P., Stauffer, A.U.: Phys. Lett. A **107** (1985) 397.
89Buc1 Buckman, S.J., Mitroy, J.: J. Phys. B **22** (1989) 1365.
89Sah1 Saha, H.P.: Phys. Rev. A **39** (1989) 5048.
90Sah1 Saha, H.P.: Phys. Rev. Lett. **65** (1990) 2003.
94Gul1 Gulley, R.J., Alle, D.T., Brennan, M.J., Brunger, M.J., Buckman, S.J.: J. Phys.B **27** (1994) 2593.

2.5.5.6 Sodium

The preferred values of σ_m for sodium are based on the swarm-derived cross section of [78Nak1] and the close-coupling calculations of [71Nor1, 98Bra1]. These are given in Table 2.5.6.

No estimate of the uncertainty is provided in this case.

References for 2.5.5.6

71Nor1 Norcross, D.W.: J. Phys. B **4** (1971) 1458.
78Nak1 Nakamura, Y., Lucas, J.: J. Phys. D **11** (1978) 337.
98Bra1 Bray, I.: Private Communication 1998.

Table 2.5.6. The preferred values of the elastic momentum transfer cross section (σ_m) for electrons in sodium.

E [eV]	σ_m [Å^2]	E [eV]	σ_m [Å^2]	E [eV]	σ_m [Å^2]
0.050	290	0.25	424	3.0	19.3
0.060	389	0.30	349	4.0	9.85
0.070	504	0.40	248	5.0	5.13
0.080	643	0.50	184	6.0	4.25
0.090	736	0.60	155	7.0	3.17
0.10	786	0.70	135	8.0	2.63
0.12	794	0.80	120	9.0	2.52
0.15	736	0.90	108	10.0	2.26
0.18	643	1.0	97.8	11.0	2.08
0.20	569	2.0	39.4		

2.5.5.7 Magnesium

There has been only one measurement of σ_m for magnesium by [78Wil1] based on integrated differential scattering cross sections. These values are given in Table 2.5.7.

It is possible that the uncertainties on these values are as large as 100 %.

Table 2.5.7. The preferred values of the elastic momentum transfer cross section (σ_m) for electrons in magnesium.

E [eV]	σ_m [Å^2]
10	7.6
20	4.1
40	0.47

References for 2.5.5.7

78Wil1 Williams, W., Trajmar, S.: J. Phys. B **11** (1978) 2021.

2.5.5.8 Argon

The preferred cross sections for argon are presented over the energy range 0.012 to 10 eV. The data are tabulated in Table 2.5.8 and presented graphically in two ranges, one which emphasises the Ramsauer-Townsend minimum in Fig. 2.5.7 and the other, Fig. 2.5.8, the range 0.012 to 10 eV. The upper limit on the energy range has been limited to 10 eV as there are serious discrepancies between the available experimental and theoretical cross sections above this energy. At lower energies (< 1 eV) the preferred cross section is based on the swarm cross sections of [94Sch1, 95Pet1], together with the theoretical calculations of [97McE1]. Between 1 and 10 eV, the preferred cross section is based on the swarm measurement of [88Nak1], the crossed beam measurements of [81Sri1, 96Gib1] and the theoretical calculations of [95Sah1, 97McE1].

The uncertainty is estimated to be: ± 5 % for $0.012 \le E < 1$ eV, although in the region of the Ramsauer-Townsend minimum (0.2…0.3 eV) ± 10 % is a more realistic estimate. For $1 \le E < 10$ eV the uncertainty is estimated to be ± 10 %. The best estimate scattering length for argon is considered to be $-1.452 \pm 0.02\ a_0$ and is based on the values of [85Fer1, 89Buc1, 93Sah1, 94Sch1, 95Pet1, 97McE1].

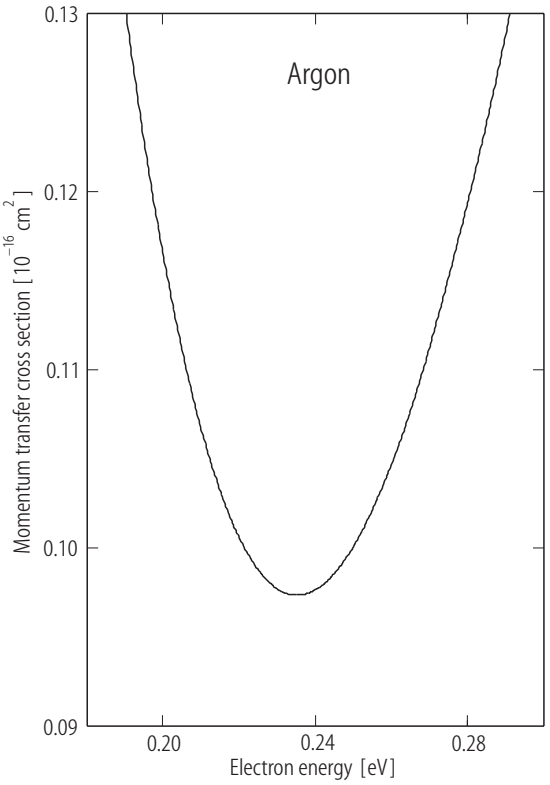

Fig. 2.5.7. Preferred values of σ_m for argon in the region of the Ramsauer-Townsend minimum.

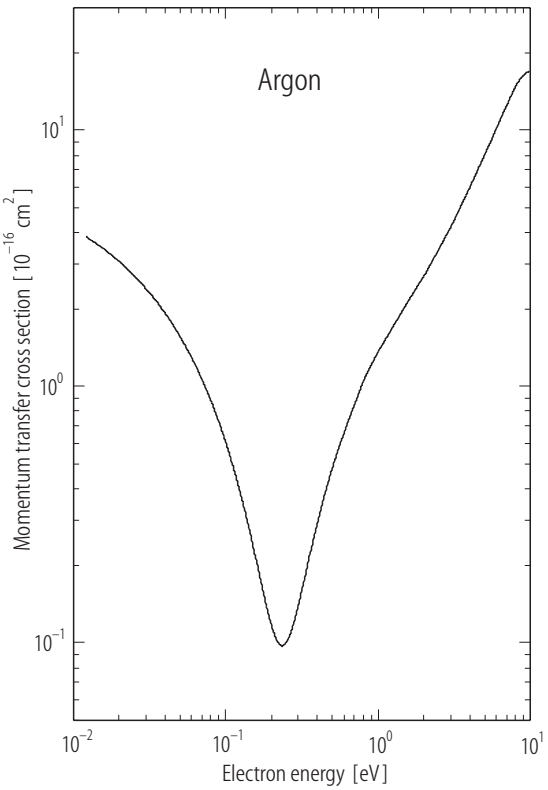

Fig. 2.5.8. Preferred values of σ_m for argon over the range 0.012 to 10 eV.

References for 2.5.5.8

81Sri1 Srivastava, S.K., Tanaka, H., Chutjian, A., Trajmar, S.: Phys. Rev. A **23** (1981) 2156.
85Fer1 Ferch, J., Granitza, B., Masche, C., Raith, W.: J. Phys. B **18** (1989) 1365.
88Nak1 Nakamura, Y., Kurachi, M.: J. Phys. D **21** (1988) 718.
89Buc1 Buckman, S.J., Mitroy, J.: J. Phys. B **22** (1989) 1365.
93Sah1 Saha, H.P.: Phys. Rev. A **48** (1993) 1163.
94Sch1 Schmidt, B., Berkhan, K., Gotz, B., Muller, M.: Phys. Scr. T **53** (1994) 30.
95Pet1 Petrovic, Z. Lj., O'Malley, T.F., Crompton, R.W.: J. Phys. B **28** (1995) 3309.
95Sah1 Private Communication, cited in [96Gib1].
96Gib1 Gibson, J.C., Gulley, R.J., Sullivan, J.P., Buckman, S.J., Chan, V., Burrow, P.D.: J. Phys. B **29** (1996) 3177.
97McE1 McEachran, R.P., Stauffer, A.D.: Aust. J. Phys. **50** (1997) 511.

Table 2.5.8. The preferred values of the elastic momentum transfer cross section (σ_m) for electrons in argon.

E [eV]	σ_m [Å^2]	E [eV]	σ_m [Å^2]	E [eV]	σ_m [Å^2]
0.012	3.86	0.17	0.174	0.60	0.664
0.015	3.53	0.18	0.150	0.65	0.756
0.018	3.24	0.19	0.131	0.70	0.847
0.020	3.08	0.20	0.117	0.80	1.05
0.025	2.71	0.21	0.107	0.90	1.21
0.03	2.41	0.22	0.101	1.0	1.36
0.04	1.93	0.23	0.0977	1.2	1.64
0.05	1.57	0.24	0.0976	1.5	2.05
0.06	1.29	0.25	0.100	1.8	2.45
0.07	1.07	0.26	0.105	2.0	2.70
0.08	0.881	0.28	0.119	2.5	3.43
0.09	0.731	0.30	0.140	3	4.20
0.10	0.607	0.32	0.165	4	6.00
0.11	0.505	0.325	0.172	5	8.01
0.12	0.420	0.35	0.209	6	10.2
0.13	0.350	0.40	0.293	7	12.6
0.14	0.292	0.45	0.384	8	14.9
0.15	0.244	0.50	0.477	9	16.4
0.16	0.205	0.55	0.571	10	17.1

2.5.5.9 Potassium

The preferred values of the elastic momentum transfer cross section (σ_m) for electrons in potassium are presented over the energy range 0.1 to 11 eV. The data, given in Table 2.5.9, are derived from theoretical calculations by [86Fab1, 98Bra1].

No estimate of the uncertainty is provided in this case.

Table 2.5.9. The preferred values of the elastic momentum transfer cross section (σ_m) for electrons in potassium.

E [eV]	σ_m [Å^2]	E [eV]	σ_m [Å^2]	E [eV]	σ_m [Å^2]
0.1	632	2.0	70.0	8.0	13.8
0.2	369	3.0	30.3	9.0	12.3
0.3	289	4.0	20.3	10.0	11.0
0.4	253	5.0	18.3	11.0	9.61
0.5	244	6.0	16.7		
1.0	182	7.0	15.4		

References for 2.5.5.9

86Fab1 Fabrikant, I.I.: J. Phys. B **19** (1986) 1527.
98Bra1 Bray, I.: Private Communication 1998.

2.5.5.10 Manganese

There has only been one determination, that of [78Wil1], of the momentum transfer cross section for manganese. This was derived from a measurement of relative angular distributions at an energy of 20 eV. The relative measurements were placed on an absolute scale using the optical oscillator normalisation technique. The value obtained was 4.2 $Å^2$ and no error limit is quoted.

References for 2.5.5.10

78Wil1 Williams, W., Cheeseborough, J.C., Trajmar, S.: J. Phys. B **11** (1978) 2031.

2.5.5.11 Copper

The preferred values of the elastic momentum transfer cross section (σ_m) for electrons in copper at energies between 6 and 100 eV are given in Table 2.5.10. They were derived from differential scattering measurements by [77Tra1].

The uncertainty on the cross section is estimated to be greater than ± 100 %.

Table 2.5.10. The preferred values of the elastic momentum transfer cross section (σ_m) for electrons in copper.

E [eV]	σ_m [$Å^2$]
6	71.1
10	38.1
20	45.9
60	7.2
100	5.7

References for 2.5.5.11

77Tra1 Trajmar, S., Williams, W., Srivastava, S.K.: J. Phys. **B** 10 (1977) 3323.

2.5.5.12 Zinc

The preferred values of the elastic momentum transfer cross section (σ_m) for electrons in zinc at energies between 2 and 30 eV are given in Table 2.5.11. These are based on three theoretical calculations contained in [94Kum1, 97McE1] which show good agreement.

No estimate of the uncertainty is provided in this case.

Table 2.5.11. The preferred values of the elastic momentum transfer cross section (σ_m) for electrons in zinc.

E [eV]	σ_m [$Å^2$]	E [eV]	σ_m [$Å^2$]	E [eV]	σ_m [$Å^2$]
2	51.0	6	16.6	10	7.1
3	38.3	7	13.0	15	3.5
4	28.4	8	10.8	20	2.3
5	21.8	9	8.4	30	1.5

References for 2.5.5.12

94Kum1 Kumar, P., Jain, A.K., Tripathi, A.N., Nahar, S.N.: Phys. Rev. A **49** (1994) 899.
97McE1 McEachran, R.P.: Private Communication 1997.

2.5.5.13 Krypton

The preferred elastic momentum transfer cross section for krypton is presented over the energy range 0.001 to 10 eV. The data are tabulated in Table 2.5.12 and presented graphically in two ranges, one which emphasises the Ramsauer-Townsend minimum in Fig. 2.5.9 and the other, Fig. 2.5.10, the range 0.010 to 10 eV. The upper limit on the energy range has been limited to 10 eV as there are serious discrepancies between the available experimental and theoretical cross sections above this energy. At lower energies (< 4 eV) the preferred cross section is based on the swarm cross sections of [93Bre1, 94Sch1], together with the theoretical calculation of [88McE1]. Between 4 and 10 eV, the preferred cross section is based on the swarm measurement of [89Nak1], the crossed beam measurements of [81Sri1, 88Dan1] and the theoretical calculation of [88McE1].

The uncertainty is estimated to be ± 5 % for $0.010 \le E < 1$ eV, although in the region of the Ramsauer-Townsend minimum (0.4…0.8 eV) ± 20 % is a more realistic estimate. For $1 \le E < 4$ eV the uncertainty is estimated to be ± 10 %, whilst for $E > 4$ eV, the uncertainty is no better than ± 30 %. The best estimate scattering length for krypton is considered to be $(-3.35 \pm 0.1)a_0$ and is based on the values of [88Wey1, 89Buc1, 90Mit1, 93Bre1, 94Sch1].

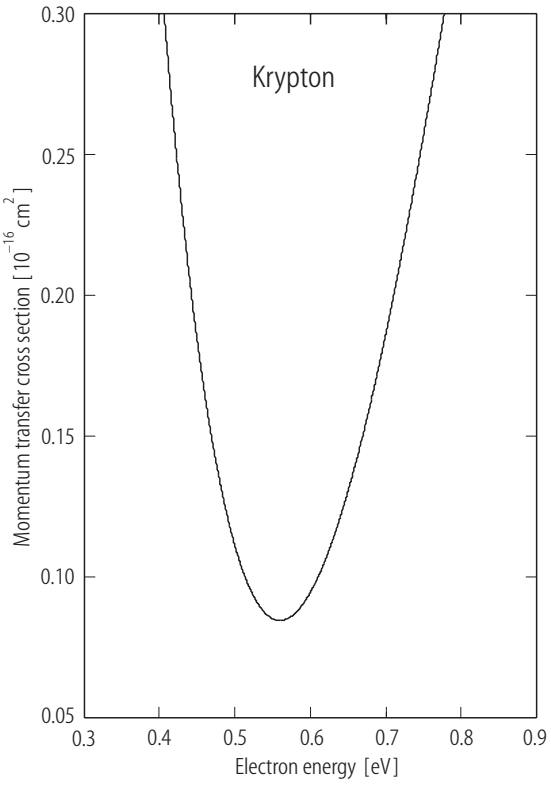

Fig. 2.5.9. Preferred values of σ_m for krypton in the region of the Ramsauer-Townsend minimum.

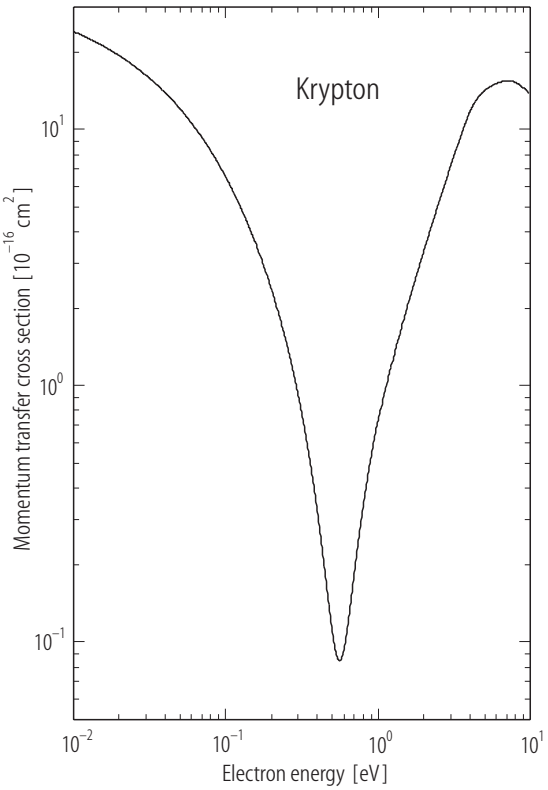

Fig. 2.5.10. Preferred values of σ_m for krypton over the range 0.01 to 10 eV.

Table 2.5.12. The preferred values of the elastic momentum transfer cross section (σ_m) for electrons in krypton.

E [eV]	σ_m [Å^2]	E [eV]	σ_m [Å^2]	E [eV]	σ_m [Å^2]
0.0001	37.4	0.510	0.102	1.10	0.929
0.001	33.1	0.515	0.0987	1.15	1.04
0.0015	32.1	0.520	0.0956	1.20	1.15
0.002	31.3	0.525	0.0929	1.25	1.26
0.0025	30.6	0.530	0.0905	1.30	1.38
0.003	30.0	0.535	0.0886	1.35	1.50
0.0035	29.4	0.540	0.0870	1.40	1.63
0.004	28.8	0.545	0.0858	1.45	1.76
0.005	27.9	0.550	0.0850	1.50	1.89
0.006	27.0	0.555	0.0845	1.55	2.02
0.007	26.2	0.560	0.0844	1.60	2.16
0.01	24.2	0.565	0.0846	1.65	2.31
0.012	23.0	0.570	0.0851	1.70	2.45
0.015	21.6	0.575	0.0860	1.75	2.60
0.017	20.6	0.580	0.0871	1.80	2.75
0.020	19.5	0.585	0.0885	1.85	2.90
0.025	17.8	0.590	0.0902	1.90	3.06
0.03	16.3	0.595	0.0922	1.95	3.22
0.035	15.1	0.60	0.0945	2.00	3.38
0.04	13.9	0.61	0.0998	2.05	3.55
0.045	13.0	0.62	0.106	2.10	3.72
0.05	12.1	0.63	0.113	2.15	3.89
0.07	9.30	0.64	0.122	2.20	4.07
0.10	6.55	0.65	0.131	2.25	4.24
0.12	5.27	0.66	0.140	2.30	4.42
0.15	3.87	0.67	0.151	2.35	4.61
0.17	3.18	0.68	0.162	2.40	4.79
0.20	2.37	0.70	0.187	2.45	4.98
0.23	1.78	0.72	0.213	2.50	5.18
0.25	1.47	0.75	0.257	2.6	5.57
0.27	1.22	0.77	0.289	2.7	5.97
0.30	0.908	0.80	0.339	3.0	7.23
0.32	0.745	0.82	0.374	3.25	8.33
0.35	0.548	0.85	0.428	3.5	9.47
0.37	0.444	0.87	0.466	4	11.7
0.40	0.321	0.90	0.525	5	14.2
0.42	0.257	0.92	0.566	6	15.1
0.45	0.184	0.95	0.629	7	15.5
0.47	0.148	0.97	0.673	8	15.3
0.50	0.111	1.00	0.729	9	14.6
0.505	0.106	1.05	0.827	10	13.7

References for 2.5.5.13

81Sri1 Srivastava, S.K., Tanaka, H., Chutjian, A., Trajmar, S.: Phys. Rev. A **23** (1981) 2156.
87Buc1 Buckman, S.J., Lohmann, B.: J. Phys. B **20** (1987) 5807.

88Dan1 Danjo, A.: J. Phys. B **21** (1988) 3759.
88McE1 McEachran, R.P., Stauffer, A.D.: Proc. Int. Symp. on Correlation and Polarisation in Electronic and Atomic Collisions, Singapore: World Scientific.
88Wey1 Weyhreter, M., Barzick, B., Mann, A., Linder, F.: Z. Phys. D **7** (1988) 333.
89Buc1 Buckman, S.J., Mitroy, J.: J. Phys. B **22** (1989) 1365.
89Nak1 Nakamura, Y.: Abstracts of 6th. Int. Swarm. Sem. (Glen Cove, NY) (1989), p1.
90Mit1 Mitroy, J.: Aust. J. Phys. **43** (1990) 19.
93Bre1 Brennan, M.J., Ness, K.F.: Aust. J. Phys. **46** (1993) 249.
94Sch1 Schmidt, B., Berkhan, K., Gotz, B., Muller, M.: Phys. Scr. T **53** (1994) 30.

2.5.5.14 Xenon

The preferred elastic momentum transfer cross section for xenon is presented over the energy range 0.005 to 10 eV. The data are tabulated in Table 2.5.13 and presented graphically in two ranges, one which emphasises the Ramsauer-Townsend minimum in Fig. 2.5.11 and the other, Fig. 2.5.12, the range 0.05 to 10 eV. The upper limit on the energy range has been limited to 10 eV as there are serious discrepancies between the available experimental and theoretical cross sections above this energy. At lower energies (< 2 eV) the preferred cross section is based on the swarm cross sections of [91Nak1, 94Sch1], the crossed beam measurements of [86Reg1, 88Wey1, 98Gib1], together with the theoretical calculation of [98Gib1]. Between 2 and 10 eV, the preferred cross section is based on the swarm measurements of [89Nak1, 94Sch1] and the crossed beam measurements of [86Reg1, 87Nis1, 98Gib1].

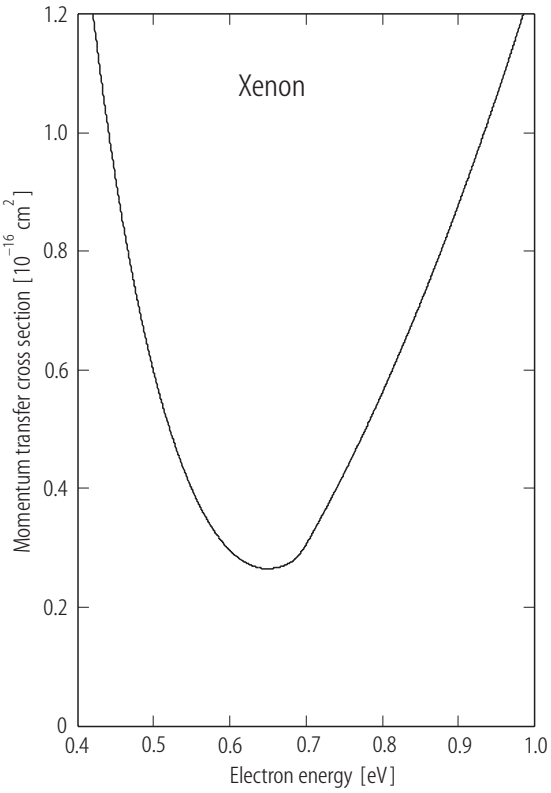

Fig. 2.5.11. Preferred values of σ_m for xenon in the region of the Ramsauer-Townsend minimum.

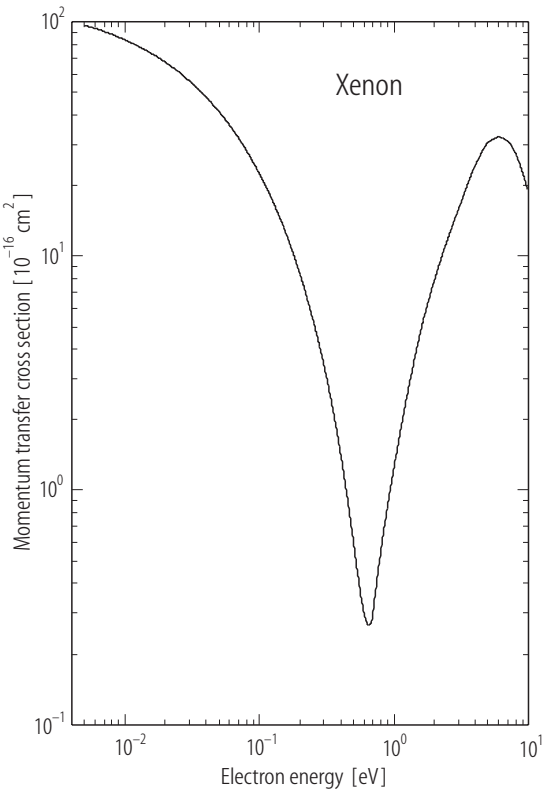

Fig. 2.5.12. Preferred values of σ_m for xenon over the range 0.01 to 10 eV.

The uncertainty is estimated to be: ± 10 % for $0.010 \le E < 1$ eV, although in the region of the Ramsauer-Townsend minimum (0.5…0.9 eV) ± 50 % is a conservative estimate. For $1 \le E < 2$ eV the uncertainty is estimated to be ± 10 %, whilst for $E > 2$ eV, the uncertainty is no better than ± 30 %. The best estimate scattering length for xenon is considered to be $(-6.3 \pm 0.3)a_0$ and is based on the values of [88Wey1, 94Sch1, 98Gib1].

Table 2.5.13. The preferred values of the elastic momentum transfer cross section (σ_m) for electrons in xenon.

E [eV]	σ_m [Å^2]	E [eV]	σ_m [Å^2]	E [eV]	σ_m [Å^2]
0.005	97.0	0.46	0.844	0.77	0.479
0.007	91.1	0.48	0.708	0.8	0.562
0.01	84.0	0.5	0.596	0.83	0.651
0.015	74.6	0.51	0.548	0.85	0.713
0.02	67.3	0.52	0.504	0.87	0.778
0.025	61.2	0.53	0.465	0.9	0.880
0.03	56.1	0.54	0.430	0.95	1.06
0.04	47.9	0.55	0.399	1	1.26
0.05	41.4	0.56	0.372	1.08	1.62
0.06	36.2	0.57	0.348	1.14	1.92
0.07	31.9	0.58	0.328	1.2	2.25
0.08	28.2	0.59	0.310	1.3	2.85
0.1	22.5	0.6	0.296	1.4	3.51
0.12	18.1	0.61	0.285	1.5	4.22
0.14	14.8	0.62	0.276	1.7	5.74
0.17	11.1	0.63	0.270	2	7.97
0.2	8.36	0.64	0.266	2.5	11.8
0.25	5.33	0.65	0.265	3	15.8
0.27	4.47	0.66	0.267	4	24.4
0.3	3.43	0.67	0.270	5	30.7
0.32	2.89	0.68	0.276	6	32.3
0.35	2.22	0.69	0.284	7	31.0
0.37	1.87	0.7	0.306	8	27.5
0.4	1.43	0.715	0.341	9	22.8
0.42	1.20	0.73	0.377	10	18.5
0.44	1.01	0.75	0.427		

References for 2.5.5.14

86Reg1 Register, D.F., Vuskovic, L., Trajmar, S.: J. Phys. B **19** (1986) 1685.
87Nis1 Nishimura, H., Matsuda, T., Danjo, A.: J.Phys. Soc. Jpn. **56** (1987) 70.
88Wey1 Weyhreter, M., Barzick, B., Mann, A., Linder, F.: Z. Phys. D **7** (1988) 333.
89Nak1 Nakamura, Y.: Abstracts of 6th Int. Swarm. Sem. (Glen Cove, N.Y.) (1989), p. 1
91Nak1 Nakamura, Y.: Joint Symp. on Electron and Ion Swarms and Low Energy Electron Scattering (Bond University) Abstracts (1991), p. 103.
94Sch1 Schmidt, B., Berkhan, K., Gotz, B., Muller, M.: Phys. Scr. T **53** (1994) 30.
98Gib1 Gibson J.C., Lun D.R., Allen, L.J., McEachran, R.P., Parcell, L.A., Buckman, S.J.: J. Phys. B **31** (1998) 3949.

2.5.5.15 Cesium

There has been a substantial amount of work, both experimental (swarm and beam) and theoretical, on low energy electron scattering from cesium. Unfortunately there is little accord for the momentum transfer cross sections derived from the various techniques (see e.g. [93Thu1]). However, the most sophisticated calculation [92Thu1] shows excellent agreement in the low energy regime with relative, angular distributions [77Geh1] and with the calculations of [72Kar1, 86Fab1].

The preferred cross sections for cesium, based on these theoretical calculations, are presented over the energy range 0.1 to 2 eV. The data are tabulated in Table 2.5.14.

No estimate of the uncertainty is provided in this case.

Table 2.5.14. The preferred values of the elastic momentum transfer cross section (σ_m) for electrons in cesium.

E [eV]	σ_m [Å^2]	E [eV]	σ_m [Å^2]
0.1	547	0.8	132
0.2	385	0.9	119
0.3	306	1.0	109
0.4	240	1.2	97.7
0.5	201	1.5	57.7
0.6	169	1.8	55.7
0.7	146	2.0	50.1

References for 2.5.5.15

72Kar1 Karule, E.M.: J. Phys. B **5** (1972) 2051.
77Geh1 Gehenn, W., Reichert, E.: J. Phys. B **10** (1977) 3105.
86Fab1 Fabrikant, I.I.: J. Phys. B **19** (1986) 1527.
92Thu1 Thumm, U., Norcross, D.W.: Phys. Rev. A **45** (1992) 6349.
93Thu1 Thumm, U., Norcross, D.W.: Phys. Rev. A **47** (1993) 305.

2.5.5.16 Barium

Table 2.5.15. The preferred values of the elastic momentum transfer cross section (σ_m) for electrons in barium.

E [eV]	σ_m [Å^2]
15	4.5
20	4.0
30	3.4
40	3.0
60	2.5
80	2.3
100	2.0

There have been two experimental measurements of σ_m in barium by [78Jen1, 94Wan1], both based on elastic differential scattering data at energies from 15 to 100 eV. These measurements differ significantly at their lowest common energy and they both vary substantially from recent calculated cross sections. The preferred cross section, based on these experimental values and the theoretical calculations of [94Kum1, 94Szm1], are given in Table 2.5.15.

The uncertainty on the cross section is estimated to be greater than ± 100 %.

References for 2.5.5.16

78Jen1 Jensen, S., Register, D., Trajmar, S.: J. Phys. B **11** (1978) 2367.
94Kum1 Kumar, P., Jaim, A.K., Tripathi, A.N., Nahar, S.N.: Z. Phys. D **30** (1994) 149.
94Szm1 Szmytkowski, R., Sienkiewicz, J.E.: Phys. Rev. A **50** (1994) 4007.
94Wan1 Wang, S., Trajmar, S., Zetner, P.W.: J. Phys. B **27** (1994) 1613.

2.5.5.17 Mercury

There have been several experimentally derived elastic momentum transfer cross sections for mercury. At low energies (<10 eV) these are all based on transport coefficient data, principally drift velocity measurements. At higher energies, there also exists a σ_m based on differential scattering measurements. The preferred values in the lower energy range were chosen on the basis of the accuracy of the drift velocity measurements of [91Eng1] in Hg vapour-gas mixtures. At higher energies, the preferred values are based on the experimental cross sections of [93Pan1] and the calculations of [87McE1, 87Hab1]. The preferred values are given in Table 2.5.16 and shown in Fig. 2.5.13.

The uncertainty is estimated to be: ± 10 % for $0.010 \leq E < 2$ eV and ± 30 % for higher energies.

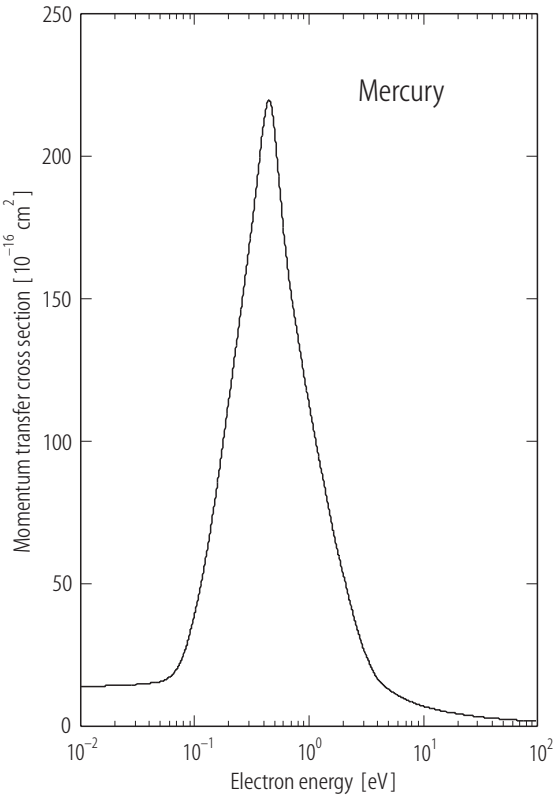

Fig. 2.5.13. Preferred values of σ_m for mercury.

Table 2.5.16. The preferred values of the elastic momentum transfer cross section (σ_m) for electrons in mercury.

E [eV]	σ_m [Å^2]	E [eV]	σ_m [Å^2]	E [eV]	σ_m [Å^2]
0.005	13.8	0.28	159	1.8	60.5
0.01	13.9	0.3	168	2	53.0
0.015	14.0	0.32	177	2.5	37.5
0.02	14.1	0.34	186	3	27.0
0.03	14.5	0.36	195	4	16.5
0.04	14.9	0.38	204	5	12.7
0.05	15.5	0.39	208	6	10.7
0.06	17.0	0.4	211	7	9.19
0.07	20.0	0.41	214	8	8.31
0.08	25.1	0.42	217	9	7.39
0.09	31.9	0.43	219	10	6.91
0.1	39.4	0.44	220	12	6.04
0.12	54.9	0.46	219	15	5.11
0.13	62.9	0.48	215	18	4.54
0.14	71.0	0.5	209	20	4.24
0.15	78.9	0.55	190	25	3.65
0.16	86.5	0.6	174	30	3.19
0.17	94.2	0.65	161	40	2.7
0.18	102	0.7	151	50	2.36
0.19	109	0.75	143	60	2.09
0.2	115	0.8	137	70	1.89
0.21	121	0.9	124	80	1.74
0.22	127	1	113	90	1.66
0.23	133	1.2	95.5	100	1.55
0.24	139	1.4	82.0		
0.26	149	1.6	70.0		

References for 2.5.5.17

87Hab1 Haberland, R., Fritsche, L.: J. Phys. B **20** (1987) 121.
87McE1 McEachran, R.P., Stauffer, A.D.: J. Phys. B **20** (1987) 5517.
91Eng1 England, J.P., Elford, M.T.: Aust. J. Phys. **44** (1991) 647.
93Pan1 Panajotovic, R., Pejcev, V., Konstantinovic, M., Filipovic, D., Bocvarski, V., Marinkovic, B.: J. Phys. B **26** (1993) 1005.

2.6 Ionization

2.6.1 Introduction and general description

General aspects of the ionization of neutral atoms by electron impact have been summarized in a number of reviews [71Ino1] and books [85Mär1]. Some surveys of the electron impact ionization data have been reported in several compilations [83Bel1, 87Taw1, 88Len1, 89Hig1] as well as in several databases (for example, NIFS [www1], JAERI [www2], ORNL [www3] and IAEA [www4]) from where relevant numerical as well as bibliographic data can be retrieved electronically.

The apparent ionization cross sections,

$$\sigma_i^a = \sum_m m\sigma_i^{m+} \quad (m \text{ is the charge state of the product ions}),$$

for most of the neutral atoms can be determined with reasonably good accuracies by crossing the energy-selected incident electrons through the gas targets and, then, measuring the secondary electrons or ions with a pair of the parallel plates, except for elements such as high melting materials which can not be easily evaporated and are hard to determine their absolute densities. Such neutral atom targets can be prepared via the electron capture into the parent ions and, then, the ionization cross sections can be determined through so-called crossed-beams technique where the target atoms cross the mono-energetic incident electrons and the product ions are charge-analyzed to determine the intensities of ions with different charges. However, it should be kept in mind that the neutral atoms prepared in such ways often include a significant fraction of the excited or metastable state beams which strongly influence the observed ionization cross sections.

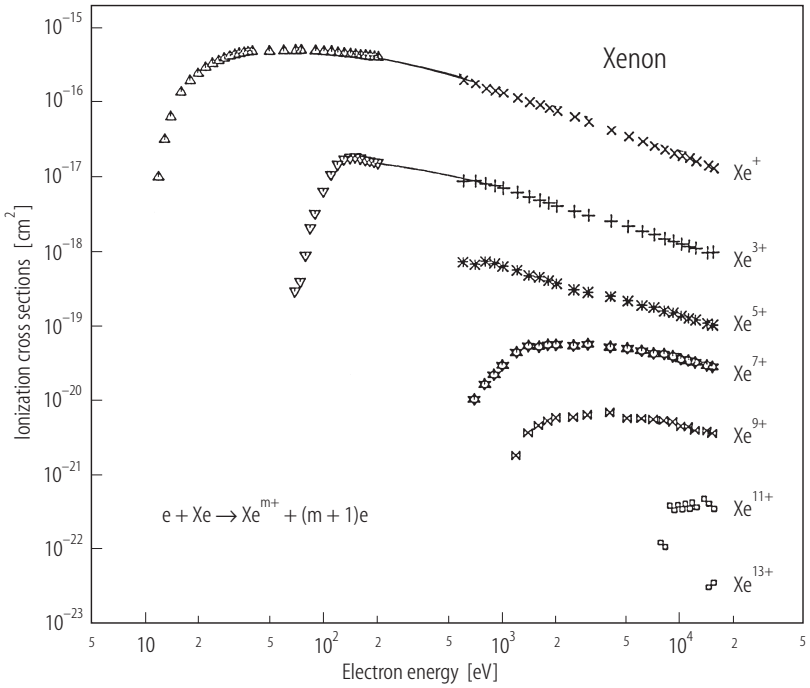

Fig. 2.6.1. Electron impact ionization cross sections for various ionization states of Xe^{m+} (m = 1, 3, 5, 7, 9, 11, 13) ions from neutral Xe atoms as a function of the electron impact energy. The solid lines are given to guide eyes (The data are taken from our database at NIFS).

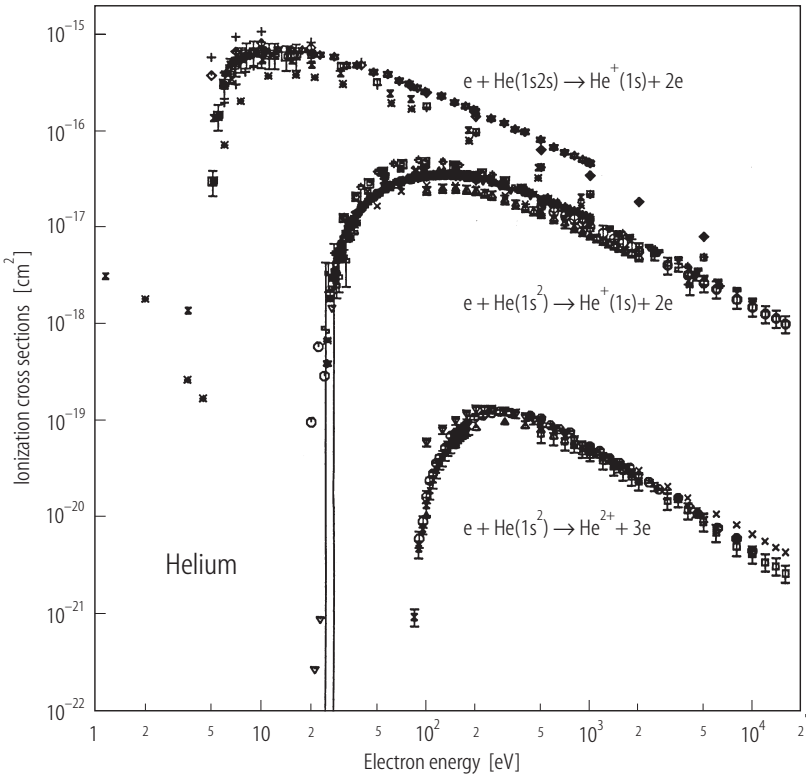

Fig. 2.6.2. Comparison of single-electron ionization cross sections for the ground and metastable He atoms under electron impact, together with those for double-electron ionization of the ground state helium atoms.

Another technique such as a time-of-flight spectrometer or magnetic analyzer is required to get the partial ionization cross sections (σ_i^{m+}) for ions with different charge states (m). Typically, as the the number of the electrons to be ionized (m) increases, the cross sections decrease drastically due to the increased binding energy, as shown in Fig. 2.6.1 where the observed cross sections of the production of multiply ionized Xe^{m+} (m = 1…13) ions from neutral Xe atoms under the single collisions of electron impact are given as a function of the electron impact energy.

Usually the metastable state beams have very large cross sections as well as the lower ionization threshold energy. In Fig. 2.6.2 is shown a comparison of the ionization cross sections for the ground $He(1s^2)$ and metastable $He(1s2s\ ^3S)$ atoms under electron impact which are prepared via electron capture into He^+ ions passing through gas targets. It is worth to note that the agreement among different experiments seems to be reasonably good for the metastable state helium atoms. Clearly the observed curve for the metastable state helium atoms shows the lower threshold energy and their cross sections are much larger than those for the ground state. Also the double-electron ionization cross sections into He^{2+} ions from the ground state He atoms are also compared in this figure.

2.6.2 Experimental techniques for neutral atom targets

2.6.2.1 Orthodox method

Here is some short description of experimental techniques relevant to the ionization of neutral atoms under electron impact. Measurements of the ionization cross sections of neutral gas atoms by electron impact are relatively simple. There are some good reviews on the ionization phenomena by electron impact and the most important aspects of these processes have been summarized [85Mär1]. So-called condenser-plate techniques can provide reliable apparent total ionization cross section, namely $\sum_m m\sigma_i^{m+}$, with the accuracies of 2…3 % [86Be1]. The partial ionization cross section for each m-electron ionization state, σ_i^{m+}, should be determined through separately measuring the relative fractions of ions in different charge states, for example by the time-of-flight techniques [87Sha1] or magnetic analyzers, and then by normalizing them to the apparent total ionization cross sections.

2.6.2.2 Magneto-optically trapped targets

This is a new technique to determine the ionization cross sections without knowing the absolute target densities. In the magneto-optical trap (MOT), the quadrupole magnetic field is shaped to be zero at the center of the trap where the laser force traps atoms at the room temperature, cool down to 100 μK and confine them to the size of a half mm with the density of about 10^6 atoms/cm^3. Then, the trapping magnetic and laser fields are switched off and the target atoms are stabilized to the ground state and the electron beam is sent into a ball of the the target atoms which are ionized. Now the trapping fields are restored where the ionized ions can leave the trapping, meanwhile the non-ionized atoms are once again retrapped and recooled down. The absolute ionization cross sections can be determined through the loss rate measurements of the trapped atoms and the accurate knowledge of the electron beam density distributions over the target. The most important merit of this method is the fact that no absolute target density is required to know. The observed cross sections represent the total ionization cross section, namely $\sum_m \sigma_i^{m+}$ (Note that "total cross section" is different from "apparent cross section" obtained through the parallel plate technique mentioned above). The accuracies are estimated to be roughly 10 %, depending slightly upon the collision energy, which comes mostly from the escape loss of the recoiling atoms from the shallow trap [96Sch1].

2.6.2.3 Excited species targets

In many applications, the excited neutral species, in particular those in the metastable states, are known to play an important and critical role [92Tra1, 96Tan1]. Therefore, it is necessary to have the reliable ionization data for such species. It is natural to expect that the cross sections for such excited species are quite large, compared with those in the ground state species. Therefore, even a very small fraction of such excited species in the target significantly influence the observed results. Unfortunately, it is not easy to get such species (specified in its electronic states) prepared with sufficient intensities under the controlled conditions. As shown in Fig. 2.6.2 (Subsect. 2.6.1), the metastable He(1s2s ^{3}S) atoms have been investigated by different authors using the crossed-beams technique and the observed cross sections show relatively good agreement with each other. Here He(1s2s ^{3}S) atoms are produced through the electron capture into He^+ ions.

Only a limited number of the experiments have been performed for some species, such as alkali or alkaline metal targets, using the three (electron + ground state species + laser)-beams crossed

technique in combination with the laser excitation. Some detailed description of the important aspects of the preparation (gas-discharge, electron beam impact, electron capture, laser excitation), detection, target density determination and comparison of the relevant cross sections over the ground state has been given [92Tra1]. It should also be noted that their production efficiencies are generally quite small and, thus, the densities of the excited species target are small, compared with those for the background gas atoms.

Indeed the absolute density determination of the excited state species is one of the most difficult tasks in measurements of the collision cross sections. The laser-based technique for the excitation of the target atoms including the species with the short life-time should be the most reliable and possible to get relative high efficiencies but the present-day lasers are still limited in applications only to alkali or alkaline metal atoms [93Gie1, 93Ric1, 97Dep1]. Also it is not straightforward to define the electronic states and the fractions in the product beams which often include some different electronic configurations, except for some neutral beam with a single metastable state.

Furthermore, in combination of a series of the lasers with different wave-lengths in multi-step excitation processes, it is possible to get quite pure excited species even in very high Rydberg states such as n = 10 where the collision cross sections can be as large as 10^{-11} cm^2 [95DeP1]. The metastable beam targets such as He*(1s2s) can be obtained through the electron capture into the proper ions such as He^+ ions and have been used in the crossed-beams technique. One of typical cross sections for the metastable He(1s2s) beam is already shown in Fig. 2.6.2, compared with those for the ground state He($1s^2$) beam.

In Table 2.6.1 are shown the metastable state species of rare gas atoms and their features.

Table 2.6.1. Energies and lifetimes of the metastable states of rare gas atoms [92Tra1].

Atom	Term	Energy [eV]	Lifetime [s]
He	$2\,^3S_1$	19.82	$6\cdot10^5$
	$2\,^1S_0$	20.61	$2\cdot10^{-2}$
Ne	$3\,^3P_2$	16.62	≈ 1
	$3\,^3P_0$	16.72	≈ 1
Ar	$4\,^3P_2$	11.55	≈ 1
	$4\,^3P_0$	11.72	≈ 1
Kr	$5\,^3P_2$	9.92	≈ 1
	$5\,^3P_0$	10.56	≈ 1
Xe	$6\,^3P_2$	8.32	-
	$6\,^3P_0$	9.45	-

2.6.3 Contribution of various processes to ionization

Not only the *direct* ionization processes in neutral atoms where some electrons in the outermost-shell as well as in the inner-shell are directly removed from the target but also the *indirect* ionization processes following the innershell excitation processes play a role in the overall ionization processes and related fields. In some electronic configurations of the target ions as will be shown in Section 3.2, the contribution of the indirect ionization processes to total ionization becomes far more significant and often are more important than that of the direct processes.

2.6.3.1 Direct processes

In simple atomic targets, the contribution to the ionization dominantly comes from so-called *direct ionization* (*DI*) process where m electrons are ionized under electron impact as expressed as follows:

$$e + A \rightarrow e + A^{m+} + me. \quad (1)$$

Also it should be noted that not only a single electron (m = 1) but also two electrons (m = 2: double ionization) can be ionized simultaneously with relatively high probabilities. The single-electron ionization cross sections are generally larger than those of double- or multiple-electron ionization, as seen in Fig. 2.6.1.

As the electron impact energy increases, some of the innershell electrons can be ionized. As the energy required to ionize the inner-shell electron is larger than that for the outermost-shell electron, the cross sections usually show some shoulders at the threshold energy of the inner-shell electron ionization, in addition to the first threshold due to the ionization of the outermost-shell electron when the cross sections are plotted as a function of the electron impact energy. A typical example of the contribution of the (4d) innershell-electron ionization is compared with that of the (5s+5p) outer-shell-electron ionization in Fig. 2.6.3 where the single-electron ionization from six 5p-shell or two 5s-shell electrons results in Xe^+ ions from Xe atoms.

Also a further deep innershell-electron ionization results mostly in the production of multiple-electron ionization through cascading processes. Among multiple ionization, the double-electron ionization (m = 2) processes are usually dominant over higher ($m \geq 3$) ionization processes and can contribute significantly to the total ionization (more than 30 % in Xe atom ionization).

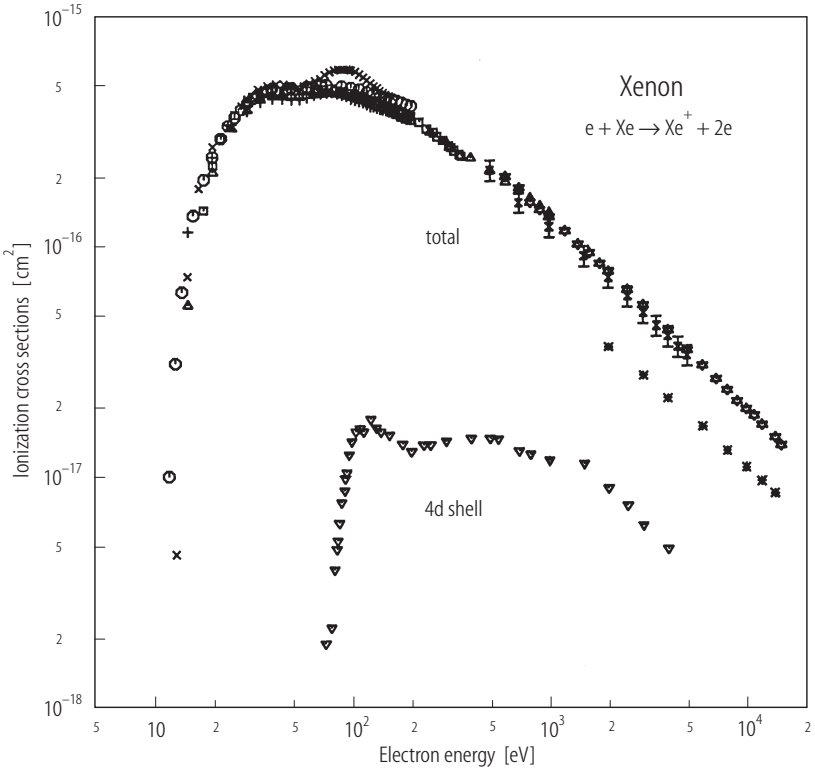

Fig. 2.6.3. A typical example of the contribution of the outer (5p+5s)- and inner (4d)-shell electron ionization of Xe atoms resulting in Xe^+ ions under electron impact. The upper curve represents the total single-electron ionization cross sections and the lower curve corresponds to the 4d-shell electron ionization.

2.6.3.2 Indirect processes

But in many-electron targets, the significant contribution often comes from so-called indirect processes which involve the innershell electrons. After one of the inner-shell electrons is excited under the incident electron impact, the doubly or triply excited states are formed which decay through the secondary (as well as ternary) processes such as the autoionization processes and finally are stabilized into the ground state of highly ionized ions.

There are a number of different types of the indirect processes. In ionization of neutral atoms, the most significant is the innershell-electron excitation followed by autoionization (EA) process where one of the inner-shell electrons in a target atom is first excited above the threshold of the ionization limit of singly-charged ions, forming the intermediate doubly excited states, a part of which are stabilized though the autoionization process:

$$e + A \rightarrow e + A^{**} \rightarrow e + A^{+} + e. \quad (2)$$

The rest is the simple excitation process and stabilized through radiative emission which does not contribute to the ionization. The double ionization processes can also be contributed by similar indirect processes mentioned above.

2.6.4 Recommended ionization cross sections for neutral atoms

2.6.4.1 General features of the ionization cross section behavior

The cross sections for single- as well as multiple-electron ionization have been measured for a large number of the neutral atoms, which can also be seen on databases, for example at NIFS. As mentioned in Introduction, there are some compilations and reviews of the ionization data for neutral atom targets under electron impact [83Bel1, 87Taw1, 88Len1, 89Hig1]. Table 2.6.2 shows a summary of the present situations on the electron impact ionization data of neutral atoms which are stored and available in our databases at NIFS.

These data have different degree of the accuracies. Therefore, we have to evaluate them to provide reliable cross sections of ionization for the basic research as well as applications.

Table 2.6.2. Summaries of the experimental electron impact ionization data of neutral atoms under electron impact seen in the databases at NIFS. The final charge of ions produced are shown on the abscissa (horizontal direction) for each element (the vertical direction) and the number in tables shows the number of the experimental investigations performed so far.

Atom	Final charge state												
	1+	2+	3+	4+	5+	6+	7+	8+	9+	10+	11+	12+	13+
H	8												
He	26	8											
Li	6	1											
Be	2												
B	1												
C	2												
N	3												
O	7	3											
F	1												

Atom	Final charge state												
	1+	2+	3+	4+	5+	6+	7+	8+	9+	10+	11+	12+	13+
Ne	20	14	14	5	2								
Na	3	1											
Mg	6	3	1	1									
Al	2												
Si	1	1											
P	1	1											
S	2	2											
Cl	1	1											
Ar	22	20	14	9	7	3	1						
K	3												
Ca	2	1											
Ti	1												
Cr	2												
Fe	3	1											
Ni	1												
Cu	2	2	1	1	1								
Zn	2												
Ga	4	4	3	1									
Ge	2	1	1										
As	1	1											
Se	2	1	1										
Br	1	1											
Kr	12	10	8	6	4	4	2	2	1				
Rb	1	6	1	1	1								
Sr	2	1											
Zr	1												
Mo	1												
Ru	1												
Pd	1												
Ag	3	2	1										
Cd	1												
In	3	1	1										
Sn	2	1	1										
Sb	1	1	1										
Te	2	1											
I	1												
Xe	10	9	9	5	5	3	1	1	1	1	1	1	1
Cs	1												
Ba	4	2	1	1									
Au	1												
Hg	2	1	1	1	1								
Tl	2	1											
Pb	3	3	2										
Bi	1	1	1										
U	1	1	1	1									

Evaluation of experimental data

In evaluating experimental data of absolute ionization cross sections in electron impact, the following issues are the most important and not only the data but also the experiments themselves should be closely scrutinized [97Taw1]:

(1) primary electron beam, (2) target species, (3) collision product and (4) detection system. There are a number of critical issues in each, as shown in Table 2.6.3. Unfortunately very few papers published have discussed the details on such issues and the access to the details is sometimes difficult. The most important but often neglected issue is the contribution of the excited or metastable state target species with relatively high internal energy. Though most of the target gases evaporated in high temperature ovens are in the ground state, the internal energy of the target atoms is critical in ionization processes, for example, in crossed-beams experiments where the neutral target atoms are formed through electron capture into charged particles. The ionization cross sections for such atoms are often much larger than those for the ground state species. Therefore, the excited states (nl) of the colliding neutralized beams have to be specified and and their fractions have to also be known accurately. Otherwise, the observed cross sections would be largely scattered.

Sometimes the observed cross sections have been, for simplicity, normalized to some known (previously observed, calculated or scaled) values. For example, the experimental cross sections for atomic hydrogens, due to difficulties in preparing the targets and in determining the absolute densities, are often normalized to those at high energies where the Born or other approximations can be assumed to be valid. In such a case, it should be noted that, if the collision energy is not sufficiently high, the Born approximations fail to give the exact values.

Table 2.6.3. Critical issues in evaluating experimental ionization cross sections in electron impact.

	Critical issues	Comments
Primary electron beam	kinetic energy spread	important in resonance observation
	beam focusing and divergence	transmission through apertures
	edge scattering	straying electrons produced
	external field	deflection of low energy beam
Target beam	contamination and residual gases	water vapor often included in gas line
	purity	high purity target gases available
	effective target density	due to diffusion through apertures
	beam overlapping with electrons	important at low energies
	internal energy or excited state	very critical in neutralized target atoms
Products	product specification	mass/charge
	collection and transmission efficiencies	discrimination in collecting system
	single collisions	correction to double collisions
	recoil/dissociation energy	loss of collection
	internal energy	
	life-time	loss of detection
	external field	charge discrimination
Detection	absolute detection efficiencies	or normalized to others
	pulse-height distributions	noise-discrimination
	secondary particle emission	spurious counting
	uniform sensitivities	detector with large area
	sensitivities to strayed particles	strayed photons or electrons
	reflection from surfaces	loss of particles

Evaluation of theoretical data

Some theoretical calculations are requisite when no experimental data are available. There are some critically important issues in evaluating the calculated cross sections. Indeed it is sometimes quite difficult to know if they are properly treated in references (see Table 2.6.4).

Table 2.6.4. Important issues in evaluating the calculated cross sections under electron impact.

Critical issues	Comments
approximation	Born, distorted-wave, close-coupling, R-matrix etc.
wave-function	distorted wave-function? electron correlation included?
interaction potential	simple electrostatic potential, exchange or distorted potential ?
number of states	not always accurate even for a large number of states considered
continuum states	quasi-continuum
validity (energy) region	limited energy region

Following some criterions as shown in Tables 2.6.3 and 2.6.4, the experimental *single-electron* ionization cross sections for a series of the ground state neutral species ranging from hydrogen to uranium atoms have been evaluated and listed in Table 2.6.5 (for neutral atoms ranging from H to Ne), Table 2.6.6 (Na-Ca), Table 2.6.7 (Sc-Zn), Table 2.6.8 (Ga-Zr), Table 2.6.9 (Mo-Xe) and Table 2.6.10 (Cs-U) as a function of the electron impact energy. It should be noted that, as the smooth variation of the cross sections as a function of the electron impact energy is assumed, some structures are not clearly seen in the present tables.

The smoothed data are also shown in Fig. 2.6.4 (H-B), Fig. 2.6.5 (C-Ne), Fig. 2.6.6 (Na-P), Fig. 2.6.7 (S-Ca), Fig. 2.6.8 (Sc-Mn), Fig. 2.6.9 (Fe-Zn), Fig. 2.6.10 (Ga-Br), Fig. 2.6.11 (Kr-Zr), Fig. 2.6.12 (Mo-In), Fig. 2.6.13 (Sn-Xe) and Fig. 2.6.14 (Cs-U). Note that the smoothed data plotted in these figures may be slightly different from those in tables.

2.6.4.2 Innershell electron ionization

The ionization of an innershell electron results in the formation of an innershell hole which follows a series of cascade processes before stabilization and finally a multiply charged ion is formed in most cases. The ionization cross sections for relativistic inner-shell electrons of neutral atom targets by relativistic electron impact have been surveyed recently [85Pow1, 90Lon1].

Table 2.6.5. Recommended cross sections for single-electron ionization of neutral atoms (H-Ne) under electron impact as a function of the electron impact energy (cf. Figs. 2.6.4 and 2.6.5).

Energy [eV]	Cross section [cm^2]									
	H	He	Li	Be	B	C	N	O	F	Ne
6			1.00E-16							
8			2.80E-16							
10			3.85E-16	2.50E-17	3.00E-17					
15	9.00E-18		4.25E-16	1.43E-16	1.25E-16		1.10E-17	1.00E-17		
20	3.10E-17		4.05E-16	2.15E-16	1.91E-16	1.10E-16	4.10E-17	3.20E-17	7.50E-18	
25	4.50E-17		3.70E-16	2.43E-16	2.20E-16	1.50E-16	7.20E-17	6.00E-17	2.10E-17	
30	5.30E-17	6.50E-18	3.40E-16	2.59E-16	2.43E-16	1.80E-16	9.00E-17	7.40E-17	3.30E-17	1.00E-17
40	6.10E-17	1.75E-17	2.90E-16	2.60E-16	2.52E-16	2.10E-16	1.21E-16	1.05E-16	5.10E-17	2.30E-17
50	6.40E-17	2.30E-17	2.50E-16	2.50E-16	2.49E-16	2.25E-16	1.39E-16	1.20E-16	6.80E-17	3.00E-17
60	6.30E-17	2.90E-17	2.20E-16	2.38E-16	2.41E-16	2.30E-16	1.48E-16	1.30E-16	8.00E-17	4.30E-17
80	5.90E-17	3.50E-17	1.70E-16	2.13E-16	2.22E-16	2.30E-16	1.57E-16	1.40E-16	9.20E-17	5.80E-17
100	5.40E-17	3.65E-17	1.45E-16	1.91E-16	2.03E-16	2.15E-16	1.56E-16	1.45E-16	9.60E-17	6.80E-17
150	4.50E-17	3.65E-17	1.00E-16	1.49E-16	1.63E-16	1.85E-16	1.41E-16	1.40E-16	9.80E-17	7.50E-17
200	3.80E-17	3.45E-17	8.00E-17	1.29E-16	1.46E-16	1.60E-16	1.28E-16	1.25E-16	9.00E-17	7.40E-17
300	2.80E-17	2.80E-17	5.60E-17	9.80E-17	1.13E-16	1.30E-16	1.05E-16	9.95E-17	7.75E-17	6.50E-17
400	2.30E-17	2.35E-17	4.40E-17	8.20E-17	9.40E-17	1.10E-16	9.10E-17	8.50E-17	6.75E-17	5.70E-17
600	1.70E-17	1.75E-17	3.00E-17	6.00E-17	7.20E-17	8.50E-17	7.20E-17	6.70E-17	5.50E-17	4.50E-17
800	1.35E-17	1.45E-17	2.35E-17	4.90E-17	5.80E-17	7.20E-17	5.90E-17	5.40E-17	4.55E-17	3.80E-17
1000	1.10E-17	1.20E-17	1.90E-17	4.10E-17	4.90E-17	6.20E-17	5.00E-17	4.65E-17	3.91E-17	3.20E-17
2000	6.30E-18	7.00E-18	1.00E-17	2.40E-17	2.90E-17	3.90E-17	3.10E-17	2.80E-17	2.40E-17	1.95E-17
4000	3.50E-18	3.90E-18	5.30E-18	1.40E-17	1.70E-17	2.20E-17	1.80E-17	1.60E-17	1.43E-17	1.15E-17
6000	2.40E-18	2.75E-18	3.80E-18	1.00E-17	1.25E-17	1.55E-17	1.30E-17	1.20E-17	1.05E-17	7.80E-18
10000	1.60E-18	1.80E-18	2.45E-18	7.00E-18	8.50E-18	1.00E-17	8.50E-18	7.60E-18	7.00E-18	5.10E-18

Table 2.6.6. Recommended cross sections for single-electron ionization of neutral atoms (Na-Ca) under electron impact as a function of the electron impact energy (cf. Figs. 2.6.6 and 2.6.7).

Energy [eV]	Cross section [cm^2]									
	Na	Mg	Al	Si	P	S	Cl	Ar	K	Ca
6	1.35E-16								5.20E-16	
8	3.30E-16	8.00E-17	2.50E-16						7.90E-16	2.50E-16
10	4.35E-16	2.80E-16	5.60E-16	9.00E-17					9.00E-16	7.40E-16
15	4.75E-16	4.90E-16	9.15E-16	5.10E-16	3.00E-16	1.9E-16	5.00E-17		9.00E-16	9.50E-16
20	4.60E-16	5.25E-16	9.60E-16	6.40E-16	4.20E-16	3.3E-16	1.80E-16	6.00E-17	8.40E-16	8.90E-16
25	4.35E-16	5.10E-16	9.70E-16	6.90E-16	4.85E-16	4.0E-16	2.55E-16	1.30E-16	7.80E-16	8.20E-16
30	4.15E-16	4.80E-16	9.60E-16	7.00E-16	5.20E-16	4.2E-16	3.00E-16	1.80E-16	7.30E-16	7.30E-16
40	3.55E-16	4.30E-16	9.30E-16	6.90E-16	5.25E-16	4.4E-16	3.40E-16	2.30E-16	6.20E-16	6.10E-16
50	3.20E-16	3.85E-16	8.90E-16	6.70E-16	5.20E-16	4.4E-16	3.55E-16	2.40E-16	5.70E-16	5.20E-16
60	2.90E-16	3.40E-16	8.30E-16	6.40E-16	5.10E-16	4.5E-16	3.60E-16	2.45E-16	5.40E-16	4.60E-16
80	2.45E-16	2.85E-16	7.30E-16	5.80E-16	4.75E-16	4.3E-16	3.50E-16	2.45E-16	5.00E-16	3.80E-16
100	2.10E-16	2.40E-16	6.50E-16	5.20E-16	4.40E-16	4.2E-16	3.30E-16	2.45E-16	4.90E-16	3.20E-16
150	1.65E-16	1.80E-16	5.00E-16	4.30E-16	3.80E-16	3.7E-16	2.90E-16	2.30E-16	4.20E-16	2.30E-16
200	1.40E-16	1.30E-16	4.10E-16	3.90E-16	3.20E-16	3.3E-16	2.60E-16	2.20E-16	3.90E-16	1.80E-16
300	1.10E-16	8.50E-17	3.30E-16			2.6E-16		1.75E-16	3.10E-16	1.30E-16
400	9.00E-17	6.00E-17	2.70E-16			2.2E-16		1.40E-16	2.50E-16	1.05E-16
600	7.30E-17		2.20E-16			1.7E-16		1.05E-16	1.90E-16	7.20E-17
800	6.00E-17		1.80E-16			1.4E-16		8.60E-17	1.50E-16	5.50E-17
1000	5.20E-17		1.50E-16			1.3E-16		7.20E-17	1.30E-16	4.50E-17
2000			9.00E-17			7.6E-17		4.25E-17	7.30E-17	2.30E-17
4000						4.5E-17		2.40E-17	4.20E-17	1.30E-17
6000						3.2E-17		1.80E-17	3.00E-17	8.30E-18
10000						2.3E-17		1.15E-17	2.10E-17	5.10E-18

Table 2.6.7. Recommended cross sections for single-electron ionization of neutral atoms (Sc-Zn) under electron impact as a function of the electron impact energy (cf. Figs. 2.6.8 and 2.6.9).

Energy [eV]	Cross section [cm^2]									
	Sc	Ti	V	Cr	Mn	Fe	Co	Ni	Cu	Zn
6										
8	6.60E-16		5.20E-16		1.40E-16				9.30E-17	
10	1.35E-15	5.70E-16	1.05E-15	2.30E-16	2.70E-16	1.30E-16	2.25E-16	1.20E-16	2.10E-16	5.00E-17
15	2.10E-15	8.05E-16	1.55E-15	5.00E-16	4.60E-16	4.00E-16	4.70E-16	3.40E-16	2.83E-16	2.00E-16
20	2.25E-15	8.20E-16	1.63E-15	6.40E-16	5.00E-16	5.00E-16	5.10E-16	4.20E-16	3.10E-16	3.40E-16
25	2.20E-15	7.90E-16	1.60E-15	7.70E-16	5.05E-16	5.20E-16	5.34E-16	4.35E-16	3.13E-16	4.10E-16
30	2.10E-15	7.45E-16	1.55E-15	8.20E-16	5.06E-16	5.25E-16	5.55E-16	4.30E-16	3.08E-16	4.20E-16
40	1.90E-15	6.40E-16	1.40E-15	7.50E-16	5.00E-16	5.15E-16	5.75E-16	4.05E-16	2.93E-16	4.10E-16
50	1.70E-15	5.70E-16	1.28E-15	6.50E-16	4.90E-16	4.90E-16	5.70E-16	3.70E-16	2.85E-16	3.90E-16
60	1.55E-15	5.10E-16	1.15E-15	5.80E-16	4.80E-16	4.60E-16	5.65E-16	3.40E-16	2.67E-16	3.70E-16
80	1.30E-15	4.25E-16	1.00E-15	4.70E-16	4.50E-16	4.15E-16	5.30E-16	2.95E-16	2.51E-16	3.25E-16
100	1.15E-15	3.50E-16	8.75E-16	4.00E-16	4.15E-16	3.70E-16	5.00E-16	2.60E-16	2.30E-16	2.80E-16
150	8.90E-16	2.70E-16	6.75E-16	3.05E-16	3.50E-16	3.10E-16	4.15E-16	2.00E-16	2.00E-16	2.30E-16
200	7.32E-16	2.20E-16	5.50E-16	2.35E-16	3.05E-16	2.70E-16	3.60E-16	1.60E-16	1.75E-16	1.95E-16
300	5.50E-16	1.70E-16	4.20E-16	1.80E-16	2.40E-16	2.10E-16	2.85E-16	1.25E-16	1.50E-16	1.45E-16
400	4.40E-16	1.35E-16	3.40E-16	1.40E-16	2.00E-16	1.70E-16	2.40E-16	1.00E-16	1.30E-16	1.20E-16
600	3.25E-16	9.80E-17	2.50E-16	1.05E-16	1.55E-16	1.27E-16	1.80E-16	7.30E-17	1.05E-16	9.00E-17
800	2.60E-16	7.60E-17	2.00E-16	8.30E-17	1.25E-16	1.05E-16	1.49E-16	5.80E-17	8.50E-17	7.30E-17
1000	2.18E-16	6.30E-17	1.65E-16	7.00E-17	1.07E-16	8.70E-17	1.25E-16	4.80E-17	7.30E-17	6.10E-17
2000	1.20E-16	3.40E-17	9.50E-17	3.90E-17	6.35E-17		7.50E-17	2.75E-17	4.40E-17	3.50E-17
4000	7.00E-17	1.90E-17	5.30E-17	2.20E-17	3.70E-17		4.35E-17	1.55E-17		2.00E-17
6000	5.00E-17	1.30E-17	3.80E-17	1.50E-17	2.60E-17		3.10E-17	1.10E-17		1.40E-17
10000	3.20E-17	8.30E-18	2.40E-17	1.00E-17	1.70E-17		2.05E-17	7.40E-18		9.00E-18

Table 2.6.8. Recommended cross sections for single-electron ionization of neutral atoms (Ga-Zr) under electron impact as a function of the electron impact energy (cf. Figs. 2.6.10 and 2.6.11).

Energy [eV]	Cross section [cm^2]								
	Ga	Ge	As	Se	Br	Kr	Rb	Sr	Zr
6							5.20E-16		
8	2.30E-16						8.00E-16	7.40E-16	3.90E-16
10	4.80E-16	1.00E-16					8.10E-16	9.80E-16	6.00E-16
15	8.60E-16	5.50E-16	2.80E-16	2.10E-16	1.05E-16	2.10E-17	7.60E-16	1.09E-15	8.10E-16
20	9.85E-16	6.30E-16	4.50E-16	3.80E-16	2.10E-16	1.20E-16	8.80E-16	1.05E-15	8.82E-16
25	1.05E-15	7.15E-16	5.50E-16	5.00E-16	3.10E-16	2.10E-16	9.30E-16	9.65E-16	8.92E-16
30	1.06E-15	7.30E-16	5.85E-16	5.40E-16	3.70E-16	2.60E-16	9.00E-16	8.85E-16	8.80E-16
40	1.03E-15	7.30E-16	6.20E-16	5.90E-16	4.30E-16	3.20E-16	8.30E-16	7.65E-16	8.18E-16
50	9.80E-16	7.20E-16	6.15E-16	5.90E-16	4.40E-16	3.40E-16	7.10E-16	6.65E-16	7.55E-16
60	9.15E-16	7.00E-16	5.95E-16	5.80E-16	4.40E-16	3.50E-16	6.30E-16	5.94E-16	6.95E-16
80	7.90E-16	6.35E-16	5.60E-16	5.55E-16	4.30E-16	3.50E-16	5.20E-16	4.94E-16	6.03E-16
100	6.90E-16	5.80E-16	5.25E-16	5.30E-16	4.05E-16	3.40E-16	4.60E-16	4.18E-16	5.23E-16
150	5.40E-16	4.60E-16	4.45E-16	4.60E-16	3.55E-16	3.20E-16	3.60E-16	3.00E-16	3.92E-16
200	4.50E-16	3.80E-16	3.98E-16	4.10E-16	3.10E-16	2.85E-16	3.10E-16	2.53E-16	3.34E-16
300	3.30E-16	2.75E-16		3.40E-16		2.35E-16	2.45E-16	1.87E-16	2.50E-16
400	2.80E-16	2.15E-16		3.00E-16		2.00E-16	2.10E-16	1.47E-16	2.01E-16
600	2.15E-16	1.60E-16		2.45E-16		1.45E-16	1.60E-16	1.08E-16	1.48E-16
800	1.80E-16	1.30E-16		2.05E-16		1.20E-16	1.40E-16	8.50E-17	1.15E-16
1000	1.50E-16	1.05E-16		1.75E-16		1.00E-16	1.25E-16	7.00E-17	9.60E-17
2000	9.00E-17	5.95E-17		1.07E-16		5.90E-17		4.00E-17	5.50E-17
4000		3.20E-17		5.90E-17		3.15E-17		2.20E-17	3.10E-17
6000		2.30E-17		4.20E-17		2.20E-17		1.60E-17	2.20E-17
10000		1.60E-17		2.90E-17		1.40E-17		1.00E-17	1.40E-17

Table 2.6.9. Recommended cross sections for single-electron ionization of neutral atoms (Mo-Xe) under electron impact as a function of the electron impact energy (cf. Figs. 2.6.12 and 2.6.13).

Energy [eV]	Cross section [cm^2]									
	Mo	Ru	Ag	Cd	In	Sn	Sb	Te	I	Xe
6					3.90E-17	8.00E-18	2.00E-18			
8	1.40E-16	9.00E-17	3.20E-17		2.00E-16	1.15E-16	5.20E-17			
10	3.50E-16	2.20E-16	1.05E-16	1.25E-16	4.20E-16	3.30E-16	1.95E-16	1.20E-16	4.00E-18	
15	6.30E-16	4.08E-16	2.00E-16	3.60E-16	7.00E-16	7.49E-16	5.70E-16	7.78E-16	1.90E-16	1.00E-16
20	7.18E-16	4.63E-16	2.60E-16	4.54E-16	7.00E-16	9.04E-16	7.26E-16	1.05E-15	3.82E-16	2.45E-16
25	7.46E-16	4.92E-16	2.90E-16	4.82E-16	6.80E-16	9.55E-16	8.10E-16	1.18E-15	4.90E-16	3.60E-16
30	7.53E-16	4.95E-16	3.00E-16	5.02E-16	6.60E-16	9.80E-16	8.30E-16	1.24E-15	5.53E-16	4.20E-16
40	7.56E-16	5.20E-16	3.00E-16	4.93E-16	6.60E-16	9.52E-16	8.10E-16	1.25E-15	6.00E-16	4.45E-16
50	7.37E-16	5.35E-16	2.90E-16	4.70E-16	7.00E-16	9.24E-16	7.85E-16	1.20E-15	5.96E-16	4.40E-16
60	7.16E-16	5.37E-16	2.70E-16	4.58E-16	7.50E-16	8.80E-16	7.60E-16	1.12E-15	5.90E-16	4.45E-16
80	6.56E-16	5.17E-16	2.60E-16	4.50E-16	8.00E-16	8.05E-16	7.20E-16	9.97E-16	5.85E-16	4.60E-16
100	6.05E-16	4.87E-16	2.60E-16	4.43E-16	7.90E-16	7.40E-16	6.70E-16	8.83E-16	5.55E-16	4.45E-16
150	4.80E-16	4.18E-16	2.35E-16	4.05E-16	7.00E-16	6.20E-16	5.70E-16	6.73E-16	4.70E-16	4.10E-16
200	4.18E-16	3.58E-16	2.10E-16	3.52E-16	6.30E-16	5.00E-16	4.50E-16	5.88E-16	4.10E-16	3.60E-16
300	3.27E-16	2.84E-16	1.65E-16	2.83E-16	5.20E-16			4.23E-16		2.90E-16
400	2.72E-16	2.34E-16	1.45E-16	2.38E-16	4.30E-16			3.42E-16		2.40E-16
600	2.05E-16	1.73E-16	1.05E-16	1.77E-16	3.40E-16			2.40E-16		1.80E-16
800	1.67E-16	1.33E-16	8.30E-17	1.44E-16	3.00E-16			1.98E-16		1.50E-16
1000	1.39E-16	1.16E-16	6.10E-17	1.20E-16	2.50E-16			1.60E-16		1.25E-16
2000	8.20E-17	6.70E-17		6.85E-17				9.30E-17		7.70E-17
4000	4.75E-17	3.80E-17		3.80E-17				5.20E-17		4.30E-17
6000	3.30E-17	2.60E-17		2.65E-17				3.80E-17		3.05E-17
10000	2.20E-17	1.75E-17		1.80E-17				2.40E-17		1.95E-17

Table 2.6.10. Recommended cross sections for single-electron ionization of neutral atoms (Cs-U) under electron impact as a function of the electron impact energy (cf. Figs. 2.6.14 and 2.6.15).

Energy [eV]	Cross section [cm^2]							
	Cs	Ba	Au	Hg	Tl	Pb	Bi	U
6	3.60E-16	4.00E-16					2.50E-17	
8	6.30E-16	1.25E-15			1.60E-16	1.05E-16	1.60E-16	1.40E-16
10	7.80E-16	1.45E-15			2.60E-16	2.10E-16	3.36E-16	1.90E-16
15	9.20E-16	1.25E-15		1.75E-16	4.10E-16	4.10E-16	6.25E-16	3.40E-16
20	8.30E-16	1.45E-15		3.30E-16	4.50E-16	5.20E-16	7.61E-16	4.35E-16
25	9.20E-16	1.40E-15		4.40E-16	4.80E-16	6.00E-16	8.40E-16	4.80E-16
30	9.35E-16	1.25E-15		5.00E-16	5.30E-16	6.20E-16	8.73E-16	5.00E-16
40	9.30E-16	1.00E-15		5.60E-16	6.10E-16	6.00E-16	8.75E-16	4.70E-16
50	9.00E-16	8.40E-16	1.15E-15	5.80E-16	6.60E-16	5.80E-16	8.61E-16	4.30E-16
60	8.40E-16	7.30E-16	1.40E-15	5.70E-16	6.90E-16	5.60E-16	8.20E-16	3.90E-16
80	7.80E-16	5.90E-16	1.45E-15	5.40E-16	7.25E-16	5.00E-16	7.75E-16	3.45E-16
100	7.10E-16	4.80E-16	1.40E-15	5.00E-16	7.20E-16	4.35E-16	7.40E-16	3.15E-16
150	5.80E-16	3.30E-16	1.25E-15	4.20E-16	6.60E-16	3.50E-16	6.20E-16	2.60E-16
200	5.20E-16	2.55E-16	1.15E-15	3.50E-16	5.85E-16	3.05E-16	5.10E-16	2.30E-16
300	4.20E-16	1.80E-16	9.60E-16	2.70E-16	4.60E-16	2.45E-16		1.90E-16
400	3.50E-16	1.35E-16	8.50E-16	2.30E-16	3.80E-16	2.10E-16		1.70E-16
600	2.80E-16	1.00E-16	7.30E-16	1.75E-16	2.90E-16	1.75E-16		1.45E-16
800	2.35E-16	7.50E-17	6.30E-16	1.45E-16	2.30E-16	1.50E-16		1.25E-16
1000	2.10E-16	6.20E-17	5.60E-16	1.30E-16	1.95E-16	1.35E-16		1.15E-16

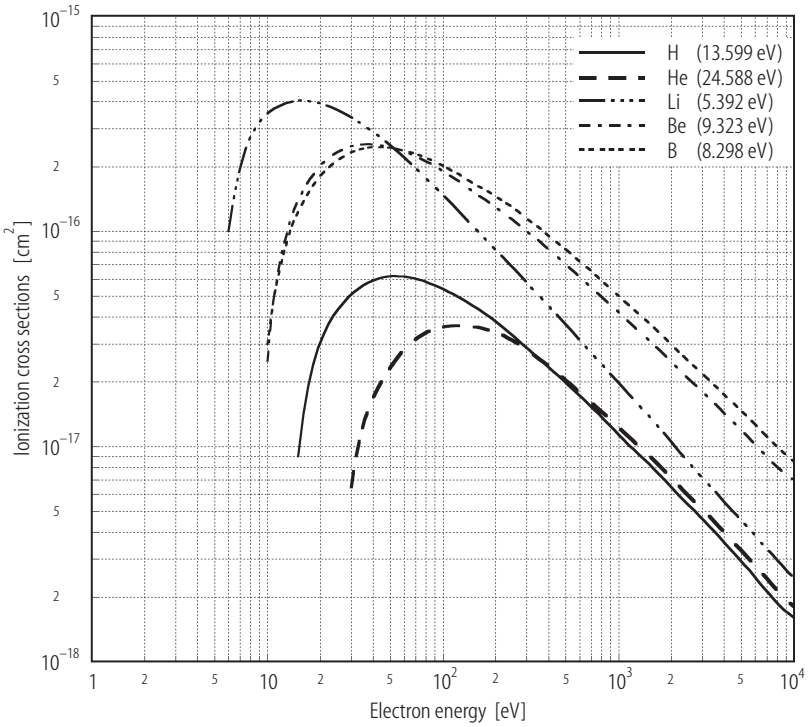

Fig. 2.6.4. Single-electron ionization cross sections for hydrogen to boron atom plotted as a function of electron impact energy (cf. Table 2.6.5).

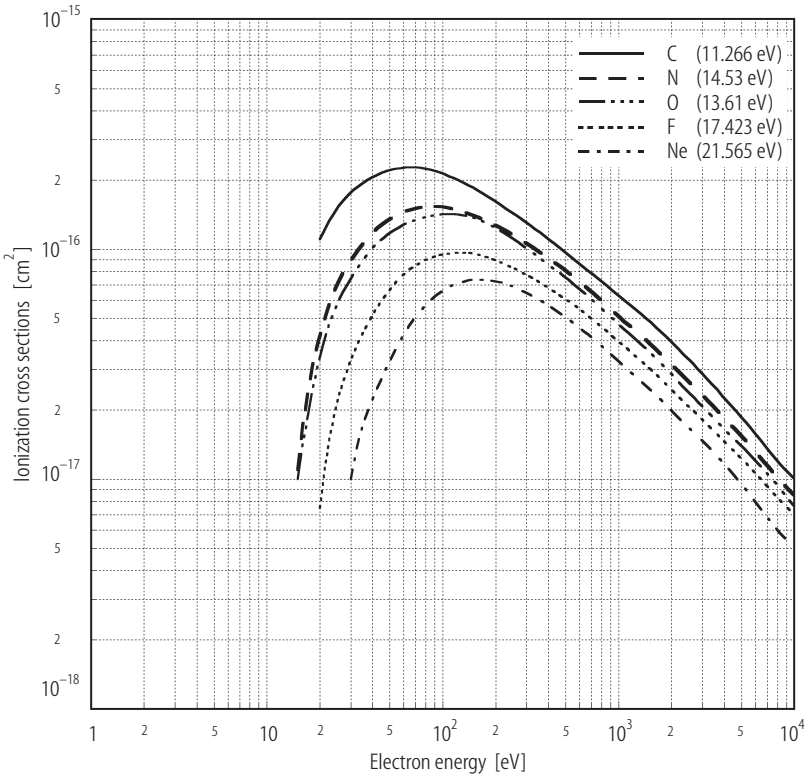

Fig. 2.6.5. Single-electron ionization cross sections for carbon to neon atom plotted as a function of electron impact energy (cf. Table 2.6.5).

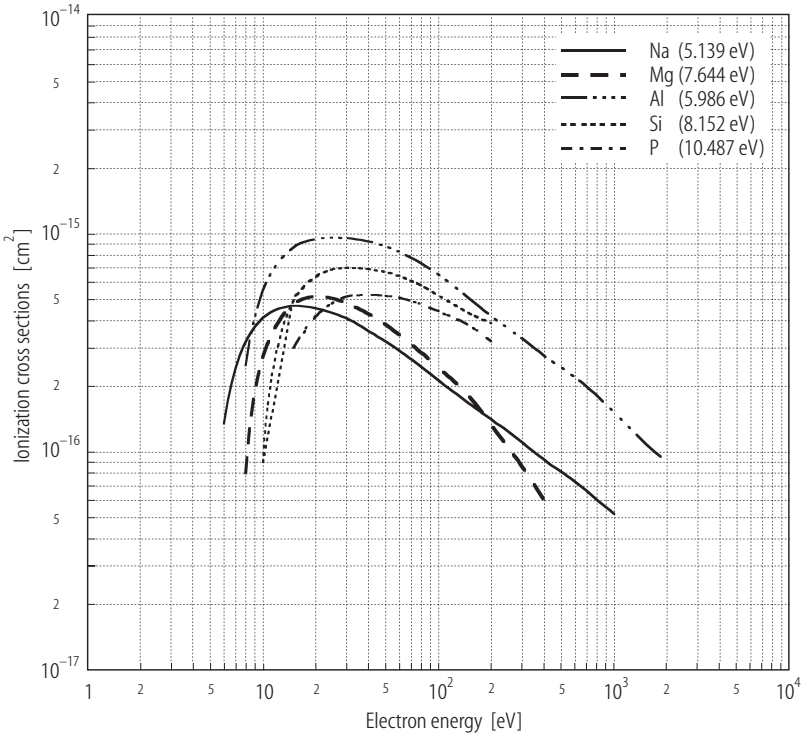

Fig. 2.6.6. Single-electron ionization cross sections for sodium to phosphor atom plotted as a function of electron impact energy (cf. Table 2.6.6).

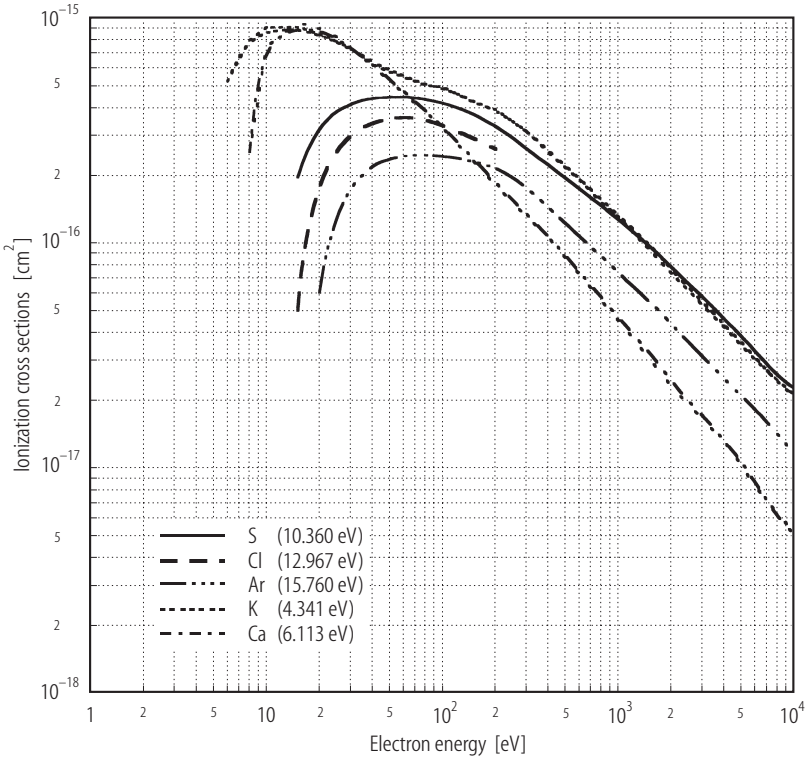

Fig. 2.6.7. Single-electron ionization cross sections for sulfur to calcium atom plotted as a function of electron impact energy (cf. Table 2.6.6).

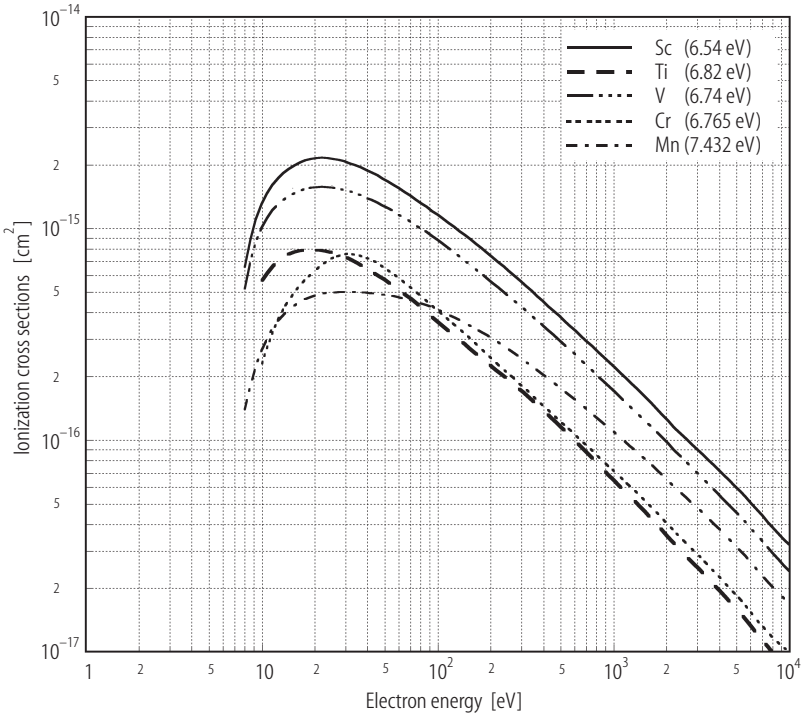

Fig. 2.6.8. Single-electron ionization cross sections for scandium to manganese atom plotted as a function of electron impact energy (cf. Table 2.6.7).

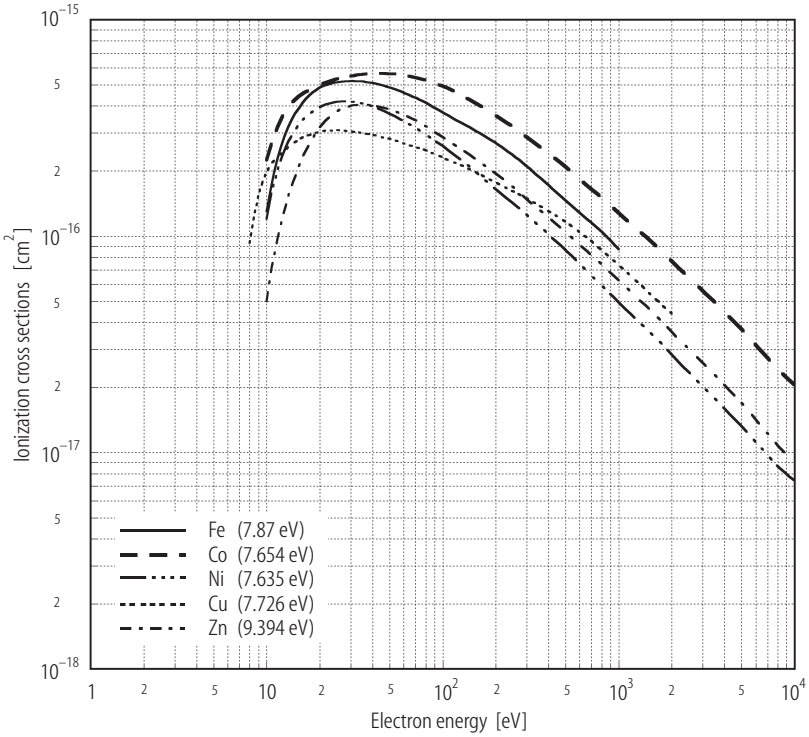

Fig. 2.6.9. Single-electron ionization cross sections for iron to zinc atom plotted as a function of electron impact energy (cf. Table 2.6.7).

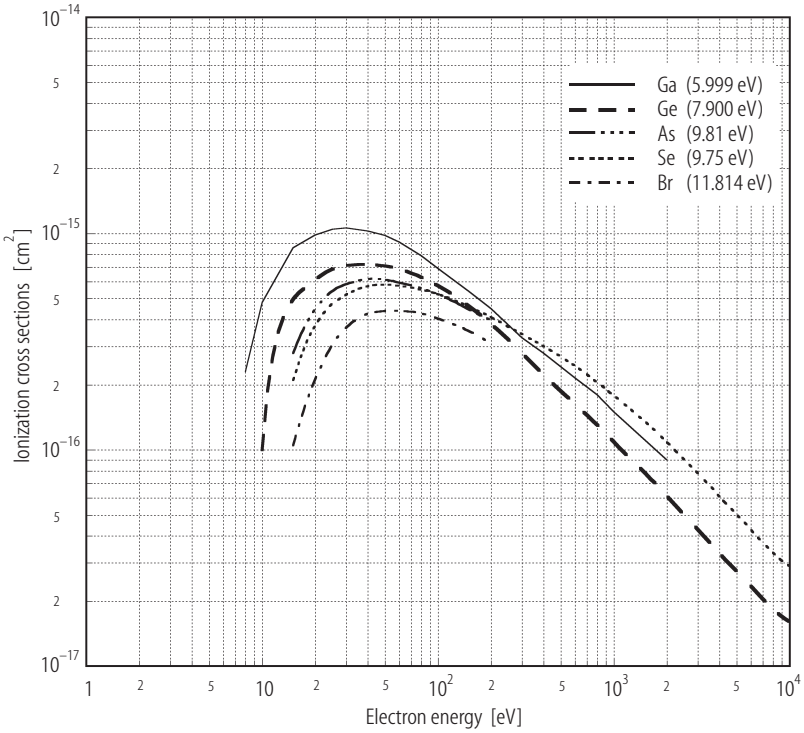

Fig. 2.6.10. Single-electron ionization cross sections for gallium to bromine atom plotted as a function of electron impact energy (cf. Table 2.6.8).

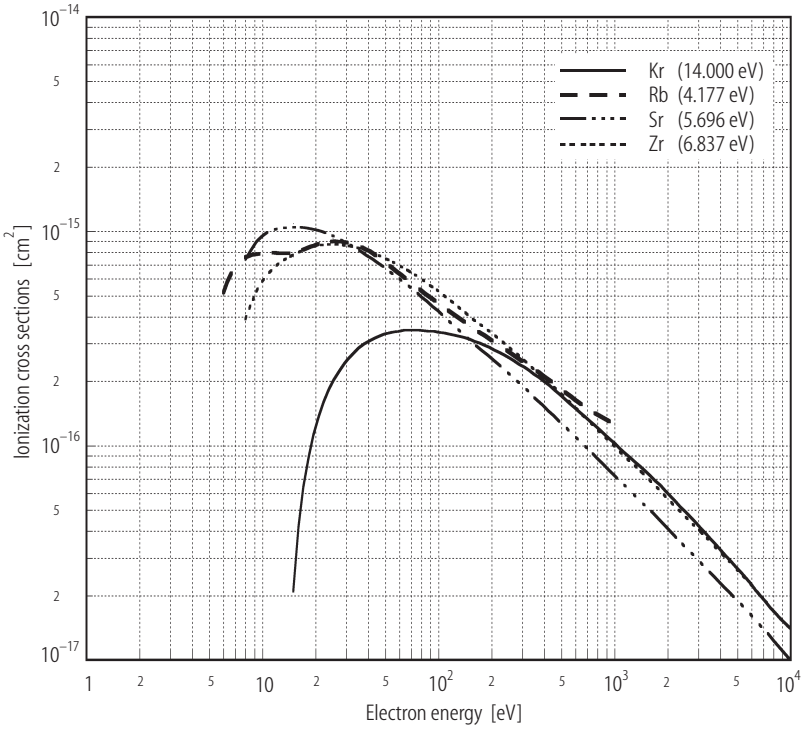

Fig. 2.6.11. Single-electron ionization cross sections for krypton to zirconium atom plotted as a function of electron impact energy (cf. Table 2.6.8).

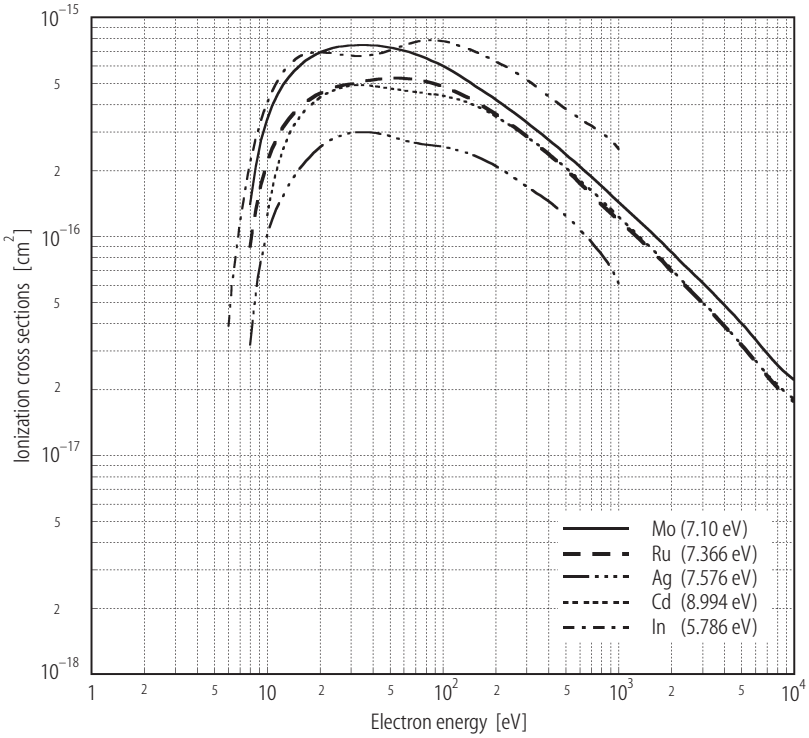

Fig. 2.6.12. Single-electron ionization cross sections for molybdenum to indium atom plotted as a function of electron impact energy (cf. Table 2.6.9).

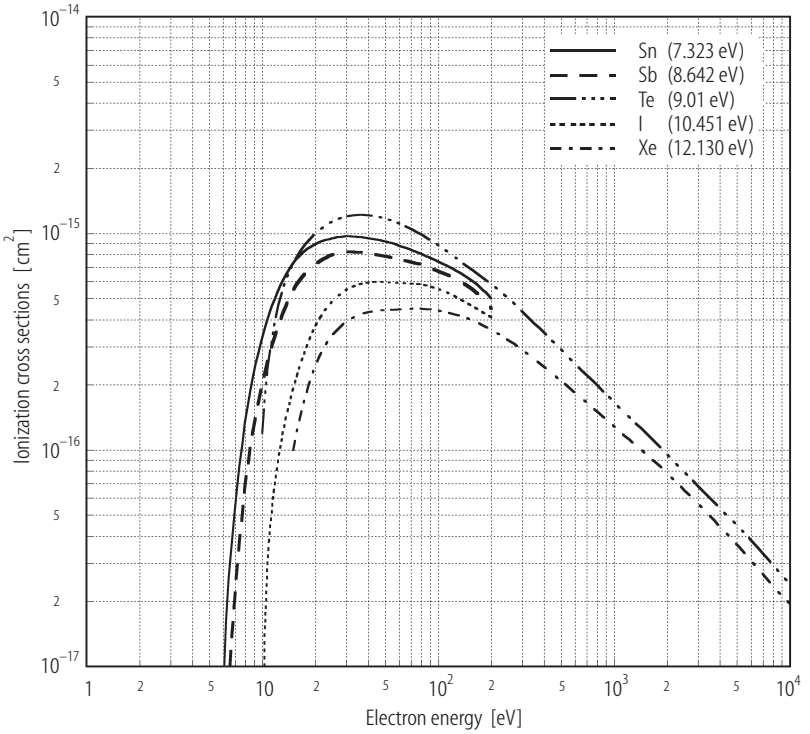

Fig. 2.6.13. Single-electron ionization cross sections for tin to xenon atom plotted as a function of electron impact energy (cf. Table 2.6.9).

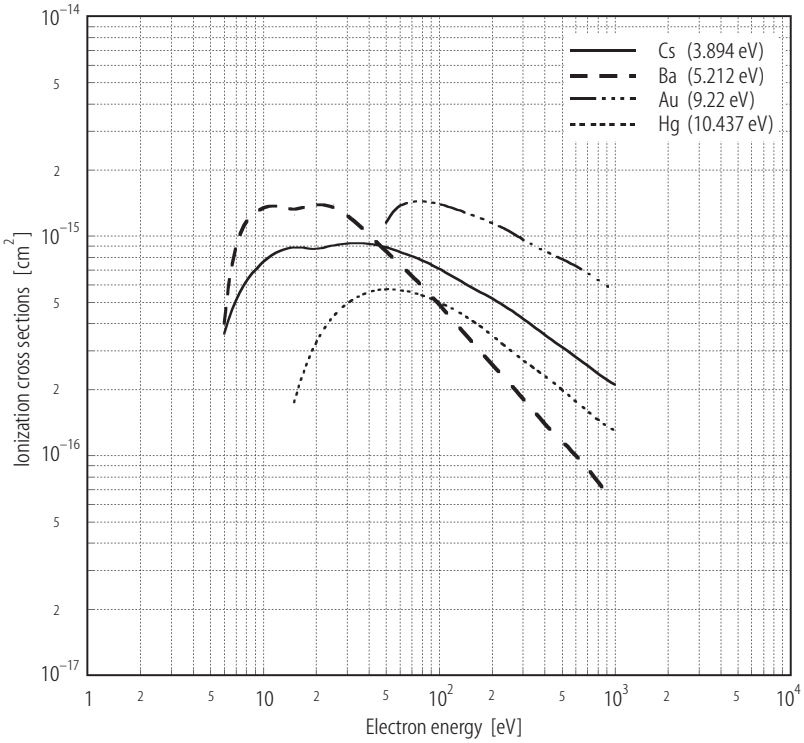

Fig. 2.6.14. Single-electron ionization cross sections for cesium to mercury atom plotted as a function of electron impact energy (cf. Table 2.6.10).

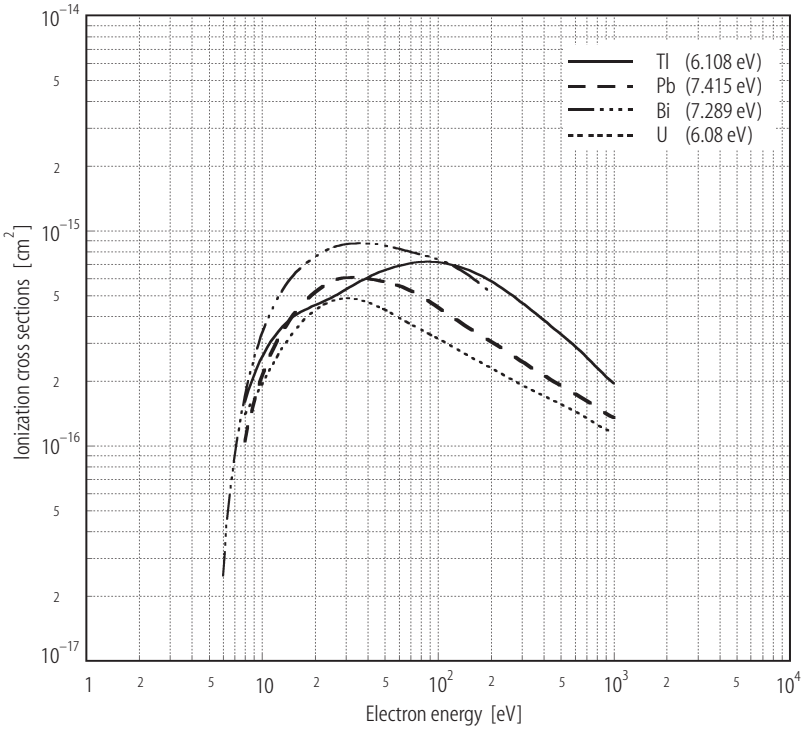

Fig. 2.6.15. Single-electron ionization cross sections for thallium to uranium atom plotted as a function of electron impact energy (cf. Table 2.6.10).

2.6.5 Short description of theories

The theories for the electron impact direct ionization have been developed for quite some time. A number of different approximation methods have been used [85Mär1].

One of the most significant progresses in theories of ionization under electron impact in recent years is the development of the convergent close-coupling (CCC) method which has been found to be very powerful and accurate not only in the ground state species but also in the excited species [92Bra1, 93Bra1]. Now realizing such progresses in theories, new and more accurate experiments are urgently required.

2.6.6 Empirical formula for ionization cross sections for outer-shell electrons

In a number of applications, it is important to have some empirical formulas to get the ionization cross sections under electron impact. So far, many basically identical but slightly different empirical formulas have been proposed [85Mär1]. There are also some critical reviews on the existing empirical formulas. Some of them are found to be convenient in many uses.

2.6.6.1 Empirical formulas for single ionization

One of the most familiar and convenient forms had been proposed by Lotz [67Lot1, 68Lot1] many years ago and is still widely in use in a number of cases. The total ionization cross sections are given as the sum of the contribution from different (sub-) shells as follows:

$$\sigma_{\mathrm{i}} = \sum_j a_j N_j \frac{\ln(u)}{u I_j^2}\left[1 - b_j \mathrm{e}^{-c_j(u-1)}\right] \tag{3}$$

where I_j is the ionization threshold energy of the j-th shell electron, the reduced electron energy $u = E/I_j$, E being the electron incident energy, N_j the number of the electrons in the j-th shell and a_j, b_j and c_j constants given for different shells [67Lot1, 68Lot1]. The total cross sections have to be summed up over all the possible j-th shells. This empirical formula is known to work surprisingly nicely even for neutral target atoms where the direct ionization processes are dominant over the indirect ionization processes (see Section 3.2 for ionization of ions).

Extensive survey of the electron ionization cross section data shows another simple analytical expression as follows:

$$\sigma_{\mathrm{i}} = \frac{1}{u I_j^2}\left[a \ln(u) + \sum_n b_n \left(1 - \frac{1}{u}\right)^n\right] \tag{4}$$

where the parameters are the same as in eq. (3) and a and b_n constants. These constants are given in [83Bel1, 88Len1, 89Hig1] for most of the neutral species (as well as typical charge state ions) of H to U. Also the number of the terms, n, which is necessary to get the best fit to the experimental data, does depend on the target species and are given [83Bel1, 88Len1, 89Hig1]. It should be, however, noted that artificial oscillations of the cross sections are sometimes seen in this type of the fitting when they are plotted as a function of the electron energy [97God1].

Empirical formula with relatively simple but physically clear background based upon the binary-encounter-dipole (BED) model has been recently discussed [94Kim1]. This formula, without requiring any fitting parameters, show a reasonable agreement with the experimental data for one-electron atoms (and ions, too). After comparing this theoretical formula with the data available, the following empirical formula based upon the BED has been proposed:

$$\sigma_{\mathrm{i}} = \frac{3.52}{u}\left[a\ln(u) + b\left(1-\frac{1}{u}\right) + c\frac{\ln(u)}{u+1}\right] \tag{5}$$

where a, b and c are the fitting parameters.

It should be pointed out that this basic empirical formula based upon BED can provide not only the total ionization cross sections but also the differential (angular and energy) cross sections of the secondary electrons which are found to be in reasonable agreement with the experiments.

Another convenient empirical formula of the single-electron ionization cross sections based upon the semiclassical approach has recently been proposed for neutral atoms ranging from hydrogen to uranium atoms [94Mar1]. The following formula for the partial ionization cross section of the sub-shell with the quantum numbers (nl) is given:

$$\sigma_{\mathrm{i}}^{j} = \pi r_j^2 g_j N_j f(u) \tag{6}$$

where r_j is the electron orbital radius of the j-th shell which is quantum-mechanically calculated, g_j the weighting factor for different shells, N_j the number of electrons in the j-th shell and the energy-dependent universal function $f(u)$ has the following form:

$$f(u) = \left(\frac{u-1}{u+1}\right)^a \frac{1}{u}\left(b + c\left\{1-\frac{1}{2u}\right\}\ln\left\{2.7+(u-1)^{1/2}\right\}\right) \tag{7}$$

with $u = E/I_j$, E and I_j representing the incident electron energy and the binding energy of the j-th shell, respectively. It has been found that, in order to get better fit to the experimental data, the constants a, b and c are varied for different shells, namely a = 7/4, b = 1, c = 1 for s-shell; a = 2, b = 1, c = 1 for p-shell; a = 3/2, b = 3, c = 2/3 for d-shell and a = 3/2, b = 1, c = 2/3 for f-shell and the factors for different shells are given [94Mar1]. Finally the total single electron ionization cross sections are given as follows:

$$\sigma_{\mathrm{i}} = \sum_j \sigma_{\mathrm{i}}^{j} \tag{8}$$

This formula has been found to be in generally good agreement with the experimental data within ± 10 % for most of the neutral species up to U and within ± 30 % for a few neutrals.

2.6.6.2 Analytical and empirical formula for ionization of inner-shell electrons

There are ab initio relativistic calculations of the inner-shell electron ionization by relativistic electron impact which show good agreement with the experimental results [78Sco1]. Yet sometimes, it is convenient to have simpler expressions for the innershell-electron ionization by the relativistic electrons.

It is well known that the relativistic collision processes can be nicely described through the Weizsacker-William method based upon the virtual photon interactions due to the electro-magnetic field generated by the passing high velocity charged particles. One of the simplest analytical formulas for total ionization cross sections [67Kol1] has been found to be in good agreement with a number of the observed data [70Mid1, 77Ish1]. The cross sections (in units of 10^{-24} cm^2) are given as the sum of two parts, namely the distant collisions (due to the virtual photon; $\sigma_{\mathrm{i}}^{\mathrm{d}}$) and close collisions (due to Coulomb interaction; $\sigma_{\mathrm{i}}^{\mathrm{c}}$):

$$\sigma_{\mathrm{i}}^{\mathrm{d}} = \frac{0.275}{I_j}\frac{(E+1)^2}{E(E+2)}\left[\ln\left\{\frac{1.19E(E+2)}{I_j}\right\} - \frac{E(E+2)}{(E+1)^2}\right] \text{ barn} \tag{9}$$

$$\sigma_{\mathrm{i}}^{\mathrm{c}} = \frac{0.99}{I_j}\frac{(E+1)^2}{E(E+2)}\left[1-\frac{E}{I_j}\left\{1-\frac{E^2}{2(E+1)^2}+\frac{2E+1}{(E+1)^2}\ln\left(\frac{E}{I_j}\right)\right\}\right] \text{ barn} \tag{10}$$

Here E and I_j represent the kinetic energy of the incident electrons and the ionization energy of the j-th inner-shell, both in the units of the electron rest mass energy (m_0c^2 where m_0 and c represent the electron rest mass and the velocity of light), respectively. It can be noted that the calculated ionization cross sections of the relativistic electrons in heavy H-like ions such U^{91+} ions are also found to be in agreement within a factor of two with those recently observed near the threshold region (see Section 3.2).

It should be pointed out that the differential cross sections of the secondary electrons caused by the inner-shell ionization have been nicely given based upon the virtual photon interactions [90May1], combined with the Møller interactions.

There is another work to find some empirical formula relevant to the ionization of the inner-shell (K, L and M) target electrons including the sub-shell electrons at the relativistic electron impact [94Deu1]. In principle, this empirical formula is the same as that given in eqs. (6)-(8), with the additional relativistic corrections. Thus the ionization cross sections are given as follows:

$$\sigma_{\mathrm{i}}^{j} = \pi r_j^2 g_j N_j f(u) F(u) \tag{11}$$

where $F(u) = R(1 + 2u^{1/4}/J^2)$ with $J = m_0c^2/I_j$, m_0c^2 being the electron rest mass energy. R, another relativistic correction factor, is given as a function of u and J [65Gry1]. Other parameters are the same as those given in eq. (6). The weighting factors g_j for K-, L- and M-(sub)shells are also given. The agreement with the experimental data is reasonable but the deviation has been clearly seen at high energies.

2.6.6.3 Empirical formula for multiple ionization of neutral atoms

Multiple electron ionization processes are much more complicated but they have been investigated to some extent [87Taw1]. It is not easy to find simple empirical formulas, even for the double-electron ionization cross sections, as many electron atoms are expected to have the significant but different contribution from the indirect processes which are not easily formulated. Yet there are some proposals to formulate such multiple electron ionizations.

One recently proposed analytical formula [95She1, 97Bél1] for m-times ($m \geq 2$) electron ionization, based upon analysis of the experimental data available, is given as follows, under the condition that the indirect processes are not significant, meaning that the empirical formula is better fitted with the observations at relatively high energies (in units of 10^{-18} cm^2):

$$\sigma_{m\mathrm{i}} = \frac{aN^b}{I_m^2}\frac{u-1}{u}\frac{\ln u}{u} \tag{12}$$

where I_m represents the threshold energy for removal of the m outer-most electrons (in Rydberg units) and is given as

$$I_m = \sum_{j}^{m-1} I_{j,j+1} \ ,$$

$I_{j,\,j+1}$ being the single-electron ionization energy from the charge j to j+1, $u = E/I_m$, E being the incident energy of electrons (in Rydberg units), N the total number of electrons in a target atom and a and b constants and given in Table 2.6.11, depending on the number of the electrons to be ionized, m. It has been found that this can provide reasonable agreement (within a factor of two) with the experimental data for multiple-electron ionization up to 13 electrons.

Table 2.6.11. Constants in empirical formula (eq. (12)) for multiple-electron ($m \geq 2$) ionization.

m	a	b
2	14.0	1.08
3	6.30	1.20
4	0.50	1.73
5	0.140	1.85
6	0.049	1.96
7	0.021	2.00
8	0.0096	2.00
9	0.0049	2.00
10	0.0027	2.00

For $m > 10$, the following asymptotic form can be used:

$$a\ (m > 10) \approx 1350\ m^{-5.7}$$
$$b\ (m > 10) \approx 2.00. \tag{13}$$

Another semiclassical formula [96Deu1] has also been proposed based upon the procedures described before. To get the cross sections of the m-electron ionization, the single ionization formula has to be summed over the contributing sub-shells:

$$\sigma_{mi} = g^m \sum_k \pi r_k^2 N_k f_k(u) \tag{14}$$

where r_k represents the mean-electron radius of the k-th sub-shell (k = 1 referring to the outermost shell, etc.), N_k the number of electrons in the k-th sub-shell and $f_k(u)$ the universal function depending upon the shell given before (see eq. (7)). g^m is the weighting factor which has been estimated from the experimental data available and has been found to be strongly dependent on the nuclear charge of the target species. So far, this formula has been shown to be in reasonable agreement with the multiple-electron ionization up to m = 5.

One more example of the empirical formulas for m-multiple electron ionization, based upon the well-understood formula, combining with some statistical consideration is given recently [95Fis1] as follows (in units of 10^{-16} cm^2):

$$\sigma_{mi} = \frac{3.52}{17^{m-1}} \frac{\zeta_m}{I_m^2} \left(1 - 2e^{-0.7u}\right) u^{-1.4} \ln(u) \tag{15}$$

where the minimum energy for removing m-electrons I_m is given in Rydberg units and ζ_m the statistical factor which depends slightly on whether m electrons are removed from the single outermost or the two more shells. It should be noted that this is not valid near the threshold where another treatment is necessary. Generally the agreement with the experimental data seems to be reasonable up to m = 7.

2.6.6.4 Ionization rate coefficients

So-called ionization rate coefficients, which are averaged over some distributions of the electron energy or temperatures such as the Maxwellian distributions, are also useful, particularly in applications involving basic and industrial plasmas [83Bel1, 88Len1, 89Hig1]. But it has been

recently realized that the original cross section data are more convenient in many applications and indeed there are a number of cases which do not follow the Maxwellian distributions and another procedure is necessary to get the rate coefficients for different energy distributions.

A number of different empirical forms for the ionization rate coefficients, namely the cross sections multiplied by the electron velocity, $<\sigma_i v_e>$, averaged over the Maxwellian velocity (temperature) distributions have been proposed.

1. One of the most commonly used forms is represented in the following [83Bel1, 88Len1, 89Hig1]:

$$\langle \sigma_i v_e \rangle = e^{-I_i/kT} \left(\frac{kT}{I_i}\right)^{1/2} \sum \alpha_n \left(\log \frac{kT}{I_i}\right)^n \qquad \text{for } I_i/10 \le kT \le 10 I_i \tag{16a}$$

$$\langle \sigma_i v_e \rangle = \left(\frac{kT}{I_i}\right)^{-1/2} \left\{ \gamma \ln \frac{kT}{I_i} + \sum \beta_n \left(\frac{I_i}{kT}\right)^n \right\} \qquad \text{for } kT > 10 I_i \tag{16b}$$

where I_i and T represent the ionization energy of ion and the electron temperature, respectively. The parameters, α_n, β_n,and γ, are given in the references for a number of atoms in various ionization [83Bel1, 88Len1, 89Hig1].

2. Based upon the recommended ionization data [83Bel1, 88Len1, 89Hig1] from H to Ni neutral atoms, another simple fitting formula for ionization rate coefficients has been recently proposed,

$$\langle \sigma_i v_e \rangle = a\left(1 + P u^{1/2}\right) u^k \frac{e^{-u}}{X+u} \tag{17}$$

where $u = I_i/T$, I_i is the ionization energy of ions and T the electron temperature. a, k and X are the adjustable parameters which have been determined from the best fit to the recommended data. P is another adjustable parameter to fit the threshold behavior (in most cases P is 0 or 1). These parameters are given in the reference [97Vor1].

Acknowledgement

The present author would like to thank Dr. I.Murakami, Mr. T.Imai and Mr. M.Kato of NIFS for their help in making some figures and tables used here.

2.6.7 References for 2.6

65Gry1 Gryzinski, M.: Phys. Rev. **138** (1965) 322.
67Kol1 Kolbenstvedt, H.: J. Appl. Phys. **18** (1967) 4785.
67Lot1 Lotz, W.: Z. Phys. **206** (1967) 205.
68Lot1 Lotz, W.: Z. Phys. **216** (1968) 241.
70Mid1 Middleman, L.M., Ford, R.L., Hofstadter, R.: Phys. Rev. A **2** (1970) 1429.
71Ino1 Inokuti, M.: Rev. Mod. Phys. **43** (1971) 297.
77Ish1 Ishii, K., Kamiya, M., Sera, K., Morita, S., Tawara, H., Oyamada, M., Chu, T.C.: Phys. Rev. A **15** (1977) 906.
78Sco1 Scofield, J.H.: Phys. Rev. A **18** (1978) 963.
83Bel1 Bell, K.L., Gilbody, H.B., Hughes, J.G., Kingston, A.E., Smith, F.J.: J. Phys. Chem. Ref. Data **12** (1983) 891.
85Mär1 Märk, T.D., Dunn, G.H.: Electron Impact Ionization, Wien, New York: Springer 1985.
85Pow1 Powell, C.J.: in [85Mär1], p. 198.

86Be1 Be, S.H., Tonuma, T., Kumagai, H., Shibata, H., Kase, M., Kambara, T., Kohno, I., Tawara, H.: J. Phys. B **19** (1986) 1771.

87Sha1 Shah, M.B., Elliot, D.S., Gilbody, H.B.: J. Phys. B **20** (1987) 3501.

87Taw1 Tawara, H., Kato, T.: At. Data Nucl. Data Tables **36** (1987) 167; Tawara, H., Kato, M. NIFS-Data 51 (1999).

88Len1 Lennon, M.A., Bell, K.L., Gilbody, H.B., Hughes, J.G., Kingston, A.E., Murray, M.J., Smith, F.J.: J. Phys. Chem. Ref. Data **17** (1988) 1285.

89Hig1 Higgins, M.J., Lennon, M.A., Hughes, J.G., Bell, K.L., Gilbody, H.B., Kingston, A.E., Smith, F.J.: CLM-R294, Culham Laboratory, UK, 1989.

90Lon1 Long, X., Liu, M., Ho, F., Peng, X.: At. Data Nucl. Data Tables **45** (1990) 353.

90May1 Mayol, R., Salvat, F.: J. Phys. B **23** (1990) 2117.

92Bra1 Bray, I., Stelbovics, A.T.: Phys. Rev. A **46** (1992) 6995.

92Tra1 Trajmar, S., Nickel, J.C.: Adv. At. Mol. Opt. Phys. **30** (1992) 45.

93Bra1 Bray, I., Stelbovics, A.T.: Phys. Rev. Lett. **70** (1993) 746.

93Gie1 Gieler, M., Aumayr, F., Schweinzer, J., Koppensteiner, W., Husinsky, W., Winter, HP., Lozkina, K., Hansen, J.P.: J. Phys. B **26** (1993) 2137.

93Ric1 Richter, C., Andersen, N., Benoit, J.C., Dowek, D., Houver, J.C., Salgado, L., Thomsen, T.W.: J. Phys. B **26** (1993) 723.

94Deu1 Deutsch, H., Margreiter, D., Märk, T.D.: Z. Phys. D **29** (1994) 31.

94Kim1 Kim, Y.K., Rudd, M.E.: Phys. Rev. A **50** (1994) 3954.

94Mar1 Margreiter, D., Deutsch, H., Märk, T.D.: Int. J. Mass Spectrom. Ion Process **139** (1994) 127.

95DeP1 DePaola, B., Huang, M.T., Winecki, S., Kanai, Y, Lundeen, S.R., Fehrenbach, C.W., Arko, S.A.: Phys. Rev. A **52** (1995) 2136.

95Fis1 Fisher, V., Ralchenko, Yu., Goldgirsh, A., Fisher, D., Martin, Y.: J. Phys. B **28** (1995) 3027.

95She1 Shevelko, V.P., Tawara, H.: J. Phys. B **28** (1995) L589.

96Deu1 Deutsch, H., Becker, K., Märk, T.D.: J. Phys. B **29** (1996) L497.

96Sch1 Schappe, R.S., Walker, T., Anderson, L.W., Lin, C.C.: Phys. Rev. Lett. **76** (1996) 4328.

96Tan1 Tan, W.S., Shin, Z., Ying, C.H., Vuskovic, L.: Phys. Rev. A **54** (1996) R3710.

97Bél1 Bélenger, C., Defrance, P., Salzborn, E., Shevelko, V.P., Tawara, H., Uskov, D.B.: J. Phys. B **30** (1997) 2667.

97Dep1 Depaola, B.: Accelerator-Based Atomic Physics Techniques and Applications (S. Shafroth, J.A. Austin, eds.), American Institute of Physics (1997), p. 677.

97God1 Godunov, A.: Abstract Book, International Conference on Physics of Electronic and Ionic Collisions (F. Aumayr, G. Betz, HP. Winter, eds.), (1997), p.TU199 and private communication (1997).

97Taw1 Tawara, H.: AIP Proceedings of International Conference on Atomic Molecular Data and Their Applications (W. Wiese, ed.), in printing, Gaithersburg, USA, (1997), p.434.

97Vor1 Voronov, G.S.: At. Data Nucl. Data Tables **65** (1997) 1.

www1 www at http://dbshino.nifs.ac.jp (accessible after getting the ID) (National Institute for Fusion Science, Toki, Japan).

www2 www at http://wwwndc.tokai.jaeri.go.jp/JEAMDL/index.html (Japan Energy Research Institute, Tokai, Japan).

www3 www at http://ornl.gov (Oak Ridge National Laboratory, Oak Ridge, TN, USA).

www4 www at http://iaea.org.at (International Atomic Energy Agency, Wien, Austria).